EVALUATING GREEN STORMWATER INFRASTRUCTURE MODELING METHODS FOR URBAN AREAS

by

Shannon Kelene Reynolds

A dissertation submitted to the faculty of
The University of Utah
in partial fulfillment of the requirements for the degree of

Doctor of Philosophy

Department of Civil and Environmental Engineering

The University of Utah

May 2015

The University of Utah Graduate School

STATEMENT OF DISSERTATION APPROVAL

The dissertation of **Shannon Kelene Reynolds**

has been approved by the following supervisory committee members:

Christine Pomeroy	, Chair	**2/25/2015** Date Approved
Steven Burian	, Member	**9/11/2014** Date Approved
Brian McPherson	, Member	**8/27/2014** Date Approved
Courtenay Strong	, Member	**8/8/2014** Date Approved
James Smullen	, Member	**9/22/2014** Date Approved

and by **Michael Barber**, Chair/Dean of

the Department/College/School of **Civil and Environmental Engineering**

and by David B. Kieda, Dean of The Graduate School.

ABSTRACT

Green Stormwater Infrastructure (GSWI) has emerged as the next-generation stormwater management solution for urban areas and can provide greater flexibility in treatment options, design type, and site locations compared to traditional stormwater management alternatives. While methodologies for simulating GSWI functionality at the individual site level are well established, the complexity of representing GSWI collectively throughout a watershed remains problematic. One reason is the lack of literature comparing methods that represent GSWI networks within urban watershed models. This research addresses this need by evaluating GSWI up-scaling methods and the associated impacts on estimated benefits from varying spatial distribution and subcatchment aggregation.

The first component of this research focuses on GSWI up-scaling methods and the impacts to the hydrologic response estimates. Comparisons are drawn from two GSWI models built to meet performance criteria metrics, such as drawdown time and runoff capture volume. One model applies a GSWI design-specific up-scaling approach, while the other model represents the GSWI network as a nonspecific collective unit. Results from an assessment of the hydrologic response output between the models show comparable estimates within ± 5% for peak discharge, average flow rate, and volume. Therefore, representing GSWI as nonspecific collectives can comparably estimate

watershed-scale benefits to those estimated using representations with design-specific details.

The second component compares various GSWI spatial distribution and aggregation modeling scenarios and identifies the impacts of each on hydrologic response estimates. Spatial targeting of GSWI is compared to output from uniformly distributed GSWI in all subcatchments. Statistical assessments using t-test methods indicate that spatial targeting does not significantly impact estimates for volume, peak flow rate, or average flow rate estimates. Increasingly aggregated GSWI subcatchments had varied hydrologic response estimates of volume, peak flow rate, and average flow rate for urban areas, though not varied enough to be statistically significant for the Philadelphia model until the subcatchments were aggregated to a single subcatchment. However, the impact at the event level was obvious for peak discharge. Thus, for watershed areas with smaller subcatchment sizes, the greatest impact is to the peak flow rates. For SLC model scenarios, aggregating GSWI subcatchments significantly influenced all flow.

Dedicated to Steven Lee Dansie

TABLE OF CONTENTS

ABBREVIATIONS AND ACRONYMS

Automated Geo-Referencing Center – AGRC

Best Management Practices – BMP

Curve Number – CN

Directly Connected Impervious Area – DCIA

Geographic Information System – GIS

Green Stormwater Infrastructure – GSWI

Hydrologic Simulation Program – HSPF

Long-term Hydrologic Impact Assessment – L-THIA

Low Impact Development – LID

National Pollutant Discharge Elimination System Stormwater – NPDES

National Resource Defense Council – NRDC

Philadelphia, Pennsylvania – PHL

Philadelphia Water Department – PWD

Salt Lake City, Utah – SLC

Stormwater Management Model Version 5 – SWMM5

System Effectiveness and Life-Cycle Evaluation of Costs Tool – SELECT

System for Urban Stormwater Treatment and Analysis Integration Model – SUSTAIN

United States Environmental Protection Agency – U.S. EPA

United States Geological Survey – USGS

Urban Drainage and Flood Control District – UDFCD

Water Environment Research Foundation – WERF

ACKNOWLEDGEMENTS

I have received support from a number of people during my tenure as a Ph.D. student, without which this document would not exist. I have a great appreciation for Dr. Christine A. Pomeroy who allowed me the freedom to develop my ideas and who provided invaluable insights to improve them. I would like to convey my gratitude and deepest respect to Dr. James T. Smullen who motivated me to return to school and who has consistently endeavored to help me succeed. Your influence on my professional development is beyond measure. A great many thanks go to my committee members Dr. Steven J. Burian, Dr. Brian J. McPherson, and Dr. Courtenay Strong for their thoughtful and instructive feedback, which has guided me to my final project.

The modeling studies herein could not have been conducted without the data and models provided by the Philadelphia Water Department. Financial support for this project was graciously provided by the Achievement Rewards for College Scientists Foundation, the Water and Environmental Research Foundation, and the University of Utah Civil and Environmental Engineering Department. Indispensable technical guidance and advice were provided by Dwayne Myers in the development of the up-scaling applications. A special thank you goes to Gary D. Martens and Rajesh Rajan for facilitating data collection and continuous support along the way. Thomas C. Walsh spent a number of hours dissecting ideas, discussing concepts and applications, and proofreading my work. He has been a valuable asset and colleague. Others I would like to thank for their

insight, feedback, and friendship include Dasch Houdeshel, Kristianne Sandoval, Megan Walsh, and Marianka Sochanska.

This section would not be complete without acknowledging the relentless support of my family throughout all my life's adventures. Collectively, their love and encouragement have carried me through this process. I would especially like to thank my mother, Susan K. Dansie, for being my biggest fan and helping me in countless ways. My success is due to your devotion and influence. I am indebted to the Smith family who provided the essentials to enjoying this journey: laughter, music, and friendship. Finally, my profound appreciation goes to my best friend, Gregory G. Smith, who pressed me to persevere when I wanted to give in and who steadfastly believed in me, even when I did not believe in myself. I cherish your support.

CHAPTER I

INTRODUCTION

The goals of this research are to assess an alternative methodology for up-scaling green stormwater infrastructure (GSWI) within urban area planning models and evaluate the hydrologic response effects from varying distribution and aggregation scenarios. This research expands the existing body of knowledge for simulating GSWI systems at the watershed-scale. A novel alternative is presented for meeting modeling objectives when design-specific details are unknown by shifting the perspective from design-specific GSWI units to a collective representation of fundamental GSWI processes. Furthermore, this work identifies the impacts to hydrologic responses from different spatial distribution patterns and subcatchment aggregation scenarios, which will help formulate special considerations in building watershed-scale GSWI networks in future planning models. This work will benefit professionals within the field of stormwater management, which includes urban area modelers, stormwater engineers, and academic researchers focused on GSWI implementation.

Background

Urbanization and the Associated Impacts

Early in the twentieth century, stormwater runoff studies discussed the need of accurately estimating the stormwater runoff volume produced from urban areas and in response, rainfall-runoff relationships were established (Lloyd-Davies 1906). These relationships were tied to the development of increasingly accurate estimations of critical urban elements. Studies focused on these areas cited impervious cover (e.g., paved areas, buildings) as one of the major sources of error in estimating runoff. These assertions have been repeatedly verified by a number of observational and modeling studies (e.g., Boyd et al. 1994; Yan and Edwards 2013). With the relationship established between rainfall and land surface change affecting runoff, it follows that studies would emerge focused on identifying surface characteristics having the most impact on stormwater runoff characteristics. Leopold (1968) summarized the algorithms necessary to quantify hydrologic impacts from urbanization, which are directly influenced by impervious cover. The report used the Brandywine Creek Basin in Pennsylvania as a case study site to apply the researched impacts, since urbanization of the basin was anticipated. Probabilistic flow frequency curves were estimated of the Brandywine Creek Basin as a function of impervious cover. Leopold (1968) reported increased flooding potential of 1.5 – 6 times that of the natural, or predevelopment, state as it is increasingly converted to impervious surfaces. Subsequent studies have re-enforced the positive correlation between impervious surfaces and changes to stormwater runoff volume, peak discharge, and time to peak discharge, identifying impervious cover as a fundamental influencing factor of urban hydrology (e.g., Schueler 1994).

Urban Watershed Modeling Studies

By the end of the twentieth century, the focus of urban areas and impervious cover studies had expanded to include research on adverse environmental impacts to downstream communities (Arnold and Gibbons 1996). Arnold and Gibbons (1996) emphasized that negative impacts to stormwater runoff from impervious surfaces were cumulative as it moves downstream. Thus, there was a need to quantify impervious surfaces to inform future community development planning decisions. The conclusions alluded to GSWI as a valuable mitigation method by stating that retaining natural land cover during urban development (i.e., reducing impervious surfaces) is a simple concept and should be applied in community development plans. The Arnold and Gibbons (2006) study presents a simplistic approach to quantify the adverse impacts to downstream locations from increasing amounts of impervious area (i.e., urbanization). However, limitations exist when applying the Arnold and Gibbons (2006) methodology to characterize the complex hydrology of urban watersheds. Subsequent studies have shown that identifying the connectivity of impervious surfaces to sewer inlets can be as important as identifying the amount of impervious surfaces. Lee and Heaney (2003) identified stormwater runoff volume sensitivity to different impervious area connectivity scenarios. Total impervious area was subcategorized based on connectivity to stormwater conveyance system inlets, specifically focused on those areas that drain directly to the sewer inlets without being intercepted or detained on-site (i.e., directly connected impervious areas (DCIA)). A 50-year rainfall timeseries was performed for four sites to quantify the magnitude of runoff attributed to DCIA (Lee and Heaney 2002). The study found 90% of all runoff produced was generated by DCIA.

The Pappas et al. (2008) study corroborated the findings from the Lee and Heaney (2003) report through observed data collected in a laboratory. Observations were conducted using simulated rainfall over three different impervious and pervious cover setups: 1) Impervious cover located upslope of pervious cover (Case 1); 2) Impervious cover located downslope of pervious cover, where impervious runoff is directly connected to the outlet (Case 2); and 3) 100% pervious cover (Case 3). The findings from the controlled study showed Case 2 produced the greatest volume of runoff, with exfiltration resulting under saturated soil conditions. The Pappas et al. (2008) results also highlighted the potential benefits of intercepting impervious runoff with pervious cover. The results for dry soil conditions (i.e., average soil moisture content equaled 16%) showed that until the soil became saturated, the system performance for Case 1 mimicked the response for Case 3 with respect to peak flow rate, time to peak, and outflow volume. For tests where the soil was considered wet (i.e., average soil moisture equaled 22%), the response from Case 1 aligned with that of Case 2, citing peak flow rate, time to peak, and outflow volume. These results imply that disconnecting impervious surfaces prior to inlets has the potential to mitigate adverse impacts where the infiltration capacity of the soil is not exceeded (i.e., dry conditions). Other studies have been conducted in the field supporting this conclusion by comparing development sites to adjacent undeveloped areas (e.g., Dietz and Clausen 2008).

More recent modeling research has focused on identifying input parameters, beyond impervious area, that influence urban hydrologic response estimates. Bormann et al. (2009) tested the influence of subcatchment aggregation and varied spatial distribution of land use types on estimated discharge. Subcatchments were increasingly aggregated

from 25-meters up to 2-kilometers grid cell size, while spatial redistribution of land cover types was performed by two methods: 1) random assignment to various locations and 2) topography-based assignment. The modified input datasets were used within three hydrologic models: the Water Flow and Balance Simulation Model (WASIM), the TOPMODEL-Based Land Surface-Atmosphere Transfer Scheme (TOPLATS), and the Soil and Water Assessment Tool (SWAT). The simulation results for all three models showed a greater sensitivity to aggregation of inputs rather than spatial redistribution.

Research studies started moving toward a predictive nature for urban area development and estimating hydrologic response. Studies have attempted to replicate the response of urban hydrology to land cover changes using a variety of numerical models, regression analysis techniques, and emerging geographic information system (GIS) tools and datasets. Bhaduri et al. (2000) developed a long-term hydrologic impact assessment (L-THIA) model to simulate the impacts to stormwater runoff from changes in urban land cover from surveyed datasets completed in 1973, 1984, and 1990. The study used long-term continuous rainfall data (e.g., 30 years) to drive the L-THIA model runoff simulations using the empirical curve number (CN) method. The GIS linked model generated results indicating an 80% increase in surface runoff between 1973 and 1990 from an 18% increase in impervious cover. The ability of predictive models to accurately simulate the urban hydrologic response based on future land cover changes has been the focus of more recent publications (e.g., Conan et al. 2003; Yang et al. 2011; Lucas and Sample 2014). Tong et al. (2012) coupled a Hydrologic Simulation Program FORTRAN (HSPF) model with a Markov Cellular Automata (CA-Markov) framework, which is a GIS-based land-use model. Using projected land use changes for the year 2050, the

resulting response was a nearly 30% increase in streamflow. The report emphasized these results would benefit urban area managers and planners in developing mitigation strategies for estimated increases (Tong et al. 2012). The results of these studies indicate that predictive models could produce beneficial information for future planning and identification of areas susceptible to urban sprawl.

GSWI Use in Urban Areas

A number of influential policy changes and federal guidance documents have contributed to the use of GSWI within urban areas, most notably: 1) The Clean Water Act of 1972, 2) the National Pollutant Discharge Elimination System (NPDES) Stormwater Program, initiated in 1990, and 3) The watershed-based NPDES permitting plan guidance document (U.S. EPA 2004). The focus of these policies is to reduce the adverse impacts from urbanization by reducing increased amounts of stormwater volume reaching downstream waterways and sewer systems. These policy changes forced municipalities to fall into compliance and thus, development of long-term control plans was initiated. For densely populated urban areas, retrofitting the urban environment to meet the NPDES policies by expanding existing conveyance, treatment, and storage facilities can be cost-prohibitive (Benedict and McMahon 2002). Therefore, site-scale treatment options (i.e., GSWI) were increasingly considered as management options to reduce the stormwater volume treated at existing facilities downstream (U.S. EPA 2000). GSWI can be defined as elements that promote infiltration or on-site detention of stormwater runoff within the urban environment in an attempt to mimic the natural hydrology of the region (Benedict and McMahon 2002). To aide in the implementation of such elements, guidance

documents began to emerge discussing the use of GSWI to manage urban area runoff (PGC 1999; Lowndes 2000). Additionally, the U.S. EPA (2000) review of GSWI presented a comprehensive review of the overall advantages and disadvantages from economic, environmental, and social perspectives. The summary discussion emphasized more observational studies are necessary to accurately assess GSWI performance.

A growing body of literature focusing on case studies and pilot projects has shown the effectiveness of using GSWI in managing urban stormwater runoff (e.g., U.S. EPA 2000; Banting et al. 2005; Abida and Sabourin 2006; Pitt and Voorhees 2010; Kazemi et al. 2013; Pitt et al. 2013). Booth et al. (1996) measured the surface and subsurface runoff results for four different permeable pavements installed in a parking lot area within the University of Washington's campus. The results were compared to traditional asphalt parking surface runoff response. Booth et al. (1996) measured no significant runoff from the permeable pavement stalls through the study period (i.e., the autumn season), while nearly all the rainfall over the traditional asphalt surface was converted to runoff. Other field studies have since followed Booth et al. (1996) that have expanded the discussion to include results after the permeable surface is clogged (e.g., Kazemi et al. 2013). The Kazemi et al. (2013) study evaluated the performance of a 28 – acre pilot project implementation of pervious pavement in Louiseville, Kentucky during less than ideal conditions. The resiliency of the system was tested by measuring system performance while the surface was clogged with sediment. The performance of the pervious pavement system was reduced from 80% runoff capture volume to 30%-40% during clogged conditions. After performing typical maintenance on the pervious surfaces and removing the accumulated sediment, Kazemi et al. (2013) reported that the

capability of the pervious pavement to capture runoff at 80% was completely restored.

GSWI Modeling Approaches and Tools

As the body of literature grows documenting the performance of pilot projects and case studies, the relative novelty of GSWI has made the predevelopment planning for these seemingly simple technologies difficult. The reality is that GSWI concepts can be quite complex and placement and design of each unit is greatly dependent on the surrounding environment it is meant to serve (Benedict and McMahon 2002). Benedict and McMahon (2002) presented seven essential initiatives to successfully implement watershed-scale GSWI, most notably, that GSWI planning prior to development is a necessity. This objective is reiterated with recent articles reviewing the state of the practice and acknowledging the benefit of master planning and developing goal oriented approaches when implementing GSWI for watershed wide stormwater management (Nickel et al. 2014). To address this, watershed-scale GSWI implementation is advancing with a variety of planning analysis tools and methods (e.g., Spicer 2008; Damodaram et al. 2010; Jia et al. 2012; Jayasooriya 2014). For example, the Philadelphia Water Department (PWD) developed a GSWI up-scaling algorithm that represented GSWI units collectively to meet Philadelphia's stormwater management requirements (Smullen et al. 2008; PWD 2009). The process was completed through the combined use of MS Excel spreadsheet capabilities and SWMM software. The approach estimated the aggregate benefits from a tiered implementation of GSWI throughout the City to manage urban stormwater runoff issues over the project timeline of 25 years (PWD 2009). Like PWD, other municipalities across the country have begun applying the GSWI paradigm as part

of long-term management plans. The National Resource Defense Council (NRDC) conducted a study entitled Rooftops to Rivers (NRDC 2006; NRDC 2011), which presented a number of case study areas where GSWI-focused watershed management plans were successfully implemented. The list of case studies included nine metropolitan areas. A follow-up report issued in 2011 included case studies for 14 metropolitan areas. However, the list of case study areas is far from complete within this report and there exist a number of other major urban city centers that have adopted and successfully implemented GSWI (e.g., PGC 1999; CTDEP 2004; EPA 2010; Struck et al. 2012; Pitt et al. 2013).

A number of studies have attempted to evaluate GSWI at the watershed-scale to estimate the hydrologic benefits (Table 1). Carter and Jackson (2007) used a GIS and the SCS Curve Number (CN) method within SWMM to estimate the runoff reduction benefits from green roofs. Weighted CN values to represent impervious areas and pervious green roof areas were developed for four spatial scales: total watershed, subwatershed, zoning (i.e., government, residential, etc.), and parcel (Carter and Jackson 2007). The distribution of green roofs within each of the spatial scale models (i.e., total watershed, subcatchment, zoning, or parcel) included applying green roofs to all rooftops and then only to flat rooftops. The results of the analysis showed significant reductions in runoff volume for the smaller storm events. The results also showed that the added detention capabilities provided by the green roofs significantly reduced peak flow rates for both scenarios (Carter and Jackson 2007). Other studies with similar modeling objectives have reported analogous reductions in runoff volume and peak flow rate estimates using different GSWI designs (Table 1).

Table 1. Summary of research conducted involving GSWI implementation at the watershed-scale.

Study	Model(s)	Scale	Focus	Peak Flow Rate	Outflow Volume	GSWI Type
Carter and Jackson 2007	SWMM; ArcGIS	Watershed	Performance	▼	▼	Green Roofs
Spicer et al. 2008	SWMM5/ L-THIA	Watershed	Performance/ Distribution	▼	▼	Multiple
Elliot et al. 2009	MUSIC	Watershed	Aggregation Influence	▲	-	Multiple
Damodaram et al. 2012	HEC-HMS/ SWMM	Watershed	Performance	▼	▼	Multiple
James et al. 2012	TR-55/ SewerGEMS	Watershed	Performance/ Distribution	▼	▼	Bioretention
Jia et al. 2012	BMPDSS/ SWMM	Watershed	Performance/ Optimization	▼	▼	Multiple
Pitt et al. 2013	WinSLAMM	Watershed	Performance/ Distribution/ Sizing	▼	▼	Bioretention
Walsh et al. 2014	SWMM	Watershed	Performance/ Distribution/ Sizing	▼	▼	Rain Barrels

James et al. (2012) looked at the performance of bioretention units when 1) multiple land uses drained to the unit and 2) impervious area only. The performance of the bioretention units for both scenarios reduced the peak discharge, runoff volume, and extended the time to peak discharge. Elliott et al. (2009) conducted a study evaluating the sensitivity of GSWI performance from increasingly aggregated subcatchments. The results showed the peak discharge was significantly affected when all original subcatchments were aggregated into one representative area. The results of this study did not include impacts to outflow volume.

Focus has shifted recently to developing built-in GSWI modules within existing modeling software or by creating stand-alone software (Jayasooriya 2014) (Table 2). This has been a direct result of the rise in planned use of GSWI in urban areas. For example, the newest release of SWMM5 is equipped with a GSWI module. The user is presented with a suite of GSWI types (e.g., Bioretention, Infiltration Trench, Permeable Pavement, Vegetated Swale, and Rain Barrels) to use within the model at the subbasin level. The GSWI module allows for a collection of GSWI types (or variations of the same type) to be used within a single subbasin area and requires the user to estimate the number of units per type to be simulated. Each GSWI type has specific input details that are necessary for the model to estimate the GSWI performance. These required inputs are different for each GSWI type, but generally include soil hydraulic conductivity, void ratio, storage depth, surface roughness, and surface slope. Unique to this model is the underdrain algorithms used to estimate discharge from the GSWI system. The discharge equations are based on the orifice equation and are defined in the model by a SWWM5 specific drain coefficient, discharge exponent, and drain height offset.

Table 2 Summary of models available for planning-level analyses of GSWI implementation.

Model Name	Model Description	Platform(s)	Scale	GSWI Type
SUSTAIN	Lee et al. 2012	ArcGIS/ HSPF /SWMM5	Watershed	Multiple
SWMM5 GSWI Module	U.S. EPA 2010	SWMM5	Watershed	Multiple
Proprietary	PWD 2009	MS Excel	Watershed	Non-Descriptive
Proprietary	Strecker et al., 2010	Proprietary	Watershed	Multiple
SELECT	WERF 2012	MS Excel	Site	Multiple
National Stormwater Calculator	U.S. EPA 2013	Web-Based/ SWMM5	Site	Multiple
DURMM	Lucas 2004	MS Excel	Watershed	Multiple
L-THIA	Jayasooriya 2014	Proprietary/Web-Based/MS Excel	Watershed	Multiple
RECARGA	Atchison and Severson 2004	Proprietary	Site	Multiple
MUSIC	Jayasooriya 2014	Proprietary	Site	Multiple
WinSLAMM	Jayasooriya 2014	Proprietary	Watershed	Multiple
LIDRA	Jayasooriya 2014	Open-Source/Web-Based	Site	Green Cover
i-Tree Hydro	Jayasooriya 2014	Proprietary	Watershed	Trees and Green Cover

The drain coefficient is a parameter that combines the area of the orifice and the discharge coefficient. The SWMM5 User's Help provides an algorithm to estimate this coefficient based on the desired drain time and the depth of water above the orifice (U.S. EPA 2010). The U.S. EPA also created the System for Urban Stormwater Treatment and Analysis Integration Model (SUSTAIN), which is focused on GSWI placement optimization at the watershed-scale. The model couples the robustness of SWMM5 hydrologic and hydraulic capabilities and HSPF sediment transport analysis with the spatial analysis capabilities of ArcGIS. The ArcGIS tool is the platform from which the model is operated. Compared with SWMM5, SUSTAIN has a larger suite of GSWI type options and provides more comprehensive results, including BMP cost estimation and spatially optimized GSWI placement (Lee et al. 2012). However, SUSTAIN requires greater time, effort, and expertise on the part of the modeler to collect and implement input data than that of other models. Furthermore, while the SUSTAIN model itself is available for free from the EPA's website, the model specifically requires the use of ArcGIS 9.3, which can be costly.

More simplistic models have emerged alongside the EPA's highly detailed watershed-scale model options. The National Stormwater Calculator is a web-based tool created to assess surface data at a specified location to estimate performance of various GSWI types (U.S. EPA 2013). A user can identify basic surface characteristics using underlying data source layers (i.e., soil type and slope) for a site and then compare the estimated performance of varying GSWI types for the location. The tool is limited to site-specific areas and does not allow for multiple GSWI units to be evaluated concurrently. Furthermore, the National Stormwater Calculator was developed with a broad spectrum

of professionals in mind and therefore, usability was prioritized over in-depth analysis capabilities and complexity. The Water Environment Research Foundation (WERF) has developed the MS Excel platform-based System Effectiveness and Life-Cycle Evaluation of Costs Tool (SELECT). SELECT combines runoff and water quality results with life-cycle costs for various GSWI types. The tool was developed in an effort to simplify GSWI representations and to provide an efficient means to check results from other more detailed model representations (e.g., SWMM5 or SUSTAIN). The SELECT model does not lend itself for use with larger urban area studies of GSWI implementation. This is mainly due to the limitations of the MS Excel Platform and the manner of representing GSWI units individually. SELECT simulates stormwater loading to GSWI units as either individual or multiple subcatchments (WERF 2012). These models function as decision support tools that offer supplemental results checks to other more robust numerical models.

The Strecker et al. (2010) distributed GSWI model attempts to bridge the gap between GSWI representation at the individual site-scale and the watershed-scale. This framework aggregates the performance of individual GSWI types into a composite watershed-scale hydrologic response. The model performs a mass balance on the hydrographs selected for routing to the aggregate GSWI component. As with the SELECT model, evaluations are conducted by parsing the contributing area into two subareas. These represent 1) the area being treated by each GSWI type (swale, cistern, and permeable pavement) prior to consolidation and 2) the remaining untreated area (Strecker et al. 2010). Each GSWI type has a specific set of required input parameters. For subareas, a weighted runoff coefficient is required, though the infiltration parameter

is established as a constant loss and the discharge from underdrains is equal to either the maximum flow rate (i.e., through the surface layer) or a user-defined use rate (i.e., time-series). As a result, this removes the reliance upon detailed design inputs (Strecker et al. 2010).

Existing literature has focused mainly on using design-specific applications of GSWI for both site-scale and watershed-scale evaluations. This approach requires input data that limit the assessment of GSWI practices within an urban environment and its applicability. Specifically, the performance of each design unit implemented hinges on assumed design variables used within the model. It is likely the design parameters have not been developed or researched at the planning stage for watershed-scale evaluations. Thus, output from these representations may be compromised by using potentially inappropriate design assumptions. Furthermore, design-level details may be unnecessary if the modeling objective is to meet watershed-scale performance criteria through some combination of GSWI types, the combination of which having yet to be defined at the planning stage. From this perspective, a combination of GSWI types is assumed to be designed and functioning to meet a standard watershed-wide performance measure. A collective representation of fundamental GSWI processes can relieve input data issues for these types of modeling objectives. Therefore, a comprehensive assessment of the methodology and its nuances is necessary to better understand its application and limitations.

Problem Statement

Increased impervious cover from urban development directly contributes to modified runoff characteristics at the watershed-scale, including higher peak flow rates, shortened times to concentration, and larger volumes of stormwater relative to pre-developed conditions (Leopold 1968). To mitigate these adverse stormwater impacts, GSWI can be introduced throughout urban areas to intercept impervious surface runoff prior to reaching sewer inlets. Site-scale studies showed GSWI was capable of mitigating the adverse impacts of urbanization (Booth et al. 1996). Subsequently, its use has increased in urban areas to meet watershed-scale stormwater management objectives (NRDC 2006; NRDC 2011; Baughman et al. 2013; Pitt et al. 2013; Nickel et al. 2014). In contrast to traditional stormwater management alternatives, GSWI provides flexibility in placement, design, and treatment options (Benedict and McMahon 2002; Shuster and Rhea 2013). Although the site-scale and watershed-scale performance of GSWI design types within urban planning models is well documented, they are limited in focus to design-specific GSWI (Damodaram et al. 2010; James et al. 2012; Carson et al. 2013; Kazemi et al. 2013; Lucas and Sample 2014).

There is a lack of literature identifying the potential variations in estimated collective benefits from GSWI networks due to sensitivities from 1) physical representation of the collective units and 2) spatial distribution and aggregation of collective units within the watershed model. Existing GSWI up-scaling literature has focused largely on using design-specific GSWI parameters (Strecker et al. 2010; Lee et al. 2012; U.S. EPA 2013). For modeling objectives aimed at comparing the performance of different GSWI types at the watershed-scale, design-oriented up-scaling approaches

are fitting. However, for modeling objectives where the collective benefit is estimated assuming a myriad of GSWI units are designed and functioning to meet specific performance criteria (regardless of unit design type and distribution density), design-level details become superfluous. Thus, introducing an alternative GSWI up-scaling method where less attention is placed on design-level details would benefit these modeling objectives.

It follows that the hydrologic response output from the collective representation of GSWI must be evaluated to identify its sensitivity to subcatchment aggregation and spatial distribution. Previous studies have evaluated influences from subcatchment aggregation and spatial distribution scenarios on the performance of specific GSWI design types (Elliot et al. 2009; James et al. 2012). These evaluations need to be expanded to include new approaches in representing GSWI watershed-wide, such as the up-scaling method presented herein. In doing so, more tools are available to evaluate the collective benefit estimates from GSWI networks. In conjunction, this research attempts to determine guidelines for acceptable aggregation practices and establish the influence of GSWI distribution patterns on resultant hydrologic response.

Research Goals and Hypotheses

The goal of this research is to introduce a novel method to represent GSWI at the watershed-scale and test the influences of spatial distribution and subcatchment aggregation on hydrologic response. These goals will be achieved by: 1) evaluating an alternative method for up-scaling GSWI within urban area planning models and developing an automated tool to generate input files for efficient model simulation; and

2) Applying the up-scaling method to models representing the Salt Lake City, Utah and Philadelphia, Pennsylvania region for a variety of spatial distribution and aggregation scenarios and compare the output. A review of the assessments will provide new insights into watershed-wide GSWI integration within planning-level models for two different climate and urban regions. Specifically, the results will relate the sensitivities of GSWI hydrologic response to basic model components such as subcatchment size and spatial distribution of the GSWI networks. The two hypotheses being explored to achieve these goals are:

Hypothesis 1: A watershed-scale up-scaling method involving the collective representation of GSWI yields comparable hydrologic results compared with existing methods based on design-level details. Performance metrics require the differences in peak flow rate, average flow rate, and volume measurements (i.e., taken from the outlet) to be within ± 5 %. Verification of Hypothesis 1 serves as proof of concept for the collective representation up-scaling method, which is subsequently used to test Hypothesis 2. Furthermore, verifying this hypothesis supports the method's use in urban area stormwater management planning and modeling.

Hypothesis 2: Variations in GSWI spatial distribution and aggregation at the subcatchment-scale influence both average and peak flow rate estimates more so than estimates of outflow volume. Evaluation of spatial distribution and subcatchment aggregation influences on hydrologic response estimates was conducted under this hypothesis. Statistical t-test methods were applied for each scenario with respect to the three hydrologic metrics of peak flow rate, average flow rate, and runoff volume to evaluate the validity of the hypothesis.

Dissertation Organization

The following chapters provide details on the execution and results of the research methodology. Chapter II presents the work completed on evaluating two up-scaling methods for use within watershed-scale planning models. This work focused on comparing the performance of an up-scaling methodology representing GSWI units as a collective to the performance from a design-oriented up-scaling approach. The article has been submitted to the J. Sustainable Water in the Built Environment and is currently under review. Subsequently, Chapter III presents comparisons of the hydrologic response from the alternative up-scaling methodology due to impacts from varying spatial distribution scenarios. These evaluations were conducted using a model representing the Salt Lake City, Utah region for single-event and long-term continuous precipitation data. The results were scrutinized for significance using t-test statistical analysis techniques. The contents of Chapter III are scheduled to be submitted to the J. Water Resources Planning and Management in January 2015 and are currently under review by its co-Author, Dr. Christine Pomeroy. Chapter IV expands the work completed in Chapter III by conducting subcatchment aggregation comparisons for a highly discretized and diversified model representing a section of the Philadelphia, Pennsylvania combined sewer area along with results from aggregating the Salt Lake City, Utah model. The content of this chapter is scheduled to be submitted to the J. Water Resources Research by May 2015. A discussion of the research results and recommendations for future work is presented within Chapter V. Appendices A, B, C, D, and E contain details regarding the tools and data sources (Appendix A), research plan and methodology (Appendix B), supplemental evaluations into the level of GSWI implementation on hydrologic response

significance (Appendix C), spatial distribution impacts for the Philadelphia, Pennsylvania model (Appendix D), and a sensitivity analysis of infiltration parameters (Appendix E).

CHAPTER II

COMPARING UP-SCALING APPROACHES FOR WATERSED-SCALE GREEN INFRASTRUCTURE

The U.S. Environmental Protection Agency (U.S. EPA) has established goals and policies in an effort to motivate urban municipalities to mitigate the negative effects of stormwater runoff. As a result, green stormwater infrastructure (GSWI) is becoming increasingly popular with urban area stormwater managers. While methodologies for simulating GSWI functionality at the individual site level are well established, the complexity of representing GSWI site characteristics collectively throughout a watershed remains problematic. This paper presents a comparison of methods to represent watershed-wide GSWI in planning models. The study uses the U.S. EPA's Stormwater Management Model (SWMM5) to estimate the collective benefit of GSWI the method presented within the Philadelphia Water Department's Green Cities, Clean Waters report and compares the results to the output produced from the built-in GSWI capabilities of SWMM5. The research objectives include: 1) implement the GSWI up-scaling procedures within the SWMM5 model to estimate stormwater runoff volume and flow reductions, and, 2) based on the results, assess the nuances of both procedures in urban

area stormwater management. The difference in watershed-wide hydrologic response estimates from the two methods range from 4% up to 12% and correlate to an increase in precipitation. Both methods infiltrate the majority of inflow, which range from 65% to 95% depending on precipitation depth. The timeseries show a close match for time to peak, peak discharge, and drawdown for the storage volume, orifice discharge, and flow that bypass the GSWI units. The results indicate both methods are useful tools in estimating watershed-wide hydrologic benefits (e.g., runoff volume reduction and decreases in peak flow) for planning-level analyses.

Background

A number of influential policy changes and federal guidance documents have contributed to the greening of urban areas and most notably include: the National Pollutant Discharge Elimination System (NPDES) Stormwater Program initiated in 1990 and the watershed-based NPDES permitting plan guidance document first published in 2003 (U.S. EPA 2004). As municipalities initiated long-term control plans to come into compliance with the NDPES policy, evaluations of nontraditional stormwater management techniques were conducted. Guidance documents began to emerge, highlighting the use of on-site controls to manage urban area runoff, such as GSWI (PGC 1999; Lowndes 2000). GSWI can simply be defined as elements that incorporate vegetation and green space into the urban environment in an attempt to mimic the natural hydrology of the region (Benedict and McMahon 2002). The U.S. EPA (2000) review of these types of controls presented a comprehensive assessment of the positive and negative side-effects from using these nontraditional stormwater management alternatives

from economic, environmental, and social perspectives. A growing body of literature focusing on case studies and pilot projects has shown the effectiveness of using LID and GSWI controls in managing urban runoff (e.g., U.S. EPA 2000; Banting et al. 2005; Abida and Sabourin 2006; Carson et al. 2013; Kazemi et al. 2013; Pitt et al. 2013; Shuster and Rhea 2013).

The expanding knowledge of individual GSWI designs and benefits has propelled the planning and implementation of these facilities, despite a lack of observed data for implemented collections of GSWI facilities throughout a catchment. The design and placement of each facility is dependent on the surrounding environment it is meant to serve (Benedict and McMahon 2002; Nickel et al. 2014), thus the natural functions GSWI are meant to mimic are quite complex. Furthermore, the observed collective benefits of multiple GSWI sites within an urban area have not been well documented or simulated as compared to individual GSWI sites. Despite these shortcomings, a growing number of United States municipalities have proposed GSWI networks within long-term watershed management plans for their reported environmental and economic benefits (PGC 1999; CTDEP 2004; National Resources Defense Council (NRDC) 2006; U.S. EPA 2010; NRDC 2011) and have created GSWI specific implementation guidance documents (e.g., UDFCD 2011). However, the UDFCD is not alone in this rite, as many regulatory and guidance documents now exist to aide in the planning, design, and implementation of GSWI within a variety of climate regions (UDFCD 2011; U.S. EPA 2014; PWD 2014).

This increased popularity and lack of an established planning-level model option has resulted in cities developing proprietary methods and algorithms to estimate the

collective benefits from implementing GSWI (e.g., Spicer 2008; Damodaram et al. 2010; Jia et al. 2012; Jayasooriya 2014). These methods up-scale individual GSWI facilities of various types to collections of multiple facilities using design-level details. Design details are essential for building and understanding GSWI facility functionality (e.g., media type and void ratio, individual rain barrel size, swale side slopes, etc.), but may not be known at the planning phase of a project when estimating watershed-wide benefits. This is especially true when a variety of GSWI design types will be implemented throughout an urban watershed to meet overall stormwater reduction goals. Understanding this reality, the Philadelphia Water Department (PWD) chose to represent GSWI using a basic water budget, tracking infiltration, storage, and controlled volume release. This enables the assessment of the collective hydrologic benefits GSWI (Smullen et al. 2008; PWD 2009).

More recently, in response to the demand for GSWI watershed planning tools, the U.S. EPA released the Stormwater Management Model (Version 5.1) equipped with a GSWI module capable of simulating one or more practices on a watershed-scale. The user is presented with a suite of GSWI types (e.g., bioretention, infiltration trench, permeable pavement, vegetated swale, and rain barrels) to use within the model at the subbasin level. The GSWI module allows for a collection of GSWI types (or variations of the same type) to be used within a single subbasin area and requires the user to estimate the number of units per type to be simulated. Each GSWI type has specific input details that are required for the model to calculate soil infiltration properties, storage requirements, and underdrain performance criteria (U.S. EPA 2010). These required inputs are different for each type, but generally include soil hydraulic conductivity, GSWI media void ratio, storage depth, surface roughness, and surface slope (Rossman

2010). Unique to this model is the underdrain algorithms used to estimate discharge from the GSWI system. The discharge equations are based on the orifice equation and are defined in the model by a SWWM5 specific drain coefficient, discharge exponent, and drain height offset (Rossman 2010). The drain coefficient is a parameter that combines the area of the orifice and the discharge coefficient. The SWMM5 User's Help provides an algorithm to estimate this coefficient based on the desired drain time and the depth of water above the orifice, thereby removing the need to define an orifice diameter (Rossman 2010). While there are a number of desirable elements to the SWMM5 GSWI module, it does have drawbacks. The structure of the storage and underdrain components within the GSWI module as described above does not allow for independent adjustment of the parameters. Instead, users are presented with the discharge equations relating the two components, which are to be used when adjusting the functionality of these two elements. The flexibility of applying timeseries data to GSWI facilities such as rain barrels to simulate reuse is complicated within the model and will require updates in subsequent releases. Furthermore, GSWI facilities are lumped within each subcatchment, which limits the ability of the model to mimic the distribution of GSWI and could potentially affect the shape of the outlet hydrograph (e.g., peak discharge and time to peak discharge).

The U.S. EPA also created the System for Urban Stormwater Treatment and Analysis Integration Model (SUSTAIN), which is focused on optimizing placement of GSWI throughout a watershed. The model couples the robustness of SWMM5 for hydrologic and hydraulic analysis with the Hydrological Simulation Program – Fortran (HSPF) for its sediment transport analysis with the spatial analysis capabilities of

ArcGIS. ArcGIS is the platform from which the aggregated model is operated. The SUSTAIN model has a much larger suite of GSWI type options and provides a more comprehensive results package as compared to SWMM5 that includes cost estimation and spatially optimized GSWI placement (Lee et al. 2012). The required input, however, is substantially more involved and time consuming to collect. While the SUSTAIN model itself is available for free from the U.S. EPA's website, the model specifically requires ArcGIS 9.3 license to be used, which can be costly, and SUSTAIN platform has not been updated to allow for more recent ArcGIS licenses. Lastly, guidance documentation and technical support is lacking for this model.

While the U.S. EPA has produced highly detailed watershed-scale modeling options for GSWI planning and implementation, less data-intensive models have also emerged. The National Stormwater Calculator is a web-based tool created to assess surface data at a specified location to estimate performance of various GSWI types (U.S. EPA 2013). A user can identify basic surface characteristics using underlying data source layers (i.e., soil type and slope) for a site and then compare the estimated performance of varying GSWI types for the location. The tool is limited to site-specific areas and does not allow for multiple GSWI units to be evaluated concurrently. Furthermore, the National Stormwater Calculator was developed with a multitude of professionals in mind and therefore usability was prioritized over in-depth analysis capabilities and complexity. The Water Environment Research Foundation (WERF) has developed the MS Excel platform-based System Effectiveness and Life-Cycle Evaluation of Costs Tool (SELECT). SELECT combines runoff and water quality results with life-cycle costs for various GSWI types. The tool was developed in an effort to simplify GSWI

representations and to provide an efficient means to check results from other more detailed model representations (e.g., SWMM5 or SUSTAIN). The SELECT model does not lend itself for use with larger urban area studies of GSWI implementation. This is mainly due to the limitations of the MS Excel Platform and the manner of representing GSWI units individually. The model allows for multiple subcatchments to load to a single GSWI alternative or to have each subcatchment load to a specific GSWI unit (WERF 2012). The costing data are derived from the WERF Whole Life Cost Model and the water quality algorithms are based on event mean concentrations of pollutants as published online within the WERF BMP database (http://www.bmpdatabase.org/). Similar decision support models have been developed, but are better suited as supplemental tools to check more robust numerical models (e.g., Osmond et al. 1995; U.S. EPA 2013; Jayasooriya 2014).

This study tests the hypothesis that the collective benefit of GSWI networks can be comparably simulated using a representation requiring fewer design-specific input parameters as compared to the SWMM5 LID module simulations. We present a comparison of the performance results produced from the PWD (2009) algorithm to the performance results produced using the built-in SWMM5 LID module for the same subcatchment and stormwater management goals.

Materials and Methods

PWD (2009) Up-Scaling Algorithm

The objective of the PWD (2009) up-scaling algorithm is to estimate the collective benefit from implementing various GSWI facilities designed to achieve a

specific level of performance. This objective assumes individual GSWI units and types within the system are designed and functioning to meet stormwater management requirements. From this perspective, type-specific and unit-level design details are superfluous. Thus, representing the fundamental processes of GSWI units as a lumped system is an appropriate approach for planning-level assessments that are not focused on comparing performance between GSWI designs.

The fundamental processes that simulate flow routing through a GSWI unit, as represented in the PWD (2009) algorithm, are: infiltration, storage with slow release through a control orifice, and GSWI unit bypass. Infiltration is estimated by routing the impervious area surface runoff directly to a pervious area (Figure 1). What does not infiltrate is routed to a storage node where the captured runoff is discharged through a control orifice. For runoff volumes that exceed the capacity of the GSWI system (i.e., infiltration plus storage capacity), flow is allowed to bypass through an overflow weir located at the top of the storage node. The bypass flow is routed, unrestricted, directly to the collection system. The elements representing these processes are created using a collection of equations presented within PWD (2009).

The PWD (2009) up-scaling algorithm organizes each fundamental process element to operate in series. At each timestep, the infiltrated volume of runoff is calculated first, followed by the amount of runoff stored and discharged through the control orifice, and ending with an estimate of bypass volume routed through the overflow weir. To isolate the GSWI hydrologic response from the area unaffected by GSWI, separate subcatchments are created (Figure 1). The area extracted for GSWI defines the amount of up-scaling within the model. The larger the area of impervious surface managed by

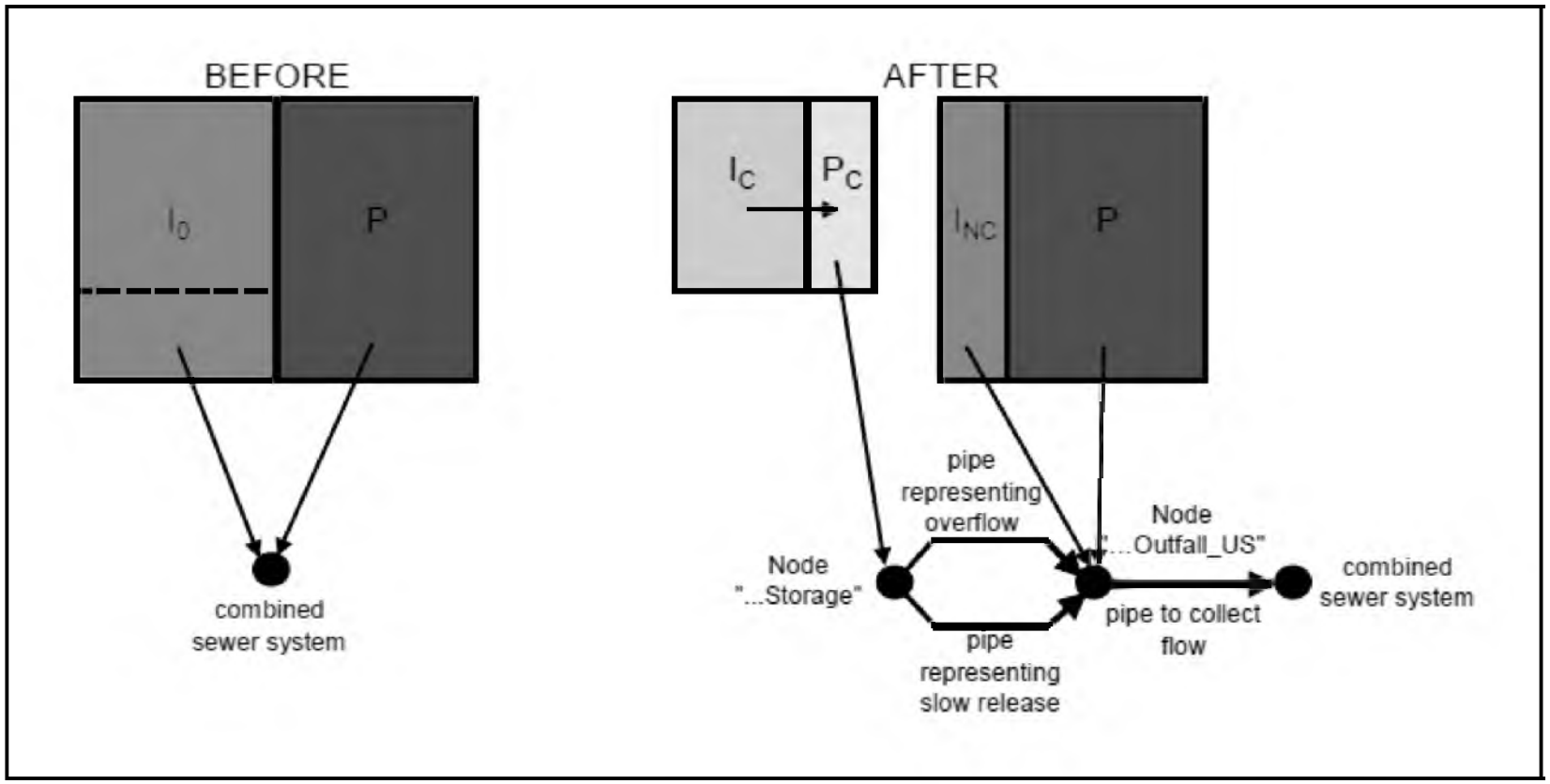

Figure 1. Conceptualization of how the PWD (2009) process and key elements are structured (adapted from PWD (2009)). The original subcatchment is separated into two new subcatchments: 1) representing the area and elements of the GSWI system (elements within the dotted line) and 2) the area unaffected by GSWI elements.

GSWI, the greater the amount of GSWI needed and simulated.

SWMM5 LID Module

The objective of applying the SWMM5 GSWI module is to estimate the collective hydrologic benefit from implementing various GSWI units and types. The benefit of this objective is in the ability to assess potential variability in hydrologic estimates from implementing an array of GSWI types within a watershed. From this perspective, GSWI design details are necessary to differentiate the level of performance for each type. Therefore, this method is appropriate for planning-level analyses where performance comparisons of specific GSWI design types are desired.

The SWMM5 GSWI design type selected for comparison in this study is the infiltration trench (S5IT), due to the component similarities to the PWD (2009) GSWI. The same fundamental processes of infiltration, storage and discharge through a control orifice, and GSWI unit bypass (Figure 2) are simulated. However, the order of simulating these processes is different from the PWD (2009) method. Surface runoff is routed through a surface layer and collected in an underlying storage layer. Infiltration to the subsurface is estimated along the bottom of the storage layer as runoff accumulates. Simultaneously, stored water is allowed to discharge through the underdrain component.

Overflow from the system occurs when all void space within the layers are at full capacity. Storage and underdrain components represent fundamental processes within the S5IT. These processes are represented by an integrated equation (Equation 1). Thus, variables for these two processes cannot be changed independently of each other. The S5IT representation also requires specific design values that are not required with the

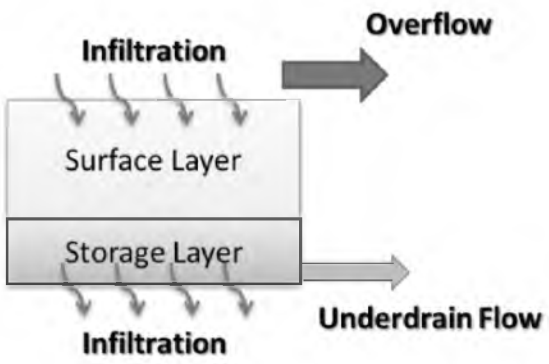

Figure 2. Profile of the S5IT fundamental processes interaction.

PWD (2009) method, such as void ratio and vegetative fraction.

$$q = C(h-H_d)^n \quad (1)$$

Where,

q = the desired peak release rate (inches/hour)

C = SWMM5 drain coefficient

h = maximum height of stored water (inches)

H_D = height of the outflow drain (inches)

n = drain exponent

The void ratio represents the media type present within the surface layer and is used to define the porosity. Vegetative fraction is the amount of plants present within the GSWI unit.

Model Simulations

The model simulations of this study are based on hydrologic response comparisons from a single hypothetical subcatchment with GSWI sized using the PWD (2009) and SWMM5 LID Infiltration Trench (S5IT) up-scaling methods. Each up-scaling method used the same subcatchment input values and sizing requirements to create the GSWI units. Two precipitation scenarios were conducted for each setup: single-event and long-term continuous. The details of the input data used for both models are discussed in the following subsections.

Precipitation Data

The single-event simulations used a SCS Type II design storm with a total precipitation volume of 2.5 inches, which represented a SCS Type II 24-hour, 25-year return period event for the Salt Lake Valley. The long-term continuous simulations used data for the years 2000 up to 2011 and were collected from the National Climatic Data Center Salt Lake International Airport rain gage (gage #427598). The long-term continuous scenarios for both models used the Salt Lake International Airport observed timeseries (TS1) followed by timeseries of 125% (TS2), 150% (TS3), and 263% (TS4) of the TS1 precipitation timeseries volume. The average annual depth, 95^{th} percentile value, and the climate regions represented by these precipitation characteristics are presented in Table 3.

Table 3. Long-term continuous precipitation characteristics and the representative climate regions.

Precipitation Timeseries ID	Average Annual Depth (inches)	95th Percentile (inches)	Representative Average Annual Precipitation
TS1	13.8	0.65	Southwest (Utah, Arizona, New Mexico) Climate Region
TS2	17.3	0.81	Northern Rockies and Plains (Wyoming, Montana, Nebraska) Climate Region
TS3	20.7	0.98	Lower Boundary of the West (California) and Northwest (Oregon) Climate Regions
TS4	36.3	1.71	South (Oklahoma), Lower Boundary Northeast (New York), and Ohio Valley (Ohio) Climate Regions

Simulated Area

The hypothetical subcatchment characteristics used for both up-scaling algorithms are presented within Table 4. These constitute baseline conditions (i.e., conditions prior to implementing GSWI) were not based on a particular urban area; however, they were selected to represent a subcatchment area with some urbanization. The Green-Ampt infiltration parameters were selected to represent a silty loam type soil that is typical for the Salt Lake City, Utah urban area. The surface slope, width, depression storage and Manning's coefficients were kept equal to the SWMM5 subcatchment default values. Both up-scaling methods (PWD (2009) and S5IT) use these conditions as the foundation for implementing GSWI.

GSWI Implementation and Performance Criteria

The level of GSWI implementation and performance criteria were equivalent between both up-scaling methods. The percent implementation of GSWI was kept to 25%

Table 4. Subcatchment characteristics inputs used for both GSWI up-scaling methods.

Description	Value
Subcatchment ID	SingleTestShed
Total Area	200 acres
Percent Impervious	25%
Surface Slope	5%
Width	500 feet
Impervious n/Pervious n	0.01/0.1 (unitless)
Impervious Depression Storage	0.05 inches
Saturated Hydraulic Conductivity	0.5 inches/hour
Suction	3.5 inches
Initial Deficit (IMDMax)	0.25 (as a fraction)

of total impervious area across all simulations. The loading ratio defining the number of impervious acres loading to 1 GSWI acre was kept constant at 15:1 for all simulations.

The GSWI units were sized to capture the first inch of runoff for the single-event precipitation simulation. For the long-term continuous simulations, the 95th percentile precipitation depth was used to size the GSWI units.

Runoff stored within the GSWI units had a drawdown requirement of 24 hours following a rainfall event for all simulations. For the purposes of this study, the result evaluation was focused only on the water balance as it pertains to the stormwater lost to infiltration, detained by the storage element and slow released through the underdrain orifice, and the flow that bypasses the GSWI facility. Antecedent moisture conditions were dry prior to simulation the design storm event. The antecedent moisture conditions for the long-term precipitation events were adjusted within SWMM5 based on the Green-Ampt soil moisture equations, and therefore varied depending on the time between subsequent storms. The water balance elements of subsurface flow or evaporation were

not evaluated with these simulations. These simulations were meant to introduce the nuances of each method as a preliminary task and not intended to be exhaustive. Further research into these additional water balance estimates are necessary and encouraged.

Representing GSWI Using the PWD (2009) Algorithm

The calculated values generated from the PWD (2009) algorithm for the single-event simulation are presented with Table 5. Between the single-event and long-term continuous simulations, the only change to these calculations was the user-defined capture volume. As the capture volume changes (i.e., 95th percentile precipitation depth), these parameters are adjusted to capture the 95th percentile runoff volumes.

Representing GSWI Using the SWMM5 LID Module

For the SWMM5 GSWI simulations, the same total subcatchment area and surface characteristics were used. The parameters defining the S5IT GSWI unit for the single-event simulation are presented in Table 6. The variables in Table 6 were updated for the long-term continuous simulations based on the 95th percentile precipitation volumes. Because capture volume requirements changed, the estimates for storage volume and peak discharge rates were adjusted.

Results and Discussion

Single Event

As expected, the distribution of the water budget for both models is greatly biased toward infiltration, followed by orifice outflow, then overflow (i.e., GSWI bypass flow).

Table 5. Calculated values derived using the PWD (2009) equations to represent GSWI for the single-event simulation.

Description	Units	Variable	Equation	Values
Baseline Subbasin Area	acres	A	Extracted From SWMM5 Input File	200
Baseline Percent Impervious Area	percent	PI	Extracted From SWMM5 Input File	25%
Percent of GSWI Implementation	percent	X	User Defined	50%
Loading Ratio	acres/acres	R	User Defined	15:1
Capture Volume	inches	CV	User Defined	1
Saturated Hydraulic Conductivity	inches/hour	K_{SAT}	User Defined	0.5
Drawdown Time for Slow Release Orifice	hours	T	User Defined	24
Maximum Height of Storage Prior to Overflow	feet	H_W	User Defined	5
Submerged Orifice Discharge Coefficient	dimensionless	C_D	User Defined	0.65
Total GSWI Controlled Area	acres	$(I_C + P_C)$	$I_0 * X$	25
Percent Impervious Controlled	percent	PI_C	$100 * (I_C)/(I_C + P_C)$	94%
GSWI Orifice Diameter (ft)	feet	D_O	$(4*(A_O)/\pi)^{(1/2)}$	0.76
GSWI Surface Depression Storage	inches	D_C	$V_I/[(P_C) * (43{,}560 \text{ sqft/ac})/(12 \text{ in/ft})]$	9.8
GSWI Storage Node Surface Area	square feet	A_N	$(V_{TR})/(H_W)$	3,403
Total Area Not Controlled	acres	TA_{NC}	$(I_{NC} + P_0)$	175
Percent Impervious Uncontrolled	percent	PI_{NC}	$100 * (I_{NC})/(TA_{NC})$	14%
Impervious Area Not Controlled	acres	I_{NC}	$I_0 - P_C - I_C$	25
Baseline Impervious Area	acres	I_0	$A * (PI/100)$	50
Average Release Rate for GSWI Storage Node	cfs/acre	Q_{AVE}	$[(CV)/(24 \text{ hrs})] * (43{,}560 \text{ sqft/ac})/[(12 \text{ in/ft}) * (3600 \text{ sec/hr})]$	0.11
Peak Controlled Release Rate for GSWI Storage Node	cfs/acre	Q_{PEAK}	$2 * (Q_{AVE})$	0.21
Baseline Pervious Area	acres	P_0	$A - I_0$	150
Bottom Area of GSWI Control	acres	P_C	$(I_C + P_C)/R$	1.6
GSWI Controlled Impervious Area	acres	I_C	$P_C * R$	23.4
GSWI Time Dependent Infiltration	cubic feet	TDI	$(P_C) * (K_{SAT}) * (T) * (43{,}560 \text{ sqft/ac})/(12 \text{ in/ft})$	68,063
Total Capture Volume	cubic feet	CV_T	$(CV) * (I_C) *(43{,}560 \text{ sqft/ac})/(12 \text{ in/ft})$	85,078
Area of GSWI Storage Node Orifice	square feet	A_O	$(Q_{PEAK}) * (I_C)/[C_D * [(2) * (g) * (H_W)]^{(1/2)}]$	0.5
GSWI Infiltration Volume	cubic feet	V_I	Minimum (CV_T, TDI)	68,063
GSWI Storage Volume	cubic feet	V_{TR}	$CV_T - V_I$	17,016

Table 6. Calculated values to represent GSWI using S5IT for the single-event simulation.

Description	Units	Variable	Equation	Values
Baseline Subbasin Area	acres	A	Extracted From SWMM5 Input File	200
Baseline Percent Impervious Area	percent	PI	Extracted From SWMM5 Input File	25%
Percent of GSWI Implementation	percent	X	User Defined	50%
Loading Ratio	acres/acres	R	User Defined	15:1
Capture Volume	inches	CV	User Defined	1
Surface Storage Depth	inches	SS_D	User Defined	0.000001
Percent of Surface Slope	percent	SS	User Defined	5%
Vegetation Volume Fraction	dimonsionless	VVF	User Defined	0
Surface Roughness	dimonsionless	SR	User Defined	0.1
Hydraulic Conductivity	inches/hour	HC	User Defined	0.5
Drain Exponent	dimonsionless	D_E	User Defined	0.5
GSWI Surface Area	acres	P_C	User Defined	1.6
Desired Peak Release Rate	inches/hour	q	User Defined	3.0
Drain Exponent	dimensionless	n	User Defined	0.5
Void Ratio	dimonsionless	VR	Default	0.75
Clogging Factor	dimonsionless	CF	Default	0
Porosity	dimonsionless	P	VR / (1 + VR)	0.4
Media Storage Depth	inches	SD_M	(12 in/ft) * V_{TR} / [P_c * (43,560 sqft/ac)]	2.9
Media Storage Depth with Voids	inches	SD_{MV}	SD_M / P	6.7
Total Storage Unit Height	inches	H_{TR}	SD_{MV} + D_{OH}	34
Drain Coefficient	inches/hour	C	q / (H_{TR} - D_{OH})^n	1.2
GSWI Storage Volume	cubic feet	V_{TR}	CV_T - V_I	17,016
Total Capture Volume	cubic feet	CV_T	(CV) * (I_C) *(43,560 sqft/ac)/(12 in/ft)	85,078
GSWI Infiltration Volume	cubic feet	V_I	Minimum (CV_T, TDI)	68,063
GSWI Infiltration Depth	inches	V_{ID}	12 * VI/(Pc * 43,560)	12
GSWI Infiltration Depth with Voids	inches	V_{IDV}	V_{ID} / VR	27
Drain Offset Height	inches	D_{OH}	V_{ID} / VR	27

A review of the timeseries presented as Figure 3 shows the timing of peak flow rates is comparable. A discrepancy is apparent in the timeseries output of the recession limb representing the storage volume. The S5IT method drains the storage volume more quickly than the PWD (2009) method. This discrepancy is a result of the process elements organization within the S5IT method. The storage and infiltration processes are layered together and therefore synergistically affect the storage volume discharge. Conversely, the PWD (2009) organizes the fundamental processes to run in series, allowing for only the storage depth of runoff to affect discharge from the unit. However, both methods drain the stored volume within the required 24-hour period.

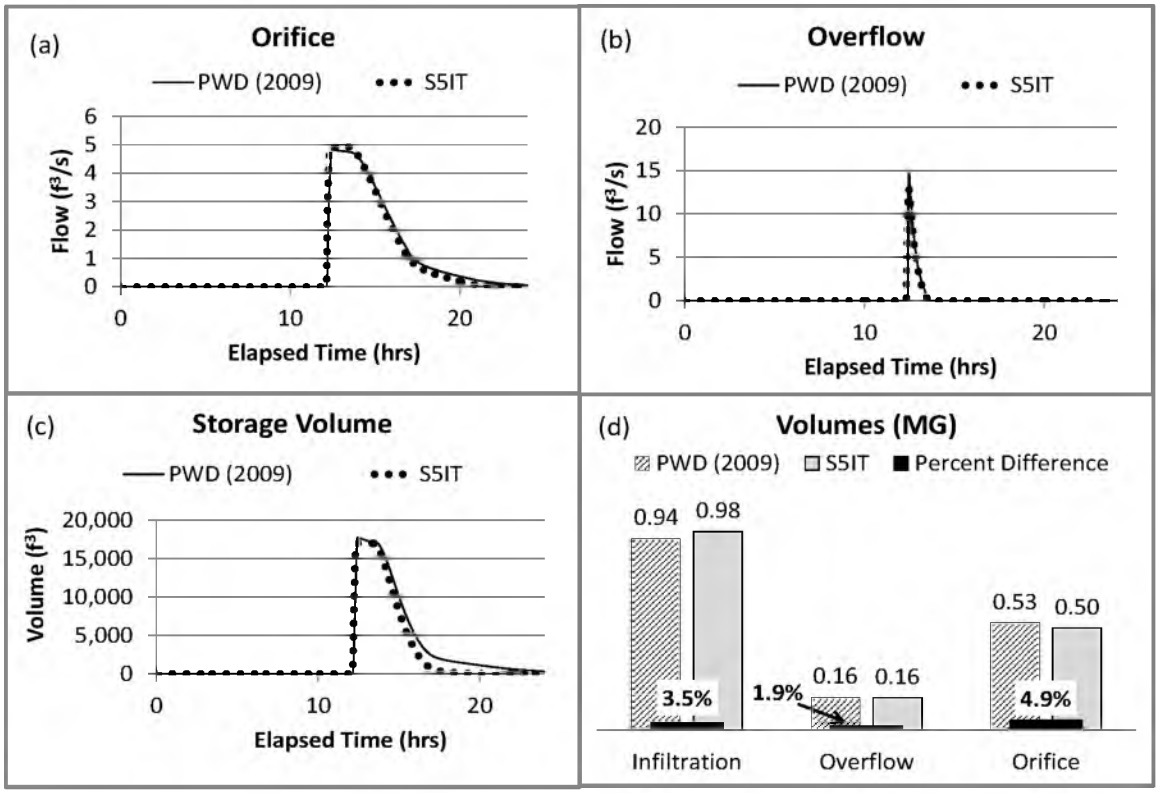

Figure 3. Comparison of the PWD (2009) algorithm and S5IT timeseries output for the orifice (a), overflow (b), and storage volumes (c). Volume results are presented for infiltration, overflow, and orifice elements (d).

Long-Term Continuous Simulations

Similar result biases are present with the long-term continuous simulations (Table 7). The water budget again shows the greatest amount of stormwater runoff volume being infiltrated. The majority of the remaining volume is managed through a slow release orifice and very little of the stormwater runoff volume bypasses the GSWI in both models. As the total volume of precipitation increases from TS1 up to TS4, both models show a gradual shift in the allocation of stormwater volume. The volume of stormwater infiltrating decreases and the volume of water being routed through the slow release orifice increases. The reason for this is that the soil reached its saturated state. As more runoff occurred, it is managed through the hydraulic elements of the system established to meet the performance criteria. Notably, the estimated volume bypassing the GSWI for both models becomes more consistent as precipitation depth increases. This result indicates that while each model has some variation in estimates for internal processes, the overall estimated management of stormwater through the GSWI from both methods is comparable. For all simulations, the PWD (2009) estimates a larger volume of infiltrated stormwater as compared to the S5IT output. Subsequently, the PWD (2009) model estimates a smaller value of stormwater volume being routed through the orifice. The divergence between the estimates for infiltrated volume and orifice discharge increases with increased precipitation depth. The infiltration estimates differ by 4 percentage points for the TS1 timeseries and up to 12 percentage points for the TS4 timeseries. This discrepancy is translated to the orifice discharge estimates.

Table 7. Results from each long-term continuous simulation. The percent of total represents the allocation of stormwater volume through each model's GSWI components.

Component	Rainfall	Volume (MG)		Percent of Total Volume	
		PWD (2009)	*S5IT*	*PWD (2009)*	*S5IT*
Infiltration	TS1	98	95	95.3%	91.8%
	TS2	123	112	95.2%	86.8%
	TS3	143	126	92.3%	81.6%
	TS4	208	175	76.7%	64.5%
Overflow	TS1	0.6	0.1	0.6%	0.1%
	TS2	0.6	0.3	0.4%	0.3%
	TS3	0.7	0.6	0.4%	0.4%
	TS4	2.0	1.8	0.7%	0.7%
Orifice	TS1	4	8	4.1%	8.0%
	TS2	6	17	4.4%	13.0%
	TS3	11	28	7.2%	18.0%
	TS4	61	94	22.6%	34.8%

Conclusions

This study compared the hydrologic output from a model representing GSWI built using the PWD (2009) algorithm to the hydrologic output using the SWMM5 GSWI module representing an infiltration trench (S5IT). The intent of the project was to determine if the collective benefit from a lumped representation of GSWI was comparable to the benefit estimated using the design-specific representation available within the SWMM5 LID module. The models were built to capture the same volume of runoff for the same contributing area produced from an SCS Type II 24-hour, 25-Year design storm and long-term continuous precipitation data from the National Climatic Data Center Salt Lake City Airport raingage.

In terms of precision between the two models, the results for the single event simulations showed comparable output results. The error for the single event simulations between the two methods was within an error tolerance of ±5%. The bias toward infiltration for both sets of simulations representing GSWI was apparent, ranging from 95% to 65%. The volume of stormwater that bypassed the GSWI systems represented the smallest volume at less than 1% of total runoff volume. When comparing the long-term continuous results, the PWD (2009) model estimated a larger fraction of infiltrated stormwater runoff volume (percent differences ranging from 4% up to 12%) and resulted in a smaller volume of stormwater routed through the orifice, as compared to the S5IT. The volume of overflow, however, remained relatively constant. These results indicate that if the modeling objective is to estimate the collective benefit of GSWI systems, then differences in fundamental process outputs (i.e., infiltration, storage, and discharge) between the models are not as critical. Both models can comparably achieve the over-

arching goal of estimating total volume reduction from the combined use of the fundamental processes. Also, this work indicates that knowing the specific type of GSWI to be implemented is not essential to estimating the collective benefits sought by implementing GSWI from a watershed-scale perspective.

As both models are only predicting estimated values, it is important to remember that this is not a test of validity with respect to observed data. While the results from this research lend support to the overall study hypothesis being correct, more simulations with multiple subcatchments would increase the credibility of these statements. With this study, a single urban subcatchment was simulated with a large portion of its impervious surface managed by GSWI. Subsequent studies should be done using a similar approach with an urban watershed model containing multiple subcatchments. It is also important to mention that both models simulated herein did not assess the spatial location of GSWI within the subcatchment. They were modeled as a lumped system for both the PWD (2009) and S5IT representations. Future studies should include a spatial component to determine how placing these systems throughout a watershed may affect the hydrologic responses, and thus the collective benefit, between each GSWI model representation.

CHAPTER III

IDENTIFYING THE EFFECT FROM SPATIAL DISTRIBUTION PATTERNS OF GREEN STORMWATER INFRASTRUCTURE

We addressed the issue of identifying potential differences in hydrologic response estimates produced from varying spatial patterns of watershed-scale green stormwater infrastructure (GSWI) networks. Simulated hydrologic response output from targeted distributions of GSWI was compared to uniformly distributed GSWI output. Our test methods included: 1) create models with targeted GSWI implementation (30 target scenarios) and a uniform GSWI distribution within the Salt Lake City, Utah watershed, 2) simulate all scenarios using a long-term rainfall record for the region (21 years, 1990-2010), and 3) apply t-test statistical test to the results to determine the significance of variation between the scenario results. Targeted distribution scenarios presented statistically comparable results for average flow, peak discharge, and volume as compared to uniform distribution outputs. However, variations in peak flows were observed in the simulated output that could influence the use of targeted distribution versus uniform distribution in modeling these systems, depending on the modeling objective(s).

Background

Green stormwater infrastructure (GSWI) has become a primary mechanism for mitigating increased stormwater runoff volume and peak discharges within many urban areas experiencing substantial growth (NRDC 2011). Conceptually, GSWI disconnects the impervious surfaces that drain directly to sewer inlets (e.g., sidewalks, roads, rooftops, etc.). Functionally, GSWI intercept stormwater runoff and detain it through some combination of infiltration, storage, and slow release (U.S. EPA 2000). GSWI is ideal for the urban environment because of the flexibility in placement options throughout the watershed and ability to manage stormwater runoff at relatively small spatial footprints (Benedict and McMahon 2002). A number of site-scale case study and pilot project implementation studies exists documenting GSWI performance (Booth et al. 1996; U.S. EPA 2006; Pitt et al. 2010; Carson et al. 2013; Pitt et al. 2013). Much of this effort has been informed by the Prince George's District's 1999 report, a comprehensive guidance document for analyzing and implementing GSWI within urban watersheds (PGC 1999). Notably, this document considered mainly East Coast environments, with arid and semi-arid climates remaining under-researched. Subsequently, the Urban Drainage and Flood Control District of Denver (UDFCD) developed an extensive regulatory document for stormwater management focused on GSWI methods and technologies (UDFCD 2011). However, the UDFCD is not alone in this rite, as many regulatory and guidance documents exist to aide in the planning, design, and implementation of GSWI within a variety of climate regions (UDFCD 2011; U.S. EPA 2014; PWD 2014).

The purported benefits and measured performance has encouraged the creation of

detailed implementation plans to distribute GSWI watershed-wide to control stormwater runoff. U.S. EPA's establishment of the National Pollutant Discharge Elimination System (NPDES) stormwater management program and inherent requirements has motivated municipalities across the country to apply the GSWI paradigm to develop mitigation strategies come into compliance with the regulations (U.S. EPA 2014). The National Resource Defense Council (NRDC) produced a report titled Rooftops to Rivers, which intended to serve as a review document highlighting GSWI management plans in urban areas (NRDC 2006; NRDC 2011). The document presented nine metropolitan areas in which GSWI oriented watershed management plans were successfully implemented. A follow-up report issued in 2011 included case studies for 14 metropolitan areas. The NRDC lists of urban metropolis areas are only a few among a larger number of other major urban city centers that have adopted and are successfully implementing GSWI (e.g., CTDEP 2004; Spicer Group 2008; PWD 2009; U.S. EPA 2010; Wang et al. 2010; MMSD 2011; Struck et al. 2012; Baughman et al. 2013; Nickel et al. 2014).

Although the popularity of GSWI has been steadily increasing and the technology for simulating these systems at the individual site level has been well established, the complexity of representing individual GSWI site characteristics at the watershed-scale remains problematic (Roy et al. 2008; Bach et al. 2014). Existing models that attempt to simulate GSWI networks are in their infancy, as well as the interface provided by models attempting to replicate type-specific GSWI. This has the potential to inaccurately estimate the collective performance of GSWI at the watershed-scale (Yeo and Guldmann 2010). Furthermore, there is a dearth of observed data for watershed-scale GWSI networks to support the assumption that a collective benefit from site-scale GSWI exists

(Roy et al. 2008). Thus, estimates of performance from simulated networks cannot yet be validated by observations. Until observations can be collected and evaluated, research has focused on improving the modeling methodology and technology. Recent publications replicated the complex nature of GSWI's infiltration and storage capabilities by developing either GSWI modules within existing modeling software (e.g., Rossman 2010) or stand-alone software and tools (e.g., Lee et al. 2009; Damodaram et al. 2010; Strecker et al. 2010; WERF 2012; Eric et al. 2013; Jayasooriya 2014). Complex models have been developed that include algorithms attempting to spatially optimize placement of type-specific GSWI (Lee et al. 2012). The complexity and system requirements of models with this detail, however, prevent it from being widely used within the water resources modeling community. Similar decision support models have been developed that serve as a supplemental results check to the more robust numerical models (e.g., Osmond et al. 1995; U.S. EPA 2013; Jayasooriya 2014). Thus, these models are not suited for watershed-wide analyses and research into up-scaling of site-specific GSWI continues to be a necessity.

Improvements to modeling technology for GSWI networks would be enabled through a better understanding of how simulated watershed-wide performance is affected by spatial. While research exists documenting the effect from varying spatial representation in watershed-scale models for urban hydrologic response without GSWI (Park et al. 2008; Bormann et al. 2009; Ghosh and Hellweger 2012), little research has been conducted to expand this concept to include GSWI. GSWI spatial distribution studies are especially limited and have not specifically addressed the issue of comparing varied distribution scenarios (Kertesz et al. 2007; James et al. 2012).

Existing literature has focused mainly on using design-specific applications of GSWI for both site-scale and watershed-scale evaluations. This approach requires input data that limit the assessment of GSWI practices within an urban environment and its applicability. Furthermore, design-level details may be unnecessary if the modeling objective is to meet watershed-scale performance criteria through some combination of GSWI types, the combination of which having not yet been defined at the planning stage. From this perspective, a combination of GSWI types is assumed to be designed and functioning to meet a standard watershed-wide performance measure. A collective representation of fundamental GSWI processes can relieve input data issues for these types of modeling objectives. Smullen et al. (2008) presented an alternative planning-level methodology to represent GSWI within a watershed-scale planning model for the City of Philadelphia, with greater details of this approach provided by the Philadelphia Water Department (PWD, 2009). The PWD (2009) up-scaling methodology for GSWI systems provides a preferable, collective representation of GSWI, such that the results would not be biased toward any given design type of GSWI, thus allowing any differences to be solely attributed to GSWI spatial distribution and aggregation impacts.

The first objective of the current study uses the PWD (2009) algorithm to evaluate output for the following sensitivity studies: 1) targeted GSWI implementation versus uniformly distributed GSWI scenarios. Conclusions derived from the results of the analysis will provide stormwater planning engineers with practical advice on creating and simulating GSWI networks at the watershed-scale. Furthermore, the content will add to the knowledge base for simulating networks of GSWI within urban area planning models.

Materials and Methods

Stormwater Management Model Version 5

Originally developed in 1971, the Stormwater Management Model Version 5.0.022 (SWMM5) model is a coupled hydrologic-hydraulic model. Calculations are based on physical processes and utilize the concepts of conservation of mass, energy, and momentum to estimate hydrologic and hydraulic responses to input datasets (U.S. EPA 2010). Because SWMM5 is a coupled hydrologic-hydraulic model, it allows the user to adjust both the surface parameters and the underlying sewer characteristics within the same model. SWMM5 compartmentalizes its computations based on the following physically based processes:

- Surface Runoff
- Groundwater
- Flow Routing
- Water Quality Routing
- Infiltration
- Snowmelt
- Surface Ponding
- LID Representation

Not all of the above processes are necessary to build a model and perform simulations. For this study, the surface runoff, flow routing, and infiltration processes are used to analyze the hypothesis and objectives. Details of these processes may be found in Rossman (2010).

Salt Lake City, Utah Model Setup

The 57-mi^2 Salt Lake City, Utah (SLC) model extended to the Wasatch Front mountain range and the western boundary was established as the Jordan River. Topography varies greatly within the area's bounds, due to the steep, canyon slopes that

characterize the eastern portion, which transition quickly to the valley floor, where the largest concentration of the population exists. Physical characteristics of the SLC model varied greatly due to the complex topography, heterogeneous soil composition, and urban density. The subcatchments were delineated using 2010 U.S. Census data and ranged in size from 17 - 6,020 acres. With census-driven delineation, smaller subcatchments represent more densely populated, urban areas.

The surface slope was estimated using Google Earth Elevation Profile capabilities. Line segments were drawn over areas where the land surface was similar. The average slope value, as calculated by Google Earth, was used within the model for the relevant subcatchments. Slope values for this region range from 0.5% (i.e., the valley) up to 24.5% (i.e., canyons) and the average slope is approximately 3.2%.

The soil and infiltration values were based on an analysis of NRCS Soil Data for the region. Soils in the region were established as varying textures of loam. These texture classifications were cross-referenced with the associated Green-Ampt parameters to establish relative infiltration performance for the areas (Table 8). Area weighted averages of all soil types, and thus Green-Ampt parameters, contained within each subcatchment were calculated and used within the SLC model.

The relative area for residential, commercial, and open space, parks or public areas for each subcatchment were used to establish the relative percent of impervious area. The corresponding area of each land use type was multiplied by the estimated percent impervious as defined by The Salt Lake County Water Quality Stewardship Plan (Table 9). Percent impervious for the subcatchments ranged from a minimum of 13% up to a maximum of 79%, with the highest values located in the valley.

Table 8. Green-Ampt infiltration parameters based on texture descriptions (adapted from The Hydrology Handbook, D.R. Maidment, Editor in Chief, McGraw-Hill, Inc., 1993, pp. 5.1 – 5.39).

Soil Texture Classification	Suction (inches)	Hydraulic Conductivity (inches/hour)	Soil Moisture Deficit (SMD)
Loamy Sand	2.41	2.35	0.312
Sandy Loam	4.33	0.86	0.246
Loam	3.5	0.52	0.193
Silt Loam	6.57	0.27	0.171
Sandy Clay Loam	8.60	0.12	0.143
Silty Clay Loam	10.75	0.08	0.105

Table 9. Estimated percent impervious values used to estimate the area weighted average percent of impervious surface in the Salt Lake City, Utah model (data adapted from SLCo, (2009)).

Type	Percent Impervious
Residential	32%
Commercial	79%
Open Space/ Parks	12%

The depression storage and surface roughness values were kept at the SWMM5 default values with the exception of the areas listed in Table 10. These areas were either canyon areas or considered to have a surface type that required a higher surface roughness and depression storage value due to the proximity to the canyon areas.

The directly connected impervious areas for the SLC model were represented indirectly by routing a portion of all runoff to pervious areas. The percentage of the surface runoff from impervious area routed to pervious areas was set to 70% for all subcatchments that were not canyon areas.

Table 10. Modified surface depression and runoff values for canyon areas and adjacent subcatchments.

Subcatchment	N-Imperv	N-Perv	S-Imperv	S-Perv
10%C/I_52	0.01	0.8	0.05	2
10%Res_10	0.01	0.8	0.05	2
Nat_54	0.01	0.8	0.05	2
Nat_55	0.01	0.8	0.05	2
38%C/I_44	0.01	0.4	0.05	1
4%Res_53	0.01	0.4	0.05	1
60%Res_5	0.01	0.4	0.05	1
80%Res_37	0.01	0.4	0.05	1
All Others	0.01	0.25	0.05	0.25

For canyon areas, the final routing percentage was set high at 90%. It was assumed that for these areas, the majority of the runoff generated by impervious areas would be intercepted by a pervious surface. Surface runoff was collected by storm sewer inlets and routed through subsurface pipes and, ultimately, discharged into the Jordan River. The untreated runoff received by the Jordan River terminated in the Great Salt Lake, located north of the City. The model mimicked this routing using 49 pipe segments, 48 junctions, and a free outfall. As this study is concerned with hydrologic influences, large pipe diameters were established to insured unrestricted flow through the system.

Precipitation

The single-event simulations used the September 16, 2006 storm event with a total precipitation volume of 1.54 inches. All long-term continuous simulations used data for the years 1990 up to 2010 and were collected from the National Climatic Data Center Salt Lake International Airport rain gage (gage #427598). The distribution of

precipitation events for this rain gage is presented with Figure 4. The 95th percentile storm event was determined to be 0.65 inches, which was used to size all GSWI units for all scenarios.

GSWI Representation

The PWD (2009) up-scaling algorithm was used to represent GSWI for all model scenarios. The fundamental processes that simulate runoff routing through a GSWI unit, as represented in the PWD (2009) algorithm, are: infiltration, storage with slow release through a control orifice, and GSWI unit bypass (Figure 1). The elements representing these processes are created using a collection of equations presented within PWD (2009).

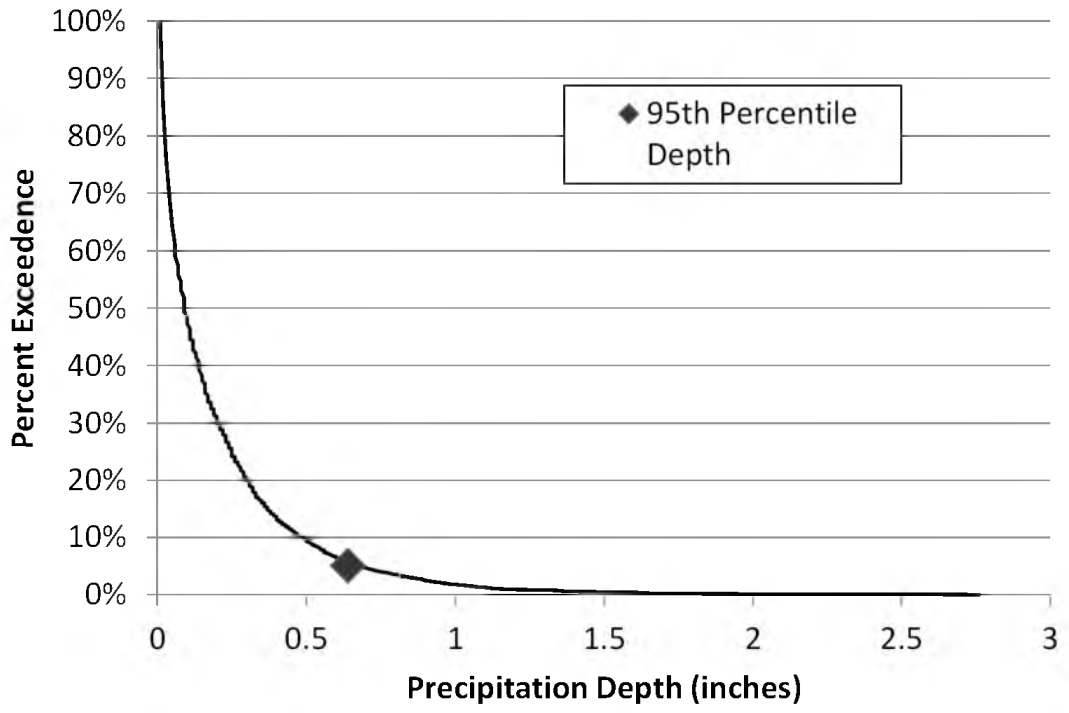

Figure 4. Salt Lake City International Airport Precipitation distribution for 1990-2010. Red marker shows the 95th percentile precipitation value of 0.65 inches.

The level of GSWI implementation and performance criteria were kept constant across all modeling scenarios. The percent implementation of GSWI was equal to 37% of total impervious area across all simulations. This value was determined through a sensitivity analysis for the SLC model and level of GSWI implementation. Through this analysis, it was determined that 37% of GSWI implementation is the level at which the difference in hydrologic response becomes statistically different from baseline (no GSWI implementation) conditions. The details of the analysis are included as Appendix C. The loading ratio defining the number of impervious acres loading to 1 GSWI acre was kept constant at 10.7:1. Runoff stored within the GSWI units had a drawdown requirement of 24 hours for all simulations.

Simulations were run with a routing timestep of 30 seconds, a wet timestep of 1 minute, a dry timestep of 1 hour, and a reporting timestep of 15 minutes. All simulations were run with dynamic wave flow routing equations. All simulations were quality checked by checking for and fixing system flooding and constraining continuity errors within ± 5%.

Two sets of modeling scenarios were simulated for this study: 1) uniform distribution of GSWI and 2) targeted distribution of GSWI. The target implementation of GSWI, referring to the total amount of impervious area managed by GSWI, was established as 4,229.5 acres.

Salt Lake City, Utah

The spatial distribution objective was evaluated by comparing output from two types of GSWI distribution scenarios within the SLC model. The uniform distribution

placed GSWI throughout all subcatchments, while the targeted distribution placed GSWI within specific subcatchments (Figure 5). The latter approach used 30 different sets of subcatchments to evaluate hydrologic response differences to the uniform distribution scenario. The same impervious surface area of 4,229.5 acres was managed by GSWI for all scenarios (uniform and targeted). Therefore, targeted spatial distribution scenarios were constrained to achieve this minimum value of stormwater management. The density of GSWI within each targeted model varied based on the cumulative impervious area available (Table 11). For the uniform distribution, the total impervious area from all subcatchments was available for management.

For the targeted scenarios, only the impervious area within the selected subcatchments was available for management. To appropriately compare the results, the same amount of impervious area managed with the uniform distribution scenario must be managed within each of the targeted scenarios. The targeted scenarios were created to meet this requirement (Table 11). The number of subcatchments where GSWI could be implemented for all targeted scenarios was limited to 30 (from the 54 subcatchments that represent the entire area within the model). In doing so, the available impervious area differed between each targeted scenario based on the impervious area within each of the individual subcatchments. Thus, the percent of GSWI implementation for each targeted scenario also varied (Table 11).

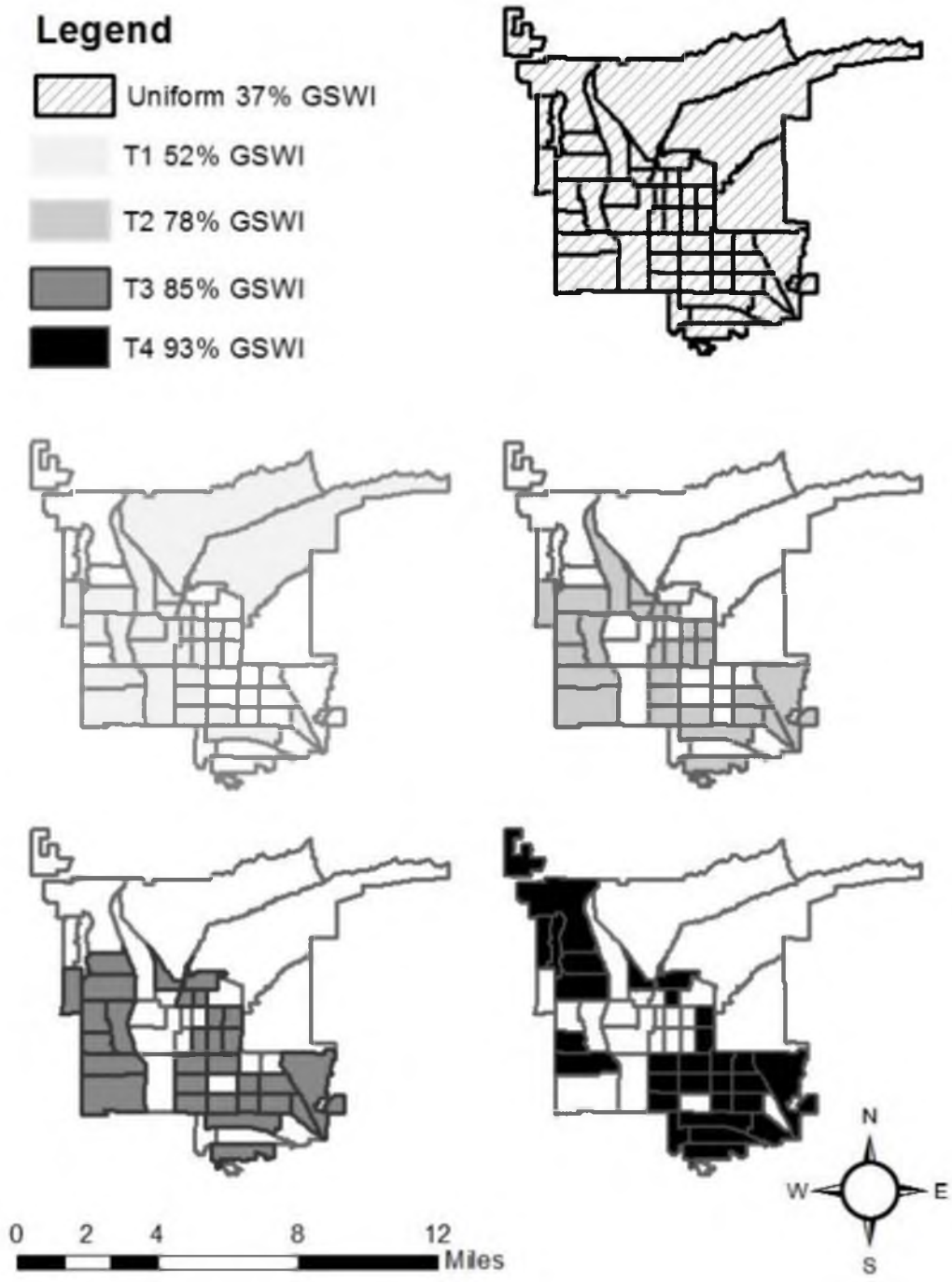

Figure 5. The uniform distribution scenario had GSWI in all subcatchments (top figure). Examples of four targeted distributions simulated where GSWI was implemented within the shaded subcatchments only (bottom four figures). Darker shading indicates a higher density of GSWI implemented within the selected subcatchments.

Table 11. Impervious area managed for each scenario and the equivalent percent of impervious area controlled relative to the number of sheds receiving GSWI.

Simulation	Percent Implementation	Impervious Area Controlled	Total Impervious Area Available to Control (acres)
Uniform	37	4,229.50	11,431
Targeted 01	52.44	4,229.38	8,065
Targeted 02	77.87	4,229.31	5,431
Targeted 03	92.64	4,229.65	4,566
Targeted 04	84.82	4,229.31	4,986
Targeted 05	60.87	4,229.52	6,948
Targeted 06	89.52	4,229.51	4,725
Targeted 07	86.39	4,229.31	4,896
Targeted 08	49.13	4,229.81	8,609
Targeted 09	48.46	4,229.16	8,727
Targeted 10	52.44	4,229.22	8,065
Targeted 11	66.76	4,229.38	6,335
Targeted 12	69.49	4,229.65	6,087
Targeted 13	72.01	4,229.20	5,873
Targeted 14	52.65	4,229.78	8,034
Targeted 15	58.28	4,229.72	7,258
Targeted 16	55.79	4,229.33	7,581
Targeted 17	61.22	4,229.14	6,908
Targeted 18	52.11	4,229.19	8,116
Targeted 19	48.87	4,229.74	8,655
Targeted 20	64.06	4,229.58	6,603
Targeted 21	52.68	4,229.66	8,029
Targeted 22	52.47	4,229.85	8,061
Targeted 23	59.23	4,229.39	7,141
Targeted 24	53.95	4,229.44	7,840
Targeted 25	58.24	4,229.16	7,262
Targeted 26	53.9	4,229.14	7,846
Targeted 27	50.68	4,229.41	8,345
Targeted 28	52.28	4,229.32	8,090
Targeted 29	71.24	4,229.75	5,937
Targeted 30	73.57	4,229.40	5,749

Results and Discussion

Hydrologic Simulations

Scatter plots of the annual data for each targeted scenario output compared against the annual uniform scenario output show discrepancies to all runoff characteristics (Figure 6). There is variance in the average flow and volume estimates, with a slight tendency to reduced values, although this is hardly noticeable. The greatest variation is within the peak flow value comparisons. There is a definite increase in the majority of peak flow values from the targeted scenarios as compared to the uniform scenario peak flow values. To further this point, Figure 7 presents the scatter plots for the 10-year average values for each scenario plotted by percent implementation. Again, variation exists for average volume and average flow values and a slight tendency toward lower average values, but without an obvious bias. The 10-year average peak flow values, however, show the same positive correlation to increased peak flow estimates for the targeted scenarios as percent implementation increases. This is while the impervious area managed remains constant among all scenarios, suggesting that peak flow estimates are sensitive to increased density of GSWI in subcatchments.

A review of an event hydrograph produced from an event occurring on September 16, 2006 (total depth = 1.54 inches) shows the time to peak for all scenario sets are a close match (Figure 8). As expected, there is a noticeable difference between peak discharge values. The uniform distribution peak discharge of 90 cubic feet per second (cfs) is lower than most other targeted scenarios. By comparison to the targeted scenarios' output, the uniform distribution appears to dampen the peak discharge estimate.

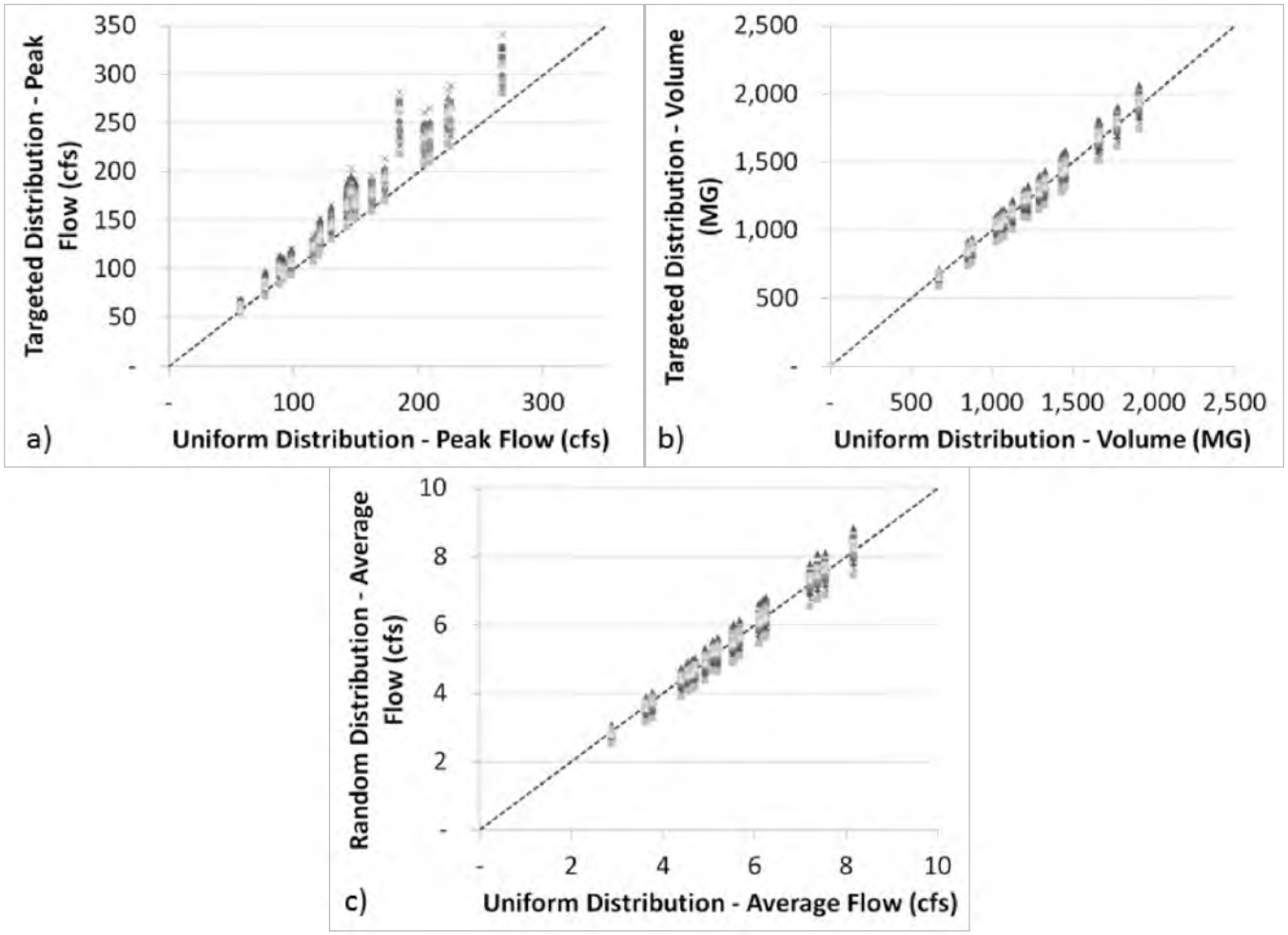

Figure 6. Scatter plots of the annual targeted distributions' results compared versus annual uniform distribution scenario output. The metrics compared are peak discharge (a), volume (b), and average flow rate (c). Only minor discrepancies are shown with the peak discharge being slightly greater for the targeted scenarios.

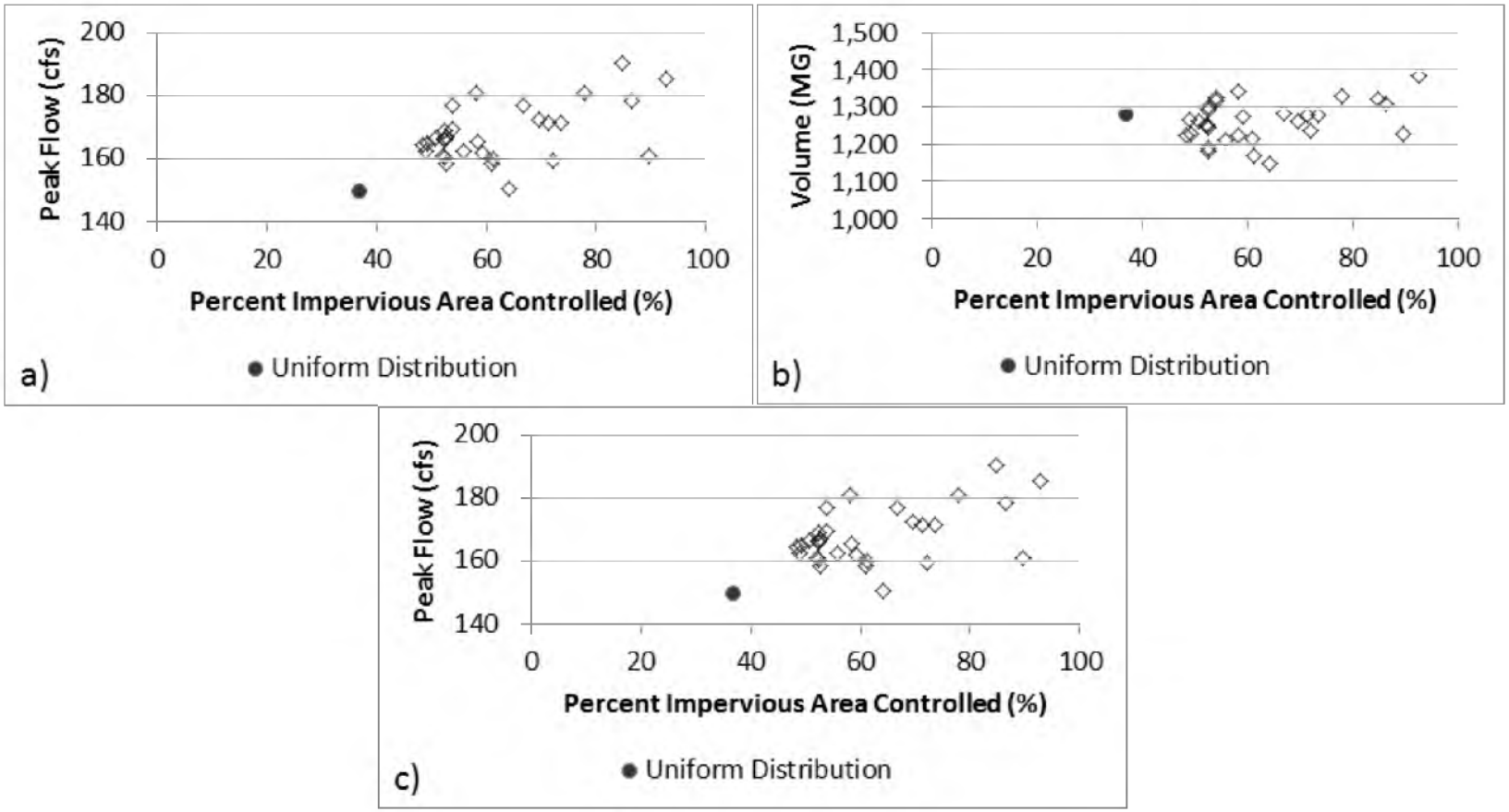

Figure 7. Scatter plot of 10-Year averaged output for all scenarios. The uniform distribution values are identified with the circular marker for peak discharge (a), volume (b), and average flow rate (c).

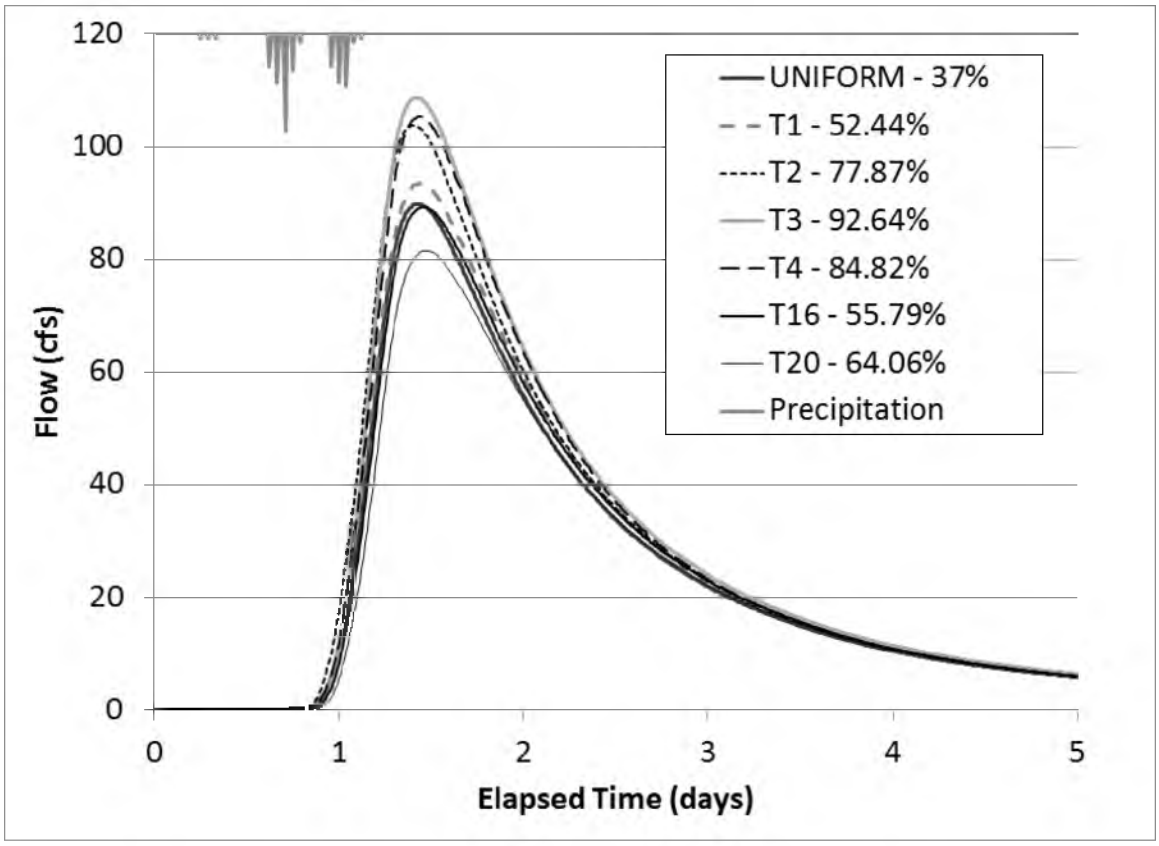

Figure 8. Hydrographs produced from the September 16, 2006 event for selected spatial distribution scenarios. The peak discharge timing is very closely correlated for all simulations. There is variation with the peak discharge estimates, with the majority of scenarios showing increases, although there are a few targeted scenarios with reduced peak discharges, as is presented in this event hydrograph for T20.

Intuitively, this is expected because the GSWI presence in all subcatchments will shave the peak discharge from all subcatchments. When implementing GSWI only in selected subcatchments for the targeted simulations, some subcatchments will be unaffected by GSWI and thus the dampening effect is reduced. Simulations performed using smaller subcatchment areas are necessary to assess the influence of spatial patterns to supplement these results in order to form a more comprehensive conclusion.

Statistical Analysis

A summary of the descriptive statistics for each scenario (uniform and targeted) are presented in Table 12. These statistics do not present any obvious bias or divergence within the results. Mean values for the average flows are within the five to six cfs range, while the peak flows vary a bit more within the 150-190 cfs range. The volumes are approximately within the 1,150 – 1,320 MG range.

Test for Normality

To ensure that the datasets were normally distributed, the average flow output from all targeted scenario results were evaluated for normalcy (n = 630). For the purposes of this evaluation, it was assumed that if the average flow datasets were normally distributed, the subsequent output (i.e., volume and peak flow) would also be normally distributed. Histograms were created based on six bins sized using the maximum and minimum values for each runoff characteristic (Figure 9). If the majority of data was grouped into the middle of the histogram, it was considered to be normally distributed. A review of the histogram in Figure 9 satisfied the criteria for normal distribution.

Test for Equal Variances

Testing for equal variances allows for the appropriate variation of significance test equations to be identified and then applied to the sample sets. The comparison was conducted for the uniform distribution average flow dataset and the average flow values for the targeted scenarios. For the variances to be considered statistically equal, the F-distribution statistic should be near 1.0 and the p-value should be near 0.5.

Table 12. Spatial distribution scenario descriptive statistics for peak discharge, volume, and average flow rate.

Peak Flow (cfs)								
Simulation	n	Mean	Standard Deviation	Standard Error	95% confidence		Minimum	Maximum
					Upper	Lower		
Uniform	21	150	54.91	3,015	173.03	126.06	58	267
Targeted 01	21	166	64.55	4,166	194.10	138.89	61	299
Targeted 02	21	181	70.01	4,902	210.99	151.10	66	328
Targeted 03	21	185	69.03	4,766	214.93	155.88	69	327
Targeted 04	21	190	74.34	5,527	222.08	158.49	67	341
Targeted 05	21	158	61.64	3,799	184.62	131.90	59	290
Targeted 06	21	161	63.23	3,998	187.94	133.85	56	294
Targeted 07	21	179	67.66	4,578	207.48	149.60	64	316
Targeted 08	21	165	64.48	4,157	192.44	137.29	60	298
Targeted 09	21	164	64.26	4,129	191.63	136.66	59	298
Targeted 10	21	160	64.19	4,121	187.94	133.03	56	292
Targeted 11	21	177	70.39	4,954	206.84	146.63	61	317
Targeted 12	21	173	65.93	4,346	200.71	144.31	61	309
Targeted 13	21	159	61.41	3,771	185.52	132.99	58	293
Targeted 14	21	159	63.33	4,011	185.61	131.44	55	290
Targeted 15	21	166	66.20	4,382	193.86	137.24	57	299
Targeted 16	21	162	64.00	4,096	189.81	135.07	59	296
Targeted 17	21	160	63.68	4,055	186.99	132.52	56	296
Targeted 18	21	161	60.53	3,664	186.98	135.20	60	288
Targeted 19	21	163	61.97	3,841	189.11	136.10	61	289
Targeted 20	21	151	59.68	3,562	176.15	125.09	56	280
Targeted 21	21	167	61.80	3,819	193.09	140.22	63	288
Targeted 22	21	169	63.07	3,978	195.67	141.72	63	292
Targeted 23	21	162	61.56	3,790	188.17	135.51	59	280
Targeted 24	21	169	63.73	4,061	196.59	142.08	63	293
Targeted 25	21	181	69.42	4,820	210.59	151.21	65	314
Targeted 26	21	177	68.73	4,724	206.17	147.38	63	313
Targeted 27	21	167	65.12	4,241	194.44	138.73	59	296
Targeted 28	21	166	64.94	4,218	193.60	138.04	58	295
Targeted 29	21	171	69.36	4,811	200.86	141.53	59	310
Targeted 30	21	171	69.33	4,807	201.02	141.71	59	308

Table 12. Continued

Volume (MG)								
Simulation	n	Mean	Standard Deviation	Standard Error	95% confidence		Minimum	Maximum
					Upper	Lower		
Uniform	21	1,280	316.30	100,048	1,415	1,145	672	1,911
Targeted 01	21	1,244	320.62	102,800	1,381	1,107	633	1,885
Targeted 02	21	1,327	339.08	114,974	1,472	1,182	681	2,005
Targeted 03	21	1,383	345.08	119,083	1,530	1,235	716	2,066
Targeted 04	21	1,322	338.48	114,569	1,467	1,177	672	2,001
Targeted 05	21	1,216	309.22	95,615	1,348	1,083	630	1,833
Targeted 06	21	1,229	311.80	97,221	1,362	1,095	628	1,856
Targeted 07	21	1,307	331.26	109,732	1,449	1,166	667	1,965
Targeted 08	21	1,228	316.97	100,468	1,363	1,092	624	1,863
Targeted 09	21	1,225	316.13	99,935	1,360	1,089	623	1,859
Targeted 10	21	1,192	310.03	96,117	1,325	1,059	602	1,817
Targeted 11	21	1,284	333.08	110,942	1,427	1,142	650	1,955
Targeted 12	21	1,263	320.19	102,521	1,400	1,126	653	1,900
Targeted 13	21	1,237	311.95	97,315	1,370	1,103	641	1,861
Targeted 14	21	1,181	307.92	94,815	1,313	1,050	596	1,802
Targeted 15	21	1,225	316.99	100,486	1,361	1,089	621	1,863
Targeted 16	21	1,210	313.86	98,507	1,344	1,075	615	1,838
Targeted 17	21	1,168	305.43	93,286	1,298	1,037	592	1,783
Targeted 18	21	1,255	318.47	101,424	1,391	1,119	648	1,891
Targeted 19	21	1,264	317.37	100,723	1,400	1,128	658	1,893
Targeted 20	21	1,146	297.52	88,517	1,274	1,019	585	1,741
Targeted 21	21	1,293	324.51	105,305	1,432	1,155	670	1,937
Targeted 22	21	1,299	326.16	106,377	1,438	1,159	673	1,946
Targeted 23	21	1,276	317.59	100,861	1,412	1,140	663	1,909
Targeted 24	21	1,319	326.37	106,517	1,458	1,179	689	1,967
Targeted 25	21	1,344	338.46	114,558	1,489	1,199	692	2,018
Targeted 26	21	1,324	332.34	110,453	1,466	1,182	685	1,990
Targeted 27	21	1,263	319.33	101,974	1,399	1,126	650	1,902
Targeted 28	21	1,251	317.81	101,001	1,387	1,115	641	1,889
Targeted 29	21	1,279	325.98	106,260	1,419	1,140	654	1,938
Targeted 30	21	1,280	326.24	106,433	1,419	1,140	653	1,938

Table 12. Continued

Average Flow (cfs)								
Simulation	n	Mean	Standard Deviation	Standard Error	95% confidence		Minimum	Maximum
					Upper	Lower		
Uniform	21	5.50	1.36	1.86	6.08	4.92	2.88	8.15
Targeted 01	21	5.35	1.38	1.91	5.94	4.75	2.71	8.04
Targeted 02	21	5.70	1.46	2.14	6.33	5.08	2.91	8.55
Targeted 03	21	5.95	1.49	2.22	6.59	5.31	3.07	8.83
Targeted 04	21	5.68	1.46	2.13	6.31	5.06	2.87	8.53
Targeted 05	21	5.23	1.33	1.78	5.80	4.66	2.70	7.83
Targeted 06	21	5.28	1.35	1.81	5.86	4.71	2.69	7.92
Targeted 07	21	5.62	1.43	2.04	6.23	5.01	2.86	8.38
Targeted 08	21	5.28	1.37	1.87	5.86	4.69	2.67	7.96
Targeted 09	21	5.27	1.36	1.86	5.85	4.68	2.67	7.94
Targeted 10	21	5.12	1.34	1.79	5.70	4.55	2.57	7.75
Targeted 11	21	5.52	1.44	2.07	6.13	4.90	2.78	8.34
Targeted 12	21	5.43	1.38	1.91	6.02	4.84	2.80	8.12
Targeted 13	21	5.32	1.35	1.82	5.90	4.74	2.75	7.95
Targeted 14	21	5.08	1.33	1.77	5.65	4.51	2.55	7.69
Targeted 15	21	5.27	1.37	1.87	5.85	4.68	2.66	7.94
Targeted 16	21	5.20	1.35	1.83	5.78	4.62	2.63	7.84
Targeted 17	21	5.02	1.32	1.74	5.59	4.46	2.53	7.61
Targeted 18	21	5.40	1.37	1.89	5.98	4.81	2.77	8.07
Targeted 19	21	5.44	1.37	1.88	6.02	4.85	2.82	8.09
Targeted 20	21	4.93	1.29	1.65	5.48	4.38	2.51	7.44
Targeted 21	21	5.56	1.40	1.96	6.16	4.96	2.87	8.27
Targeted 22	21	5.58	1.41	1.98	6.19	4.98	2.88	8.31
Targeted 23	21	5.49	1.37	1.87	6.07	4.90	2.84	8.14
Targeted 24	21	5.67	1.41	1.99	6.27	5.07	2.95	8.40
Targeted 25	21	5.78	1.46	2.14	6.40	5.15	2.96	8.62
Targeted 26	21	5.69	1.43	2.06	6.31	5.08	2.93	8.49
Targeted 27	21	5.43	1.38	1.90	6.02	4.84	2.78	8.12
Targeted 28	21	5.38	1.37	1.88	5.96	4.79	2.74	8.06
Targeted 29	21	5.50	1.41	1.98	6.10	4.90	2.80	8.27
Targeted 30	21	5.50	1.41	1.98	6.10	4.90	2.79	8.26

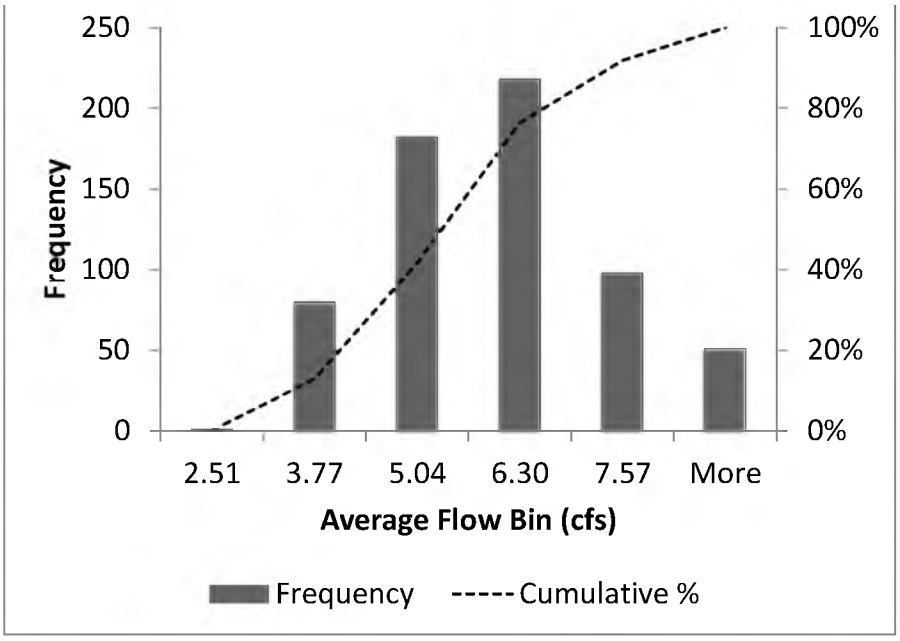

Figure 9. Histogram of average flow data points (n = 630) produced from the targeted scenarios. The distribution represents a normal distribution of the data.

Based on these criteria and reviewing the results in Table 13, the results suggest the variances to be equal for average flow and volume results. The peak flow datasets have unequal variances. Thus, for the average flow and volume datasets, the equal variances approach will be used, while the unequal variances equations will be applied to the peak flow result dataset.

T-Test

The t-test results showed the targeted distribution means were not statistically different with respect to any of the hydrologic metrics as compared to the uniform distribution simulation. The values were calculated based on an alpha value = 0.05 and n = 31 observations (1 uniform distribution scenario and 30 targeted scenarios). To determine the statistical significance of the results, each hydrologic characteristic (i.e.,

Table 13. F-distribution values and results for the uniform distribution and averaged targeted scenario. Results are included for average flow, peak flow, and volume values. With an F-value near 1.0 and a p-value close to 0.5, the results show the variances to be equal for the average flow and volume metrics. The reverse is true for the peak flow metric.

Statistic	Average Flow (cfs)		Peak Flow (cfs)		Volume (MG)	
	Uniform	Targeted	Uniform	Targeted	Uniform	Targeted
Mean	5.50	5.42	150	1,261	1,280	1,261
Variance	1.86	1.92	3,015	103,153	100,048	103,153
Observations	21	21	21	21	21	21
Degrees of Freedom	20	20	20	20	20	20
F-statistic	0.967		0.029		0.970	
P(F<=f) one-tail	0.470		0.000		0.473	
F Critical one-tail	0.471		0.471		0.471	

average flow, peak flow, and volume) was evaluated using three statistical metrics: 1) The calculated t-statistic was compared against the t-critical value, 2) the confidence intervals were calculated, and 3) the calculated p-value was compared to the alpha value. For the means for the targeted scenarios to be statistically different from the mean of the uniform distribution results, the following criteria must be met:

1. The calculated t-statistic > the t-critical value (2.04);
2. The value of the null hypothesis (i.e., difference in means = 0) must fall outside the bounds of the confidence interval; and
3. The calculated p-value must be less than the alpha value (i.e., 0.05).

By all metrics, the targeted scenario means are not statistically different from the uniform distribution mean (Table 14).

Table 14. T-test results comparing the targeted scenario dataset means to the uniform dataset mean for average flow, peak flow, and volume estimates. The results show no statistically significant difference between the means (n=31, alpha = 0.05).

Statistic/Metric	Uniform - Flow	Targeted - Flow	Uniform - Peak	Targeted - Peak	Uniform - Volume	Targeted - Volume
Mean	5.50	5.42	149.55	167.96	1,280	1,261
Variance	1.86	1.92	3,015	4,270	100,048	103,293
Standard Deviation	1.36	1.39	54.91	65.25	316	321
Degrees of Freedom	29		29		29	
Pooled Variance	3.78		7,273		203,222	
t-Statistic (Calculated)	0.157		(0.836)		0.162	
P(T<=t) one-tail	0.427		0.164		0.424	
t Critical one-tail	2.04		2.04		2.04	
95% CI of difference in Means (lower bound)	-0.94		-63.33		-218.58	
95% CI of difference in Means (upper bound)	1.10		26.51		256.32	

Conclusions

The results show that varying spatial distribution has the greatest influence on peak discharge and, to a lesser degree, impacts the volume and average flow estimates. One of the purported benefits of GSWI is its ability to minimize peak runoff. Thus, our peak discharge results indicate spatial distribution of GSWI within a watershed planning model and, more importantly, GSWI density within a subcatchment is the most important factor to consider, although the output from the targeted scenarios was not found to be statistically different between simulations that managed the same area of impervious runoff. For use as a planning tool to estimate total volume and average flow, the uniform distribution is sufficient.

For peak discharge specific estimates, a targeted distribution approach that more closely mimics the reality of implementing GSWI networks may be necessary and understanding the driving factors behind the peak flow variations is essential. The differences in peak discharge among the targeted scenarios can be attributed to a couple of factors. First, it can be attributed to the selection (or nonselection) of subcatchments where GSWI was implemented. Those that do not have GSWI may have a higher percent impervious area, thus contributing more runoff directly to the sewer inlet than the other scenarios. Alternatively, the density of GSWI within the subcatchments selected for GSWI implementation (which is dictated by the amount of impervious area contained within) may adversely impact the output hydrograph.

The limitations of these results are related to the size of the subcatchments used to generate results and the lack of observed data to evaluate output accuracy. First, the subcatchment sizes were, on average, greater than 100 acres for the SLC model. This

limits the discussion with respect to peak discharge results. As subcatchments increase in size, the effect from travel time diminishes due to the lumped representation of subcatchment parameters within SWMM5. Thus, smaller sized subcatchments introduce greater distribution of placement options that would broaden the distribution of GSWI, potentially affecting the timing and magnitude of the peak discharge for the spatial distribution evaluation. Supplemental spatial distribution evaluations on a model representing Philadelphia, Pennsylvania with greater subcatchment resolution and subcatchment characteristic details were conducted and the results are presented in Appendix D. The results of the Philadelphia model simulations show variation with the average flow and peak flow values still exists, but minimal variation was shown with respect to the volume estimates. This indicates that smaller subcatchments may improve the estimate precision for at least one of the metrics. The Philadelphia results are only supplemental and further analysis is necessary to support this conclusion.

For all simulations, the output was evaluated for relative precision between approaches and not accuracy of output estimates. It is impossible to deduce the accuracy of these results without observed data against which to validate. To improve the robustness of these types of evaluations, observed data from watershed-scale GSWI networks are required. Lastly, the simulated results are only estimations of the watershed-scale benefit from GSWI networks, not individual GSWI site performance. Therefore these results cannot be interpreted for site-level design development or modeling approaches.

Understanding how GSWI representation within urban planning models affects the potential hydrologic benefits will improve the overall engineering process of GSWI

networks from conception through design and construction. Refining the methodology to simulate more accurate estimated benefits at the planning stage will reduce costs throughout the lifespan of the project by minimizing adjustments to the design from large errors in simulated benefits. Furthermore, our work adds to the growing body of knowledge identifying the necessary considerations when building planning models for GSWI networks.

CHAPTER IV

EVALUATIONS ON AGGREGATING GREEN STORMWATER INFRASTRUCTURE SUBCATCHMENTS

We further address the issue of identifying influences on hydrologic response estimates produced from aggregating subcatchments containing green stormwater infrastructure (GSWI). Resultant hydrologic responses were compared from increasingly aggregated subcatchments containing GSWI. Our test methods included: 1) create models of increasingly aggregated subcatchments (301, 142, 37, 4, and 1 subcatchment(s)) containing GSWI within the Philadelphia, Pennsylvania watershed, 2) create models of increasingly aggregated subcatchments (54, 7, 3, and 1 subcatchment(s)) containing GSWI within the Salt Lake City, Utah watershed, 3) simulate all scenarios using a long-term rainfall record for the region, and 4) apply statistical t-test significance test to determine the magnitude of variation between the scenario results. Results support previous studies implying aggregation scenarios can produce comparable results with respect to peak discharge and volume, but average flow rate results showed statistically different results between aggregation scenarios ($n = 46$, $\alpha = 0.05$). However, these metrics become increasingly more sensitive and variable as aggregated subcatchments increase in representative area. Time to peak and recession

limb characteristics were substantially influenced by increasingly aggregated scenarios.

Background

Green stormwater infrastructure (GSWI) has become a primary mechanism for mitigating increased stormwater runoff volume and peak discharges within many urban areas experiencing substantial growth (NRDC 2011). Conceptually, GSWI disconnects the impervious surfaces that drain directly to sewer inlets (e.g., sidewalks, roads, rooftops, etc.). Functionally, GSWI intercept stormwater runoff and detain it through some combination of infiltration, storage, and slow release (U.S. EPA 2000). GSWI is ideal for the urban environment because of the flexibility in placement options throughout the watershed and ability to manage stormwater runoff at relatively small spatial footprints (Benedict and McMahon 2002). A number of site-scale case study and pilot project implementation studies exists documenting GSWI performance (Booth et al. 1996; U.S. EPA 2006; Pitt et al. 2010; Carson et al. 2013). Much of this effort has been informed by the Prince George's District's 1999 report, a comprehensive guidance document for analyzing and implementing GSWI within urban watersheds (PGC 1999). Notably, this document considered mainly East Coast environments, with arid and semi-arid climates remaining under-researched. Subsequently, the Urban Drainage and Flood Control District of Denver (UDFCD) developed an extensive regulatory document for stormwater management focused on GSWI methods and technologies (UDFCD 2011).

The purported benefits and measured performance has encouraged the creation of detailed implementation plans to distribute GSWI watershed-wide to control stormwater runoff. U.S. EPA's establishment of the National Pollutant Discharge Elimination System

(NPDES) stormwater management program and inherent requirements has motivated municipalities across the country to apply the GSWI paradigm to develop mitigation strategies come into compliance with the regulations (U.S. EPA 2014). The National Resource Defense Council (NRDC) produced a report titled Rooftops to Rivers, which intended to serve as a review document highlighting GSWI management plans in urban areas (NRDC 2006; NRDC 2011). The document presented nine metropolitan areas in which GSWI oriented watershed management plans were successfully implemented. A follow-up report issued in 2011 included case studies for 14 metropolitan areas. The NRDC lists of urban metropolis areas are only a few among a larger number of other major urban city centers that have adopted and are successfully implementing GSWI (e.g., CTDEP 2004; Spicer Group 2008; PWD 2009; U.S. EPA 2010; Wang et al. 2010; MMSD 2011; Struck et al. 2012).

Although the popularity of GSWI has been steadily increasing and the technology for simulating these systems at the individual site level has been well established, the complexity of representing individual GSWI site characteristics at the watershed-scale remains problematic (Roy et al. 2008; Bach et al. 2014). Existing models that attempt to simulate GSWI networks are in their infancy, as well as the interface provided by models attempting to replicate type-specific GSWI. This has the potential to inaccurately estimate the collective performance of GSWI at the watershed-scale (Yeo and Guldmann 2010). Furthermore, there is a dearth of observed data for watershed-scale GWSI networks to support the assumption that a collective benefit from site-scale GSWI exists (Roy et al. 2008). Thus, estimates of performance from simulated networks cannot be validated by observations. Until observations can be collected and evaluated, research has

focused on improving the modeling methodology and technology. Recent publications replicated the complex nature of GSWI's infiltration and storage capabilities by developing either GSWI modules within existing modeling software (e.g., Rossman 2010) or stand-alone software and tools (e.g., Lee et al. 2009; Damodaram et al. 2010; Strecker et al. 2010; WERF 2012; Eric et al. 2013). Complex models have been developed that include algorithms attempting to spatially optimize placement of type-specific GSWI (Lee et al. 2012). The complexity and system requirements of models with this detail, however, prevent it from being widely used within the water resources modeling community. Similar decision support models have been developed that serve as a supplemental results check to the more robust numerical models (e.g., Osmond et al. 1995; U.S. EPA 2013). Thus, these models are not suited for watershed-wide analyses and research into up-scaling of site-specific GSWI continues to be a necessity.

Improvements to modeling technology for GSWI networks would be enabled through a better understanding of how simulated watershed-wide performance is affected by spatial distribution and subcatchment aggregation. Recent studies emphasize the need to investigate the hydrologic sensitivity of spatial aggregation and siting of GSWI within watershed-scale models (Elliott and Trowsdale 2007; Hamel et al. 2013; Bach et al. 2014). While research exists documenting the effect from varying spatial representation in watershed-scale models for urban hydrologic response without GSWI (Park et al. 2008; Bormann et al. 2009; Ghosh and Hellweger 2012), little research has been conducted to expand this concept to include GSWI. The few existing studies show that aggregation of subcatchments containing GSWI has little impact on total runoff volume estimates, but may have a notable influence on peak discharge and water quality

estimates (Arabi et al. 2006; Carter and Jackson 2007; U.S. EPA 2007; Elliott et al. 2009). Results also indicate that differences in simulated output correlate with increased aggregation (Arabi et al. 2006; Elliott et al. 2009). GSWI spatial distribution studies are especially limited and have not specifically addressed the issue of comparing varied distribution scenarios (Kertesz et al. 2007; James et al. 2012).

Existing literature has focused mainly on using design-specific applications of GSWI for both site-scale and watershed-scale evaluations. This approach requires input data that limit the assessment of GSWI practices within an urban environment and its applicability. Furthermore, design-level details may be unnecessary if the modeling objective is to meet watershed-scale performance criteria through some combination of GSWI types, the combination of which having not yet been defined at the planning stage. From this perspective, a combination of GSWI types is assumed to be designed and functioning to meet a standard watershed-wide performance measure. A collective representation of fundamental GSWI processes can relieve input data issues for these types of modeling objectives. Smullen et al. (2008) presented an alternative planning-level methodology to represent GSWI within a watershed-scale planning model for the City of Philadelphia, with greater details of this approach provided by the Philadelphia Water Department (PWD 2009). The PWD (2009) up-scaling methodology for GSWI systems provides a preferable, collective representation of GSWI, such that the results would not be biased toward any given design type of GSWI. Thus, allowing any differences to be solely attributed to GSWI spatial distribution and aggregation impacts.

The first objective of the current study uses the PWD (2009) algorithm to evaluate output for sensitivity studies identifying the influences on hydrologic response from

increasingly aggregated subcatchments that contain GSWI. Conclusions derived from the results of the analysis will provide stormwater planning engineers with practical advice on creating and simulating GSWI networks at the watershed-scale. Furthermore, the content will add to the knowledge base for simulating networks of GSWI within urban area planning models.

Materials and Methods

Stormwater Management Model Version 5 (SWMM5)

Originally developed in 1971, the Stormwater Management Model Version 5 (SWMM5) model is a coupled hydrologic-hydraulic model. Calculations are based on physical processes and utilize the concepts of conservation of mass, energy, and momentum to estimate hydrologic and hydraulic responses to input datasets (U.S. EPA 2010). Because SWMM5 is a coupled hydrologic-hydraulic model, it allows the user to adjust both the surface parameters and the under-lying sewer characteristics within the same model. SWMM5 compartmentalizes its computations based on the following physically based processes:

- Surface Runoff
- Groundwater
- Flow Routing
- Water Quality Routing
- Infiltration
- Snowmelt
- Surface Ponding
- LID Representation

Not all of the above processes are necessary to build a model and perform simulations. For this study, the surface runoff, flow routing, and infiltration processes are used to analyze the hypothesis and objectives. Details of these processes may be found in

Rossman (2010).

Philadelphia, Pennsylvania Model

The model used for this research was a 14.2-mi^2 section within Philadelphia, Pennsylvania (PHL) that represents the southeast drainage district of the city. The area is a densely populated urban portion of the city and is represented by an average impervious area of 58%, with values ranging from 7% up to 80%. Slope values for this region range from 0.4% up to 27% and the average slope is approximately 3.4%. More details of the surface characteristics are available in PWD (2009).

Surface runoff was collected by storm sewer inlets and routed through subsurface pipes and, ultimately discharge through various an unrestricted outfalls. There model contains 443 pipe segments, 401 junctions, and 38 unrestricted outfalls. Pipe sizing ensured unrestricted flow through the system. Model build was conducted using observed data collected from years of monitoring conducted by the Philadelphia Water Department for a number of parameters including: flow, infiltration, rainfall, impervious area, and others. More details of the model calibration using this collected data are available in PWD (2009).

Precipitation

All long-term continuous simulations used data from a single raingage for the years 1990 up to 2013 and were provided by the Philadelphia Water Department (Figure 10). The 95^{th} percentile rainfall depth for the entire collection of rainfall data from a single raingage was calculated as 1.5 inches (Figure 11).

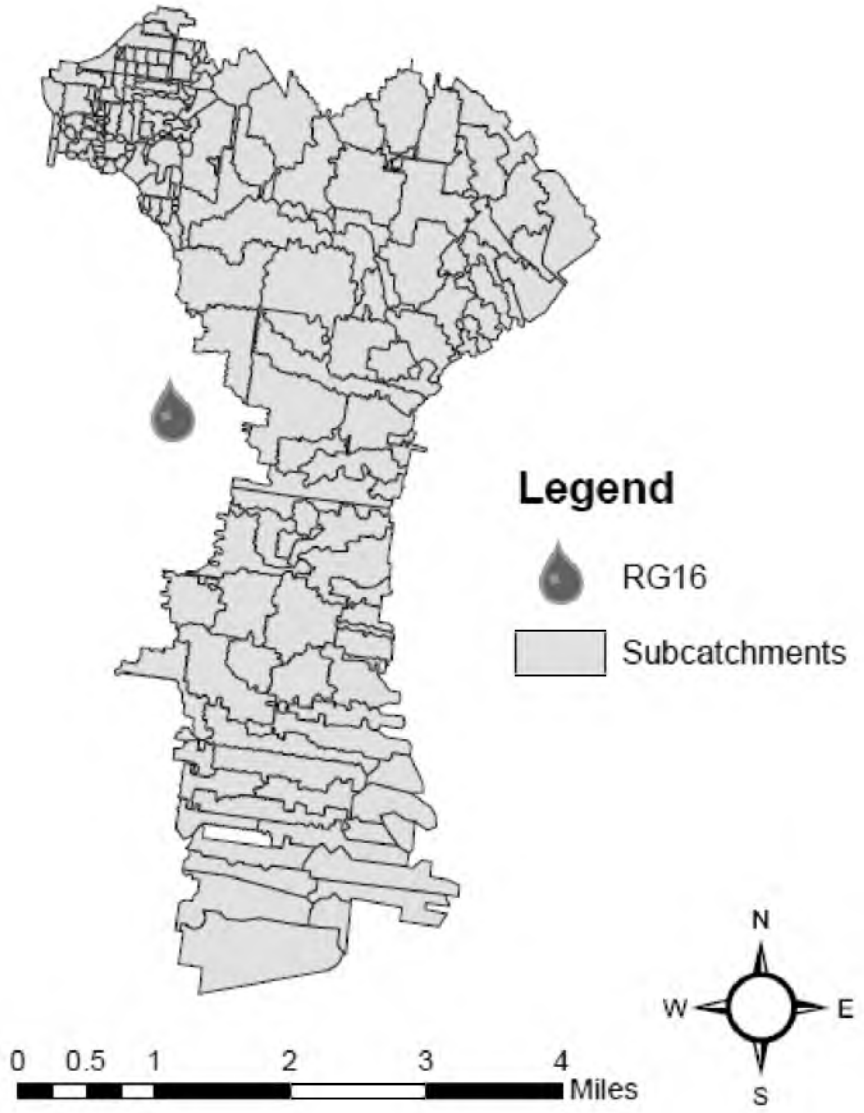

Figure 10. Locations of the raingage used to run the simulations for this study. The subcatchments associated with each raingage are grouped by color.

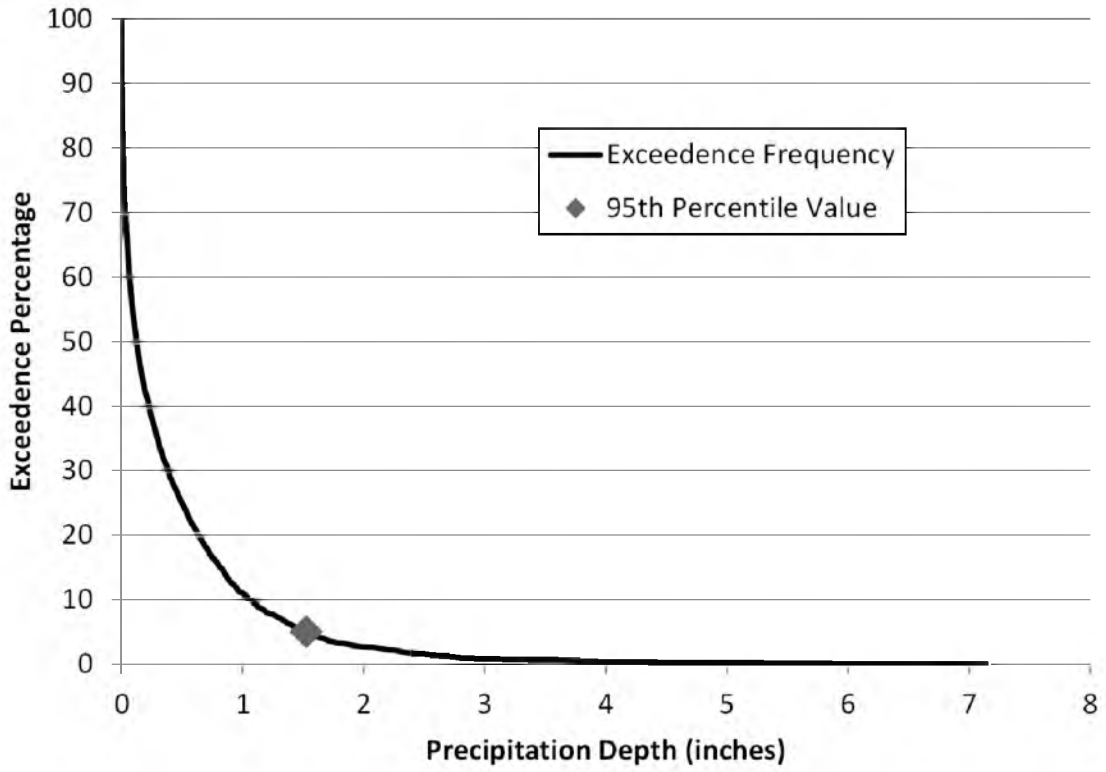

Figure 11. Exceedence Frequency of the four rain gages combined. The 95th percentile value is identified as 1.5 inches.

GSWI Representation

The PWD (2009) up-scaling algorithm was used to represent GSWI for all model scenarios. The fundamental processes that simulate runoff routing through a GSWI unit, as represented in the PWD (2009) algorithm, are: infiltration, storage with slow release through a control orifice, and GSWI unit bypass (Figure 1). The elements representing these processes are created using a collection of equations presented within PWD (2009).

Percent implementation of GSWI was equal to 45% of total impervious area across all simulations. This value was determined through an analysis of increasing levels of implementation, which is documented in Appendix C. The loading ratio defining the number of impervious acres loading to 1 GSWI acre was kept constant at 10.7:1. The

GSWI units were sized to capture the first inch of runoff for the single-event precipitation simulations. For the long-term continuous simulations, the 95th percentile precipitation depth was used to size the GSWI units and was equal to 1.5 inches. Runoff stored within the GSWI units had a drawdown requirement of 24 hours for all simulations.

Modeling Scenarios

Two sets of modeling scenarios were simulated for this study: 1) uniform distribution of GSWI and 2) aggregation of subcatchments containing GSWI. The target implementation of GSWI, referring to the total amount of watershed impervious area managed by GSWI, was established as 45%, or 2,427 acres, for all scenarios.

The spatial aggregation objective was tested by systematically aggregating the subcatchments within the PHL model and making adjustments to the hydraulic loading (Figure 12 and Figure 13). As subcatchment areas were aggregated, surface characteristics controlling stormwater runoff detention and infiltration had to be re-evaluated. All surface characteristics, except the overland flow width parameter and impervious area, were derived by area weighted averaging. Overland flow width was calculated by doubling the square root of the aggregated area, as suggested in the SWMM5 manual. Percent impervious was recalculated to reflect the cumulative impervious area within the aggregated subcatchments and thus the percent impervious value distribution tended toward the average (Figure 14). Hydraulic characteristics (e.g., pipe length and diameter) were kept constant for all scenarios.

Each aggregation scenario had some combination of adjustments made to the hydraulic loading and surface routing conditions. With the original model (representing

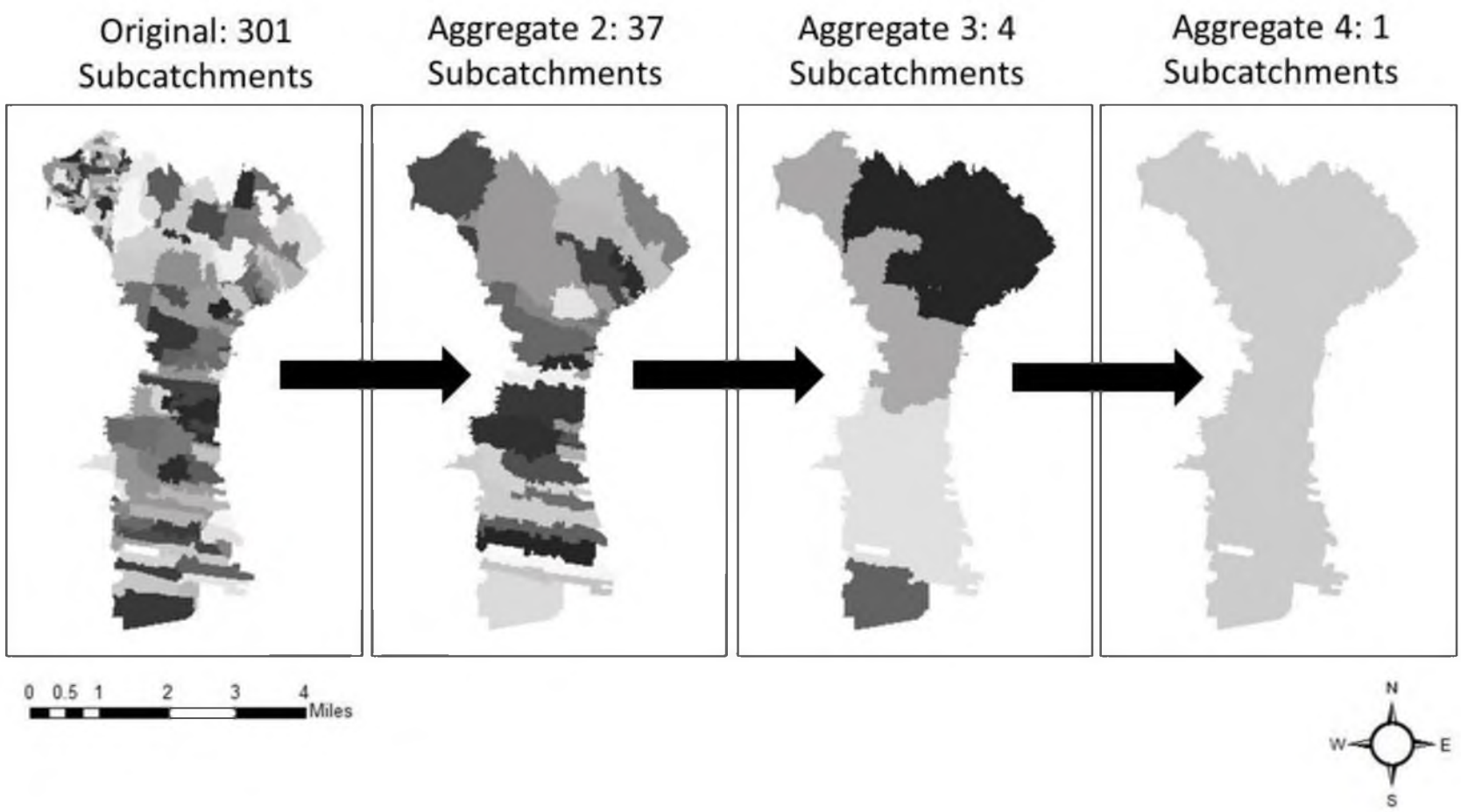

Figure 12. Four simulated aggregate scenarios. The baseline (original) condition represents a fully disaggregated situation. Aggregate 2, 3, and 4 represent progressive lumping of the subcatchments, with Aggregate 4 representing a fully aggregated model.

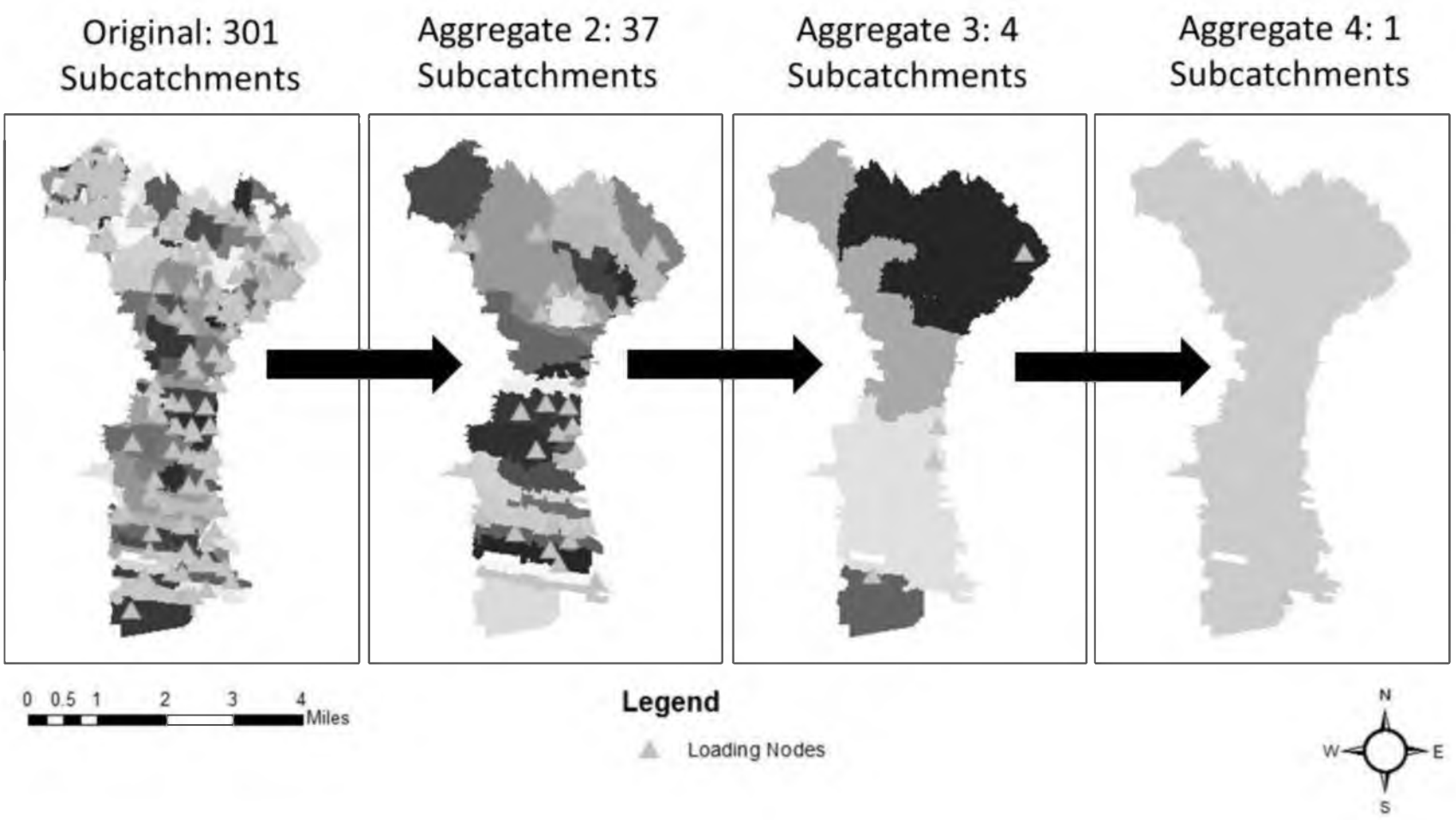

Figure 13. The triangles represent loading junctions used for each scenario. Progressively aggregated subcatchments contribute to an increasingly lumped loading, potentially affecting the shape of the outfall hydrograph for the watershed.

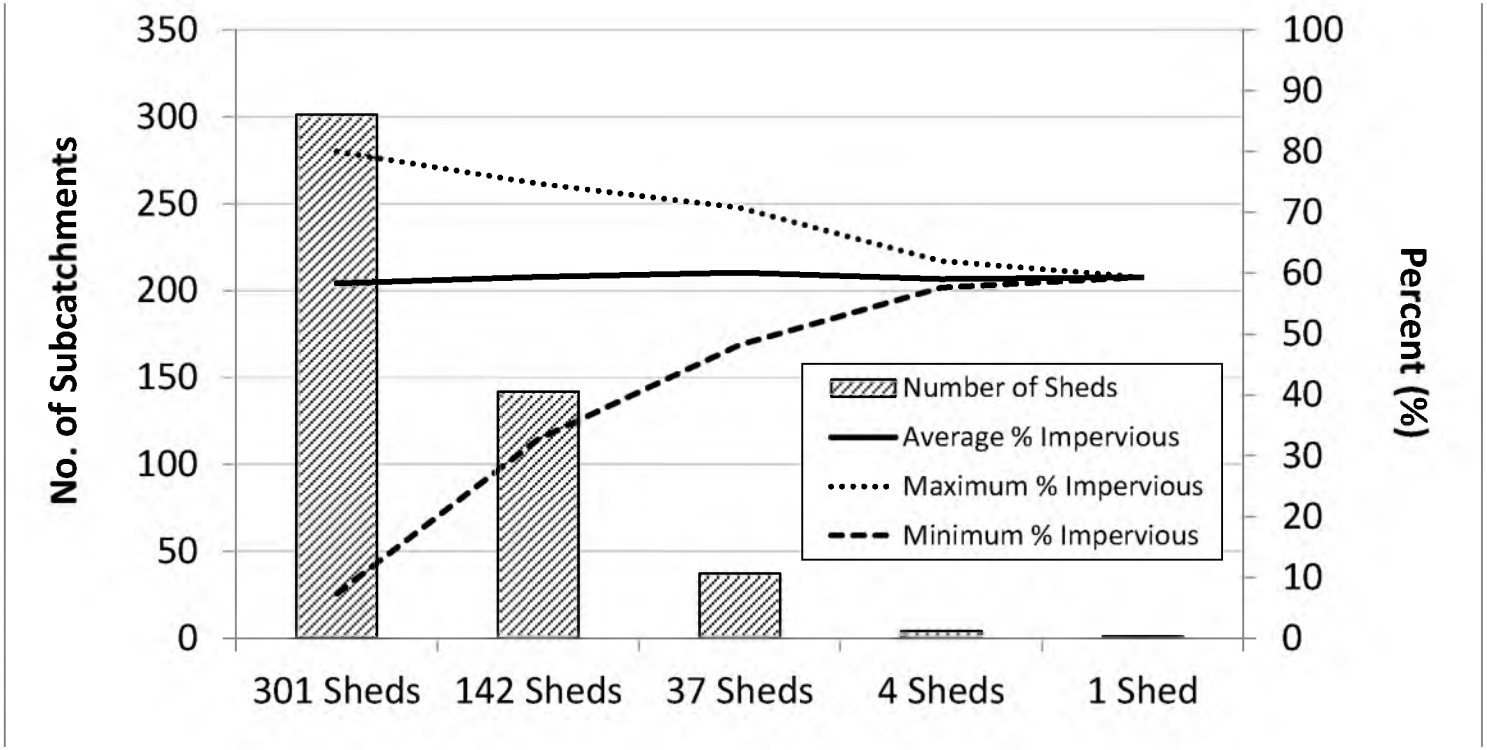

Figure 14. The percent impervious values as subcatchments were aggregated for the PHL.

the highest level of discretization), 159 loading points were used to collect surface runoff from the subcatchments (Figure 13). SWMM5 creates surface runoff hydrographs for each subcatchment and then transfers the flow profile to the assigned downstream collection node to be routed through the pipe network. It follows that more subcatchments mean greater surface routing granularity and diversification within the model (Figure 13).

For the Aggregate 1 scenario, the number of subcatchments was aggregated from 301 to 142. This translates to a reduced surface runoff granularity and aggregates the individual subcatchment hydrographs into 142 cumulative hydrographs. This has the effect of manipulating peak discharge timing and minimizing distribution over the aggregated area that was present within the original scenario. This compounded loading continues for the subsequent three aggregation scenarios (Figure 13).

Salt Lake City, Utah Model

The spatial aggregation objective was tested by systematically aggregating the subcatchments within the SLC model in the same manner as was applied for the Philadelphia model (Figure 15). Each aggregation scenario had some combination of adjustments made to the hydraulic loading and surface routing conditions. With the baseline model (representing the highest level of discretization), eight loading points were used to collect surface runoff from the subcatchments (Figure 16). Long-term continues precipitation data and GSWI setup was the same as described in Chapter III.

For the Aggregate 1 scenario, the number of subcatchments was aggregated from 54 to 31. The number of loading junctions for the Aggregate 1 scenario remained

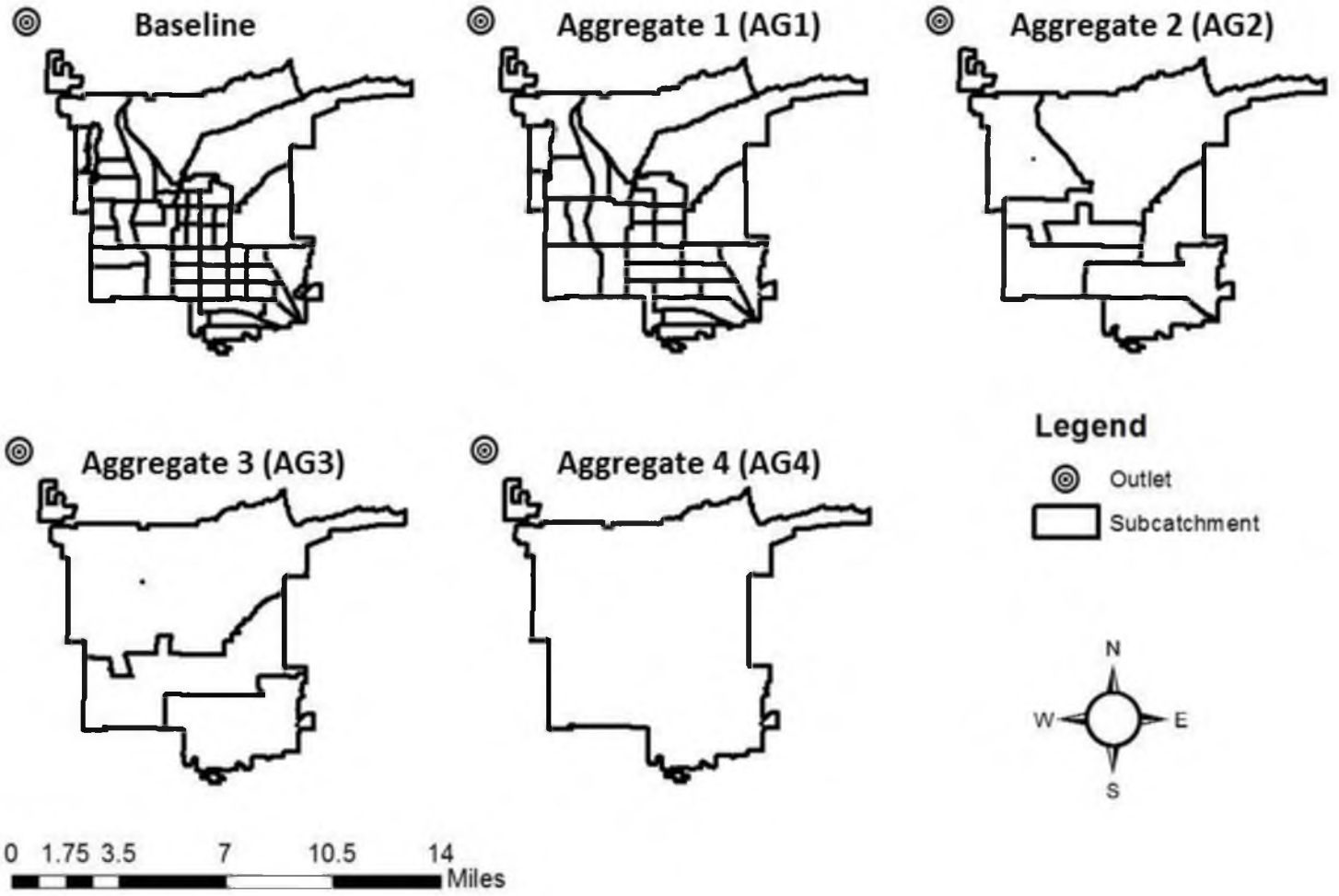

Figure 15. The five simulated aggregate scenarios. The baseline condition represents a fully disaggregated situation. Aggregate 1, 2, 3, and 4 represent progressive lumping of the subcatchments, with Aggregate 4 representing a fully aggregated model.

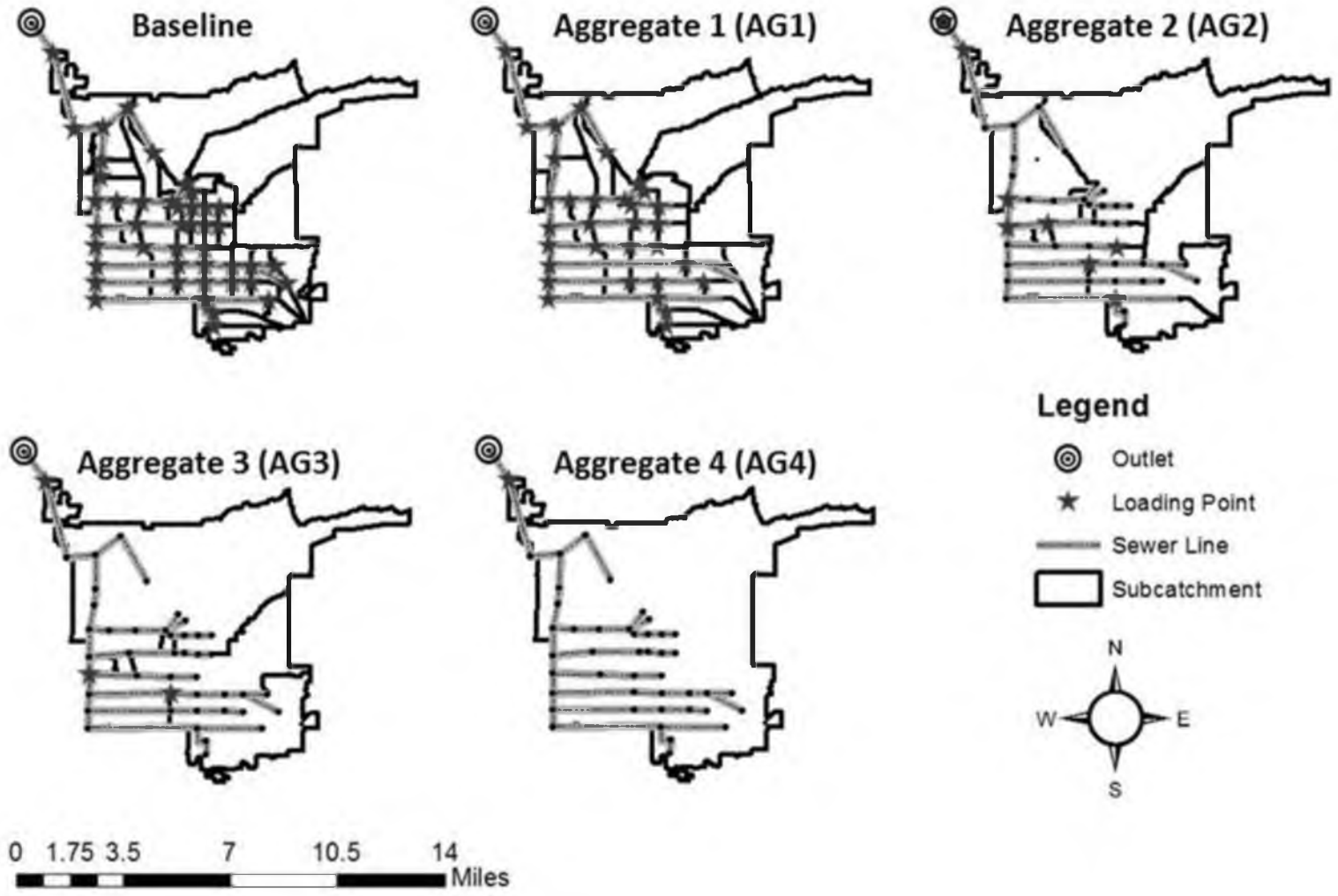

Figure 16. The stars represent the loading junctions used for each scenario. Progressively aggregated subcatchments contribute to an increasingly lumped loading, potentially affecting the shape of the outfall hydrograph for the watershed.

consistent with the Baseline conditions, with the only difference being the loading was shifted downstream to the main sewer line for the Aggregate 1 scenario. This compounded loading continues for the subsequent three aggregation scenarios (Figure 16). Percent impervious was recalculated to reflect the cumulative impervious area within the aggregated subcatchments and thus, the percent impervious value distribution tended toward the average (Figure 17).

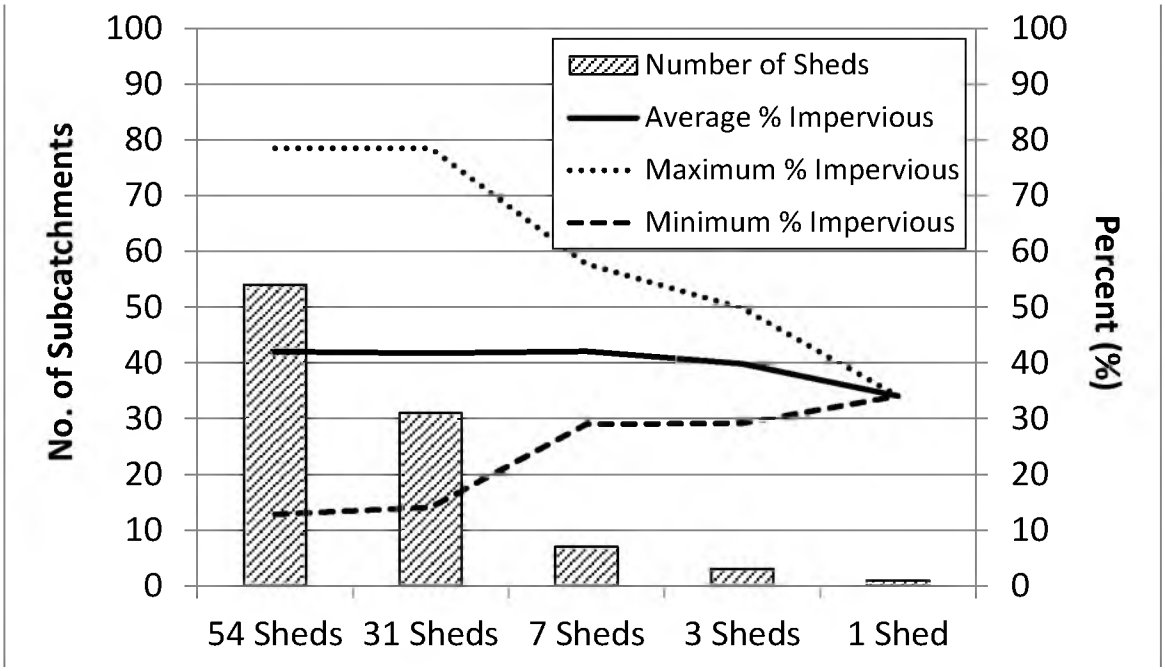

Figure 17. The percent impervious values as subcatchments were aggregated for the SLC model.

Results and Discussion

PHL Hydrologic Simulations

Scatter plots show large variations with the annual flow rate and to a lesser extent with peak discharge values for larger volume events (Figure 18). There could be a couple of reasons for this phenomenon. First, the aggregated overland flow width parameter may be adversely influencing the surface routing. Generally, this parameter is used as a calibration value, and is adjusted to minimize adverse effects to the simulated hydrographs after comparing to observed timeseries data. Since observed data do not exist with which to calibrate these data inputs, it is impossible to know the correct hydrograph response to mimic. The second possible influence can be the hydraulic loading changes. As the subcatchments are aggregated, the loading of the runoff to the sewer system is also aggregated. For this particular model, the hydraulic loading points are progressively pushed further downstream, thereby reducing travel time for flow within the sewer system.

Upon inspection of the outlet hydrograph for the June 2, 2006 event, it appears the greatest influence from aggregating subcatchments is on peak discharge and an associated reduction in volume (Figure 19). The greatest change occurs when the subcatchment number is reduced to 4 and 1. The reason for this may be attributed to the lumping of GSWI's pervious areas and subcatchment surface characteristics over larger areas (Table 15). For the PHL model specifically, the 37 shed aggregation scenario is the highest level of aggregation where result data are comparable to the fully discretized scenario.

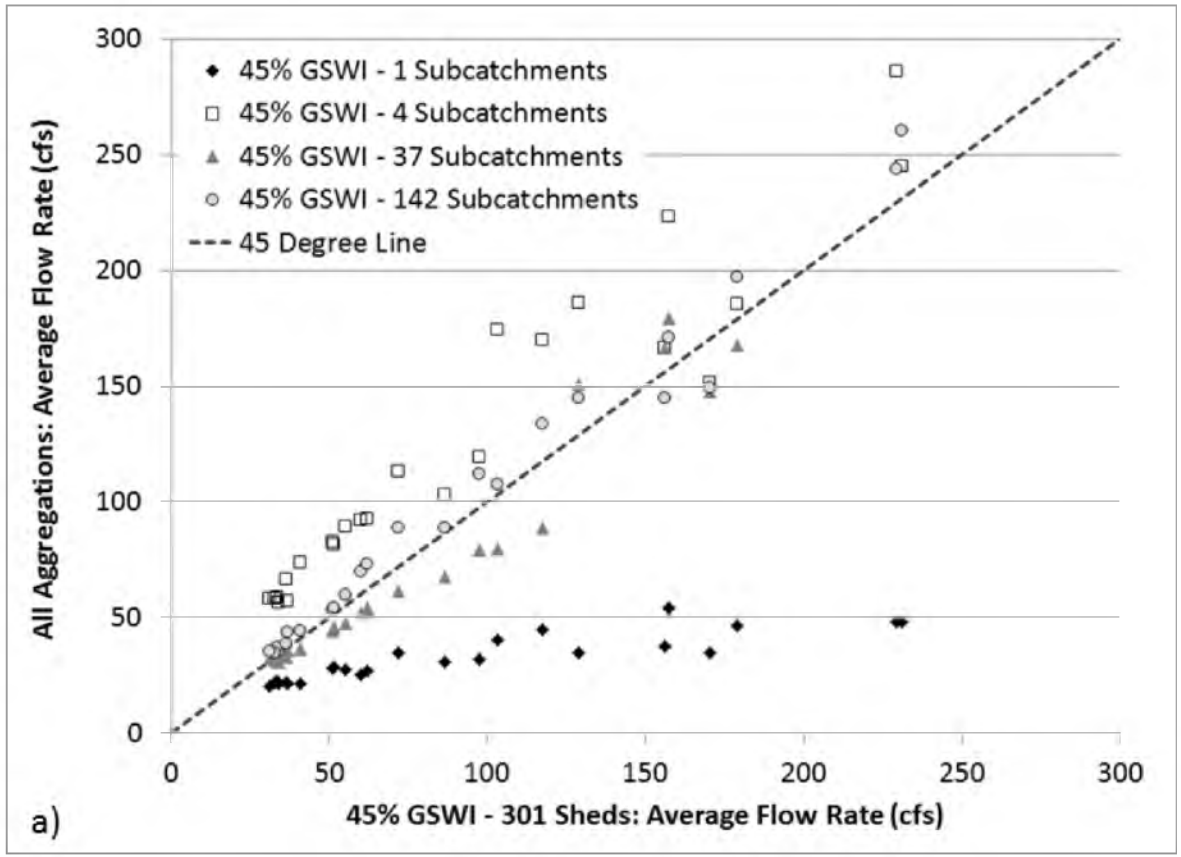

Figure 18. PHL Scatter plots of the aggregated scenarios' results compared against the baseline scenario output. Results for average flow rate (a), peak discharge (b), and volume (c) are plotted. Some variation in peak discharge is present for the larger values.

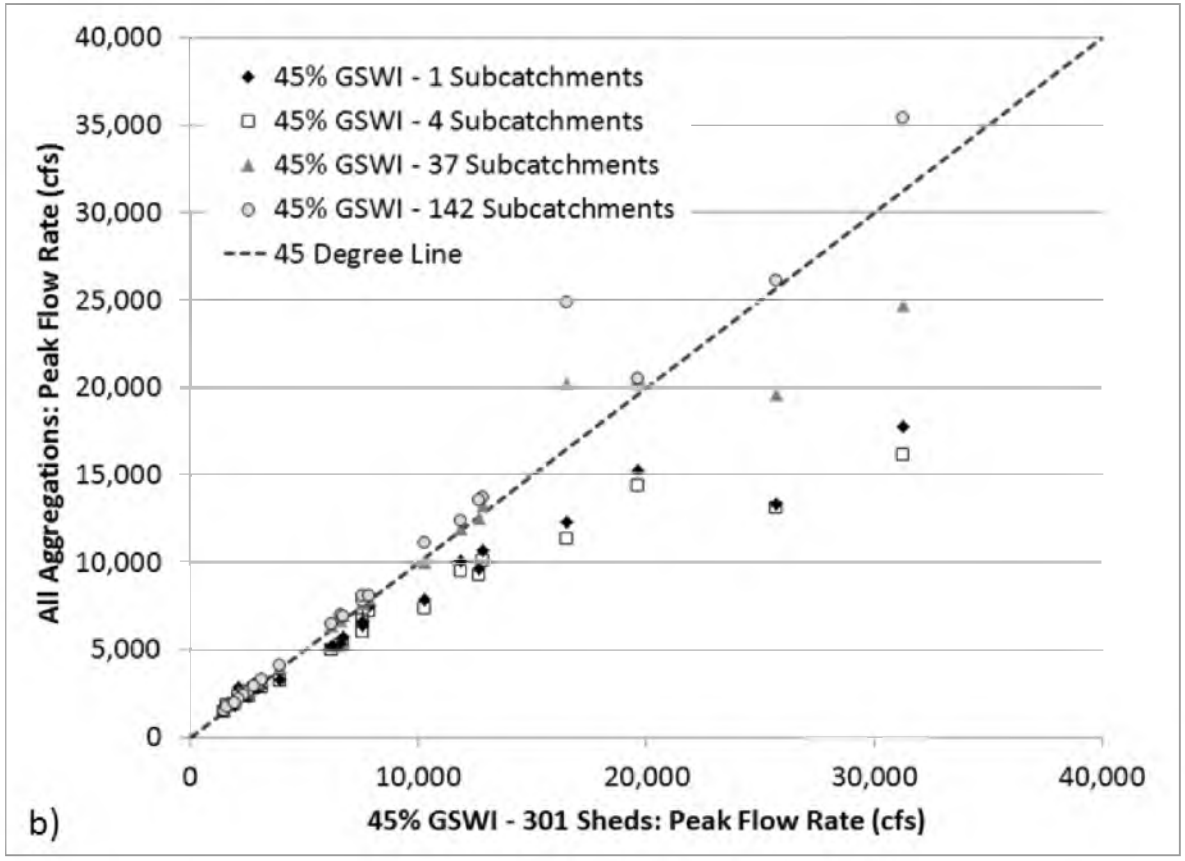

Figure 18. Continued

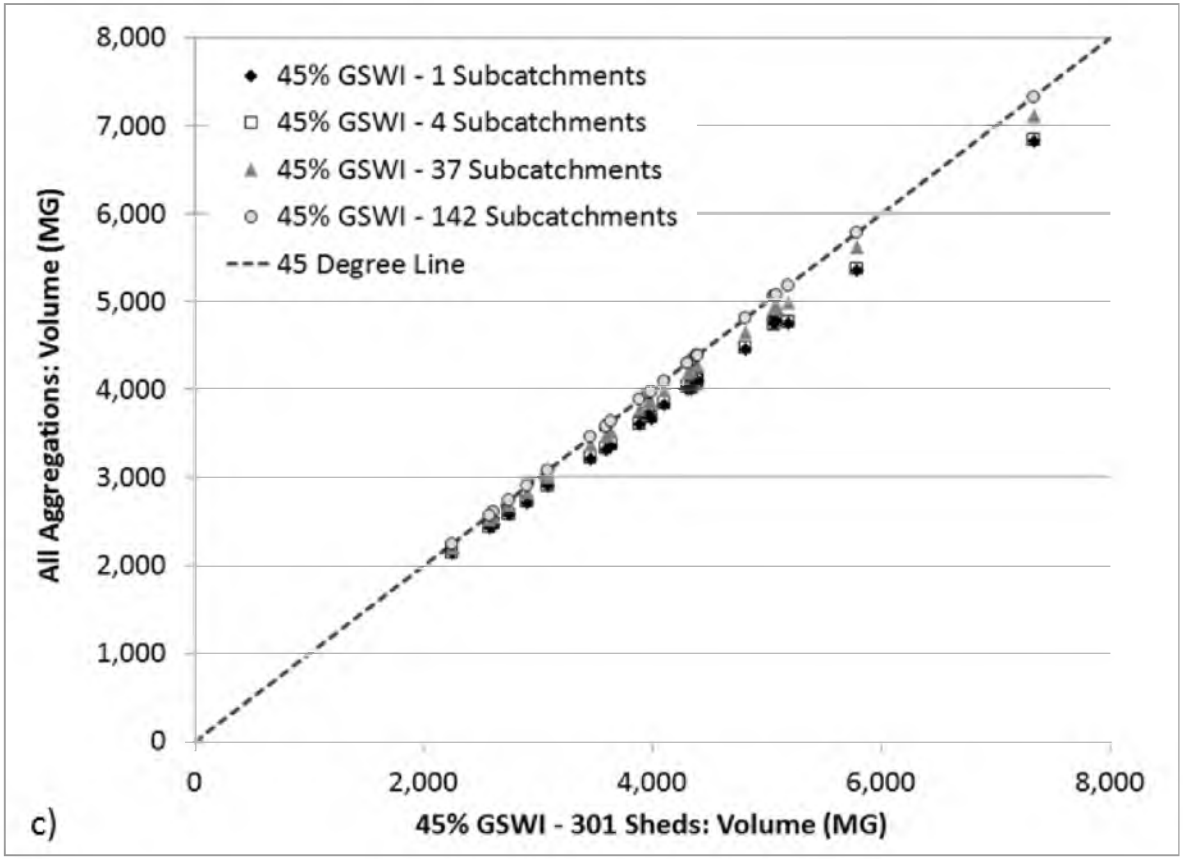

Figure 18. Continued

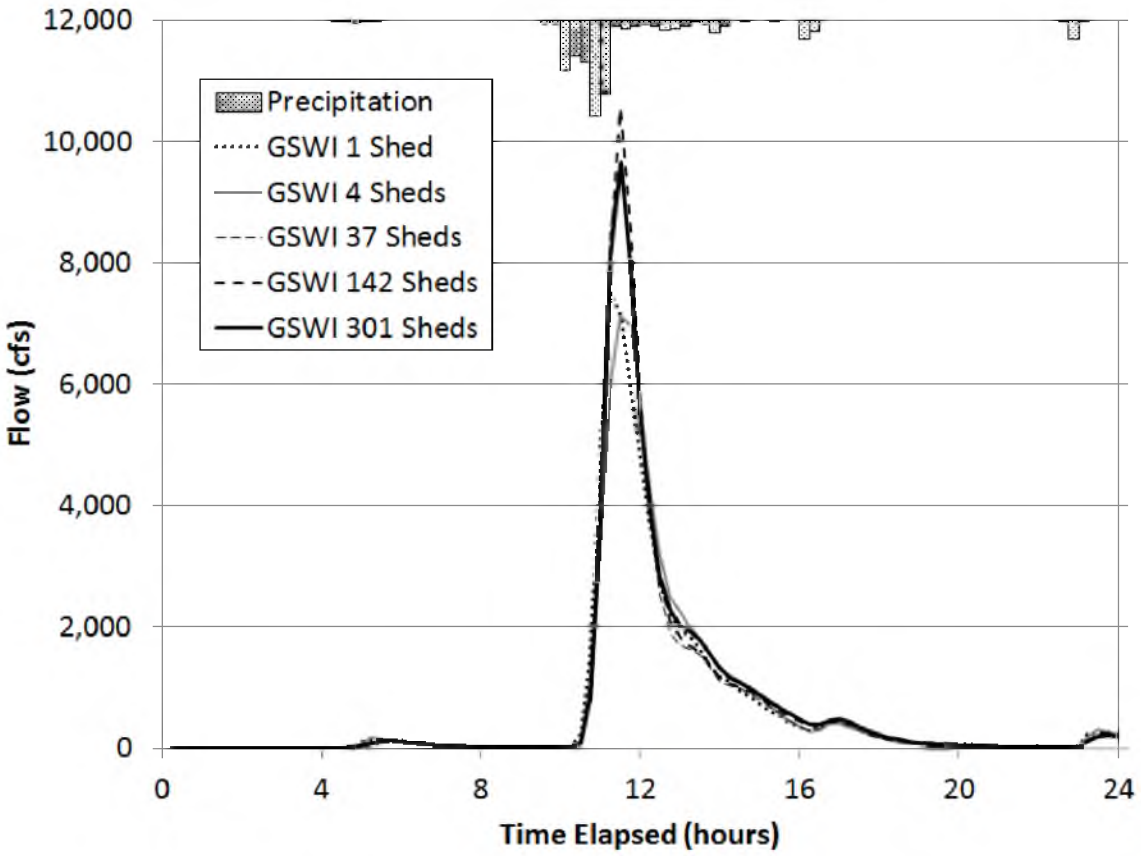

Figure 19. Hydrographs produced from the June 2, 2006 event for all scenarios. The peak discharge is substantially impacted by aggregation of the subcatchments. Large variations of peak discharge between each scenario are apparent for this event timeseries and are most likely affected by the hydraulic and overland flow routing.

Table 15. Subcatchment area values and statistics for each level of aggregation.

Simulation ID	Maximum Subcatchment Area (acres)	Minimum Subcatchment Area (acres)	Average Subcatchment Area (acres)
301 Sheds	311	0.12	30
142 Sheds	311	1.42	64
37 Sheds	1,601	3.04	246
4 Sheds	3,619	607	2,273
1 Shed	9,094	9,094	9,094

PHL Statistical Analysis

A summary of the descriptive statistics for each scenario (original – fully discretized and aggregated) are presented in Table 16. These statistics reiterate the scatter variance from the plotted results in the previous section. Clearly, the mean average flow values have large variations between each aggregation scenario. Of notable interest is the single subcatchment scenario where the average flow is one third of the other aggregation and original-fully discretized scenarios. This observation is apparent with the maximum and minimum values. The mean, maximum, and minimum peak values produced from aggregation scenarios 3 and 4 (4 subcatchments and 1 subcatchment, respectively) also show a large decrease in value as compared to the other scenarios. The volume statistics were not as affected by the increased aggregation.

Test for Normality

To ensure that the datasets were normally distributed, the average flow, peak flow, and volume output from the original-fully discretized scenario results were evaluated for normalcy (n = 24). For the purposes of this study, if the results for this set of scenarios were found to be normal, then it was assumed the results for the aggregated scenarios for the PHL and SLC models would also be normally distributed. Histograms were created based on five bins sized using the maximum and minimum values for each runoff characteristic (Figure 20). If the majority of data was grouped into the middle of the histogram, it was considered to be normally distributed. A review of the histograms in Figure 20 satisfied the criteria for normal distribution.

Table 16. PHL Subcatchment aggregation scenarios descriptive statistics for average flow rate, peak discharge, and volume.

Average Flow (cfs)								
Simulation	n	Mean	Standard Deviation	Standard Error	95% confidence		Minimum	Maximum
					Upper	Lower		
45% GSWI - 301 Subcatchments	24	94	63	4,005	119	69	31	231
45% GSWI - 142 Subcatchments	24	101	67	4,489	128	74	35	260
45% GSWI - 37 Subcatchments	24	96	84	7,067	129	62	31	331
45% GSWI - 4 Subcatchments	24	124	66	4,380	151	98	56	286
45% GSWI - 1 Subcatchments	24	32	10	102	36	28	20	54
Peak Flow (cfs)								
Simulation	n	Mean	Standard Deviation	Standard Error	95% confidence		Minimum	Maximum
					Upper	Lower		
45% GSWI - 301 Subcatchments	24	8,671	7,897	62,363,247	11,831	5,512	1,485	31,280
45% GSWI - 142 Subcatchments	24	9,494	9,001	81,024,823	13,095	5,893	1,530	35,413
45% GSWI - 37 Subcatchments	24	8,468	6,833	46,691,489	11,201	5,734	1,574	24,702
45% GSWI - 4 Subcatchments	24	6,277	4,316	18,629,791	8,004	4,551	1,431	16,144
45% GSWI - 1 Subcatchments	24	6,615	4,637	21,501,000	8,470	4,760	1,497	17,748
Volume (MG)								
Simulation	n	Mean	Standard Deviation	Standard Error	95% confidence		Minimum	Maximum
					Upper	Lower		
45% GSWI - 301 Subcatchments	24	4,108	1,166	1,360,416	4,575	3,642	2,251	7,334
45% GSWI - 142 Subcatchments	24	4,102	1,164	1,354,805	4,567	3,636	2,248	7,320
45% GSWI - 37 Subcatchments	24	3,990	1,127	1,269,637	4,441	3,539	2,200	7,118
45% GSWI - 4 Subcatchments	24	3,836	1,079	1,163,835	4,268	3,405	2,136	6,842
45% GSWI - 1 Subcatchments	24	3,826	1,076	1,158,701	4,257	3,396	2,135	6,818

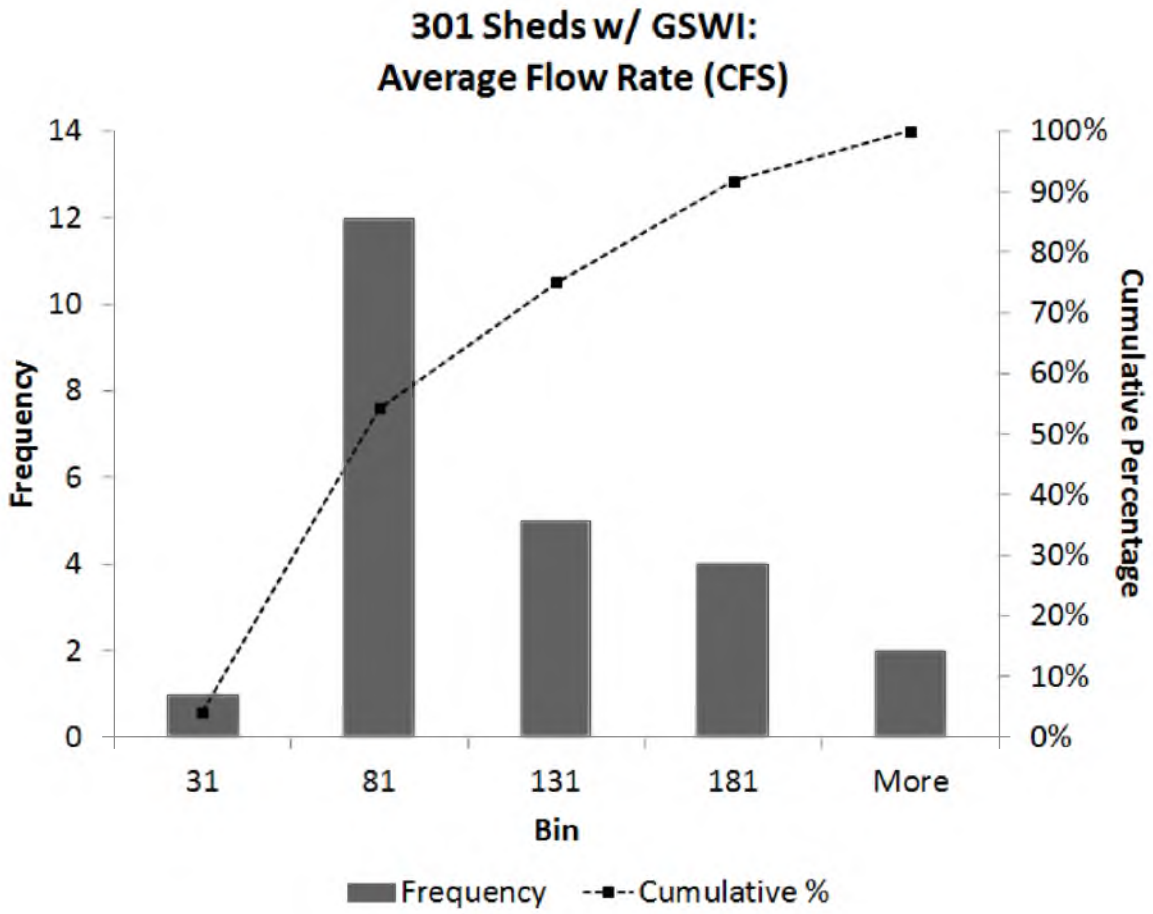

Figure 20. Histogram of average flow data points (n = 24) produced from the original-fully discretized scenario. The average flow (a), peak flow (b), and volume (c) distributions represent a normal distribution of the data, although the average flow and peak flow distribution have a slight skew.

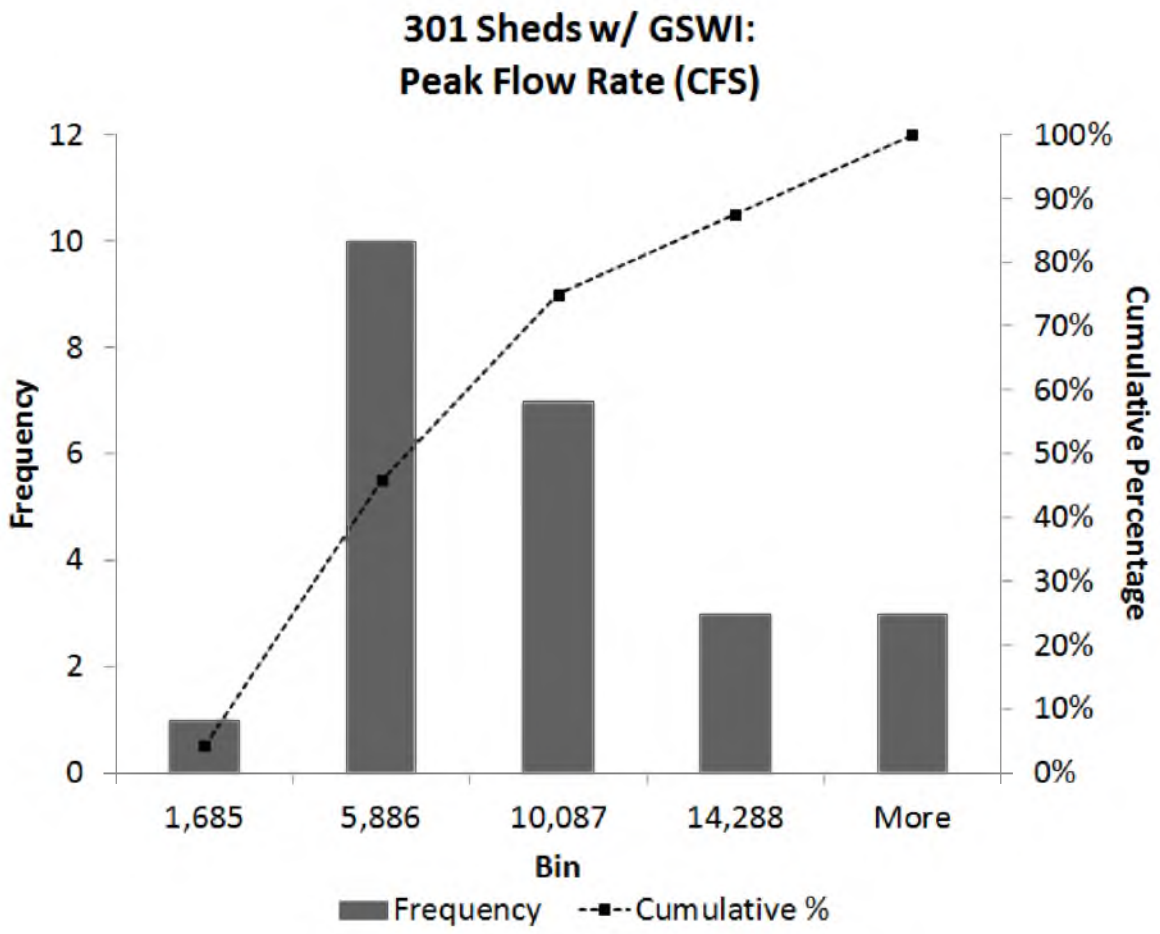

Figure 20. Continued

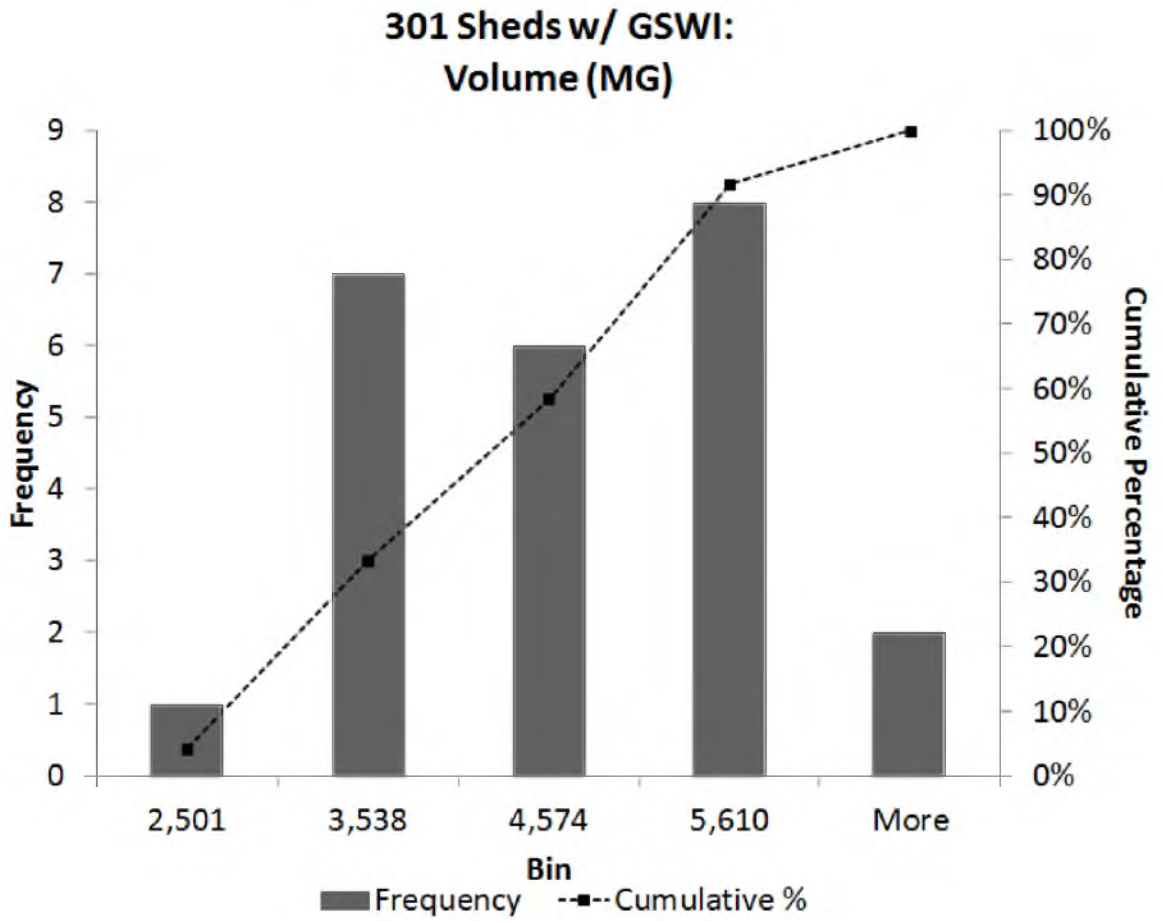

Figure 20. Continued

Test for Equal Variances

Testing for equal variances allows for the appropriate variation of significance test equations to be identified and then applied to the sample sets. The comparison was conducted for the original-fully distributed average flow, peak flow, and volume datasets and the average flow values for the aggregated scenarios. For the variances to be considered statistically equal, the F-distribution statistic should be near 1.0 and the p-value should be near 0.5. Based on these criteria and reviewing the results in Table 17, the results suggest the variances to be unequal between the datasets for the majority of scenarios. Therefore, a t-test with unequal variances will be applied to compare these datasets.

T-Test

The t-test results showed the targeted distribution means were not statistically different with respect to any of the hydrologic metrics as compared to the uniform distribution simulation. The values were calculated based on an alpha value = 0.05 and n = 24 observations (24-year precipitation). To determine the statistical significance of the results, each hydrologic characteristic (i.e., average flow, peak flow, and volume) was evaluated using three statistical metrics: 1) The calculated t-statistic was compared against the t-critical value, 2) the confidence intervals were calculated, and 3) the calculated p-value was compared to the alpha value. For the means representing the targeted scenarios to be statistically different from the mean of the uniform distribution results, the following criteria must be met:

Table 17. F-distribution values and results for all scenarios' average flow, peak flow, and volume result metrics. Using the criteria of an F-value near 1.0 and a p-value close to 0.5, the results show the variances to be unequal for a majority of the datasets.

Statistic	Average Flow (cfs)		Peak Flow (cfs)		Volume (MG)	
	Original (301)	Aggregate 1 (142)	Original (301)	Aggregate 1 (142)	Original (301)	Aggregate 1 (142)
Mean	94	101	8,671	9,494	4,108	4,102
Variance	4,005	4,489	62,363,247	81,024,823	1,360,416	1,354,805
Observations	24	24	24	24	24	24
Degrees of Freedom	23	23	23	23	23	23
F-statistic	0.892		0.770		1.004	
P(F<=f) one-tail	0.393		0.268		0.496	
F Critical one-tail	0.496		0.496		2.014	
Statistic	Average Flow (cfs)		Peak Flow (cfs)		Volume (MG)	
	Original (301)	Aggregate 2 (37)	Original (301)	Aggregate 2 (37)	Original (301)	Aggregate 2 (37)
Mean	94	96	8,671	8,468	4,108	3,990
Variance	4,005	7,067	62,363,247	46,691,489	1,360,416	1,269,637
Observations	24	24	24	24	24	24
Degrees of Freedom	23	23	23	23	23	23
F-statistic	0.567		1.336		1.071	
P(F<=f) one-tail	0.090		0.247		0.435	
F Critical one-tail	0.496		2.014		2.014	
Statistic	Average Flow (cfs)		Peak Flow (cfs)		Volume (MG)	
	Original (301)	Aggregate 3 (4)	Original (301)	Aggregate 3 (4)	Original (301)	Aggregate 3 (4)
Mean	94	124	8,671	6,277	4,108	3,836
Variance	4,005	4,380	62,363,247	18,629,791	1,360,416	1,163,835
Observations	24	24	24	24	24	24
Degrees of Freedom	23	23	23	23	23	23
F-statistic	0.914		3.348		1.169	
P(F<=f) one-tail	0.416		0.003		0.356	
F Critical one-tail	0.496		2.014		2.014	
Statistic	Average Flow (cfs)		Peak Flow (cfs)		Volume (MG)	
	Original (301)	Aggregate 4 (1)	Original (301)	Aggregate 4 (1)	Original (301)	Aggregate 4 (1)
Mean	94	32	8,671	6,615	4,108	3,826
Variance	4,005	102	62,363,247	21,501,000	1,360,416	1,158,701
Observations	24	24	24	24	24	24
Degrees of Freedom	23	23	23	23	23	23
F-statistic	39.350		2.900		1.174	
P(F<=f) one-tail	0.000		0.007		0.352	
F Critical one-tail	2.014		2.014		2.014	

1. The calculated t-statistic > the t-critical value (2.04);
2. The value of the null hypothesis (i.e., difference in means = 0) must fall outside the bounds of the confidence interval; and
3. The calculated p-value must be less than the alpha value (i.e., 0.05).

By all metrics, the targeted scenario means are not statistically different from the uniform distribution mean (Table 18).

SLC Hydrological Simulations

Upon inspection of the SLC outlet hydrograph for the May 25, 2004 event, aggregating subcatchments for this particular model has large impacts to peak discharge timing, recession limb characteristics, as well as the volume (Figure 21). Increasing the aggregation to a single subcatchment creates an almost instantaneous peak discharge response and decreases the estimated volume. There could be a couple of reasons for this phenomenon. First, the aggregated overland flow width parameter may be adversely influencing the surface routing and subsequently affecting modeled performance of the GSWI. Generally, this parameter is used as a calibration value, and is adjusted to minimize adverse effects to the simulated hydrographs after comparing to observed timeseries data. Longer overland flow distances within the increasingly aggregated scenarios may be allowing for increased infiltration or evaporation to occur. The second possible influence can be the hydraulic loading changes. As the subcatchments are aggregated, the loading of the runoff to the sewer system is also aggregated. For this particular model, the hydraulic loading points are progressively pushed further downstream, thereby reducing travel time for flow within the sewer system.

Table 18. T-test results comparing the aggregated scenarios' dataset means to the original-fully discretized dataset means. The three metrics of average flow, peak flow, and volume estimates are evaluated. Statistically significant differences were not apparent between the means for any scenarios except the average flow metric of the Aggregation 3 and 4 scenario comparisons (n=46, alpha = 0.05).

Statistic/Metric	Original - Flow	Aggregation 1 - Flow	Original - Peak	Aggregation 1 - Peak	Original - Volume	Aggregation 1 - Volume
Mean	94	101	8,671	9,494	4,108	4,102
Variance	4,005	4,489	62,363,247	81,024,823	1,360,416	1,354,805
Standard Deviation	63.29	67.00	7,897	9,001	1,166	1,164
Degrees of Freedom	46		46		46	
Pooled Variance	8,678.97		146,505,202		2,774,248	
t Stat	(0.006)		(0.000)		0.000	
P(T<=t) one-tail	0.359		0.369		0.492	
t Critical one-tail	2.04		2.04		2.04	
95% CI of difference in Means (lower bound)	-34.56		-4428		-489.8	
95% CI of difference in Means (upper bound)	20.94		2783		502.5	

Table 18. Continued

Statistic/Metric	Original - Flow	Aggregation 2 - Flow	Original - Peak	Aggregation 2 - Peak	Original - Volume	Aggregation 2 - Volume
Mean	94	96	8,671	8,468	4,108	3,990
Variance	4,005	7,067	62,363,247	46,691,489	1,360,416	1,269,637
Standard Deviation	63.29	84.07	7,897	6,833	1,166	1,127
Degrees of Freedom	46		46		46	
Pooled Variance	11,312.78		111,425,491		2,687,228	
t Stat	(0.001)		0.000		0.000	
P(T<=t) one-tail	0.467		0.462		0.361	
t Critical one-tail	2.04		2.04		2.04	
95% CI of difference in Means (lower bound)	-33.46		-2941		-369.8	
95% CI of difference in Means (upper bound)	29.90		3348		606.7	

Table 18. Continued

Statistic/Metric	Original - Flow	Aggregation 3 - Flow	Original - Peak	Aggregation 3 - Peak	Original - Volume	Aggregation 3 - Volume
Mean	94	124	8,671	6,277	4,108	3,836
Variance	4,005	4,380	62,363,247	18,629,791	1,360,416	1,163,835
Standard Deviation	63.29	66.18	7,897	4,316	1,166	1,079
Degrees of Freedom	46		46		46	
Pooled Variance	8,567.02		82,753,756		2,579,125	
t Stat	(0.025)		0.000		0.001	
P(T<=t) one-tail	0.055		0.100		0.203	
t Critical one-tail	2.04		2.04		2.04	
95% CI of difference in Means (lower bound)	-58.05		-316		-206.7	
95% CI of difference in Means (upper bound)	(2.91)		5104		750.1	

Table 18. Continued

Statistic/Metric	Original - Flow	Aggregation 4 - Flow	Original - Peak	Aggregation 4 - Peak	Original - Volume	Aggregation 4 - Volume
Mean	94	32	8,671	6,615	4,108	3,826
Variance	4,005	102	62,363,247	21,501,000	1,360,416	1,158,701
Standard Deviation	63.29	10.09	7,897	4,637	1,166	1,076
Degrees of Freedom	46		46		46	
Pooled Variance	4,196.15		85,687,383		2,573,880	
t Stat	0.104		0.000		0.001	
P(T<=t) one-tail	0.000		0.139		0.194	
t Critical one-tail	2.04		2.04		2.04	
95% CI of difference in Means (lower bound)	42.60		-701		-195.9	
95% CI of difference in Means (upper bound)	81.19		4813		759.8	

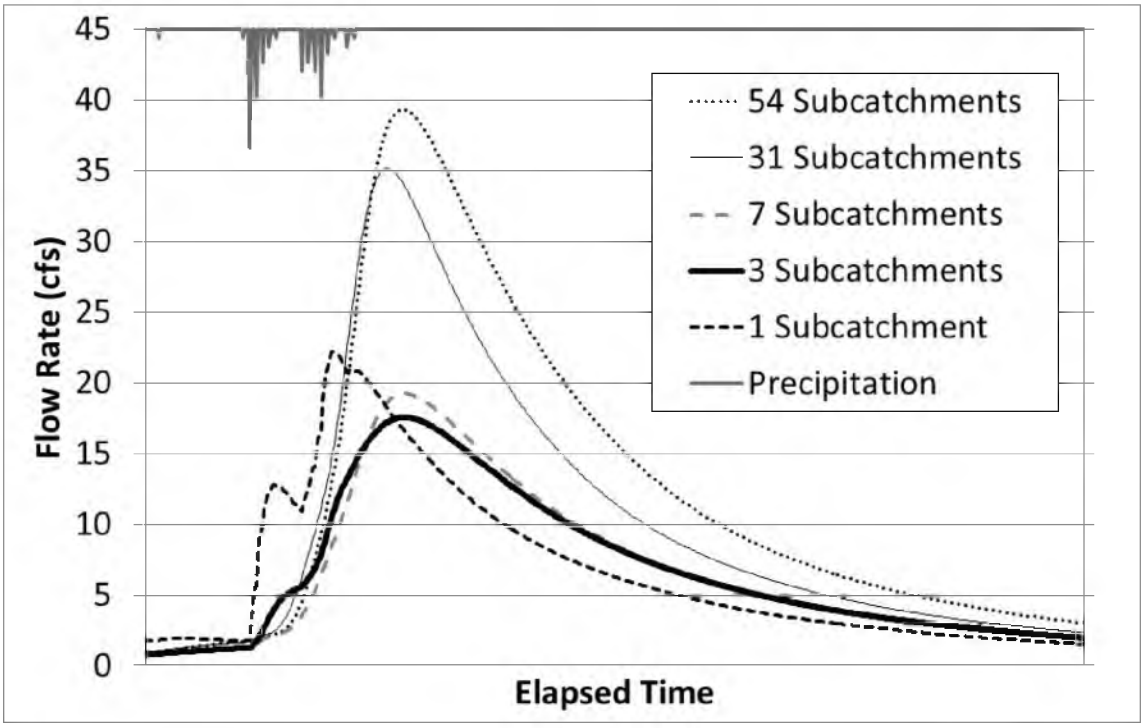

Figure 21. Hydrographs produced from the May 25, 2004 event for the 7, 3, and 1 subcatchment(s) scenarios. Time to peak, peak discharge, and volume estimates are substantially impacted by aggregation of the subcatchments.

The issue of reduced volume is more exaggerated for the SLC model and a review of the area distributions for each scenario reinforces the opinion that lumping GSWI systems and other surface characteristics over large subcatchment areas produces large variations in output results (Table 19). For this model, the 31 subcatchment scenario is the only aggregated scenario that is comparable to the original-fully discretized scenario. However, this scenario still produces consistently lower average flow and volume estimates as compared to the fully discretized results.

Table 19. Subcatchment area statistics for the SLC model.

Simulation ID	Maximum Subcatchment Area (acres)	Minimum Subcatchment Area (acres)	Average Subcatchment Area (acres)
54 Sheds	6,020	16.68	676.2
31 Sheds	6,020	257.73	1,178
7 Sheds	20,516	888.86	5,217
3 Sheds	25,245	5,490	12,172
1 Shed	36,517	36,517	36,517

SLC Statistical Analysis

A summary of the descriptive statistics for each scenario (original – fully discretized and aggregated) is presented in Table 20. These statistics reiterate the scatter variance from the plotted results in the previous section. The variation in values is large for all aggregation scenarios for this model and may be a direct influence from the large subcatchment sizes simulated.

T-Test

The t-test results showed the targeted distribution means were not statistically different with respect to any of the hydrologic metrics as compared to the uniform distribution simulation. The values were calculated based on an alpha value = 0.05 and n = 40 observations. To determine the statistical significance of the results, each hydrologic characteristic (i.e., average flow, peak flow, and volume) was evaluated using three statistical metrics: 1) The calculated t-statistic was compared against the t-critical value, 2) the confidence intervals were calculated, and 3) the calculated p-value was compared to the alpha value.

Table 20. Subcatchment aggregation scenarios descriptive statistics for average flow rate, peak discharge, and volume.

Average Flow (cfs)								
Simulation	n	Mean	Standard Deviation	Standard Error	95% confidence		Minimum	Maximum
					Upper	Lower		
37% GSWI Baseline: 54 Sheds	21	5.1	1.3	1.7	5.7	4.5	2.6	7.7
37% GSWI Aggregate 1: 31 Sheds	21	4.1	1.0	1.1	4.6	3.7	2.1	6.2
37% GSWI Aggregate 2: 7 Sheds	21	2.7	0.6	0.4	3.0	2.5	1.5	4.0
37% GSWI Aggregate 3: 3 Sheds	21	2.7	0.6	0.4	3.0	2.5	1.5	3.9
37% GSWI Aggregate 4: 1 Sheds	21	2.7	0.6	0.3	2.9	2.4	1.5	3.8
Peak Flow (cfs)								
Simulation	n	Mean	Standard Deviation	Standard Error	95% confidence		Minimum	Maximum
					Upper	Lower		
37% GSWI Baseline: 54 Sheds	21	162	65	4,241	190	134	56	298
37% GSWI Aggregate 1: 31 Sheds	21	170	84	6,979	206	135	48	350
37% GSWI Aggregate 2: 7 Sheds	21	68	34	1,143	83	54	25	145
37% GSWI Aggregate 3: 3 Sheds	21	58	28	773	70	46	22	126
37% GSWI Aggregate 4: 1 Sheds	21	74	54	2,939	97	50	34	289
Volume (MG)								
Simulation	n	Mean	Standard Deviation	Standard Error	95% confidence		Minimum	Maximum
					Upper	Lower		
37% GSWI Baseline: 54 Sheds	21	1,186	305	92,876	1,317	1,056	606	1,803
37% GSWI Aggregate 1: 31 Sheds	21	959	242	58,518	1,063	856	485	1,463
37% GSWI Aggregate 2: 7 Sheds	21	638	144	20,673	699	576	353	943
37% GSWI Aggregate 3: 3 Sheds	21	631	140	19,517	690	571	352	923
37% GSWI Aggregate 4: 1 Sheds	21	623	133	17,668	680	566	353	885

For the means for the targeted scenarios to be statistically different from the mean of the uniform distribution results, the following criteria must be met:

1. The calculated t-statistic > the t-critical value (2.04);
2. The value of the null hypothesis (i.e., difference in means = 0) must fall outside the bounds of the confidence interval; and
3. The calculated p-value must be less than the alpha value (i.e., 0.05).

By all metrics, the aggregated scenario means are statistically different from the original-fully discretized scenario mean (Table 21).

Conclusions

Average flow rate was significantly affected by increasingly aggregating the subcatchments, while the peak discharge and volume estimates were less affected across all PHL aggregate scenarios. However, all metrics were significantly impacted by the aggregation of the SLC model, which is represented by larger subcatchments as compared to the PHL model. The effect on average flow is thought to be a product of aggregating subcatchment area parameters that have a large influence on hydrologic response estimates (e.g., overland flow width and percent impervious) and simplification of the hydraulic network. Aggregating subcatchments can have a substantial impact on the time to peak runoff and can substantially modify the recession limb of the outlet hydrograph. Sensitivity analyses targeting the subcatchment size to further evaluate the influences these parameters have on aggregating GSWI subcatchments.

This research can be expanded to include sensitivity analyses on critical subcatchment characteristics, such as overland flow width, infiltration parameters, and

Table 21. T-test results comparing the aggregated scenario dataset means to the original-fully discretized dataset mean for average flow, peak flow, and volume estimates. The results show statistically significant difference between the means (n=40, alpha = 0.05)

Statistic/Metric	Original - Flow	Aggregation 1 - Flow	Original - Peak	Aggregation 1 - Peak	Original - Volume	Aggregation 1 - Volume
Mean	5	4	162	170	1,186	959
Variance	2	1	4,241	6,979	92,876	58,518
Standard Deviation	1.32	1.04	65	84	305	242
Degrees of Freedom	40		40		40	
Pooled Variance	2.89		11,501		155,178	
t Stat	3.781		-0.50		3.786	
P(T<=t) one-tail	0.005		0.363		0.005	
t Critical one-tail	2.04		2.04		2.04	
95% CI of difference in Means (lower bound)	0.44		-42.25		102.09	
95% CI of difference in Means (upper bound)	1.52		26		352.57	

Table 21. Continued

Statistic/Metric	Original - Flow	Aggregation 2 - Flow	Original - Peak	Aggregation 2 - Peak	Original - Volume	Aggregation 2 - Volume
Mean	5	3	162	68	1,186	638
Variance	2	0	4,241	1,143	92,876	20,673
Standard Deviation	1.32	0.62	65	34	305	144
Degrees of Freedom	40		40		40	
Pooled Variance	2.17		5,519		116,388	
t Stat	10.520		8.31		10.549	
P(T<=t) one-tail	0.000		0.000		0.000	
t Critical one-tail	2.04		2.04		2.04	
95% CI of difference in Means (lower bound)	1.89		70.48		440.02	
95% CI of difference in Means (upper bound)	2.83		118		656.94	

Table 21. Continued

Statistic/Metric	Original - Flow	Aggregation 3 - Flow	Original - Peak	Aggregation 3 - Peak	Original - Volume	Aggregation 3 - Volume
Mean	5	3	162	58	1,186	631
Variance	2	0	4,241	773	92,876	19,517
Standard Deviation	1.32	0.60	65	28	305	140
Degrees of Freedom	40		40		40	
Pooled Variance	2.14		5,140		115,203	
t Stat	10.721		9.52		10.746	
P(T<=t) one-tail	0.000		0.000		0.000	
t Critical one-tail	2.04		2.04		2.04	
95% CI of difference in Means (lower bound)	1.93		81.18		447.96	
95% CI of difference in Means (upper bound)	2.86		127		663.78	

Table 21. Continued

Statistic/Metric	Original - Flow	Aggregation 4 - Flow	Original - Peak	Aggregation 4 - Peak	Original - Volume	Aggregation 4 - Volume
Mean	5	3	162	74	1,186	623
Variance	2	0	4,241	2,939	92,876	17,668
Standard Deviation	1.32	0.57	65	54	305	133
Degrees of Freedom	40		40		40	
Pooled Variance	2.11		7,360		113,307	
t Stat	10.941		6.77		10.978	
P(T<=t) one-tail	0.000		0.000		0.000	
t Critical one-tail	2.04		2.04		2.04	
95% CI of difference in Means (lower bound)	1.96		61.27		456.18	
95% CI of difference in Means (upper bound)	2.88		116		670.21	

slope to better understand the magnitude of influence each may have on watershed-scale GSWI estimates. The profession would also benefit from conducting similar analyses on a variety of urban areas in different climates. Furthermore, the response of GSWI networks to climate change impacts could broaden the scope of understanding among professional planners, engineers, and others within the Water Resources profession.

Understanding how GSWI representation within urban planning models affects the potential hydrologic benefits will improve the overall engineering process of GSWI networks from conception through design and construction. Refining the methodology to simulate more accurate estimated benefits at the planning stage will reduce costs throughout the lifespan of the project by minimizing adjustments to the design from large errors in simulated benefits. Furthermore, our work adds to the growing body of knowledge identifying the necessary considerations when building planning models for GSWI networks.

CHAPTER V

CONCLUSIONS AND RECOMMENDATIONS

The first goal of this project was to evaluate the performance of a novel watershed-scale GSWI up-scaling algorithm. The second goal was to identify influences on GSWI hydrologic response estimates from varying spatial distribution and subcatchment aggregation scenarios. These goals were achieved by meeting the following objectives: 1) compare watershed-scale output from a nondescript collective representation of GSWI to output produced from design-specific representations, 2) use t-test statistical significance testing to identify the effect from spatial targeting of GSWI versus uniformly distributing GSWI and 3) use use t-test statistical significance testing to identify the effect from increasingly aggregated subcatchments containing GSWI a the watershed-scale. The key conclusions derived from these analyses are:

- Watershed-scale up-scaling methods representing GSWI as collective units can perform comparably to other design-specific GSWI up-scaling tools. Differences between the two methods for average flow rate, peak discharge, and volume were within a tolerance of ±5%. Thus, depending on the modeling objective, the collective representation is determined to be suitable for use in urban area planning studies.
- For the SLC model, using targeted GSWI implementation patterns yielded

greater peak discharge estimates versus uniform distribution patterns, though the differences were not statistically significant ($n=630$, $\alpha=0.05$, $p=0.164$). The differences are attributed to the dampening effect generated by the uniform distribution scenario. The average flow and volume estimates showed minor variations, but were not statistically different from the uniform distribution ($n=630$, $\alpha=0.05$, $p=0.427$; $n=630$, $\alpha=0.05$, $p=0.424$).

- The increasingly aggregated SLC model results produced substantial modifications to the outlet hydrograph time to peak and recession limb characteristics. Specifically, as subcatchments were increasingly aggregated, more volume of runoff was shifted into the peak and a simultaneous reduction in volume was observed in the recession limb. Furthermore, the time to peak moved toward an instantaneous response as aggregation increased.
- For SLC model scenarios, aggregating GSWI subcatchments significantly influenced all flow metrics ($n = 40$, $\alpha=0.05$, $p=0.000$; $n = 40$, $\alpha=0.05$, $p= 0.000$; $n = 40$, $\alpha=0.05$, $p= 0.000$). The influence of aggregation was less substantial for the PHL sceanarios, although the variation was still high. Increases and reductions in average flow rate and peak discharge were recorded, which were influenced from changes in hydraulic loading locations. Volume estimates were the least impacted by subcatchment aggregation within the PHL model, but substantially more affected within the SLC model.
- Hydrologic response sensitivity is far less from model adjustments for spatial distribution scenarios than that of subcatchment aggregation. Subcatchment aggregation requires adjustments to critical surface characteristics (e.g.,

impervious area, infiltration, slope, overland flow width), which if not handled properly during aggregation, can produce large variances in hydrologic response estimates. It also appears that subcatchment size plays a significant role in the variation on hydrologic response.

While this research lends support to the use of an alternative GSWI up-scaling method and elucidates important influences from GSWI distribution and aggregation on a watershed-scale, it also opens up a number of opportunities for further research. Expanding the hydrologic output sensitivity analyses from aggregating influences to include surface characteristics such as overland flow width and slope are needed. Both parameters can have substantial influences on surface routing performance and therefore warrant a thorough analysis when incorporating GSWI into watershed-scale models. This is especially true for urban areas like Salt Lake City, Utah where surface characteristics are highly variable across the watershed.

More applications using the up-scaling algorithm representing GSWI as a collective unit are needed to further substantiate the results herein. Furthermore, evaluations into the different scales and urban environments to which this method can be reasonably applied would help further define its use in urban area modeling studies. Indeed, research of this nature is essential for all GSWI up-scaling tools to define an appropriate scope of applicability.

Perhaps most importantly, the need to calibrate and validate GSWI output using watershed-scale observed data is paramount to improve simulations of watershed-scale GSWI benefits. It is acknowledged that this component is not an easily performed, nor should it be an arbitrarily conducted, task; however, it is a critical component in further

developing tools and methods that accurately depict the complex interaction of GSWI on a watershed-scale. Without these data, the information produced from all watershed-scale GSWI up-scaling algorithms can only be evaluated relative to one another and therefore none can explicitly be identified as better or worse at representing GSWI networks.

APPENDIX A

TOOLS AND DATA SOURCES

Research Tools

Three existing programs will be used to meet each objective of the research plan: ArcGIS, MS Excel, and SWMM5. The up-scaling processes of H1O will be automated using MS Excel software. The H2O spatial selection algorithms are carried out using ArcGIS software and spatial datasets identifying surface characteristics of the study area within ArcGIS. The H3O model simulations are completed using the U.S. EPA Stormwater Management Model version 5.0.022 (SWMM5). A description of each program is included in the sections that follow.

ArcGIS

ArcGIS is geographical information system software that combines the efficiency of databases and the usefulness of spatial information. It is a powerful tool to use for spatial research and problem solving and is ideal in choosing spatially significant locations for a variety of spatial problems. The development software can be used to create code for specific functionality and spatial tool development. The software may also be used in conjunction with outside programs such as MS Excel.

MS Excel

The spreadsheet program from the Microsoft office suite allows for data to be easily organized, used, and edited through the use of tabbed sheets and a variety of internal equations and algorithms. Macros may be created using the internal VBA code software to create specific tools for increased functionality. VBA uses an object-oriented coding paradigm, which is incredibly user-friendly and easy to use.

SWMM5

Originally developed in 1971, the SWMM5 model is a 2-dimensional coupled hydrologic-hydraulic model. Calculations are based on physical processes and use the concepts of conservation of mass, energy, and momentum to estimate hydrologic and hydraulic responses to input datasets (U.S. EPA 2010). Because SWMM5 is a coupled hydrologic-hydraulic model, it allows the user to adjust both the surface parameters as well as underlying sewer characteristics within the same model. It is open-source modeling software and is available at no cost from the U.S. EPA website.

Data Sources

Rainfall Data

Salt Lake City, Utah Model

Long-term continuous rainfall data for the Salt Lake City, Utah models was downloaded from the National Climatic Data Center (NCDC) rain gage located at the Salt Lake International Airport (Gage ID: 427598). The dataset was downloaded from the NCDC site for the years 1990 through 2010. For the single-event simulations, the rainfall

depth of 0.81 inches from the May 25, 2004 storm for Salt Lake City, Utah was used.

Philadelphia, Pennsylvania Model

The long-term continuous rainfall data for the Philadelphia, Pennsylvania model were received from the Philadelphia Water Department (PWD). The PWD has collected rainfall throughout the city since 1990. For the model used in this research, rainfall data from four raingages were used to run the model simulations. The raingages were associated to subcatchments based on its proximity to the sheds.

GIS Data

Salt Lake City, Utah

The GIS data used to represent the Salt Lake City, Utah area were obtained through the Utah Automated Georeferencing Center (AGRC). Layers downloaded for this research are included Table 22.

Philadelphia, Pennsylvania

All GIS layers used to represent the Philadelphia, Pennsylvania study area were provided courtesy of the Philadelphia Water Department (PWD). PWD collects and maintains its own set of extensive spatial datasets for use within the department for various studies and infrastructure maintenance assessments. These datasets include raingage, subcatchment, subsurface hydrology, and hydraulics information.

Table 22. GIS datasets used and the source of the data.

Layer Name	Source
SGID10.Geoscience.Soils	Utah AGRC, NRCS
SGID10.Demographic.CensusBlocks2010	U.S. Census Bureau
State, County, Municipal Boundaries	Utah AGRC
SGID10.Water.Watersheds_Area	BLM, NRCS, U.S. Forest Service, USGS

APPENDIX B

RESEARCH PLAN

H1O: Developing an Automated Version of the PWD (2009) Up-Scaling Algorithm

This section will first describe the PWD (2009) up-scaling algorithm and its calculations in detail. Following the algorithm introduction is a description of the tasks, reiterated below, to meet the H1O objective.

1. Import the algorithm into MS Excel and perform a mass balance analysis using the elements generated through the up-scaling algorithm.
2. Simulate the same generated elements created in (1) using SWMM5.
3. Validate the simulated results produced from SWMM5 in (2) to the mass balance spreadsheet solution of (1).
4. Automate the algorithm using MS Excel Visual Basic for Applications (VBA) coding language.
5. Perform an assessment of simulated results of the up-scaling algorithm to results produced by a comparable system represented with the LID module of SWMM5.

Introduction to the Up-Scaling Algorithm

H1O involves automating the PWD (2009) up-scaling algorithm. Required inputs from the user to use the algorithm include:

- Percent Implementation (X) – Percent of DCIA to be managed by GSWI;
- Loading Ratio (LR) – The desired ratio of drainage area managed per acre of GSWI (typical values range from 10:1 to 20:1);
- Water Quality Capture Volume (WQCV) – The volume of surface runoff to be managed by the GSWI;
- Drawdown Time (T) – The maximum time allowed to drain the ponded water from the GSWI;
- Weir Height (HW) – The maximum depth of storage before overflow occurs in the GSWI;
- Average Release Rate (Q_{AVG}) – The average allowable rate of flow discharged from the storage element per unit of impervious area;
- Orifice Discharge Coefficient (C_D) – Accounts for the geometry of the orifice that discharges flow from the storage element of the GSWI.

Once the modeler has provided the above inputs, the algorithm begins by identifying the total impervious area (TIA) for each subcatchment as provided by the baseline model input file. This value is designated as I_o (Figure 22). The pervious area of the subcatchment is calculated using Equation 2.

$$P = A_T - I_o \quad (2)$$

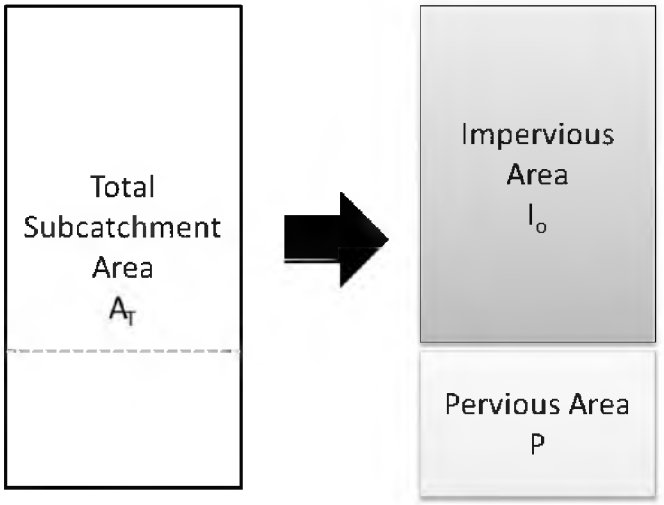

Figure 22. Subcatchment schematic showing the total subcatchment area and the subareas representing the TIA designated as I_o and the total pervious area designated as P.

Where,

P = Original pervious area (acres)

A_T = Total subcatchment area (acres)

I_o = Total impervious area (TIA) (acres)

Using the percent of GSWI implementation (X), the total area to be controlled (I_c + P_c) may be calculated by Equation 3:

$$(I_c + P_c) = I_o(X) \quad (3)$$

Where,

I_c = Impervious area managed by the GSWI (acres)

P_c = Pervious surface area of GSWI (acres)

The pervious surface area of GSWI and the controlled DCIA may be determined using the loading ratio (LR) within Equation 4 and Equation 5.

$$P_c = (I_c + P_c) / (LR + 1) \quad (4)$$

$$I_c = P_c(LR) \quad (5)$$

Where,

LR = Ratio of controlled DCIA draining to a unit of GSWI area (ac/ac)

These areas are used to create a new subcatchment where the total area is equal to ($I_c + P_c$), as shown in Figure 23. The impervious area that is not being managed by GSWI is calculated in Equation 6 by subtracting the new subcatchment area as represented by ($I_c + P_c$). Figure 24 provides a schematic of the resulting subcatchments and the relative areas.

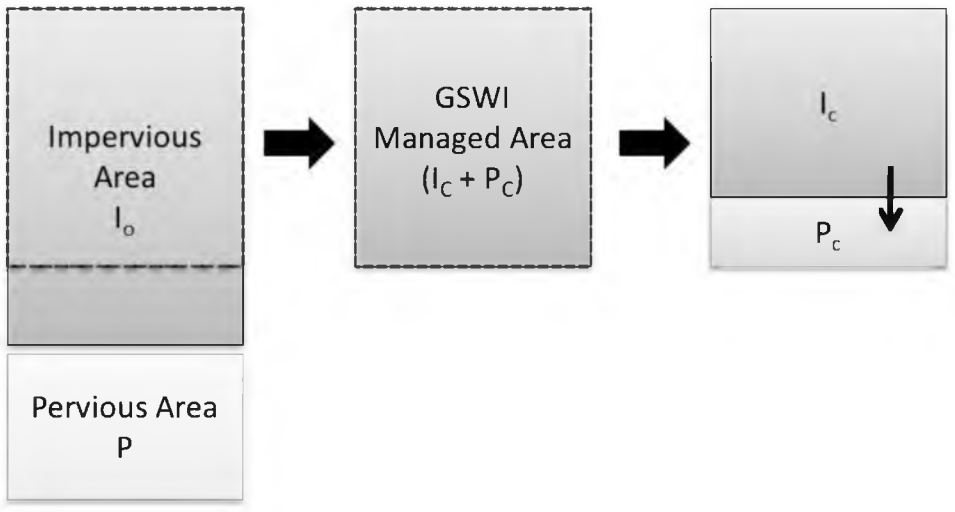

Figure 23. Schematic of the new subcatchment created to represent GSWI and the portion of DCIA draining to the GSWI.

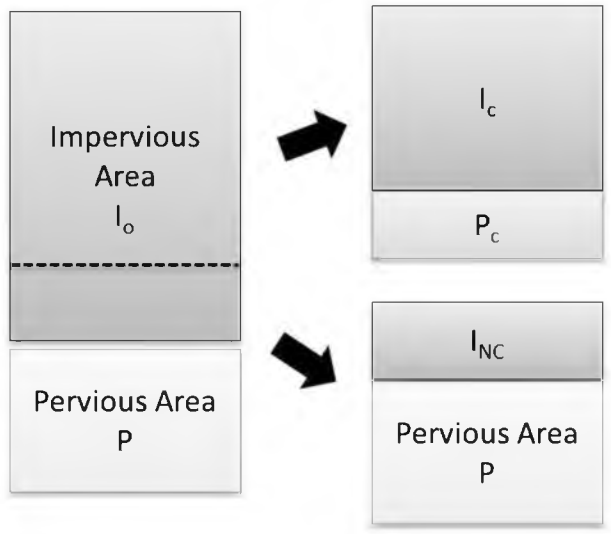

Figure 24. Final subcatchments created from Equations 2 through 6.

$$I_{NC} = I_o - (I_c + P_c) \quad (6)$$

Where,

I_{NC} = The area of TIA not managed by GSWI (acres)

The new subcatchment comprised of I_c and P_c represents the impervious area loading to GSWI and the GSWI area itself. This allows the runoff generated by the impervious portion to run-on to the adjacent GSWI parcel prior to entering the sewer system.

The next series of calculations estimates the minimum volume of infiltration to be expected from the GSWI pervious surface (P_c). The minimum volume between the WQCV produced from the managed DCIA (I_c) area and the volume of ponded water that can reasonably expected to be infiltrated within the designated drawdown time (T). The equations for these estimates are identified as Equation 7, Equation 8, and Equation 9.

$$WQCV_T = (WQCV)(I_c)[43{,}560\ (ft^2/ac) / 12\ (in/ft)] \quad (7)$$

$$TDI = (P_c)(K_{sat})(T)[43{,}560\ (ft^2/ac) / 12\ (in/ft)] \quad (8)$$

$$V_I = \text{Minimum}\ (WQCV_T, TDI) \quad (9)$$

Where,

K_{sat} = The saturated soil hydraulic conductivity taken from the baseline input file for the respective subcatchment (in/hr)

$WQCV_T$ = The total volume of runoff to manage over the controlled DCIA based on the WQCV defined by the user (ft^3)

WQCV = The depth of runoff to manage (inches)

TDI = The volume of ponded water that can reasonably be expected to infiltrate within the designated drawdown time (ft^3)

V_I = Estimated infiltration volume of the GSWI (ft^3)

Now that the infiltration volume is estimated, the GSWI pervious area depression storage may be calculated using Equation 10.

$$D_C = [V_I / (P_C)(43{,}560\ ft^2/ac)](12\ in/ft) \quad (10)$$

Where,

D_C = GSWI surface depression storage (inches)

The hydraulic elements of the up-scaling algorithm consist of a storage node, an

orifice, and the overflow conduit (Figure 25). The storage node is sized to capture and detain the volume in excess of what can be infiltrated as calculated with Equations 7 through 10. Therefore, the combined capacity of the depression storage of P_c and the storage node is equal to the required volume to manage as defined by the user for the controlled DCIA (i.e., $WQCV_T$). Sizing the hydraulic elements requires an estimate of the volume of runoff that will need to be stored and the surface area of the unit. These are calculated with Equation 11 and Equation 12.

The storage node has two outlets: 1) a controlled slow release orifice and 2) an overflow pipe. The slow release orifice regulates flow from the storage node to the sewer system and is set equal to a user-defined value (e.g., cubic feet per second (cfs)/acre). The algorithm assumes the maximum discharge allowed is twice the average discharge value provided by the user (i.e., a peaking factor of 2). Equation 13, Equation 14, and Equation 15 are used to define the geometry of the orifice.

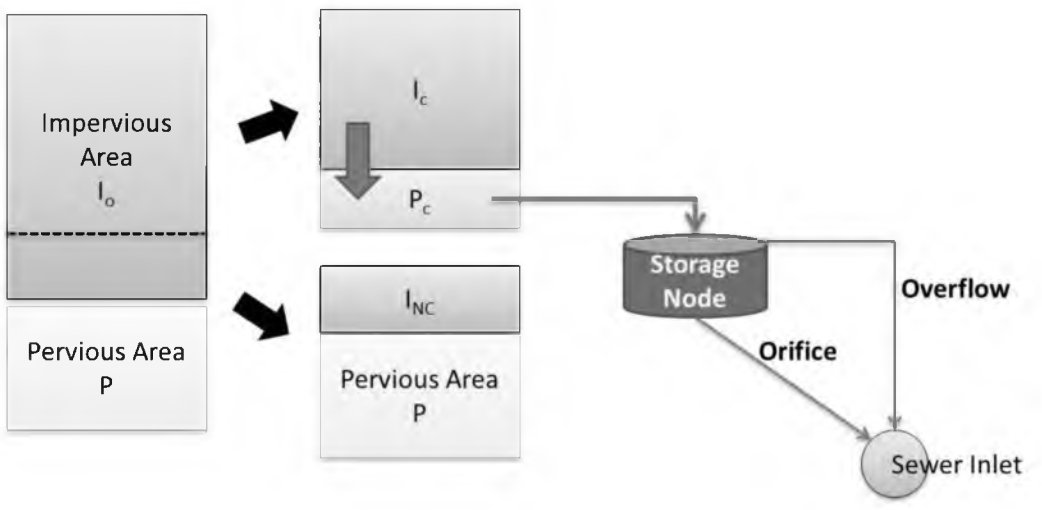

Figure 25. Schematic of the hydraulic setup produced by the PWD (2009) up-scaling algorithm.

$$V_{TR} = WQCV_T - V_I \quad (11)$$

$$A_N = V_{TR} / HW \quad (12)$$

Where,

V_{TR} = the total required storage volume to manage (ft^3)

A_N = The surface area of the storage node (ft^2)

HW = the maximum depth of the storage node (ft)

$$Q_{PEAK} = 2Q_{AVG} \quad (13)$$

$$A_o = (Q_{PEAK})(C_D)(2gHW)^{1/2} \quad (14)$$

$$D_o = (4A_o/\pi)^{1/2} \quad (15)$$

Where,

Q_{PEAK} =Maximum allowable release rate from orifice (ft^3/s)

Q_{AVG} = Average allowable release rate for the controlled DCIA (ft^3/s)

A_o = Area of the orifice (ft^2)

C_D = Discharge coefficient (unitless)

g = Gravitational constant (ft/s^2)

D_o = Orifice diameter (ft)

The second outlet from the storage node is meant to track the bypass from the

GSWI element. This is accomplished through the use of an overflow weir with its offset height equal to the maximum depth of the storage node (HW). The overflow weir is meant to be unrestrictive and therefore, the size of the weir is exaggerated to provide uninhibited routing from the storage node to the sewer inlet. The weir depth is set equal to 10 feet and the length of the weir is set equal to 100 feet.

Both outlet pipes are routed to an outfall node, as is the unmanaged impervious and pervious areas of the subcatchment (I_{NC} and P, respectively). This represents the entire flow entering the sewer system from a particular subcatchment (Figure 26).

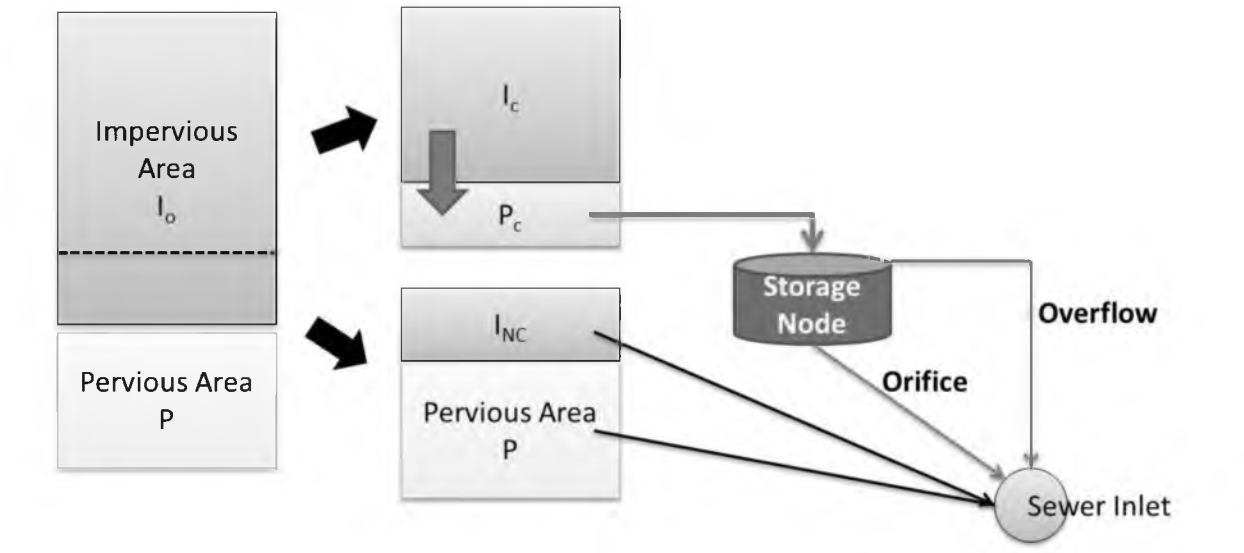

Figure 26. A complete schematic of the structure and flow routing of surface runoff for the GSWI up-scaling procedure.

SWMM5 LID Representation

SWMM5 compartmentalizes its computations based on the following physically based processes:

- Surface Runoff
- Groundwater
- Flow Routing
- Water Quality Routing
- Infiltration
- Snowmelt
- Surface Ponding
- LID Representation

Not all of the above processes are necessary to build a model and perform simulations. For this study, the Surface Runoff, Flow Routing, Infiltration, and LID Representation processes are used to analyze the hypotheses and objectives. A description on the processes employed for this study is provided in the subsections below.

Surface Runoff

Subcatchments represented in SWMM5 are divided into impervious and pervious sections based on the percent impervious value provided by the modeler (Figure 27). Each of these sections (i.e., the impervious area and the pervious area) has specific input data defining the surface. These parameters include depression storage, surface roughness, and surface slope. Both sections of the subcatchment are modeled independently as nonlinear reservoirs. The model performs a mass balance of inflows and outflows for the reservoir to determine surface runoff. The inflows to the reservoir are precipitation and any runoff directed from another subcatchment. The outflows include evaporation, infiltration, and surface runoff (represented as Q in Figure 27).

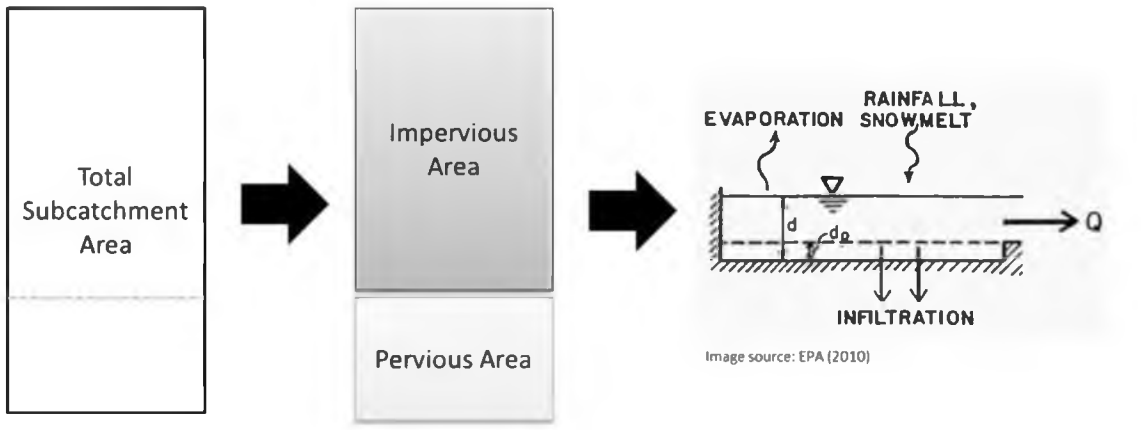

Figure 27. A schematic of the surface runoff conceptual methods employed by SWMM5. The total subcatchment area is divided into impervious and pervious subsections. Each subsection is then modeled as a nonlinear reservoir that produces surface runoff (Q) when the depression storage depth (d_p) has been exceeded.

The depression storage parameter (d_p in Figure 27) defines the amount of water ponded or stored on the surface. Surface runoff will occur when the depression storage depth has been exceeded. For pervious areas, the depression storage parameter is commonly used to represent the detention volume necessary to manage a particular depth of runoff produced from rainfall in order to minimize adverse impacts from urban stormwater runoff. This volume is referred to as the water quality capture volume (WQCV).

It is possible to internally route surface runoff generated from one section of the subcatchment to another within SWMM5 (Figure 28). For the situation presented in Figure 28, the surface runoff generated by the impervious section of the subcatchment is routed to the pervious section. SWMM5 allows the modeler to designate all or only a portion of a subarea to be routed to another subarea. This provides great flexibility in simulating urban area runoff and pervious area interception.

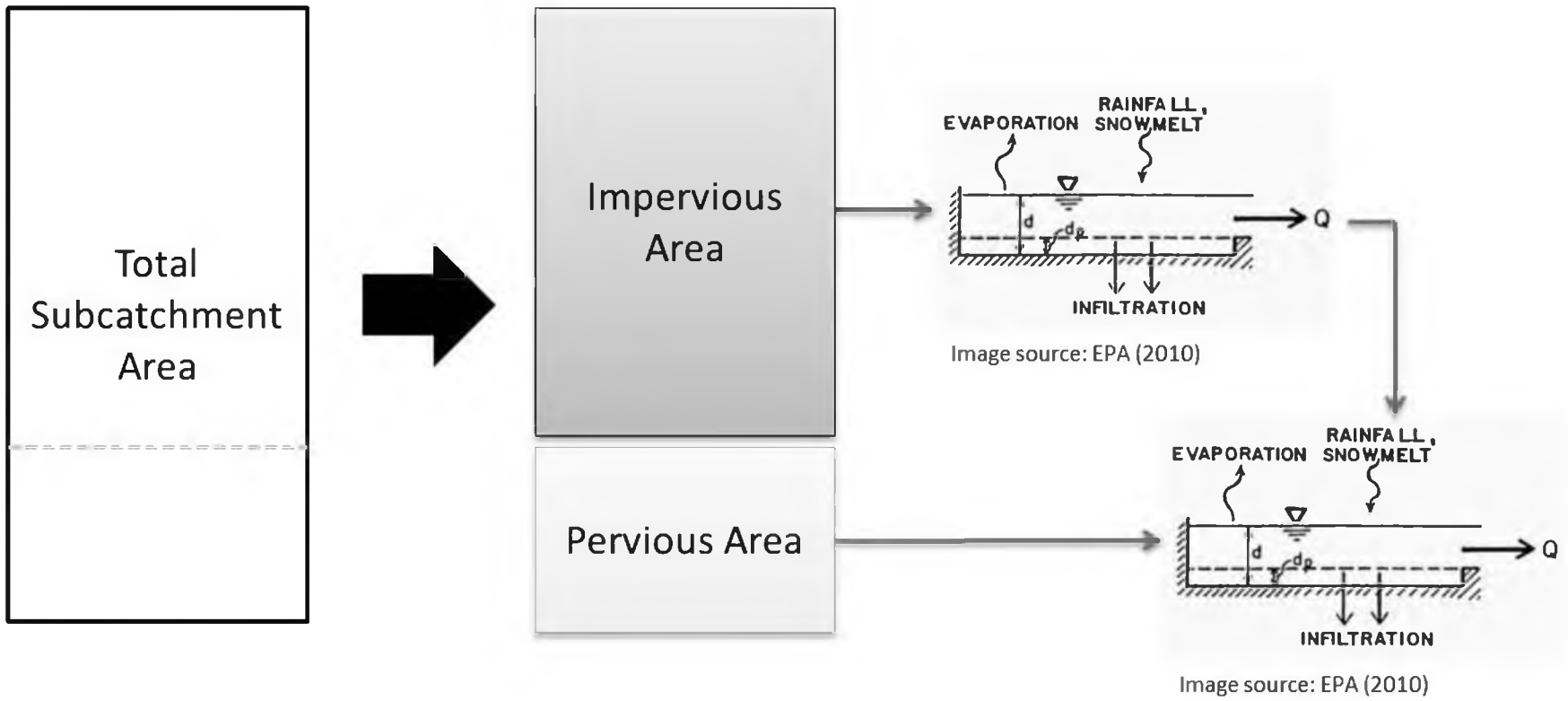

Figure 28. Subarea routing diagram showing the nonlinear reservoir concept for each subarea (i.e., impervious and pervious). The runoff calculated from the impervious area is routed to the pervious area and is used as inflow to the pervious area's nonlinear reservoir calculations.

Oftentimes, this internal routing capability is used to separate directly connected impervious area (DCIA) runoff (i.e., roadway stormwater runoff draining to a street gutter) from impervious area runoff that is intercepted by pervious land cover (i.e., rooftop runoff routed to rain gutters draining to a lawn). Impervious area runoff that is intercepted by pervious area is referred to in this proposal as nondirectly connected impervious area (nDCIA). Figure 29 presents a simplified schematic of how SWMM5 portions the total impervious area (TIA) into DCIA and nDCIA areas and the subsequent routing pathways.

Infiltration

The Green-Ampt method defines the soil infiltration characteristics using an initial soil moisture deficit, a soil hydraulic conductivity, and a wetting front suction head.

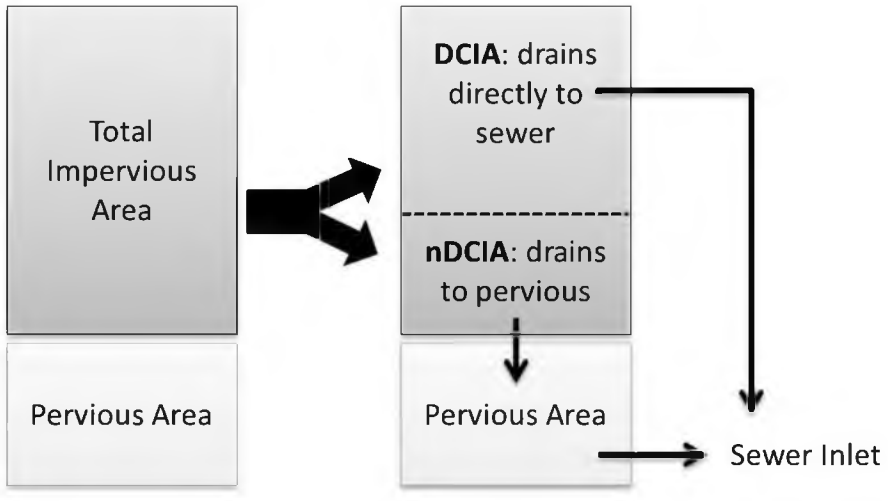

Figure 29. Schematic of internal routing capabilities of SWMM5 subcatchments. The TIA may be divided to have a portion of the surface runoff drain directly to the sewer inlet (i.e., representing DCIA) and the remaining surface runoff be intercepted by the pervious area of the subcatchment (i.e., representing nDCIA).

The initial soil moisture deficit describes the antecedent conditions of the soil prior to receiving any precipitation and essentially represents the maximum volume of storage available in the soil's pore space. The hydraulic conductivity defines the speed at which water flows through the soil under saturated conditions. The maximum suction head describes the capillary suction force from the dry soil pulling the wetting front down through the soil column (Figure 30).

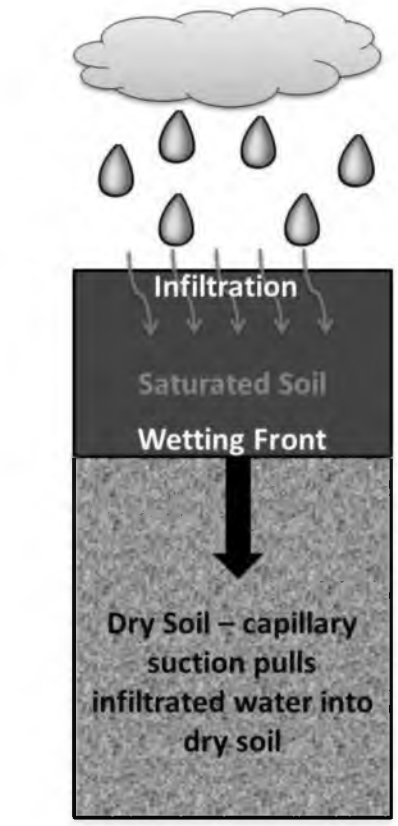

Figure 30. Schematic of the movement of water through a soil column as represented by the Green-Ampt infiltration methodology. Infiltrated water fills available pore space and creates a wetting front, which is pulled down through the soil column from gravitational and capillary suction forces in the dry soil.

Flow Routing

SWMM5 provides three algorithms to simulate flow through a pipe network: steady-state, kinematic wave, and dynamic wave. The three types provide varying degrees of computational complexity. Steady-state assumes uniform and steady flow through the pipe network and does not account for any potential changes to the flow (i.e., friction losses, entrance and exit minor losses, backwater effects, pressurized flow, etc.). The inflow at the upstream end of the conduit will exactly match that of the downstream end of the conduit, meaning the inflow hydrograph is indifferent to time. The use of steady-state routing is not advised for in-depth urban area simulations.

The kinematic wave routing method allows for the inflow timeseries to a conduit to vary spatially and temporally by solving the complete continuity equation and a simplified version of the momentum equation (U.S.EPA 2010). Flow can be lost from downstream nodes due to flooding or it can be allowed to pond and then reintroduced to the system as capacity in the pipe becomes available over time. This means that flow through the conduit may be attenuated, lost, or delayed at each timestep as it moves through the pipe network. The limitations to this flow routing option are that it is not capable of representing backwater effects, pressurized pipes, flow reversal, or minor losses (U.S.EPA 2010).

To be able to account for the backwater, pressurized pipe, flow reversal, or minor loss phenomena, the dynamic wave routing method must be employed. Dynamic wave routing uses an iterative process to solve the St. Venant flow equations, which are derived from the full continuity and momentum equations for flow in conduit sections and volume continuity at the upstream and downstream nodes (U.S.EPA 2010). The use of

this routing method is appropriate for all network types and is necessary for complex systems (e.g., urban drainage networks) experiencing pressurized flows and backwater effects produced from pipe constrictions in downstream sections (i.e., bottlenecking). Therefore, the dynamic wave routing methodology will be used with this study. The drawbacks of this routing technique lie in the computational requirements. A significantly reduced computational timestep is required for the St. Venant equations to converge on a solution. The timestep required is generally less than 1 minute, which means longer runtimes for larger pipe networks.

LID Representation

The functionality of the most current version of SWMM5 has been updated to include a suite of commonly built LID designs, including: bioretention, vegetated swales, infiltration trenches, permeable pavement, and rain barrels. Within SWMM5, these LID types are simulated as a collection of vertical layers representing the surface layer, the soil layer, and the storage/underdrain layer (Figure 31). The surface layer represents ground cover exposed to the atmosphere and is the only layer that directly intercepts precipitation and any runoff from other subcatchments (represented as "Runoff" in Figure 31). The soil layer represents the media used within bioretention LID design types to route the infiltrated water from the surface layer through the media and into the storage layer. The storage layer collects the water and releases it either through an underdrain system and/or through infiltration.

Not all vertical layers are applicable to each of the LID design types. For example, the rain barrel type does not use a surface or soil layer; it only requires the

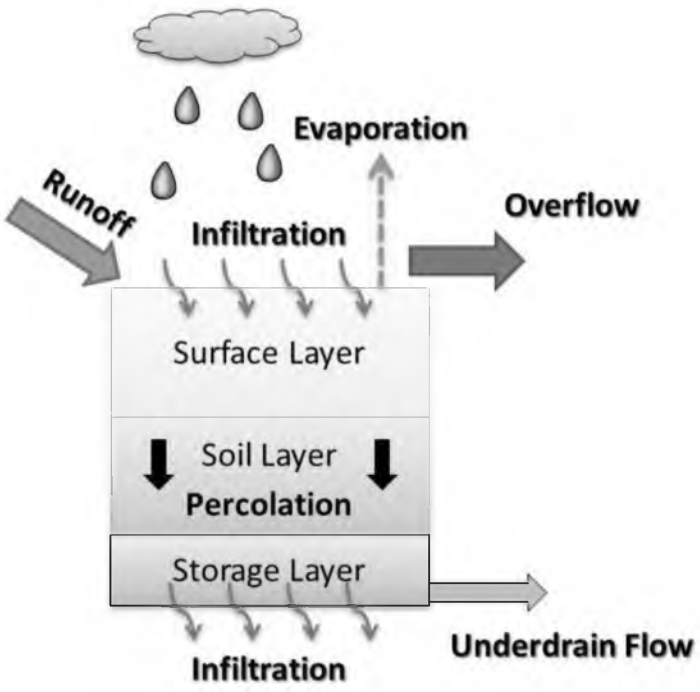

Figure 31. Schematic of the vertical layers used to track the flow through an LID design type within SWMM5. Each LID design type may require data for all vertical layers or a combination of layers to calculate flow through the LID element.

storage and underdrain layer. Alternatively, the bioretention type requires all three vertical layers to simulate flow through the element. Table 23 outlines which of the vertical layers are required for each LID design type.

SWMM5 provides two options for implementing LID design types within a model. The first allows multiple LID design types to displace a portion of the subcatchment's area (Figure 32). With this option, the collection of different LID design types work in parallel to treat portions of the impervious area.

To simulate GSWI treatment in series, the modeler must use the second option, which allows the modeler to simulate an entire subcatchment as a specific LID design type. With this option, runoff from an upstream subcatchment may be directed to the

Table 23. Outline of the required vertical layers for each LID design type available within SWMM5.

LID Element Name	Description of Key Processes	Simulated Vertical Layers
Bioretention	• Infiltration allowed through surface Layer • Evaporation simulated for ponded water on surface layer • Percolation of infiltrated water through the soil layer • Infiltration allowed in storage layer • Optional underdrain system allowed to drain stored water volume	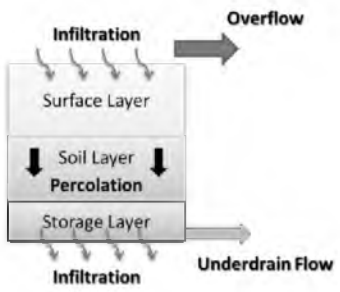
Infiltration Trench	• Infiltration allowed through surface layer • Evaporation simulated for ponded water on surface layer • Infiltration allowed in storage layer • Optional underdrain system allowed to drain stored water volume	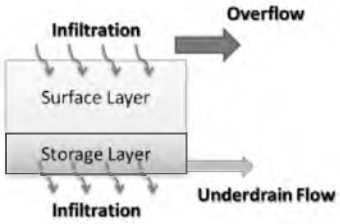
Porous Pavement	• High infiltration rate (i.e., represents permeability of porous asphalt) through surface layer • Evaporation simulated for ponded water on surface layer • Infiltration allowed in storage layer • Optional underdrain system allowed to drain stored water volume	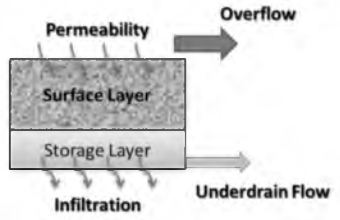
Rain Barrel	• Storage layer collects precipitation and runoff from upstream subcatchments • No infiltration allowed • Underdrain system required to drain stored water volume	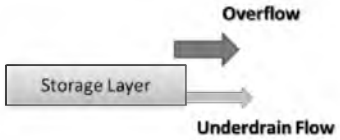
Vegetated Swale	• No infiltration allowed with surface layer • Evaporation of ponded water simulated on surface layer	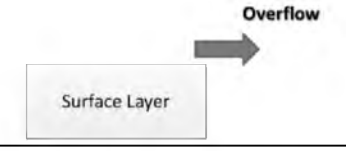

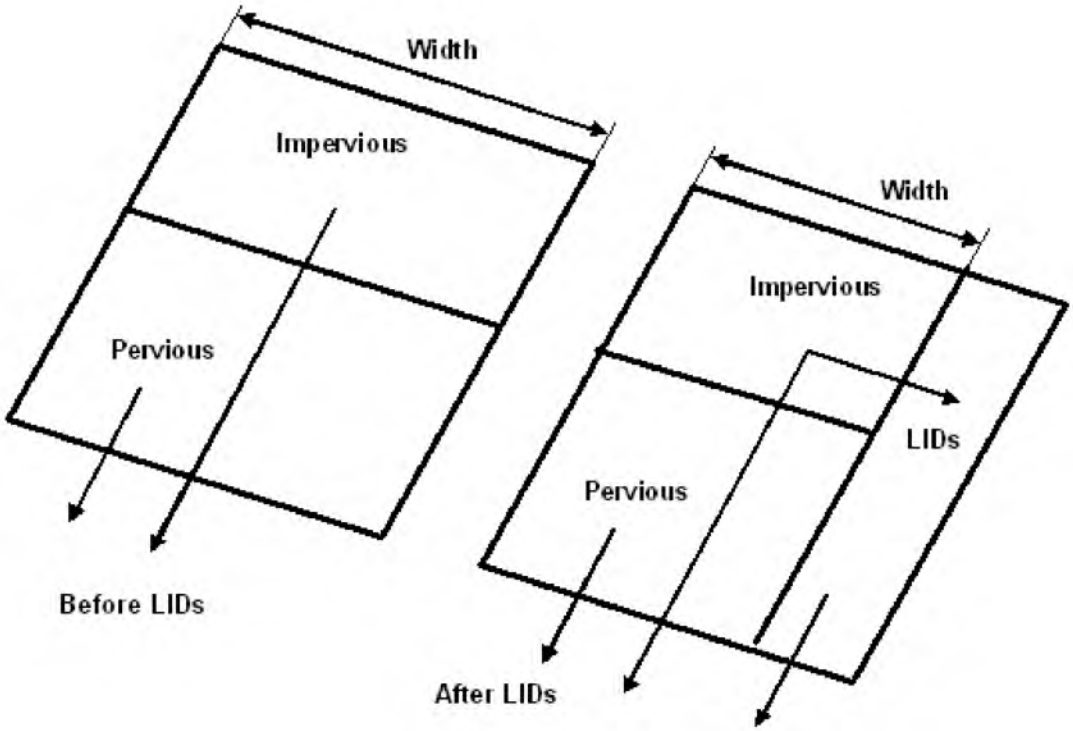

Figure 32. The U.S. EPA (2010) conceptual overview for implementing LID elements in SWMM5 and the routing pathway.

GSWI represented as its own subcatchment. The subsequent runoff from the GSWI may be further managed by routing it to another GSWI represented as a subcatchment (Figure 33). When using the LID elements, it is imperative the modeler understand the limitations with SWMM5 in appropriately distinguishing TIA, DCIA, and nDCIA and the implications on system results. As SWMM5 LID design types are created and implemented within the subcatchment, accounting for these areas becomes increasingly complicated (Figure 34). This is especially true if subarea routing is being used to separate DCIA and nDCIA. Ideally, the LID element should displace the DCIA area to minimize the adverse impact of the runoff loading directly to the sewer system, as is depicted in Figure 34.

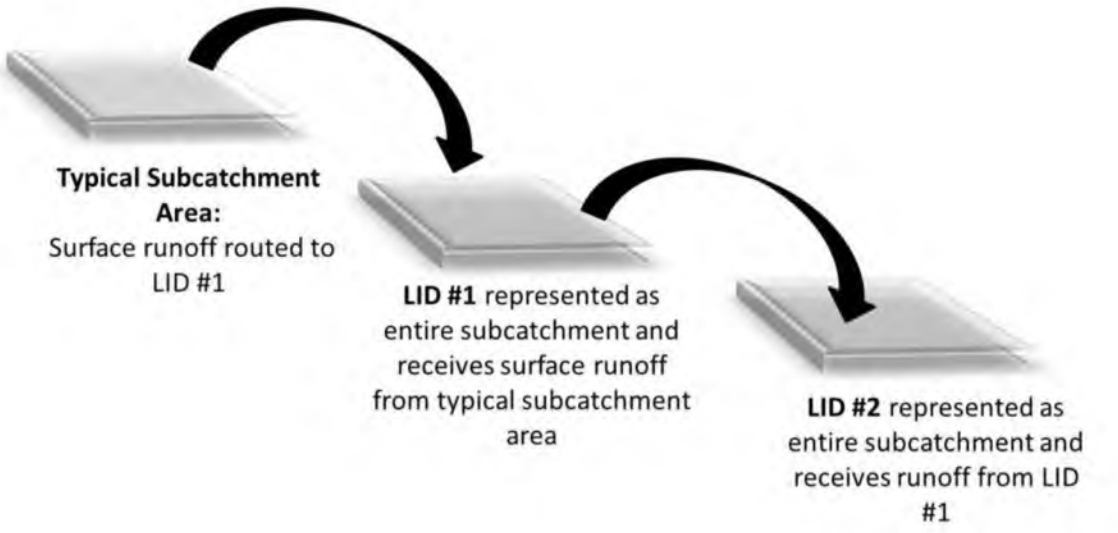

Figure 33. Conceptual diagram of how SWMM5 LID elements are simulated in series.

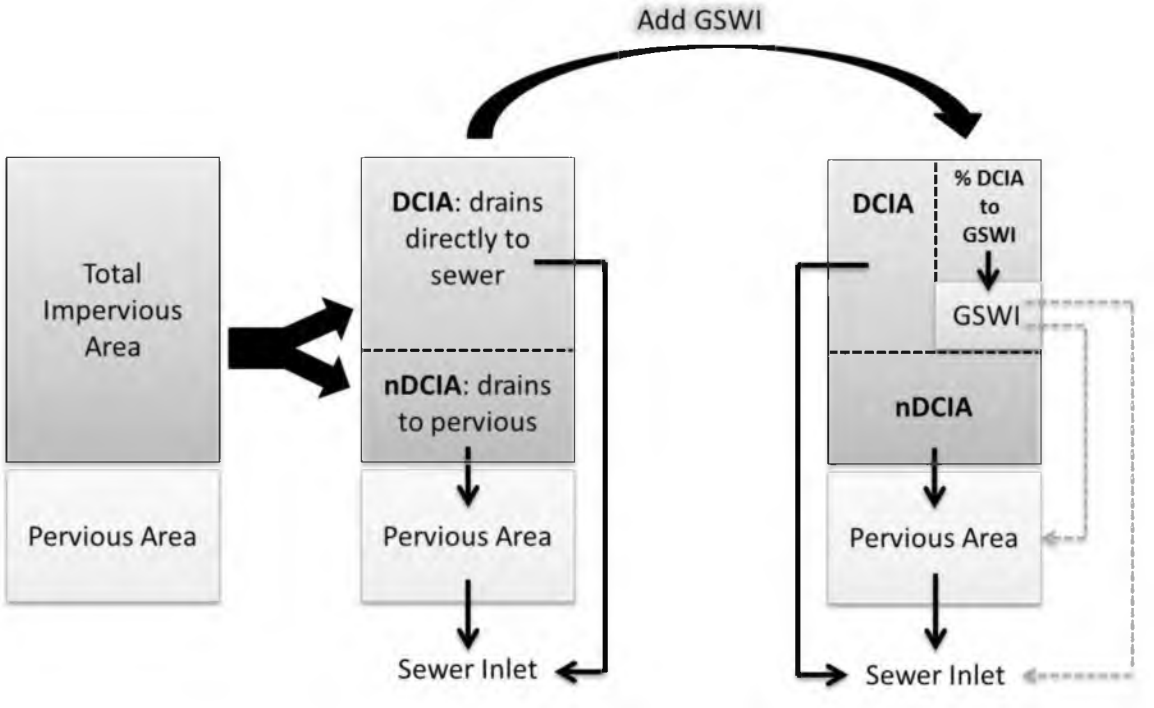

Figure 34. Conceptual overview of the appropriate area accounting after an LID element is introduced in a SWMM5 subcatchment.

Unfortunately, there is no way to explicitly assign a percentage of DCIA to be treated with the SWMM5 LID element. Instead, the amount of area displaced by the LID element is based on the TIA in the model. The modeler must be mindful of this and adjust the percent of impervious area treated accordingly. SWMM5 does not automatically do this for the modeler. If allocated properly, the amount of TIA and DCIA should be reduced by an amount equal to the LID element surface area. The original nDCIA should be unchanged. Subsequently, the percent of total subcatchment area should be re-calculated using the new TIA and DCIA areas. Lastly, the routing to the LID subcatchment is received as runoff from an upstream subcatchment and is not able to differentiate between runoff generated by TIA or DCIA, unless these areas are physically split from the upstream subcatchment and directed to the LID subcatchment, which is essentially one of the methods the research in this document is proposing.

The issues discussed above have the potential to substantially affect the hydrologic response of a simulated GSWI system. The research proposed in this document provides an alternative methodology for simulating GSWI that does not create these adverse impacts, thus providing more appropriate model results. The subsequent section details the research plan to develop the proposed alternative methodology.

H1O Task Descriptions

1. The calculations introduced in the previous section will be imported to an Excel spreadsheet. A generic subcatchment will be created to perform preliminary calculations using the imported equations. The resulting GSWI subcatchment (i.e., $I_C + P_C$) will be simulated within SWMM5 to generate a

runoff timeseries that will be used as input to the GSWI hydraulic system. The hydraulic system created from the calculations will be used to perform a mass balance on the system within Excel.

2. A fully simulated version of the same GSWI system created in Task 1 will be completed. The Task 1 subcatchment and hydraulic system elements will be imported to SWMM5 simulated using the same precipitation input as was used to generate the runoff timeseries for Task 1.
3. To validate that the algorithm functions as expected within SWMM5, the simulated results for each hydraulic element and hydrologic output (Task 2 result) will be required to match within a margin of error of ±5% to the results of the mass balance spreadsheet solution (Task 1 result). The characteristics compared will be peak discharge, time to peak of the timeseries, and total volume.
4. The next task following the validation of the algorithm performance within SWMM5 is to automate the algorithm. This task will be completed within Excel using Visual Basic for Application (VBA) code. The automated tool will provide the user with a graphical user interface where the required user inputs values, as outlined in the previous section, will be requested. A SWMM5 model input file and a list of subcatchments selected to receive GSWI will also be required. The inputs will be used in internal calculations to create a new SWMM5 input file that will contain the split subcatchments representing GSWI and any existing subcatchments that were not selected to receive GSWI. The input file created will be complete and intended to be used

directly within SWMM5.

5. An assessment of the simulated results from the up-scaled subcatchment and from a comparable subcatchment using the SWMM5 LID module sized to treat an equivalent volume of runoff (i.e., equivalent WQCV) will be completed. The presentation of results will highlight differences in hydrologic response results to include peak discharge, total volume, and time-to-peak. A discussion on the findings and the implications to applicability for urban watershed planning will also be included.

Results

Task #1: Develop Manual Approach

The first step in creating the spreadsheet solution was to assume some basic input parameters. The assumptions made for the validation process are listed in Table 24. Using these assumed parameters and applying the equations discussed in Chapter 3, GSWI elements were sized for a single subbasin and include: the managed area ($I_C + P_C$); overflow weir offset height; storage volume; and orifice diameter. Once the GSWI elements were created, it was necessary to generate a runoff timeseries to use as inflow to the spreadsheet.

The managed area ($I_C + P_C$) was simulated in SWMM5 with a design storm volume of 2.5 inches to generate a runoff timeseries. The simulated output timeseries temporal resolution was set equal to 1-minute.

The volume associated with each hydraulic element was calculated at each 1-minute interval using the calculated storage volume, orifice discharge, and bypass

Table 24. Summary of the input data used in the equations to derive the spreadsheet solution.

Description	Value
Area (A)	200
Percent Impervious (PI)	25
Percent of GI Implementation (X):	50
Loading Ratio (R):	15
Water Quality Capture Volume (V_{WQ}):	1
Saturated Hydraulic Conductivity (K_{SAT}):	0.5
Drawdown Time for Slow Release (T):	24
Weir Height in GI (H_W):	5
Submerged Orifice Discharge Coefficient (C_D):	0.60

(overflow) volume (Figure 35). Calculated results from the spreadsheet solution are presented in Table 25. Hydrographs for each of the hydraulic elements and the controlled area runoff volume are presented in Figure 36.

Task #2 and Task #3: Simulating and Validating the Up-Scaling Algorithm with SWMM5

The same subcatchment and hydraulic elements used for the spreadsheet solution for the GSWI were simulated within SWMM5. The simulated results are presented in Table 26 along with the results from the spreadsheet solution results. Hydrograph comparisons for each element are available in Figures 37 thru 39.

The results show an acceptable level of accuracy, with all volumes and peak percent differences well within the error tolerance of ±5% (Table 26). A review of the timeseries figures show that the timing of peaks and recession limbs match nicely and positively supplement the quantitative comparison results (Figures 37 thru 39). This match indicates the resulting input parameters produced from the PWD (2009) up-scaling

TR Node Storage Volume (ft3):	*17,016*					
TR Node Storage Area (ft2):	*3,403*					
TR Orifice Area (ft2):	*0.46*					
Table - Subcatch SingleTestShed_Ic+Pc			Io	O1		
		Runoff	Runoff Volume	TR Orifice Discharge	TR Overflow Rate	Effective storage Volume
Days	*Hours*	*(CFS)*	(ft3)	(cfs)	(cfs)	(ft3)
0	*12:29:00*	*19.42*	1,165	4.92	14	17,015.63
0	*12:30:00*	*18.84*	1,130	4.92	14	17,015.63
0	*12:31:00*	*18.25*	1,095	4.92	13	17,015.63
0	*12:32:00*	*17.67*	1,060	4.92	13	17,015.63
0	*12:33:00*	*17.12*	1,027	4.92	12	17,015.63
0	*12:34:00*	*16.58*	995	4.92	12	17,015.63
0	*12:35:00*	*16.07*	964	4.92	11	17,015.63
0	*12:36:00*	*15.58*	935	4.92	11	17,015.63
0	*12:37:00*	*15.1*	906	4.92	10	17,015.63
0	*12:38:00*	*14.63*	878	4.92	10	17,015.63
0	*12:39:00*	*14.19*	851	4.92	9	17,015.63
0	*12:40:00*	*13.76*	826	4.92	9	17,015.63
0	*12:41:00*	*13.35*	801	4.92	8	17,015.63
0	*12:42:00*	*12.96*	778	4.92	8	17,015.63

Figure 35. Screen shot of the mass balance spreadsheet solution setup. At each timestep, the volume and/or flow is accounted for through each hydraulic element.

Table 25. Summary of the spreadsheet results for the GSWI hydraulics and inflow values.

Element	Spreadsheet
Subcatchment Runoff Volume (cu.ft)	92,530
Slow Release Volume (cu.ft)	71,315
Overflow Volume (cu.ft)	21,162
BMP Storage Volume (cu.ft)	3,049,935
Peak Slow Release (cfs)	4.92
Peak Slow Release (cfs/acre)	0.197
Peak Slow Release (cfs/ac. Imp)	0.210
Peak Overflow (cfs)	16.38
Peak Overflow + Peak Slow Release (cfs)	21.30

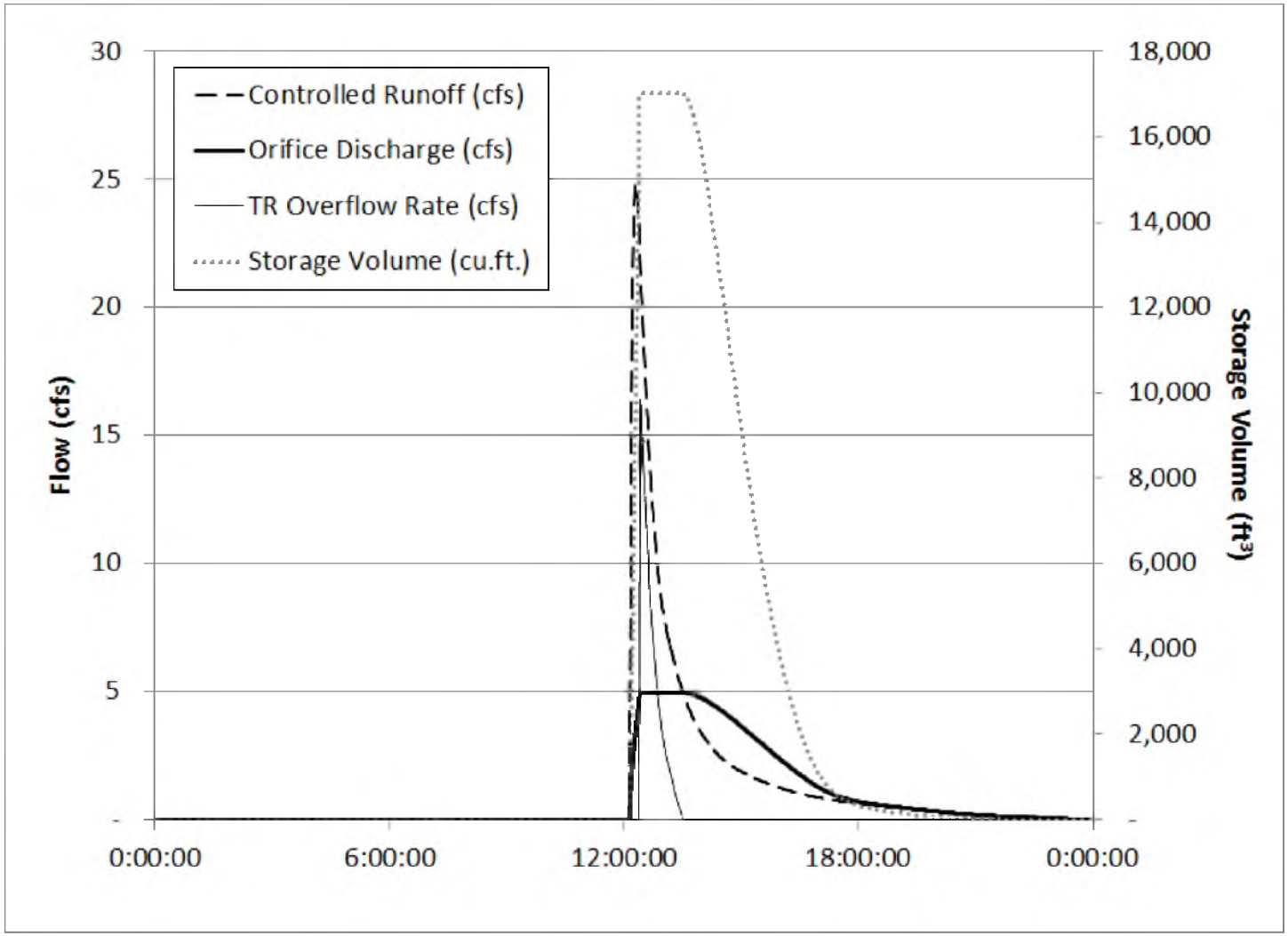

Figure 36. Controlled Area runoff, orifice discharge, overflow weir discharge, and storage volume curve for the spreadsheet solution.

Table 26. Summary of the spreadsheet and SWMM5 results for the storage node, orifice, and overflow weir.

Element	Spreadsheet	SWMM5	% Difference
Subcatchment Runoff Volume (cu.ft)	92,530	92,529	0.00%
Slow Release Volume (cu.ft)	71,315	71,746	0.60%
Overflow Volume (cu.ft)	21,162	20,539	-2.94%
BMP Storage Volume (cu.ft)	3,049,935	3,175,282	4.11%
Peak Slow Release (cfs)	4.92	4.99	1.35%
Peak Slow Release (cfs/acre)	0.197	0.200	1.35%
Peak Slow Release (cfs/ac. Imp)	0.210	0.213	1.35%
Peak Overflow (cfs)	16.38	15.84	-3.28%
Peak Overflow + Peak Slow Release (cfs)	21.30	20.83	-2.21%

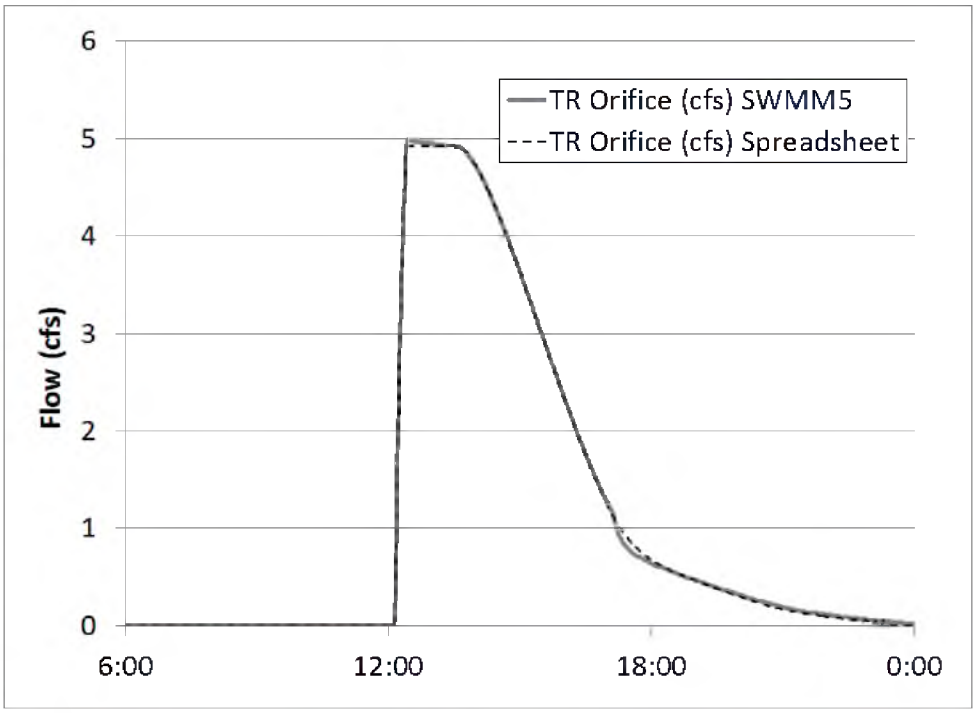

Figure 37. Comparison of the spreadsheet solution and SWMM5 orifice hydrographs.

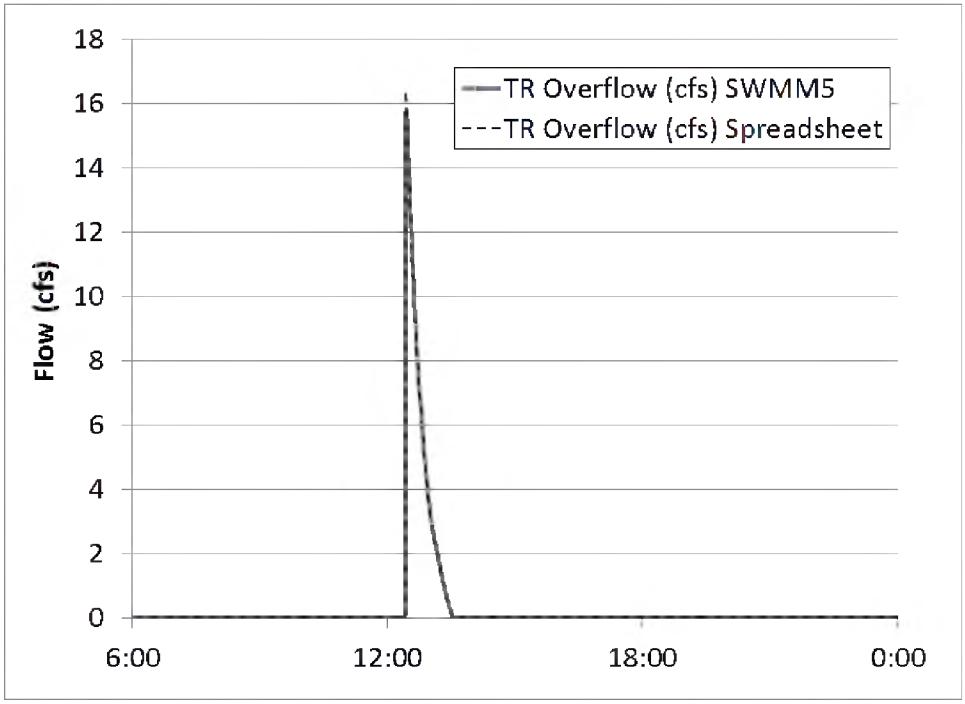

Figure 38. Comparison of the spreadsheet solution and SWMM5 overflow weir hydrographs.

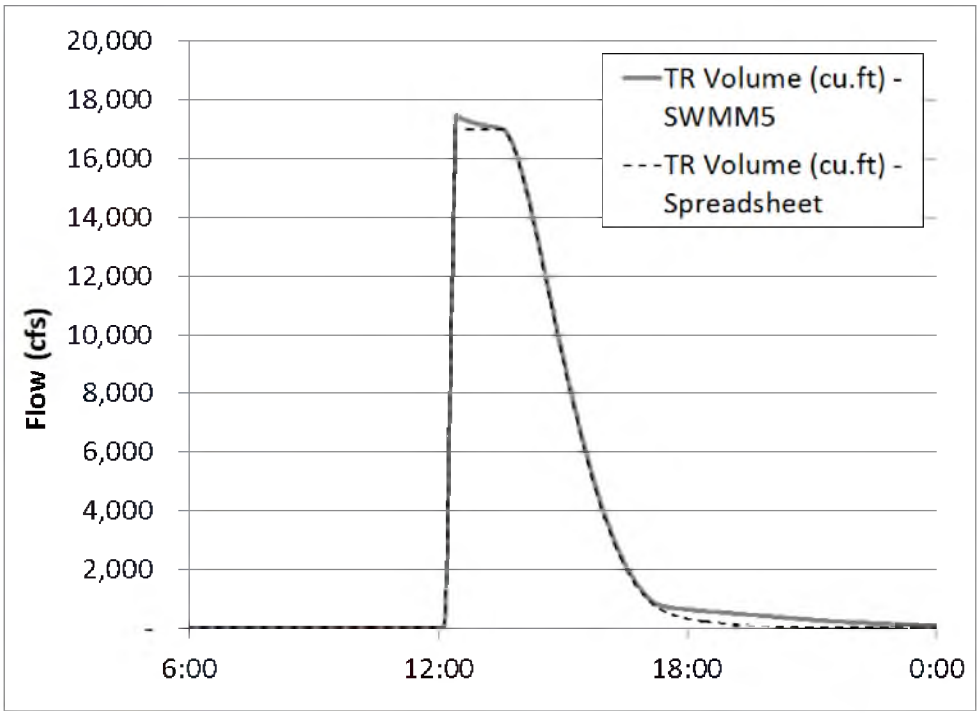

Figure 39.Comparison of the spreadsheet solution and SWMM5 storage node volume curves.

algorithm function as expected when used as input to the SWMM5 model.

Task #4: Develop Automated Approach

A graphical user interface (GUI) has been developed to collect the user inputs necessary to execute the GSWI algorithm (Figure 40). The GUI requires the user to navigate to the location of necessary input files. These files include: the baseline SWMM5 input file, the list of subbasins to receive GSWI, and a list identifying the subbasins not receiving GSWI.

Once the 'Process' button is clicked, the program populates the workbook tabs with GUI data (Figure 41) and through a series of subroutines, creates a new input file

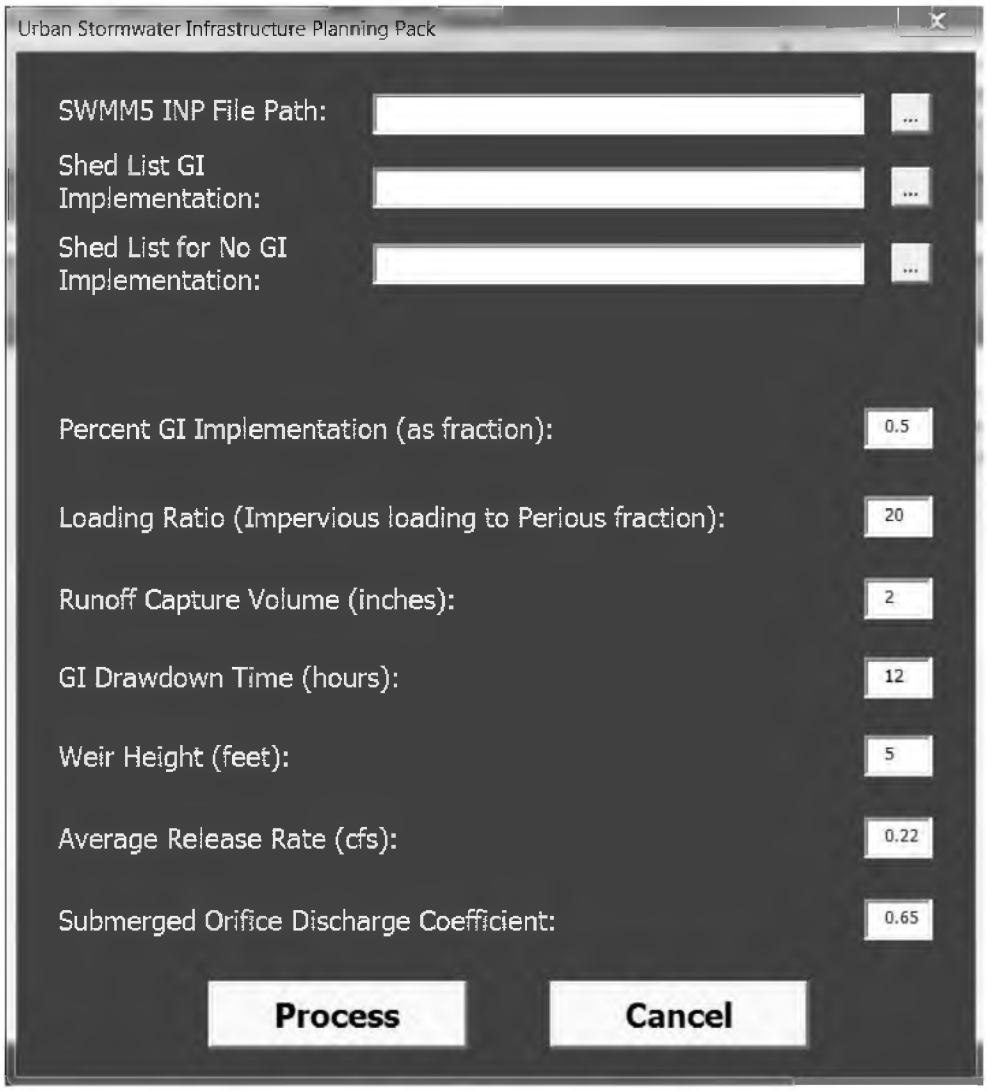

Figure 40. The GSWI automated up-scaling tool GUI.

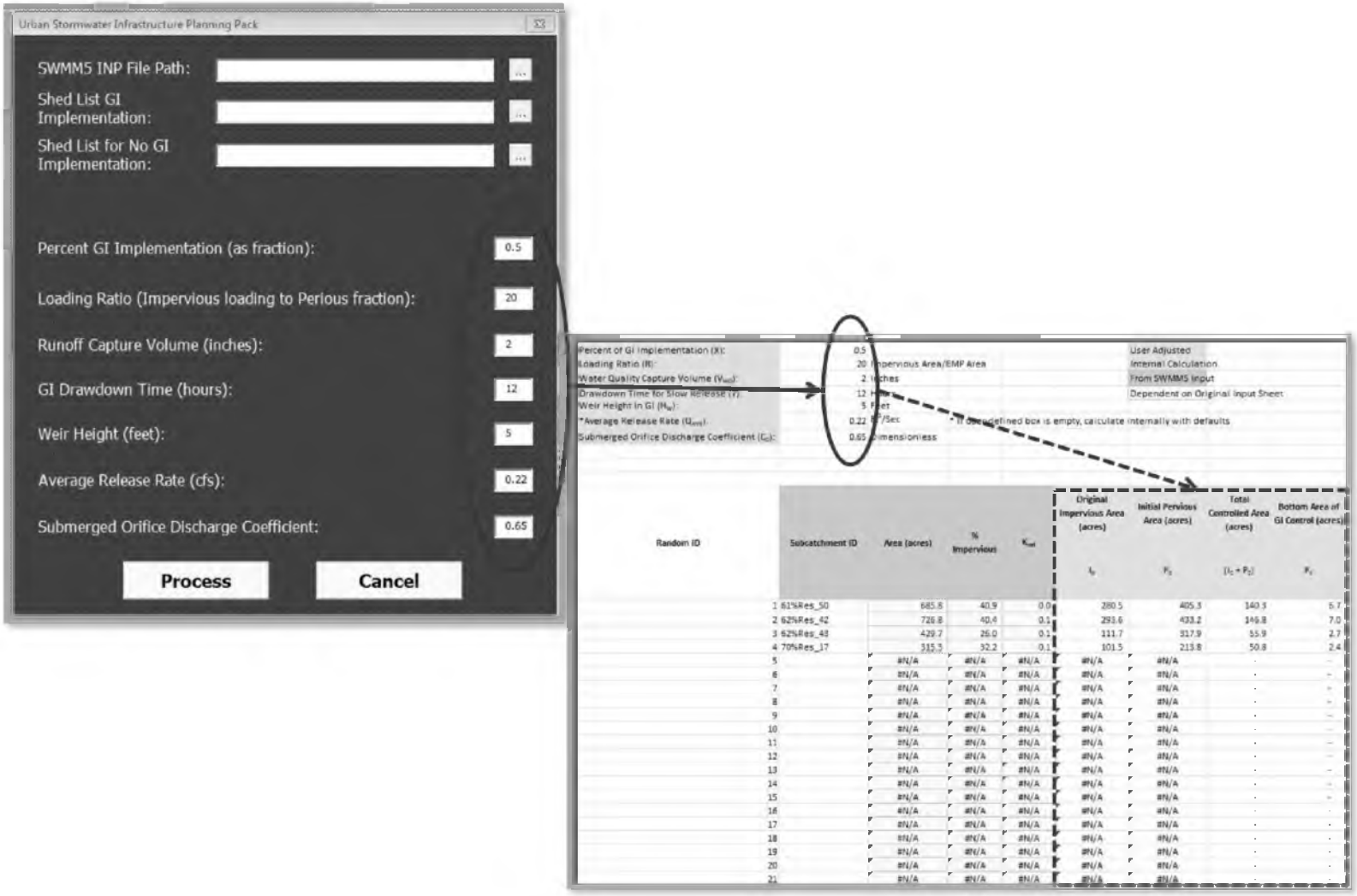

Figure 41. The data entered into the GUI by the user is placed into internal sheets and used to perform the calculations from Chapter 3.

with the new GSWI subbasins (Figure 42). The GSWI input file can be used directly in SWMM5 because the automated procedure creates a complete file using the information from the baseline model (Figure 43). with the new GSWI subbasins (Figure 42). The GSWI input file can be used directly in SWMM5 because the automated procedure creates a complete file using the information from the baseline model (Figure 43).

Task #5: Simulated Results and Comparisons to SWMM5 LID Module

A SWMM5 LID module has been created to assess the hydrologic response and hydraulic output to the results produced from the algorithm presented in H1O. The SWMM5 LID (S5IT) element was built to manage the same WQCV as was used in the previous H1O tasks. The selected LID design type used was the infiltration trench. It was selected due to the similarities in the conceptual structure of the model representations (i.e., both have surface layers, a storage element, and underdrain system).

The result comparisons show a strong positive correlation for the orifice discharges (Figure 44). The peak discharge and overall shape of the hydrograph matches nicely. The overflow peak discharge comparisons show a relatively close match. The comparison is further positively matched when reviewing the volumes produced by each GSWI element. It is concluded that the collective representation can be used to perform watershed-scale GSWI research with comparable accuracy to the SWMM5 LID module capabilities.

Figure 42. Image of the baseline input file subbasins (top left) and the GSWI subbasins created using the up-scaling GUI (bottom right).

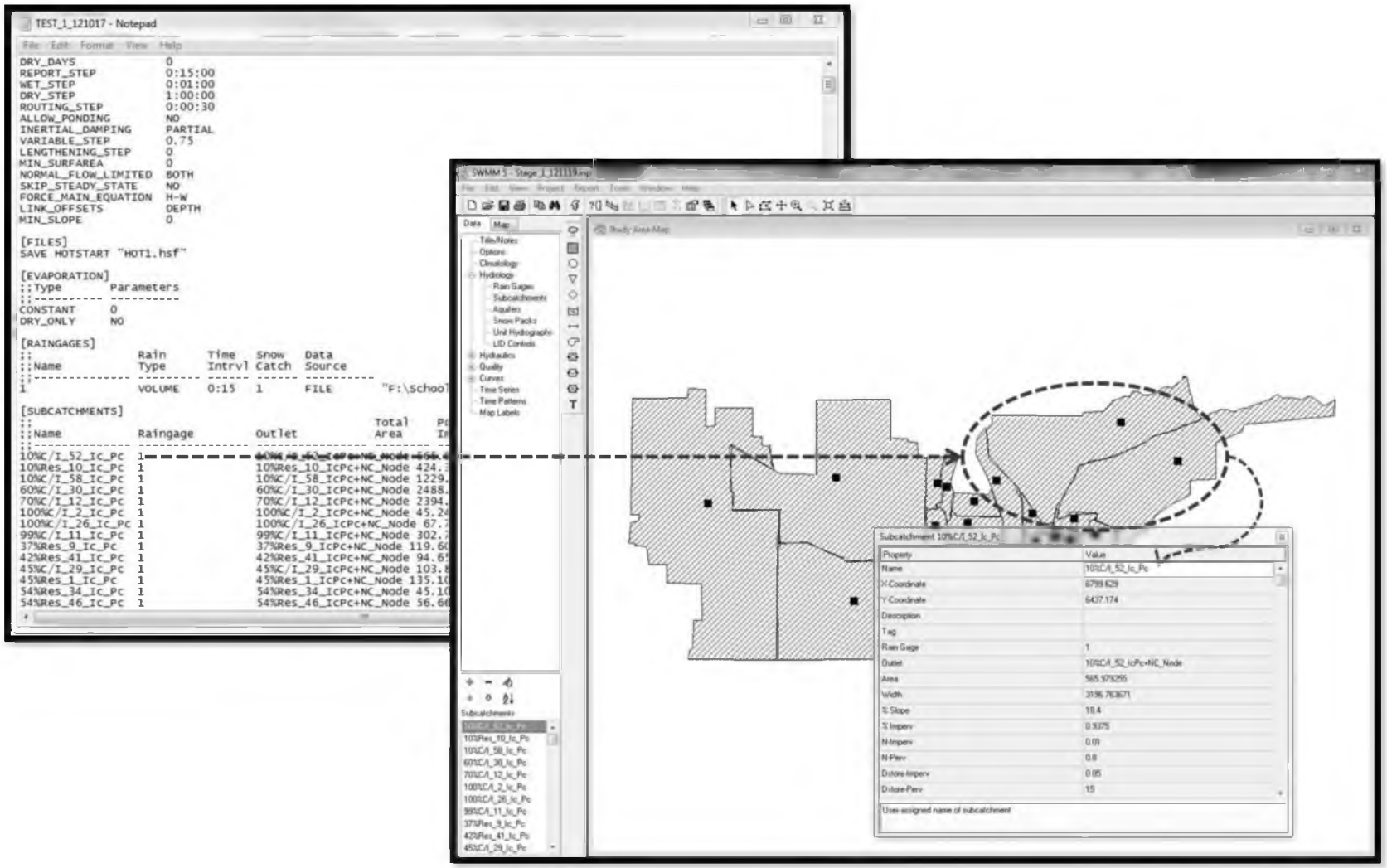

Figure 43. Visualization of the input file opened within the SWMM5 modeling environment.

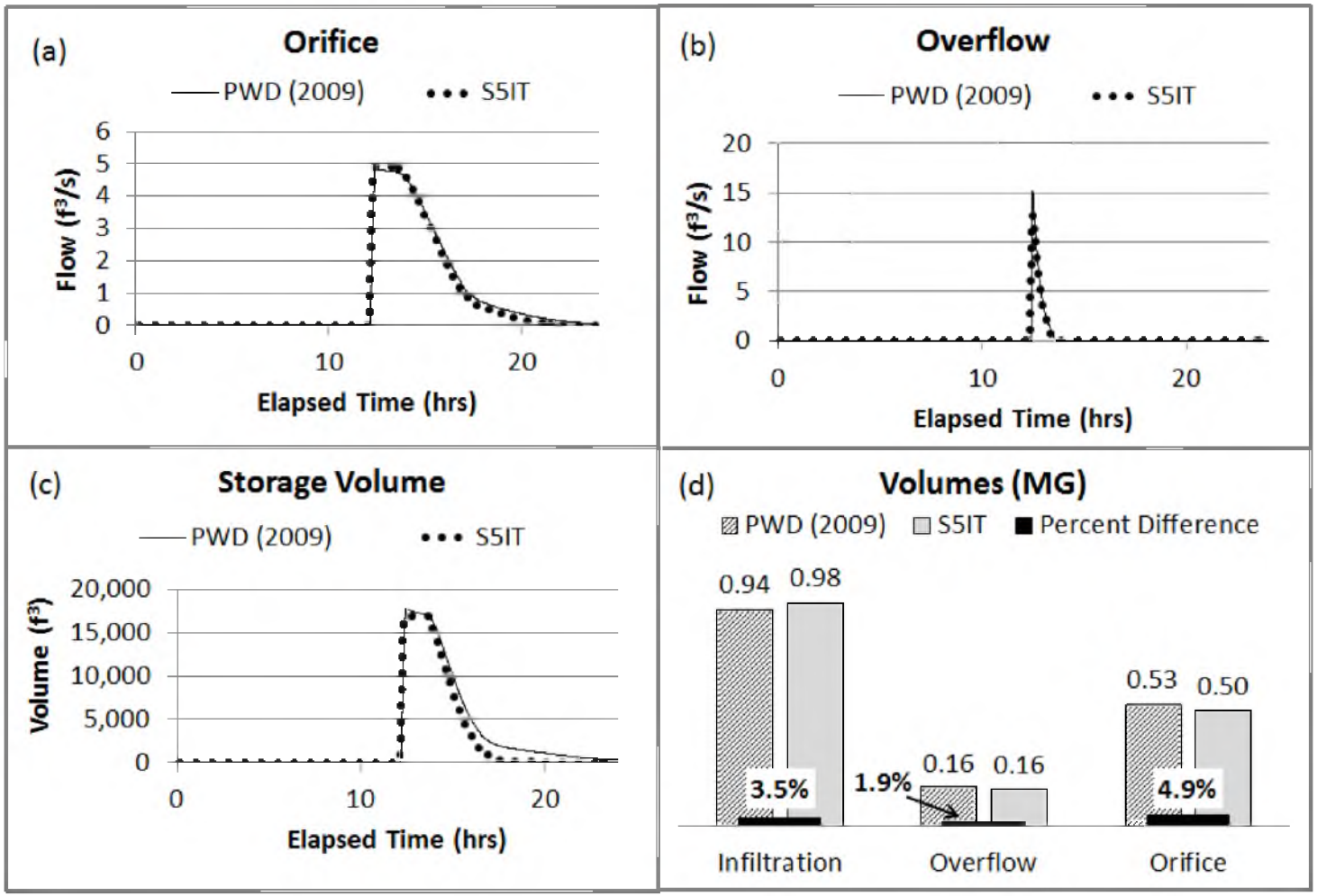

Figure 44. Hydrograph and volume results for the SWMM5 LID (S5IT) module output and the PWD (2009) collective representation of GSWI up-scaling algorithm. Timeseries results are presented for the orifice (a), overflow (b), and storage volume (c). Total volume comparisons are also included (d).

H2O and H3O: Compare GSWI Hydrologic Response to Spatial Distribution and Aggregation Influences

The following sections will present a discussion on the approach used to meet the H2O and H3O objectives. These objectives were focused on quantifying the influence of variations in GSWI spatial distribution and subcatchment aggregation on GSWI hydrologic response. The H2O objective uses the Salt Lake City, Utah urban area, which is characterized as a semi-arid, strongly heterogeneous surface profile, 57-mi^2 urban area. Conversely, the H3O objective uses a portion of the Philadelphia, Pennsylvania urban area, which is characterized by a wet climate, less heterogeneous surface profile (as compared to the SLC area), densely populated, 14-mi^2 urban area. The following steps were completed for both the H2O and H3O modeling objectives and are further addressed in the subsections below.

1. Prepare the models to incorporate the collective representation of GSWI for model simulations.
2. Create and simulate a number of spatial distribution patterns and increasingly aggregated model scenarios.
3. Perform single-factor ANOVA statistical testing on each set of output and generate other supplemental support graphics and tables.

H2O & H3O Task Descriptions

1. The first task to complete was to prepare the existing conditions model for each objective. This required simulation of all rainfall datasets to ensure the foundation model was functioning as expected and without any adverse

system nuances, such as flooding or instability issues. This step contributed to fewer potential issues when introducing watershed-scale GSWI and any issues could be narrowed to the GSWI implementation, distribution method, or the aggregation procedure.

2. Once the existing conditions models have been evaluated and cleared for use, the next step is to create the scenarios to be evaluated. All scenarios were organized and created using a combination of MS Excel workbooks and ArcGIS capabilities. Specifically, subcatchments were modified (e.g., aggregated) using MS Excel functions and the spatial representations of the modified subcatchments were verified within ArcGIS. Furthermore, spatial distribution loading patterns were evaluated by spatially reviewing the model within ArcGIS, which was then translated to the MS Excel spreadsheets to build representative SWMM5 models. Once the models were modified to suit the objective, they were used within the automated up-scaling tool created in H1O to generate GSWI within the models. Following model creation, the simulations were conducted through batch script commands to increase modeling efficiency.
3. All sets of data underwent significance testing using the t-test statistical test method. The factors considered were spatial distribution and aggregation for both the H2O and H3O objectives. The t-test allowed for a straightforward comparison of multiple output datasets and assumes the data comes from a Gaussian distribution. Three metrics used to evaluate sensitivity: average flow rate, peak discharge, and volume. To supplement the t-test statistical results,

comparisons were made by plotting output data for each model representing watershed-wide conditions. The SLC model also used event hydrographs to evaluate time to peak discharge and influences on hydrograph shape characteristics.

H2O & H3O Task Completion Results

Task #1 and #2: Prepare Models

Tasks 1 and 2 required extensive use of MS Excel spreadsheets and ArcGIS software. Existing models needed adjustments to the underlying sewer system to ensure flow could be routed through without restriction. Therefore, some sewer lines were enlarged and all unnecessary elements that were not essential to the integrity of the model for the purposes of this study's goals were removed. This included any pumps, flap gates, regulating device, syphons, etc. The quality assessment of each baseline model simulation included a check for low runoff and hydraulic continuity error and that system flooding did not exist (Figure 45).

With the baseline models created, work commenced on creating the spatial distribution and subcatchment aggregation input files. The baseline hydrology characteristics were imported to an MS Excel workbook, where the data underwent various modifications depending on the specific modeling objective. For the spatial distribution scenarios, subcatchments were selected within which GSWI would be implemented. The amount of GSWI to implement was calculated based on the selected subcatchments total impervious area availability (Figure 46). Hydraulic loading adjustments were aided by visualizations of the sewer systems in ArcGIS (Figure 47).

Runoff Quantity Continuity	Volume acre-feet	Depth inches
Total Precipitation	57422.384	18.870
Evaporation Loss	0.000	0.000
Infiltration Loss	50965.037	16.748
Surface Runoff	6403.110	2.104
Final Surface Storage	56.933	0.019
Continuity Error (%)	-0.005	

Flow Routing Continuity	Volume acre-feet	Volume 10^6 gal
Dry Weather Inflow	0.000	0.000
Wet Weather Inflow	6403.109	2086.549
Groundwater Inflow	0.000	0.000
RDII Inflow	0.000	0.000
External Inflow	0.000	0.000
External Outflow	6427.043	2094.348
Internal Outflow	0.000	0.000
Storage Losses	0.000	0.000
Initial Stored Volume	0.006	0.002
Final Stored Volume	19.969	6.507
Continuity Error (%)	-0.686	

Figure 45. Example of the typical continuity values for the baseline models for runoff and flow routing. The internal outflow value represented system flooding and was required to be zero for all simulations.

Total Area (P + I) to Control:	4229.5							
Number of sheds to include:	30		Old Name	New Name				
Total Impervious Area	8,065.2	52%	Random 1	Targeted 1				
	5,431.2	78%	Random 2	Targeted 2				
	4,565.7	93%	Random 3	Targeted 4				
	6,741.8	63%	Random 4	-				
	4,986.2	85%	Random 5	Targeted 3				

Subcatchment ID	Area (acres)	% Impervious	Total Impervio Area (acres)	ID	Simulatic Random 1	Simulati Random 2	Simulati Random 3	Simulati Random 5
10%C/I_52	5,865.1	19.3	1131.96	51	Random 1			
10%Res_10	6,019.6	14.1	848.77	52	Random 1			
100%C/I_2	115.3	78.5	90.49	1	Random 1			
100%C/I_26	172.7	78.5	135.59	2	Random 1			
19%C/I_51	2,422.2	27.6	668.52	48			Random 3	
37%Res_9	595.1	40.2	239.22	23	Random 1	Random 2	Random 3	Random 5
4%Res_53	65.3	12.8	8.36	53	Random 1			
42%Res_41	444.4	42.6	189.32	18	Random 1	Random 2		Random 5
45%C/I_29	415.3	50.0	207.65	13	Random 1	Random 2		Random 5

Figure 46. Sample of a spatial distribution spreadsheet used to identify subcatchments selected to receive GSWI and calculation of the relative GSWI implementation.

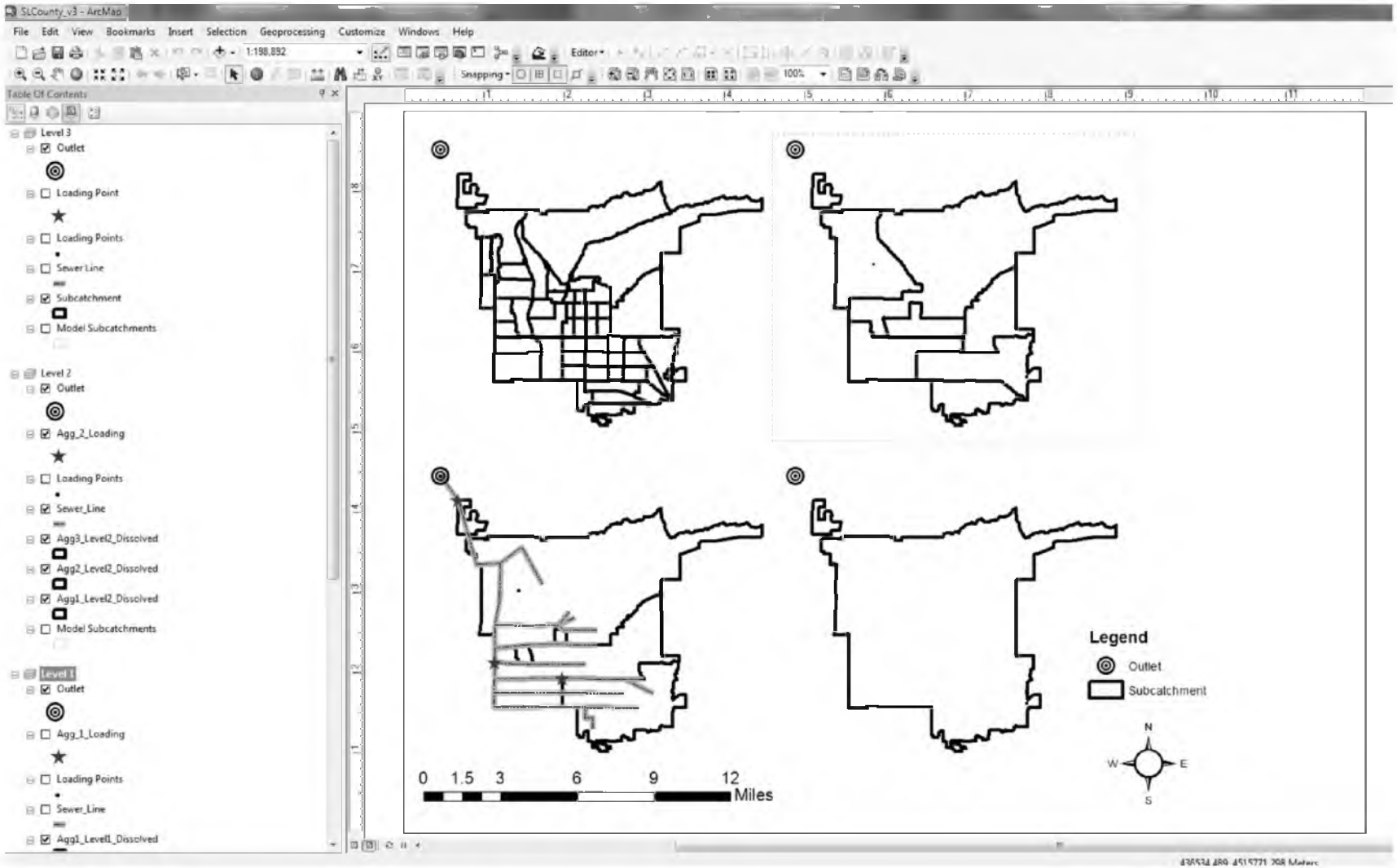

Figure 47. Sample of the spatial distribution hydraulic loading visualization within ArcGIS.

For the subcatchment aggregation, more extensive calculations and organization within MS Excel was required (Figure 48). Subcatchment surface characteristics were all aggregated to varying levels and therefore required separate calculations for each characteristic at each level. ArcGIS was instrumental in helping identify subcatchments that were spatially adjacent and therefore available to merge together (Figure 49). When all the models were created, GSWI units were introduced by using the collective up-scaling algorithm of H1O.

Task #3: T-test Statistical Testing and Supplemental Decision Support Graphics

T-test significance testing was conducted using the data analysis capabilities of MS Excel. Output from each model was first organized into the workbook (Figure 50). This information is linked to other sheets that calculate exceedance and generate associated plots. The statistical calculations are contained in another worksheet within the same workbook (Figure 51). These results are used to identify the magnitude of influence on the hydrologic response from spatial distribution and subcatchment aggregation of GSWI on a watershed-scale.

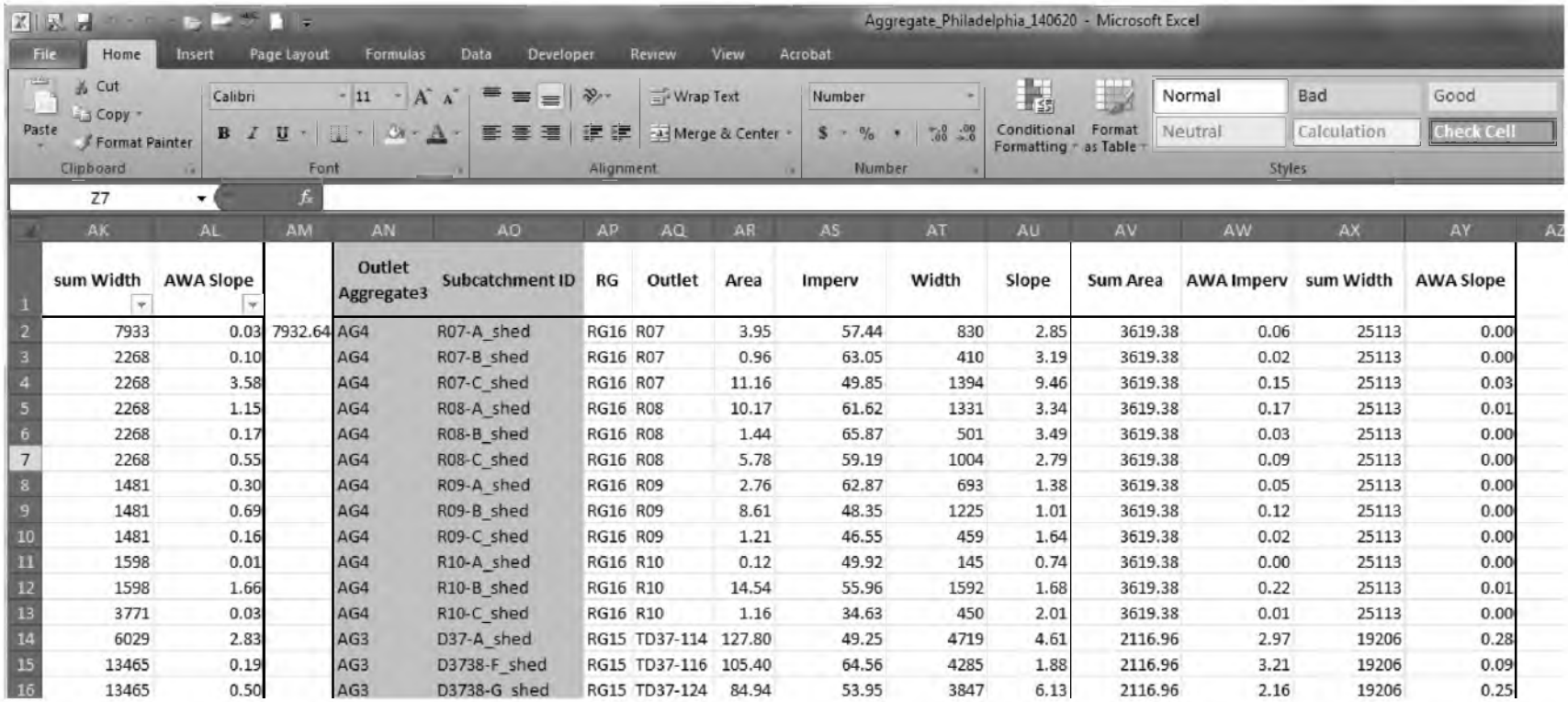

	AK	AL	AM	AN	AO	AP	AQ	AR	AS	AT	AU	AV	AW	AX	AY
1	sum Width	AWA Slope		Outlet Aggregate3	Subcatchment ID	RG	Outlet	Area	Imperv	Width	Slope	Sum Area	AWA Imperv	sum Width	AWA Slope
2	7933	0.03	7932.64	AG4	R07-A_shed	RG16	R07	3.95	57.44	830	2.85	3619.38	0.06	25113	0.00
3	2268	0.10		AG4	R07-B_shed	RG16	R07	0.96	63.05	410	3.19	3619.38	0.02	25113	0.00
4	2268	3.58		AG4	R07-C_shed	RG16	R07	11.16	49.85	1394	9.46	3619.38	0.15	25113	0.03
5	2268	1.15		AG4	R08-A_shed	RG16	R08	10.17	61.62	1331	3.34	3619.38	0.17	25113	0.01
6	2268	0.17		AG4	R08-B_shed	RG16	R08	1.44	65.87	501	3.49	3619.38	0.03	25113	0.00
7	2268	0.55		AG4	R08-C_shed	RG16	R08	5.78	59.19	1004	2.79	3619.38	0.09	25113	0.00
8	1481	0.30		AG4	R09-A_shed	RG16	R09	2.76	62.87	693	1.38	3619.38	0.05	25113	0.00
9	1481	0.69		AG4	R09-B_shed	RG16	R09	8.61	48.35	1225	1.01	3619.38	0.12	25113	0.00
10	1481	0.16		AG4	R09-C_shed	RG16	R09	1.21	46.55	459	1.64	3619.38	0.02	25113	0.00
11	1598	0.01		AG4	R10-A_shed	RG16	R10	0.12	49.92	145	0.74	3619.38	0.00	25113	0.00
12	1598	1.66		AG4	R10-B_shed	RG16	R10	14.54	55.96	1592	1.68	3619.38	0.22	25113	0.01
13	3771	0.03		AG4	R10-C_shed	RG16	R10	1.16	34.63	450	2.01	3619.38	0.01	25113	0.00
14	6029	2.83		AG3	D37-A_shed	RG15	TD37-114	127.80	49.25	4719	4.61	2116.96	2.97	19206	0.28
15	13465	0.19		AG3	D3738-F_shed	RG15	TD37-116	105.40	64.56	4285	1.88	2116.96	3.21	19206	0.09
16	13465	0.50		AG3	D3738-G_shed	RG15	TD37-124	84.94	53.95	3847	6.13	2116.96	2.16	19206	0.25

Figure 48. Sample of a subcatchment aggregation spreadsheet used to lump subcatchment surface characteristics for each level of aggregation.

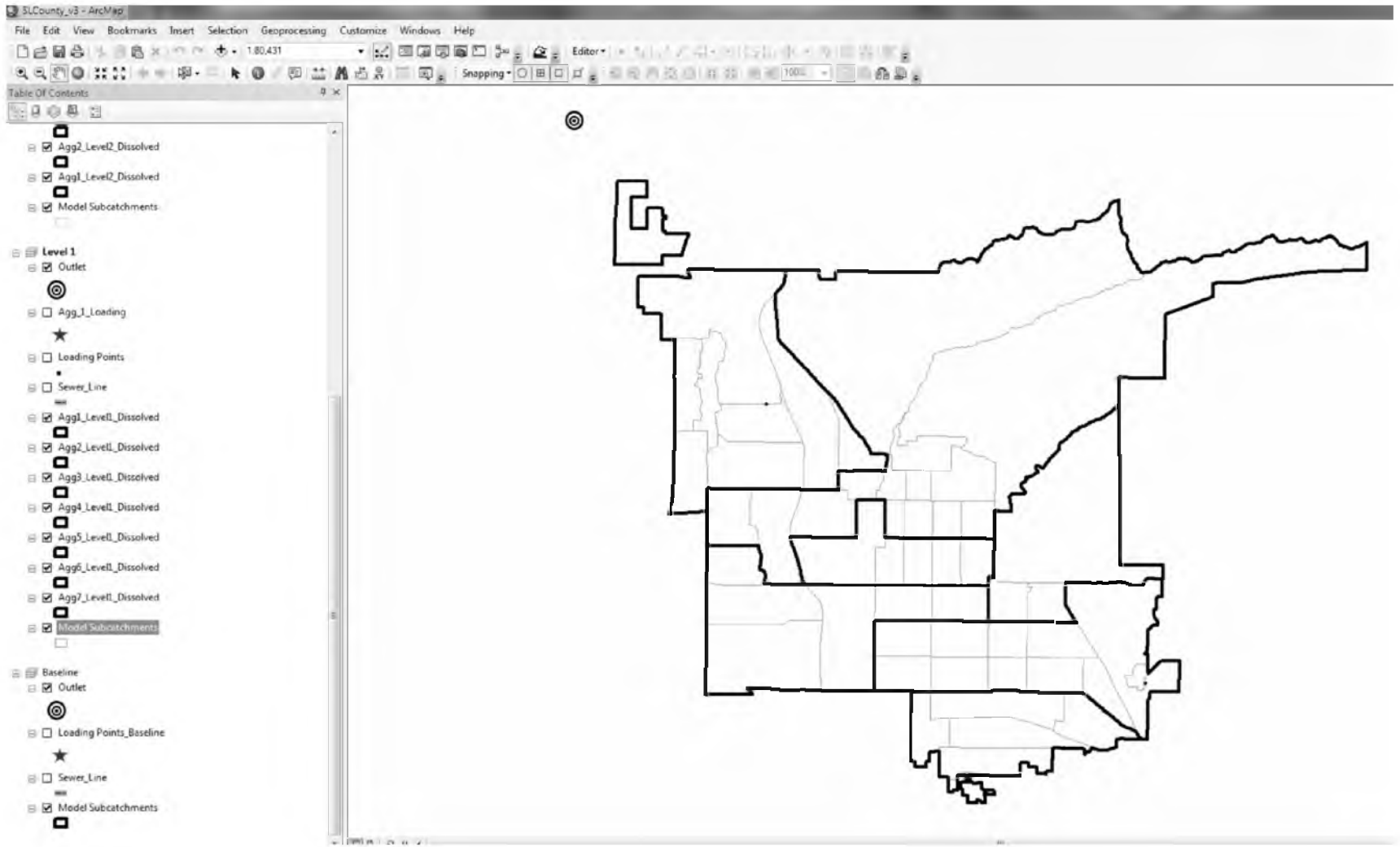

Figure 49. Sample of visualizing the subcatchments to aggregate within ArcGIS.

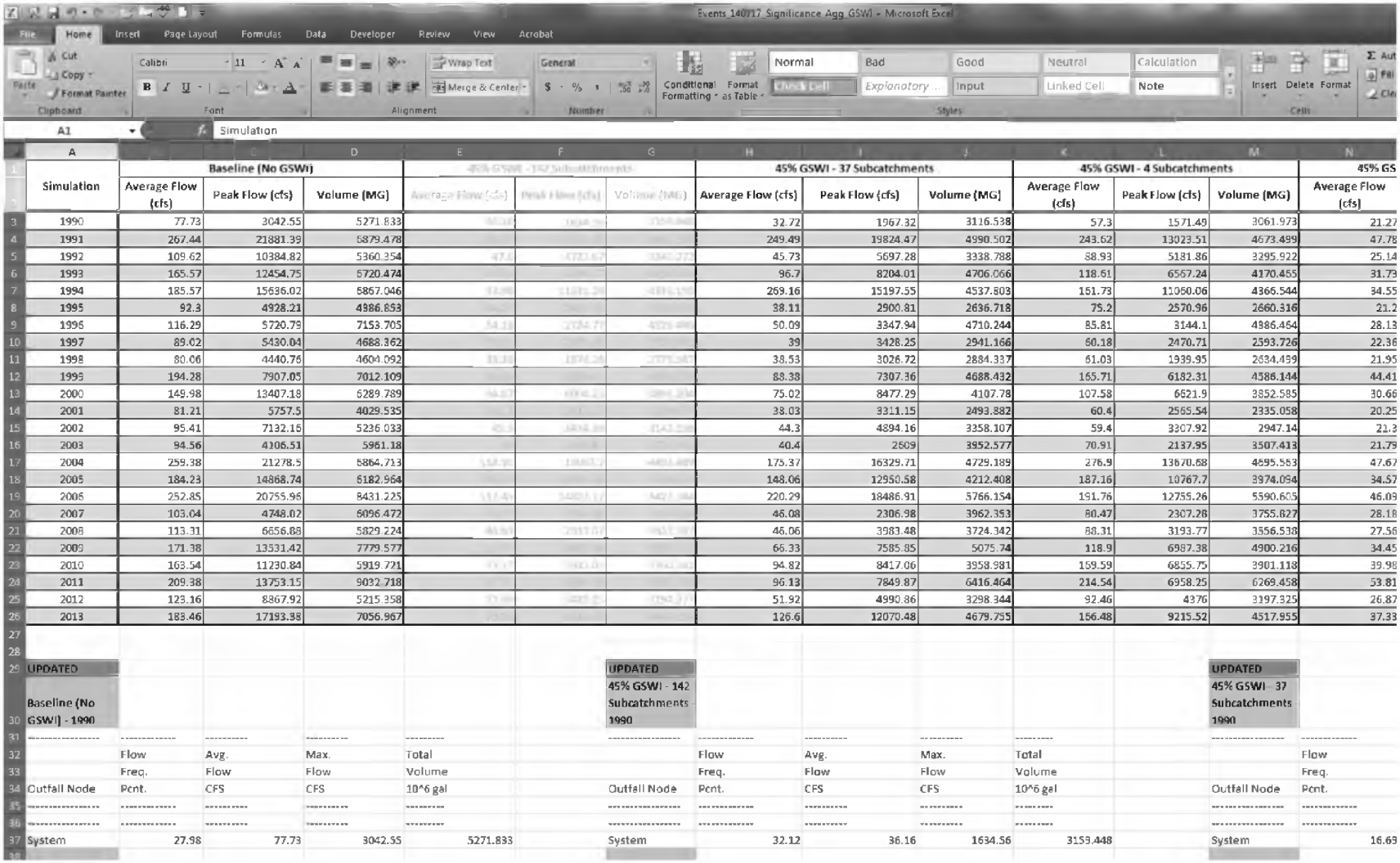

Simulation	Baseline (No GSWI)			45% GSWI - 37 Subcatchments			45% GSWI - 4 Subcatchments			45% GS
	Average Flow (cfs)	Peak Flow (cfs)	Volume (MG)	Average Flow (cfs)	Peak Flow (cfs)	Volume (MG)	Average Flow (cfs)	Peak Flow (cfs)	Volume (MG)	Average Flow (cfs)
1990	77.73	3042.55	5271.833	32.72	1967.32	3116.538	57.3	1571.49	3061.973	21.27
1991	267.44	21881.39	5879.478	249.49	19824.47	4990.502	243.62	13023.51	4673.499	47.78
1992	109.62	10384.82	5360.354	45.73	5697.28	3338.788	88.93	5181.86	3295.922	25.14
1993	165.57	12454.75	5720.474	96.7	8204.01	4706.066	118.61	6567.24	4170.455	31.79
1994	185.57	15636.02	5867.046	269.16	15197.55	4537.803	151.73	11060.06	4366.544	34.55
1995	92.3	4928.21	4986.853	38.11	2900.81	2636.718	75.2	2570.96	2660.316	21.2
1996	116.29	5720.79	7153.705	50.09	3347.94	4710.244	85.81	3144.1	4986.464	28.13
1997	89.02	5430.04	4688.362	39	3428.25	2941.166	60.18	2470.71	2593.726	22.36
1998	80.06	4440.76	4604.092	38.53	3026.72	2884.337	61.03	1939.95	2634.499	21.95
1999	194.28	7907.05	7012.109	88.38	7307.36	4688.432	165.71	6182.31	4586.144	44.41
2000	149.98	13407.18	6289.789	75.02	8477.29	4107.78	107.58	6621.9	3852.585	30.66
2001	81.21	5757.5	4029.535	38.03	3311.15	2493.882	60.4	2565.54	2335.058	20.25
2002	95.41	7132.16	5236.033	44.3	4894.16	3358.107	59.4	3307.92	2947.14	21.3
2003	94.56	4106.51	5961.18	40.4	2609	3952.577	70.91	2137.95	3507.413	21.79
2004	259.38	21278.5	5864.713	175.37	16329.71	4729.189	276.9	13670.68	4595.563	47.67
2005	184.23	14868.74	6182.964	148.06	12950.58	4212.408	187.16	10767.7	3974.094	34.57
2006	252.85	20755.96	8431.225	220.29	18486.91	5766.154	191.76	12755.26	5590.605	46.09
2007	103.04	4748.02	6096.472	46.08	2306.98	3962.353	80.47	2307.26	3755.827	28.18
2008	113.31	6656.88	5829.224	46.06	3983.48	3724.342	88.31	3193.77	3556.538	27.56
2009	171.38	13531.42	7779.577	66.33	7585.85	5075.74	118.9	6987.38	4900.216	34.45
2010	163.54	11230.84	5919.721	94.82	8417.06	3958.981	159.59	6855.75	3901.118	39.98
2011	209.38	13753.15	9032.718	96.13	7849.87	6416.464	214.54	6958.25	6269.458	53.81
2012	123.16	8867.92	5215.358	51.92	4990.86	3298.344	92.46	4376	3197.325	26.87
2013	183.46	17193.38	7056.967	126.6	12070.48	4679.755	156.48	9215.52	4517.955	37.33

UPDATED Baseline (No GSWI) - 1990					UPDATED 45% GSWI - 142 Subcatchments 1990					UPDATED 45% GSWI - 37 Subcatchments 1990	
	Flow Freq.	Avg. Flow	Max. Flow	Total Volume		Flow Freq.	Avg. Flow	Max. Flow	Total Volume		Flow Freq.
Outfall Node	Pcnt.	CFS	CFS	10^6 gal	Outfall Node	Pcnt.	CFS	CFS	10^6 gal	Outfall Node	Pcnt.
System	27.98	77.73	3042.55	5271.833	System	32.12	36.16	1634.56	3159.448	System	16.69

Figure 50. Sample of the model output organization within the results spreadsheets to calculate statistical results.

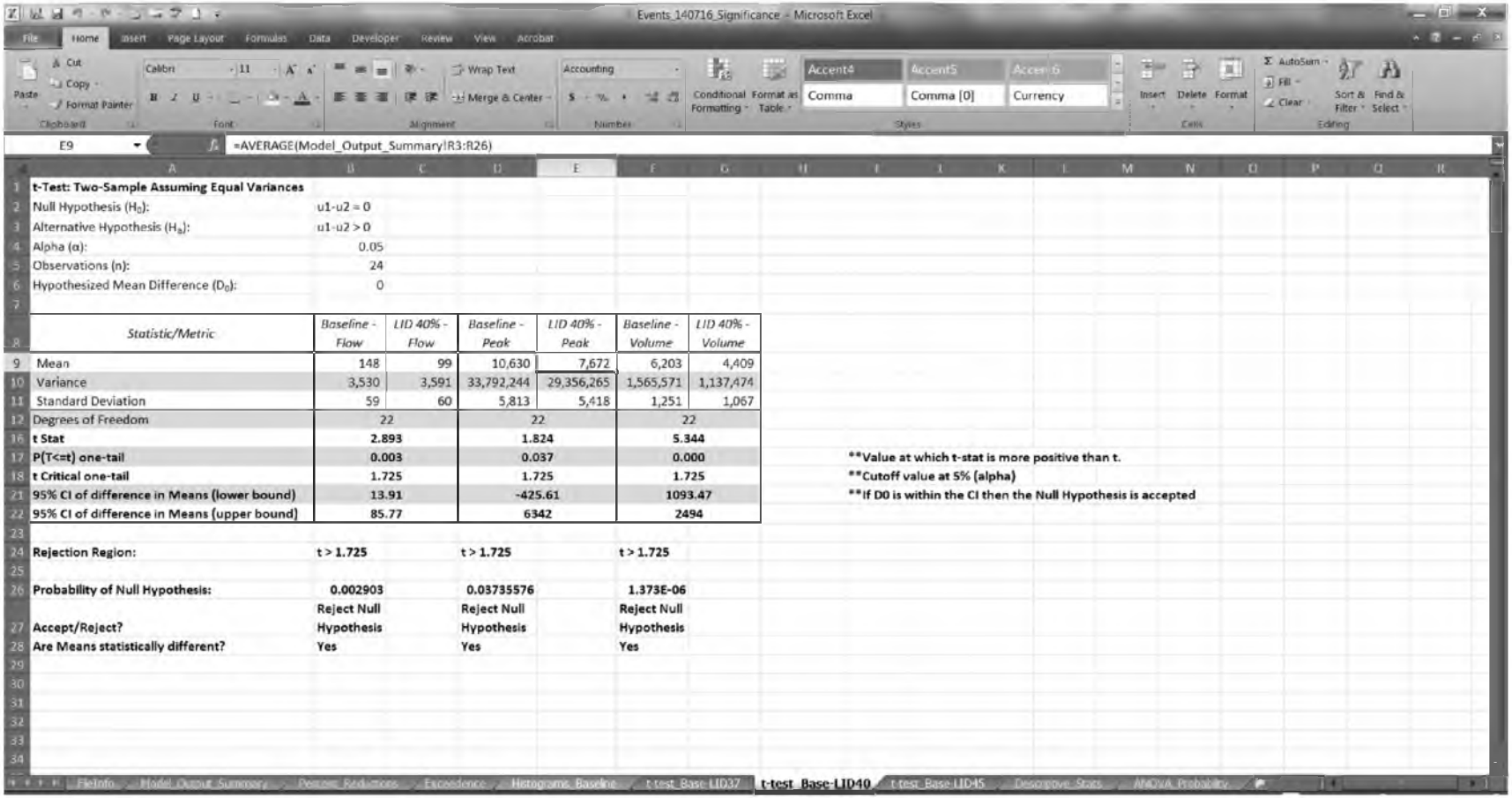

t-Test: Two-Sample Assuming Equal Variances						
Null Hypothesis (H_0):	u1-u2 = 0					
Alternative Hypothesis (H_a):	u1-u2 > 0					
Alpha (α):	0.05					
Observations (n):	24					
Hypothesized Mean Difference (D_0):	0					
Statistic/Metric	*Baseline - Flow*	*LID 40% - Flow*	*Baseline - Peak*	*LID 40% - Peak*	*Baseline - Volume*	*LID 40% - Volume*
Mean	148	99	10,630	7,672	6,203	4,409
Variance	3,530	3,591	33,792,244	29,356,265	1,565,571	1,137,474
Standard Deviation	59	60	5,813	5,418	1,251	1,067
Degrees of Freedom	22		22		22	
t Stat	**2.893**		**1.824**		**5.344**	
P(T<=t) one-tail	**0.003**		**0.037**		**0.000**	
t Critical one-tail	**1.725**		**1.725**		**1.725**	
95% CI of difference in Means (lower bound)	**13.91**		**-425.61**		**1093.47**	
95% CI of difference in Means (upper bound)	**85.77**		**6342**		**2494**	
Rejection Region:	**t > 1.725**		**t > 1.725**		**t > 1.725**	
Probability of Null Hypothesis:	**0.002903**		**0.03735576**		**1.373E-06**	
Accept/Reject?	**Reject Null Hypothesis**		**Reject Null Hypothesis**		**Reject Null Hypothesis**	
Are Means statistically different?	**Yes**		**Yes**		**Yes**	

**Value at which t-stat is more positive than t.
**Cutoff value at 5% (alpha)
**If D0 is within the CI then the Null Hypothesis is accepted

Figure51. Sample of the statistical testing worksheet containing all statistical measurement calculations and results.

APPENDIX C

QUANTIFYING THE SIGNIFICANCE OF GREEN STORMWATER INFRASTRUCTURE ON URBAN RUNOFF CHARACTERISTICS

Salt Lake City, Utah Model

Introduction

During a convening of my Ph.D. committee on December 17, 2013 to review my qualifying exam responses, it was requested by Dr. Burian that an evaluation be conducted to test the significance of GSWI on urban runoff characteristics. This appendix presents the evaluation conducted and subsequent results in response to this request.

Method

The data used for this evaluation was produced from a SWMM5 model of the Salt Lake City drainage area east of the Jordan River (Figure 52). In total, 107 subcatchments drain to the Jordan River in this model setup. The evaluation uses the annual average flow, annual peak discharge, and total annual volume at the system outlet to define the characteristic runoff from the area. Samples for evaluation were taken for each year from 2000 to 2010, for a total of 11 years (i.e., sample size = 11).

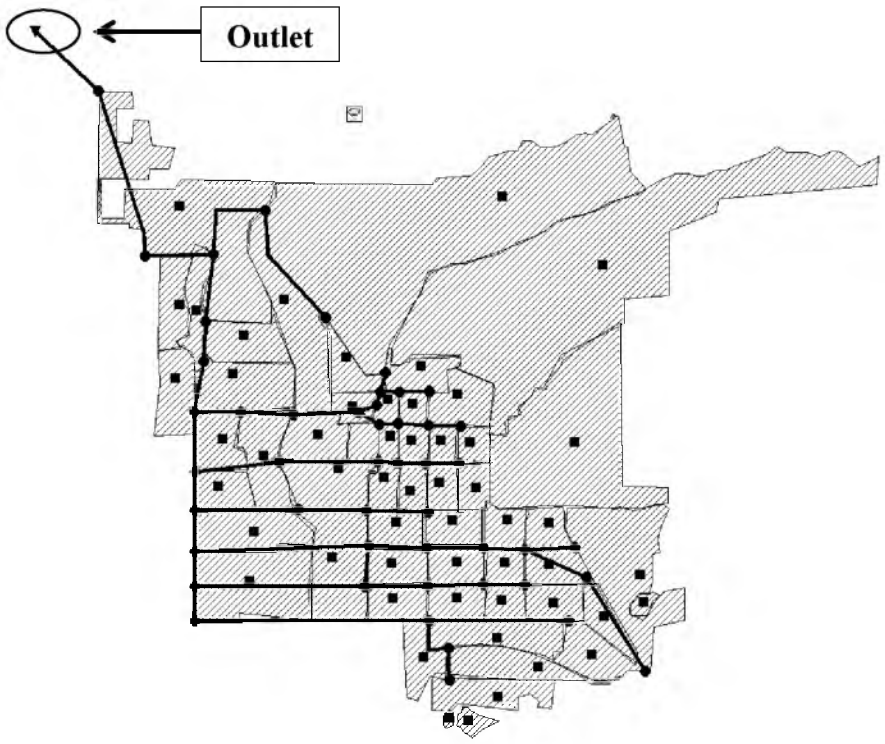

Figure 52. Layout of the model subcatchments, conduits, and outlet for the Jordan River model used for this evaluation.

Simulation results representing baseline conditions (i.e., no LID implementation) for the 11 years were compared against the results produced from simulating 10, 25, 50, and 75% LID implementation. LID implementation for all simulations used a 10.7 loading ratio, a 1-inch capture volume, and a 24-hour drawdown time. The only change between LID representations was the amount of impervious surface converted to LID (i.e., 10, 25, 50, or 75%). LID was represented as pervious surface to allow infiltration and supplemental storage to manage the full inch of required capture volume and then release to the Jordan River within the required 24 hours. The loading ratio dictated the amount of impervious area loading to an acre of pervious LID (i.e., 10.7 acres of impervious area loading to 1 acre of LID). The evaluation performed included the

following steps in the order they were performed: 1) Data Simulation; 2) Test for Normality; 3) Test for Equal Variances; and 4) Test for Significance.

Results and Discussion

Data Simulations

Simulations were completed for the baseline, 10%, 25%, 50%, and 75% LID implementation models for each year from 2000-2010. The average annual flow, peak discharge, and total volume were documented for each year and the mean, standard deviation, and variance were calculated for each sample set. The collected output is presented as Table 27. As expected, the magnitude of the runoff characteristics decrease as LID implementation increases.

Test for Normality

The sample sets produced from the baseline scenario were evaluated to ensure the datasets were normally distributed. For the purposes of this evaluation, it was assumed that if the datasets were normally distributed, the subsequent LID simulations would be as well. To test for normality, histograms were created based on six bins sized using the maximum and minimum values for each runoff characteristic (Figure 53). If the majority of data was grouped into the middle of the histogram, it was considered to be normally distributed. A review of the histograms in Figure 53 satisfied the criteria for normal distribution.

Table 27. Descriptive statistics for the 0% (Baseline), 10%, 25%, 50%, and 75% GSWI implementation scenarios

Average Flow (cfs)								
Simulation	N	Mean	Standard Deviation	Standard Error	95% confidence Intervals		Minimum	Maximum
					Upper	Lower		
Baseline (No GSWI)	11	6.06	1.43	2.04	7	5	3.41	8.81
10% GSWI	11	5.80	1.33	1.76	7	5	3.33	8.35
25% GSWI	11	5.40	1.25	1.56	6	5	3.08	7.82
50% GSWI	11	4.71	1.12	1.25	5	4	2.65	6.90
75% GSWI	11	3.99	0.99	0.99	5	3	2.18	5.97
Peak Flow (cfs)								
Simulation	n	Mean	Standard Deviation	Standard Error	95% confidence Intervals		Minimum	Maximum
					Upper	Lower		
Baseline (No GSWI)	11	188	63.3	4,003	226	151	74.1	278.2
10% GSWI	11	164	56.0	3,133	197	131	65.6	249.7
25% GSWI	11	154	52.6	2,770	185	123	61.3	236.9
50% GSWI	11	138	48.3	2,336	166	109	53.8	214.9
75% GSWI	11	124	45.4	2,063	151	98	46.2	196.9
Volume (MG)								
Simulation	n	Mean	Standard Deviation	Standard Error	95% confidence Intervals		Minimum	Maximum
					Upper	Lower		
Baseline (No GSWI)	11	1,407	321	102,735	1,596	1,217	797	1,978
10% GSWI	11	1,348	298	88,621	1,524	1,172	779	1,875
25% GSWI	11	1,254	280	78,533	1,420	1,089	720	1,755
50% GSWI	11	1,094	251	63,118	1,243	946	619	1,551
75% GSWI	11	926	223	49,633	1,058	794	509	1,340

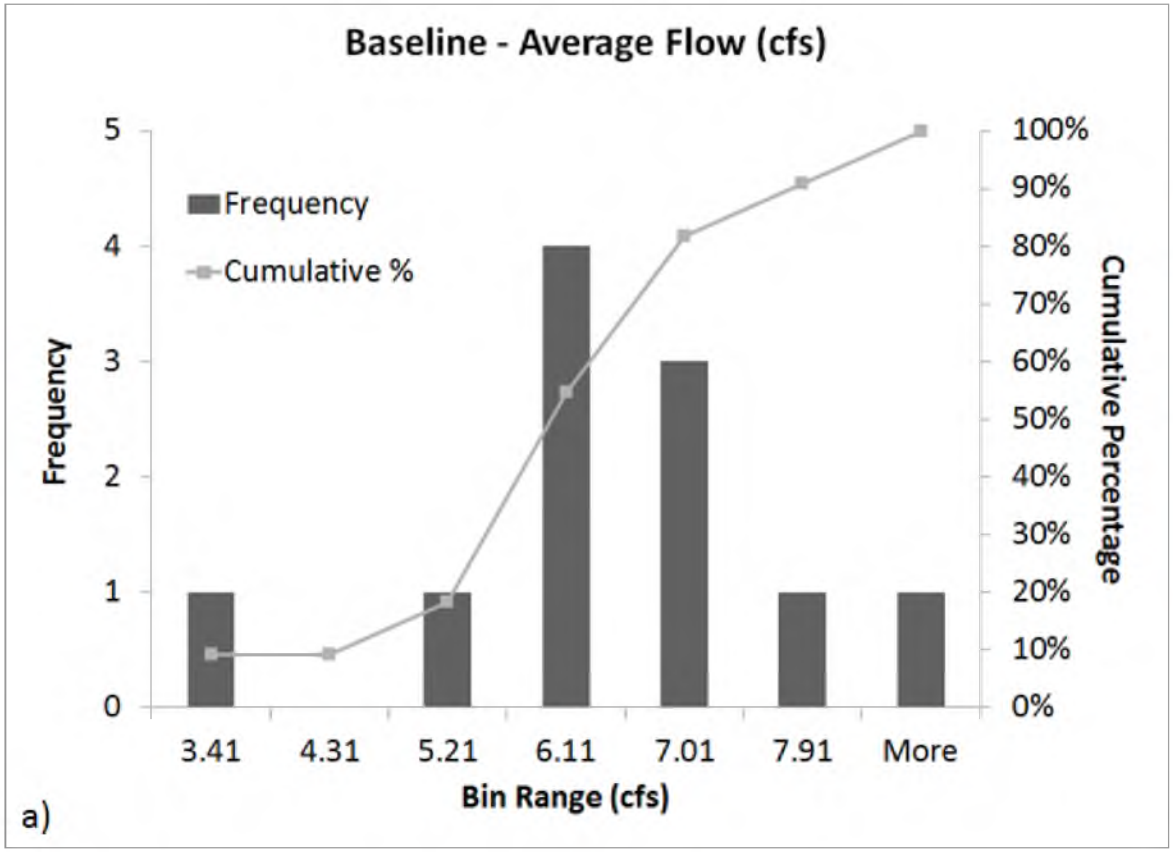

Figure 53. Histograms for the baseline simulations created to test the annual average flow (a), peak discharge (b), and total volume (c) for normality.

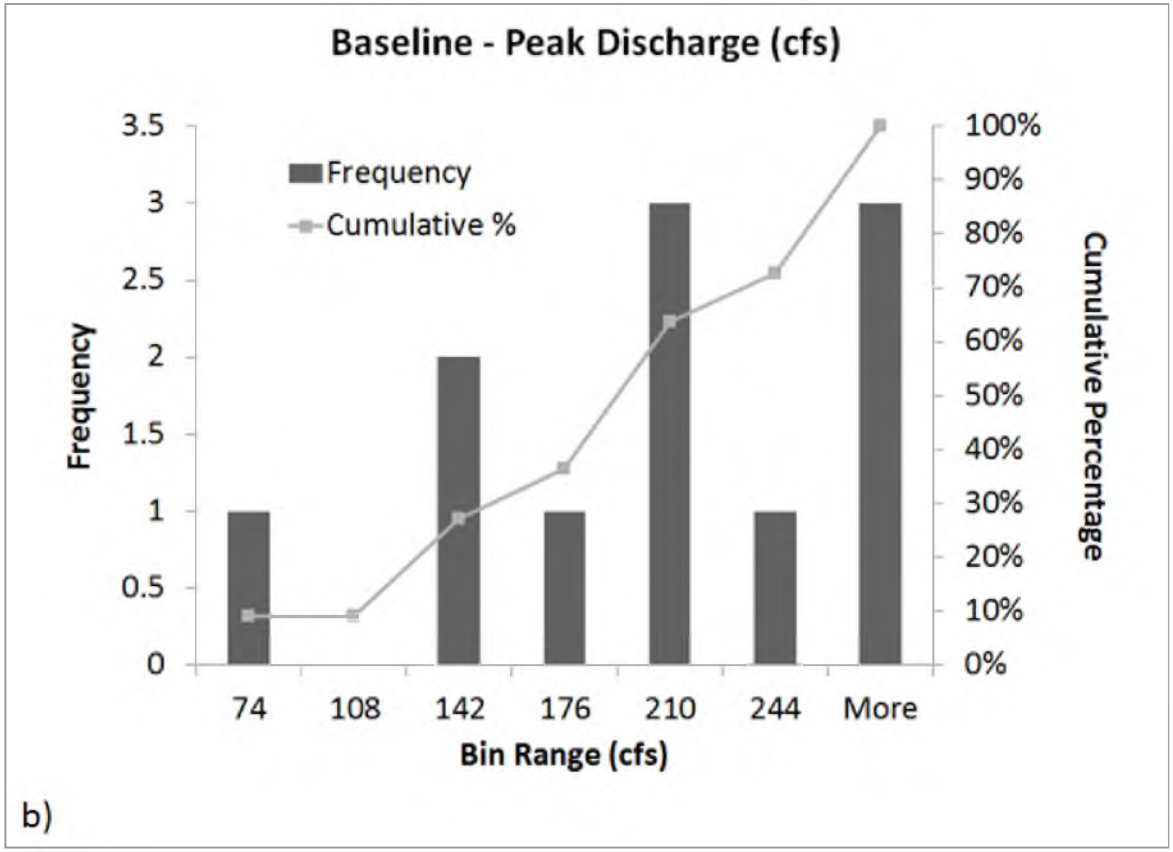

Figure 53. Continued

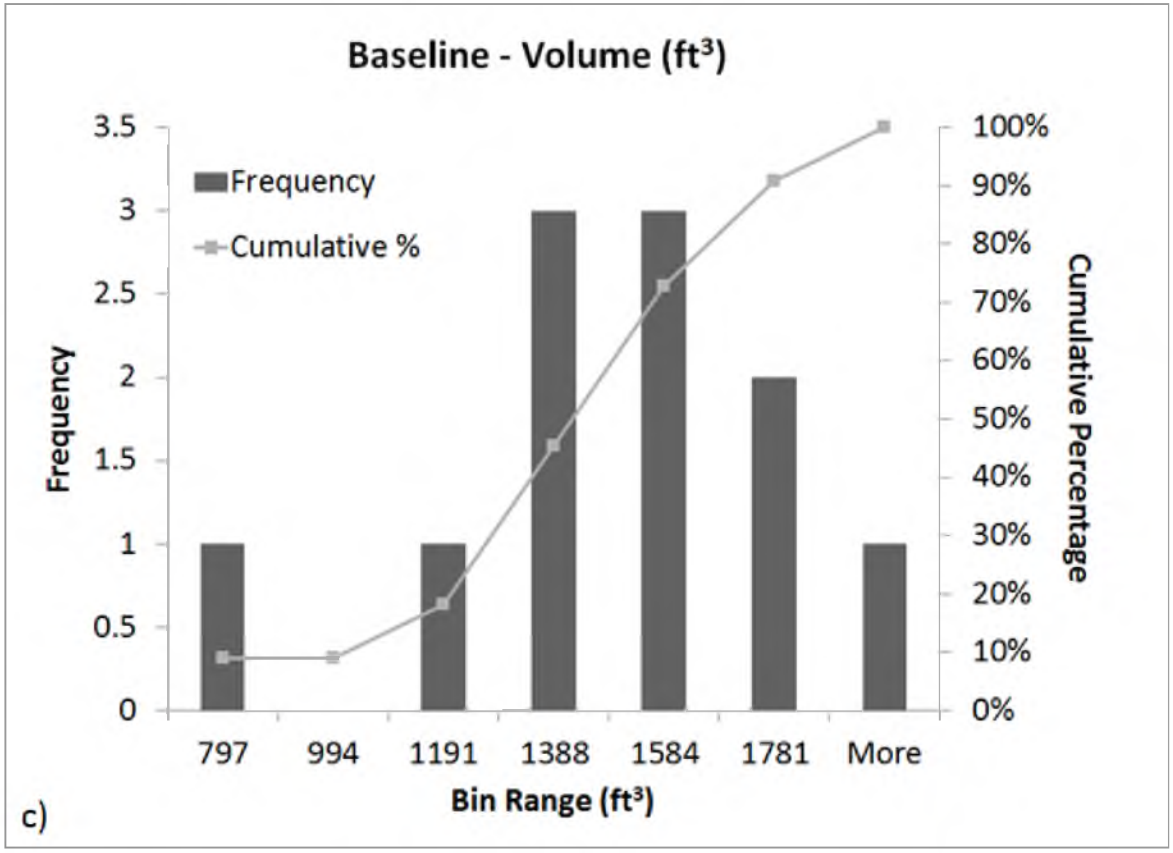

Figure 53. Continued

Test for Equal Variances

To appropriately evaluate the sample sets for significance, it is essential to utilize the most relevant equations. Testing for equal variances allows for the appropriate variation of significance test equations to be identified and then applied to the sample sets. MS Excel has built-in functions to generate the necessary metrics to evaluate the equality of sample variances and these capabilities were applied for this evaluation. The comparison was conducted for the baseline sample set and the 10% LID sample set only (Table 28). For the variances to be considered statistically equal, the F-distribution statistic should be near 1.0 and the p-value of (F <= f) should be near 0.5. Based on these criteria, the results suggest the variances to be unequal between the sample sets. Therefore, it was assumed that increasing the percent of LID implementation would exacerbate this inequality. Thus, the equations used for the next step were based on an unequal variance model for all sample sets.

Test for Significance

The sample size of this evaluation was small, therefore the t-test equation was used (as opposed to the z-score) to compare the means of each runoff characteristic (i.e., flow, peak discharge, and volume) produced from the baseline and each LID sample set. The fundamental equations deemed most appropriate for the unequal variance model are collectively referred to as the Smith-Satterthwaite test (Equations 16, 17, and 18).

$$t = \frac{\overline{x_{baseline}} - \overline{x_{LID}} - D_0}{\sqrt{\left(s^2_{baseline}/_n\right) + \left(s^2_{LID}/_n\right)}} \tag{16}$$

Table 28. Sample statistics to compare the variances for annual average flow, peak discharge, and volume between the baseline and 10% LID implementation sample sets. The f-distribution and probability statistics are greater than 1 and less than 0.5, indicating the variances are not equal.

Statistic	Average Flow		Peak Discharge		Volume	
	Baseline	10% LID	Baseline	10% LID	Baseline	10% LID
Mean	6.06	5.80	188	164	1,407	1,348
Variance	2.04	1.76	4,003	3,133	102,735	88,621
No. of Samples	11	11	11	11	11	11
Degrees of Freedom	10	10	10	10	10	10
F-distribution	1.16		1.28		1.16	
P(F<=f) one-tail	0.41		0.35		0.41	
F Critical one-tail	2.98		2.98		2.98	

$$v = \frac{\left[\left(s^2_{baseline}/_n\right)+\left(s^2_{LID}/_n\right)\right]^2}{\left[\left(s^2_{baseline}/_n\right)^2+\left(s^2_{LID}/_n\right)^2\right]/\,(n-1)} \quad (17)$$

$$95\%\,CI = (\overline{x_{baseline}} - \overline{x_{LID}}) \pm t_{\alpha/2}\sqrt{\frac{s^2_{baseline}+s^2_{LID}}{n}} \quad (18)$$

Where,

t = test statistic of dataset

v = degrees of freedom

95% CI = upper and lower bound confidence interval for the difference in means

$x_{baseline}$ = mean value of the baseline sample set

x_{LID} = mean value of the LID sample set

$s_{baseline}$ = standard deviation of baseline sample set

s_{LID} = standard deviation of baseline sample set

D_0 = null hypothesis allowable difference in means (0).

n = sample size

$t_{\alpha/2}$ = t-critical value for α/2

These equations were applied to each paired sample set to evaluate if the runoff characteristics for each LID implementation level were significantly different from the baseline values. The boundary conditions for the significance tests were established as:

- Null Hypothesis: The difference in mean values for annual average flow, peak discharge, and total volume = 0 (i.e., $H_0 = 0$)
- Alternative Hypothesis: The difference in mean values for annual average

flow, peak discharge, and total volume $\neq 0$ (i.e., $H_a \neq 0$)

- 95% Confidence: $\alpha = 0.05$

Three metrics were used to determine if the difference in the mean runoff variables are statistically significant. These are:

1. If the test statistic > $t_{\alpha,\text{degrees of freedom}}$;
2. If the probability of the Null Hypothesis < α, where $\alpha = 0.05$; and
3. If the Null Hypothesis value of zero is outside the 95% confidence interval for the difference in means.

The results of the significance tests for each pairing using the equations and boundary conditions above are presented in Table 29. All results for the three runoff characteristics produced from the 10% and 25% LID implementation support the null hypothesis that the mean runoff characteristics are not statistically different. First, the t-statistic value for both pairings is less than the t-critical value of 1.725. Second, the probability that the null hypothesis is true is greater than the chosen alpha value of 0.05. Furthermore, the confidence interval for each pairing contains the null value – meaning the null value is within the region of acceptance. The 50% and 75% LID implementation results proved to be statistically significant.

All t-statistics were greater than the respective t-critical values, the probability of the null hypothesis was less than the alpha value, and the null hypothesis is within the rejection region of the 95% confidence intervals for all three runoff characteristics.

Table 29. Results of the statistical analysis for the 10%, 25%, 50%, and 75% LID implementation simulations compared to the baseline condition. T-stat values > the t-critical value are indicative of the means being significantly different. Other metrics to show significant differences are if P(T<=t) values < 0.05 and exclusion of zero within the confidence interval.

Statistic/Metric	Baseline - Flow	10% LID - Flow	Baseline - Peak	10% LID - Peak	Baseline - Volume	10% LID - Volume
Mean	6.06	5.80	188	164	1,407	1,348
Variance	2.04	1.76	4,003	3,133	102,735	88,621
Standard Deviation	1.43	1.33	63.27	55.98	321	298
Degrees of Freedom	20		20		20	
t Stat	0.433		0.956		0.447	
P(T<=t) one-tail	0.335		0.175		0.330	
t Critical one-tail	1.725		1.725		1.725	
95% CI of difference in Means (lower bound)	-0.97		-28.78		-216.18	
95% CI of difference in Means (upper bound)	1.48		77.49		334.1	

Table 29. Continued

Statistic/Metric	Baseline - Flow	25% LID - Flow	Baseline - Peak	25% LID - Peak	Baseline - Volume	25% LID - Volume
Mean	6.06	5.40	188	154	1,407	1,254
Variance	2.04	1.56	4,003	2,770	102,735	78,533
Standard Deviation	1.43	1.25	63.27	52.63	321	280
Degrees of Freedom	20		19		20	
t Stat	1.148		1.393		1.188	
P(T<=t) one-tail	0.132		0.089		0.124	
t Critical one-tail	1.725		1.729		1.725	
95% CI of difference in Means (lower bound)	-0.54		-17.37		-115.29	
95% CI of difference in Means (upper bound)	1.85		86.50		420.3	

Table 29. Continued

Statistic/Metric	Baseline - Flow	50% LID - Flow	Baseline - Peak	50% LID - Peak	Baseline - Volume	50% LID - Volume
Mean	6.06	4.71	188	138	1,407	1,094
Variance	2.04	1.25	4,003	2,336	102,735	63,118
Standard Deviation	1.43	1.12	63.27	48.33	321	251
Degrees of Freedom	19		19		19	
t Stat	2.455		2.102		2.547	
P(T<=t) one-tail	0.012		0.024		0.010	
t Critical one-tail	1.729		1.729		1.729	
95% CI of difference in Means (lower bound)	0.19		0.01		54.73	
95% CI of difference in Means (upper bound)	2.50		100.89		570.7	

Table 29. Continued

Statistic/Metric	Baseline - Flow	75% LID - Flow	Baseline - Peak	75% LID - Peak	Baseline - Volume	75% LID - Volume
Mean	6.06	3.99	188	124	1,407	926
Variance	2.04	0.99	4,003	2,063	102,735	49,633
Standard Deviation	1.43	0.99	63.27	45.42	321	223
Degrees of Freedom	18		18		18	
t Stat	3.936		2.719		4.085	
P(T<=t) one-tail	0.000		0.007		0.000	
t Critical one-tail	1.734		1.734		1.734	
95% CI of difference in Means (lower bound)	0.96		14.51		233.56	
95% CI of difference in Means (upper bound)	3.17		113.19		728.1	

Following the comparison of the 4 LID implementation levels, the evaluation was extended to identify the percent of implementation at which the three metrics become significantly different from the baseline, which must occur between 25% and 50% implementation, based on the previous results analysis. The significance equations were applied to a number of LID implementation levels, but only the results from the identified percent implementation level where the significance occurs are presented in addition to the original 4 implementation levels. The value was determined to be 37% LID implementation. The simulation descriptive statistics are presented in Table 30. Beyond this implementation level, all runoff characteristics are significantly different from the baseline condition for this model representation of the Jordan River drainage area. Two of the three metrics to measure statistical significance were met by the results: the t-statistic was greater than t-critical and the probability of the null hypothesis is below 0.05. The confidence interval metric did contain the null hypothesis value within the region of acceptance. Because the results are so close to the cutoff values, it is deduced that any implementation level greater than 37% would produce significantly different runoff characteristics compared to the baseline condition.

These results are only applicable for the simulated results from the SWMM5 model that generated them. The statistics for LID implementation level and the resulting significance on runoff adjustment would be different given changes to surface characteristics and representation of LID within the model. Therefore, it is imperative that subsequent statistical assessments be conducted to supplement any changes to the SWMM5 model. A potential expansion of this study would be to conduct similar statistical analyses using various methods to generate output, such as various methods to

Table 30. Statistical results for the 37% LID implementation comparison to the baseline model. The same significance metrics were applied to this pairing as was used above. Because the significance tests are so close to the cutoff values, it is assumed that all implementations greater than 37% would produce significantly different runoff as compared to the baseline model.

Statistic/Metric	Baseline - Flow	37% LID - Flow	Baseline - Peak	37% LID - Peak	Baseline - Volume	37% LID - Volume
Mean	6.06	5.07	188	146	1,407	1,178
Variance	2.04	1.41	4,003	2,538	102,735	70,934
Standard Deviation	1.43	1.19	63.27	50.38	321	266
Degrees of Freedom	19		19		19	
t Stat	1.756		1.740		1.819	
P(T<=t) one-tail	0.047		0.049		0.042	
t Critical one-tail	1.729		1.729		1.729	
95% CI of difference in Means (lower bound)	-0.19		-8.61		-34.37	
95% CI of difference in Means (upper bound)	2.16		93.47		491.6	

represent LID, and evaluate the difference in estimated implementation levels that produce significantly different runoff results. This could lend insight into the potential to define a standard measure of significance for LID implementation.

Philadelphia, Pennsylvania Model

The same methods that were presented in the previous section were applied to identify the level of GSWI implementation within the Philadelphia, Pennsylvania model (PHL) that produced significantly different hydrologic output results. The modeling and evaluation specifics for the PHL model are presented in the sections that follow.

Method

The data used for this evaluation were produced from a SWMM5 model of the southeast portion of the Philadelphia, Pennsylvania drainage area (Figure 54). In total, 301 subcatchments are used to represent the area in this model setup. The evaluation uses the annual average flow, annual peak discharge, and total annual volume for the system to define the characteristic runoff from the area. Samples for evaluation were taken for each year from 1990 to 2014, for a total of 24 years (i.e., sample size = 24). Simulation results representing baseline conditions (i.e., no LID implementation) for the 24 years were compared against the results produced from simulating 37-, 40-, and 45% LID implementation. LID implementation for all simulations used a 10.7 loading ratio, a 1-inch capture volume, and a 24-hour drawdown time. The only change between LID representations was the amount of impervious surface converted to LID (i.e., 37-, 40-, and 45%). LID was represented as pervious surface to allow infiltration and

Figure 54. Representation of the southeast portion of Philadelphia, Pennsylvania used in this evaluation.

supplemental storage to manage the full inch of required capture volume and then release sewer system within the required 24 hours. The loading ratio dictated the amount of impervious area loading to an acre of pervious LID (i.e., 10.7 acres of impervious area loading to 1 acre of LID). The evaluation performed included the following steps in the order they were performed: 1) Data Simulation; 2) Assumed Normality; 3) Assumed Unequal Variances; and 4) Test for Significance.

Results and Discussion

Data Simulations

Simulations were completed for the baseline, 37%, 40%, and 45% LID implementation models for each year from 1990-2014. The average annual flow, peak discharge, and total volume were documented for each year and the mean, standard deviation, and variance were calculated for each sample set. The collected output is presented as Table 31. As expected, the magnitude of the runoff characteristics decrease as LID implementation increases.

Assumed Normality

For the purposes of this evaluation, it was assumed that if the datasets from the SLC evaluation were normally distributed, the subsequent LID simulations for PHL would be as well.

Assumed Unequal Variances

For the purposes of this evaluation, it was assumed that if the datasets from the SLC evaluation were normally distributed, the subsequent LID simulations for PHL would be as well.

Test for Significance

As with the SLC evaluations, the t-test equations were used (as opposed to the z-score) to compare the means of each runoff characteristic (i.e., flow, peak discharge, and volume) produced from the baseline and each LID sample set. The fundamental

Table 31. Descriptive statistics for each PHL simulation, which includes the baseline condition (no LID) and three LID scenarios.

Average Flow (cfs)								
Simulation	n	Mean	Standard Deviation	Standard Error	95% confidence Intervals		Minimum	Maximum
					Upper	Lower		
Baseline	24	148	59	3,530	172	125	78	267
37% GSWI	24	100	60	3,543	124	77	41	230
40% GSWI	24	99	60	3,591	123	75	39	228
45% GSWI	24	96	60	3,636	120	71	36	226
Peak Flow (cfs)								
Simulation	n	Mean	Standard Deviation	Standard Error	95% confidence Intervals		Minimum	Maximum
					Upper	Lower		
Baseline	24	10,630	5,813	33,792,244	12,955	8,304	3,043	21,881
37% GSWI	24	7,774	5,409	29,260,940	9,938	5,610	1,828	18,617
40% GSWI	24	7,672	5,418	29,356,265	9,839	5,504	1,774	18,565
45% GSWI	24	7,499	5,431	29,490,493	9,672	5,326	1,685	18,489
Volume (MG)								
Simulation	n	Mean	Standard Deviation	Standard Error	95% confidence Intervals		Minimum	Maximum
					Upper	Lower		
Baseline	24	6,203	1,251	1,565,571	6,703	5,702	4,030	9,033
37% GSWI	24	4,545	1,080	1,166,463	4,977	4,113	2,775	7,074
40% GSWI	24	4,409	1,067	1,137,474	4,836	3,983	2,672	6,914
45% GSWI	24	4,183	1,044	1,090,350	4,601	3,765	2,501	6,646

equations deemed most appropriate for the unequal variance model are collectively referred to as the Smith-Satterthwaite test and were presented in the previous discussion on the SLC model evaluations. These equations were applied to each paired sample set to evaluate if the runoff characteristics for each LID implementation level were significantly different from the baseline values. The boundary conditions for the significance tests were the same as for the SLC evaluations:

- Null Hypothesis: The difference in mean values for annual average flow, peak discharge, and total volume = 0 (i.e., $H_0 = 0$)
- Alternative Hypothesis: The difference in mean values for annual average flow, peak discharge, and total volume $\neq 0$ (i.e., $H_a \neq 0$)
- 95% Confidence: $\alpha = 0.05$

Three metrics were used to determine if the difference in the mean runoff variables are statistically significant. These are:

1. If the test statistic > $t_{\alpha,\text{degrees of freedom}}$ (value obtained from Table 24);
2. If the probability of the Null Hypothesis < α, where $\alpha = 0.05$; and
3. If the Null Hypothesis value of zero is outside the 95% confidence interval for the difference in means.

All results for the three runoff characteristics produced from the LID implementation levels proved to be statistically significant (Table 32). All t-statistics were greater than the respective t-critical values, the probability of the null hypothesis was less than the alpha value, and the null hypothesis is within the rejection region of the 95% confidence intervals for most of the three runoff characteristics.

Table 32. T-test results for the 37%-, 40%-, and 45% LID implementation levels. All sets of hydrologic metrics were determined to be statistically different from baseline (no LID) conditions.

Statistic/Metric	Baseline - Flow	LID 37% - Flow	Baseline - Peak	LID 37% - Peak	Baseline - Volume	LID 37% - Volume
Mean	148	100	10,630	7,774	6,203	4,545
Variance	3,530	3,543	33,792,244	29,260,940	1,565,571	1,166,463
Standard Deviation	59	60	5,813	5,409	1,251	1,080
Degrees of Freedom	22		22		22	
t Stat	2.798		1.762		4.914	
P(T<=t) one-tail	0.004		0.042		0.000	
t Critical one-tail	1.725		1.725		1.725	
95% CI of difference in Means (lower bound)	12.22		-525.46		954.20	
95% CI of difference in Means (upper bound)	83.84		6237		2362	

Table 32. Continued

Statistic/Metric	Baseline - Flow	LID 40% - Flow	Baseline - Peak	LID 40% - Peak	Baseline - Volume	LID 40% - Volume
Mean	148	99	10,630	7,672	6,203	4,409
Variance	3,530	3,591	33,792,244	29,356,265	1,565,571	1,137,474
Standard Deviation	59	60	5,813	5,418	1,251	1,067
Degrees of Freedom	22		22		22	
t Stat	2.893		1.824		5.344	
P(T<=t) one-tail	0.003		0.037		0.000	
t Critical one-tail	1.725		1.725		1.725	
95% CI of difference in Means (lower bound)	13.91		-425.61		1093.47	
95% CI of difference in Means (upper bound)	85.77		6342		2494	

Table 32. Continued

Statistic/Metric	Baseline - Flow	LID 45% - Flow	Baseline - Peak	LID 45% - Peak	Baseline - Volume	LID 45% - Volume
Mean	148	96	10,630	7,499	6,203	4,183
Variance	3,530	3,543	33,792,244	29,260,940	1,565,571	1,166,463
Standard Deviation	59	60	5,813	5,409	1,251	1,080
Degrees of Freedom	22		22		22	
t Stat	3.081		1.932		5.986	
P(T<=t) one-tail	0.002		0.030		0.000	
t Critical one-tail	1.725		1.725		1.725	
95% CI of difference in Means (lower bound)	17.08		-250.35		1315.92	
95% CI of difference in Means (upper bound)	88.70		6512		2724	

APPENDIX D

SUPPLEMENTAL SPATIAL DISTRIBUTION STUDY

Philadelphia, Pennsylvania

The spatial distribution objective was evaluated by comparing output from two types of GSWI distribution scenarios within the PHL model. The uniform distribution placed GSWI equally throughout all subcatchments, while the targeted distribution placed GSWI within specific subcatchments (Figure 55). The latter approach used four different sets of subcatchments to evaluate hydrologic response differences to the uniform distribution scenario. The same impervious surface area of 2,427 acres was managed by GSWI for all scenarios. Therefore, targeted spatial distribution scenarios were constrained to achieve this minimum value. The density of GSWI within each targeted model varied based on the cumulative impervious area available (Table 33). For the uniform distribution, the total impervious area from all subcatchments was available for management. For the targeted scenarios, only the impervious area within the selected subcatchments was available for management. To appropriately compare the results, the same amount of impervious area managed with the uniform distribution scenario must be managed within the targeted scenarios.

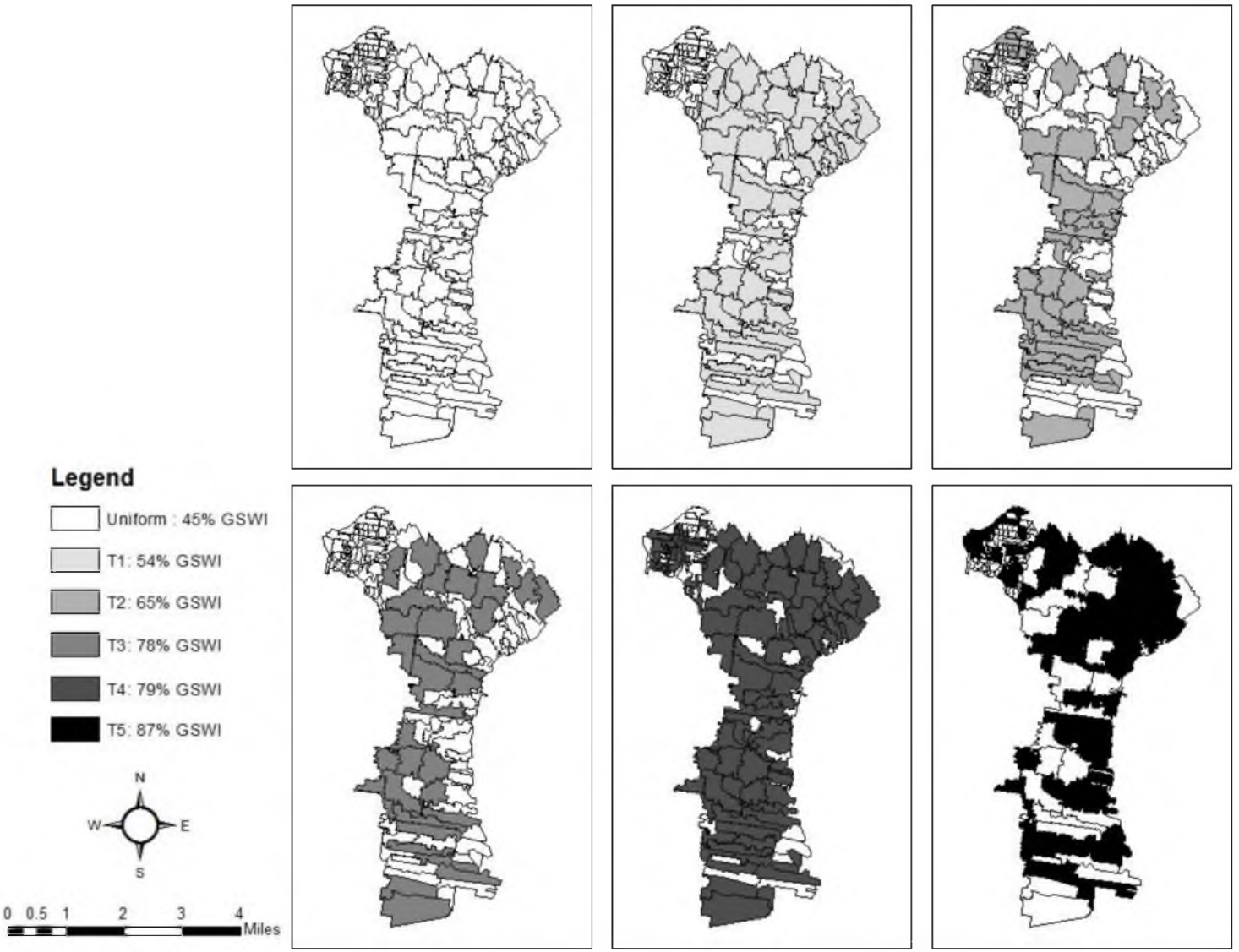

Figure 55. The uniform distribution scenario had GSWI in all subcatchments (top-left figure). Five targeted distributions were simulated where GSWI was implemented within the shaded subcatchments only.

Table 33. Impervious area managed for each scenario and the equivalent percent of impervious area controlled relative to the number of sheds receiving GSWI.

Distribution Type/ Simulation	Total Impervious Area of Sheds with GSWI (acres)	Impervious Area Managed with GSWI (acres)	% Impervious Area Controlled within GSWI Sheds
Uniform	11,431	2,427	45%
T1	4,518	2,427	54%
T2	3,734	2,427	65%
T3	3,099	2,427	78%
T4	3,087	2,427	79%
T5	2,789	2,427	87%

PHL Statistical Analysis

The descriptive statistics show minor variations in values (Table 34). The effect of spatial distribution is not immediately apparent after reviewing these data.

PHL Hydrologic Simulations

Scatter plots of the data plotting each target scenario against the uniform scenario output show only minor discrepancies (Figure 56). The targeted distribution average flow rate showed some variations compared to the baseline condition. This can be attributed to the dampening effect from uniformly distributing GSWI within the baseline model.

Table 34. Spatial distribution scenario descriptive statistics for average flow rate, peak discharge, and volume.

Average Flow (cfs)								
Simulation	n	Mean	Standard Deviation	Standard Error	95% confidence Intervals		Minimum	Maximum
					Upper	Lower		
45% GSWI - UNIFORM	24	96	60	3,636	120	71	36	226
54% GSWI - Distribution 1	24	92	53	2,856	114	71	36	208
65% GSWI - Distribution 2	24	99	49	2,415	118	79	43	209
78% GSWI - Distribution 3	24	97	55	3,013	119	75	41	219
79% GSWI - Distribution 4	24	97	53	2,766	118	76	41	219
87% GSWI - Distribution 5	24	105	49	2,354	124	85	47	208
Peak Flow (cfs)								
Simulation	n	Mean	Standard Deviation	Standard Error	95% confidence Intervals		Minimum	Maximum
					Upper	Lower		
45% GSWI - UNIFORM	24	7,499	5,431	29,490,493	9,672	5,326	1,685	18,489
54% GSWI - Distribution 1	24	7,219	5,232	27,369,510	9,312	5,126	1,492	18,142
65% GSWI - Distribution 2	24	7,853	5,468	29,902,935	10,041	5,665	1,557	20,109
78% GSWI - Distribution 3	24	7,794	5,626	31,646,705	10,045	5,544	1,706	18,918
79% GSWI - Distribution 4	24	7,714	5,469	29,910,851	9,902	5,526	1,645	19,603
87% GSWI - Distribution 5	24	7,699	5,477	30,002,326	9,890	5,508	1,532	20,459
Volume (MG)								
Simulation	n	Mean	Standard Deviation	Standard Error	95% confidence Intervals		Minimum	Maximum
					Upper	Lower		
45% GSWI - UNIFORM	24	4,183	1,044	1,090,350	4,601	3,765	2,501	6,646
54% GSWI - Distribution 1	24	4,085	1,046	1,094,424	4,504	3,667	2,389	6,785
65% GSWI - Distribution 2	24	4,155	1,045	1,091,103	4,573	3,737	2,445	6,780
78% GSWI - Distribution 3	24	4,178	1,032	1,064,429	4,591	3,765	2,516	6,519
79% GSWI - Distribution 4	24	4,172	1,034	1,068,190	4,585	3,758	2,496	6,628
87% GSWI - Distribution 5	24	4,110	1,005	1,010,123	4,512	3,708	2,463	6, 534

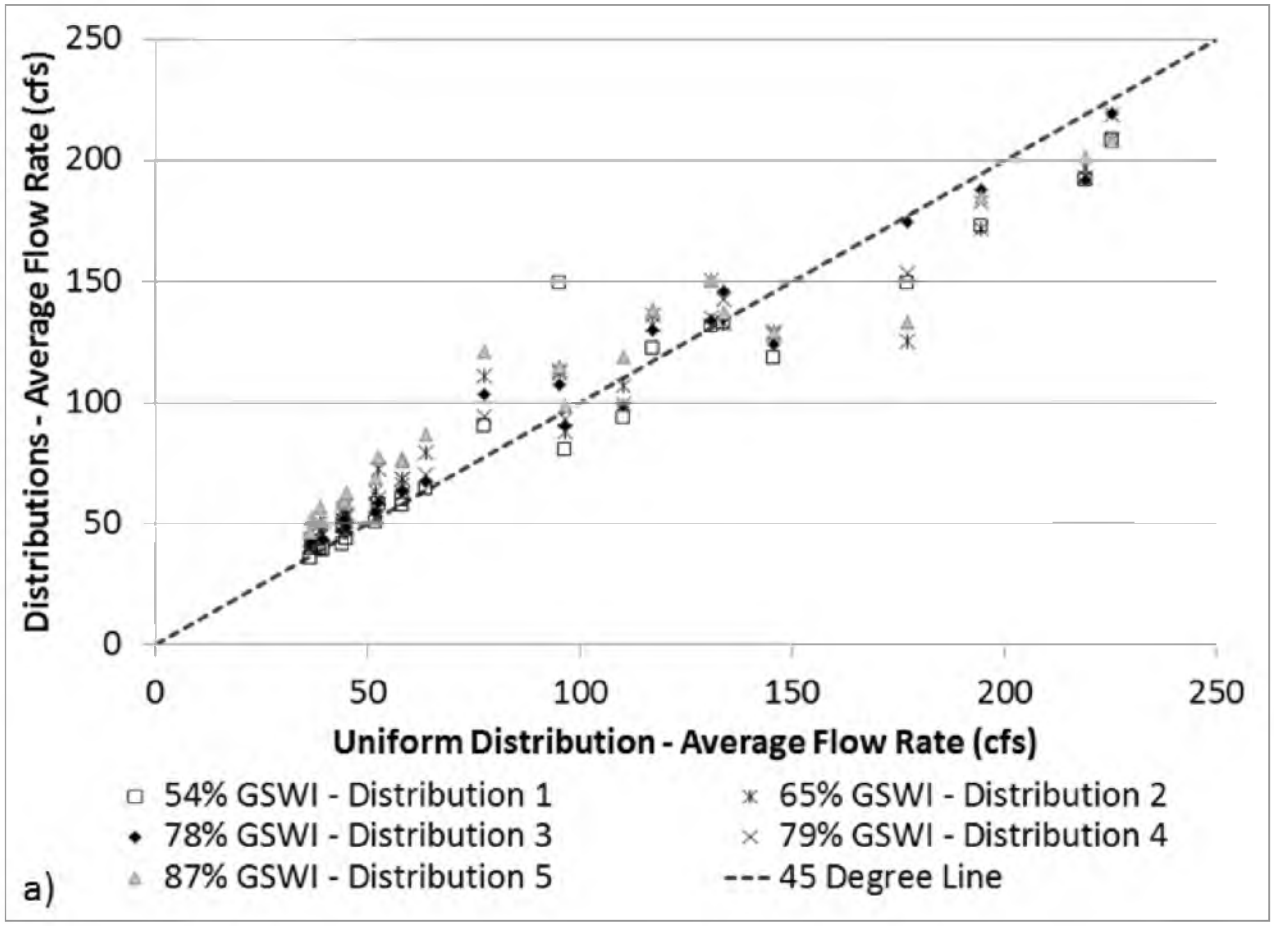

Figure 56. Scatter plots of the targeted distributions' average flow rate (a), peak discharge (b), and volume (c) compared against the uniform distribution scenario output. Only minor discrepancies are shown with the peak discharge being slightly greater for the targeted scenarios.

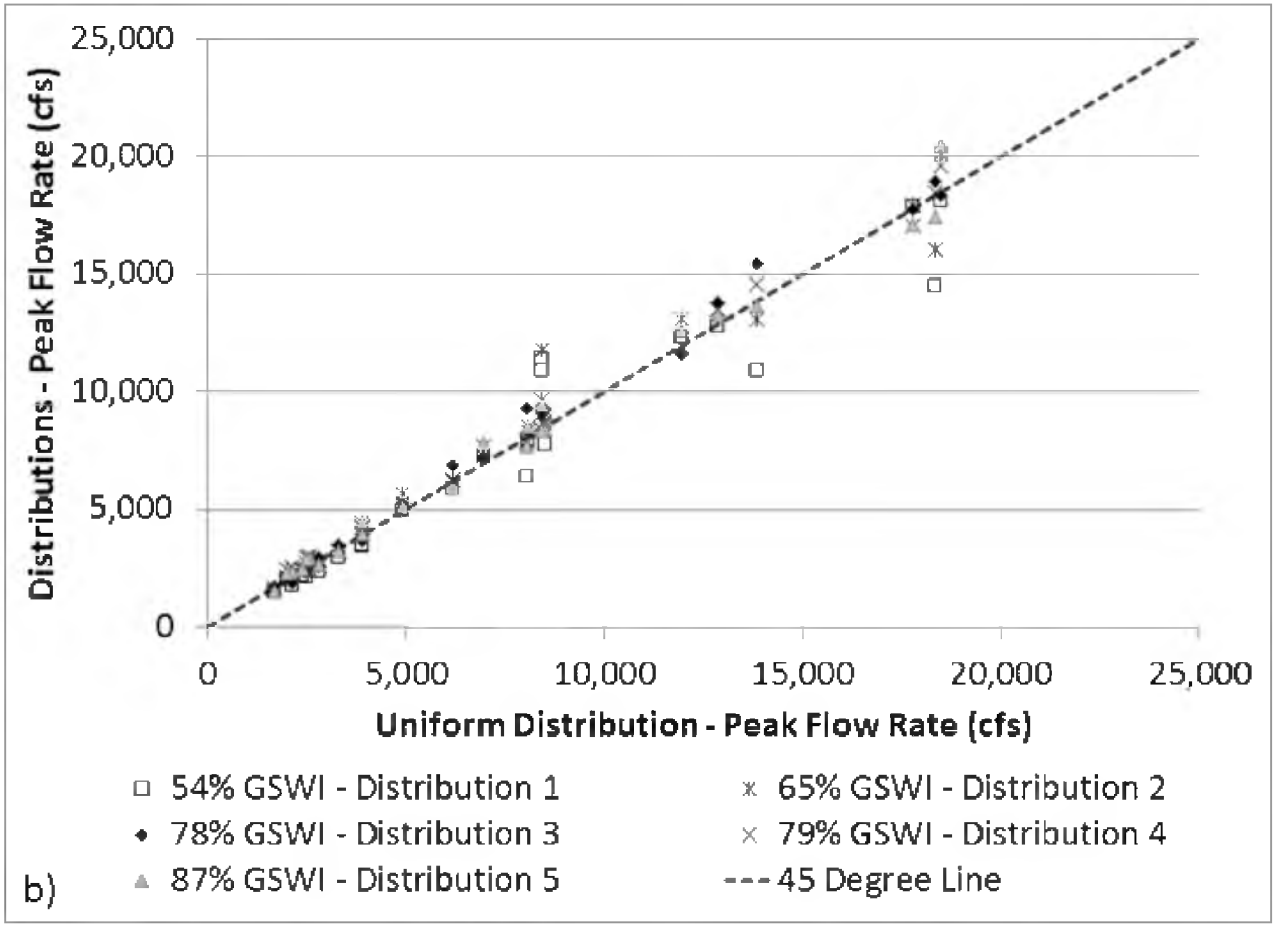

Figure 56. Continued

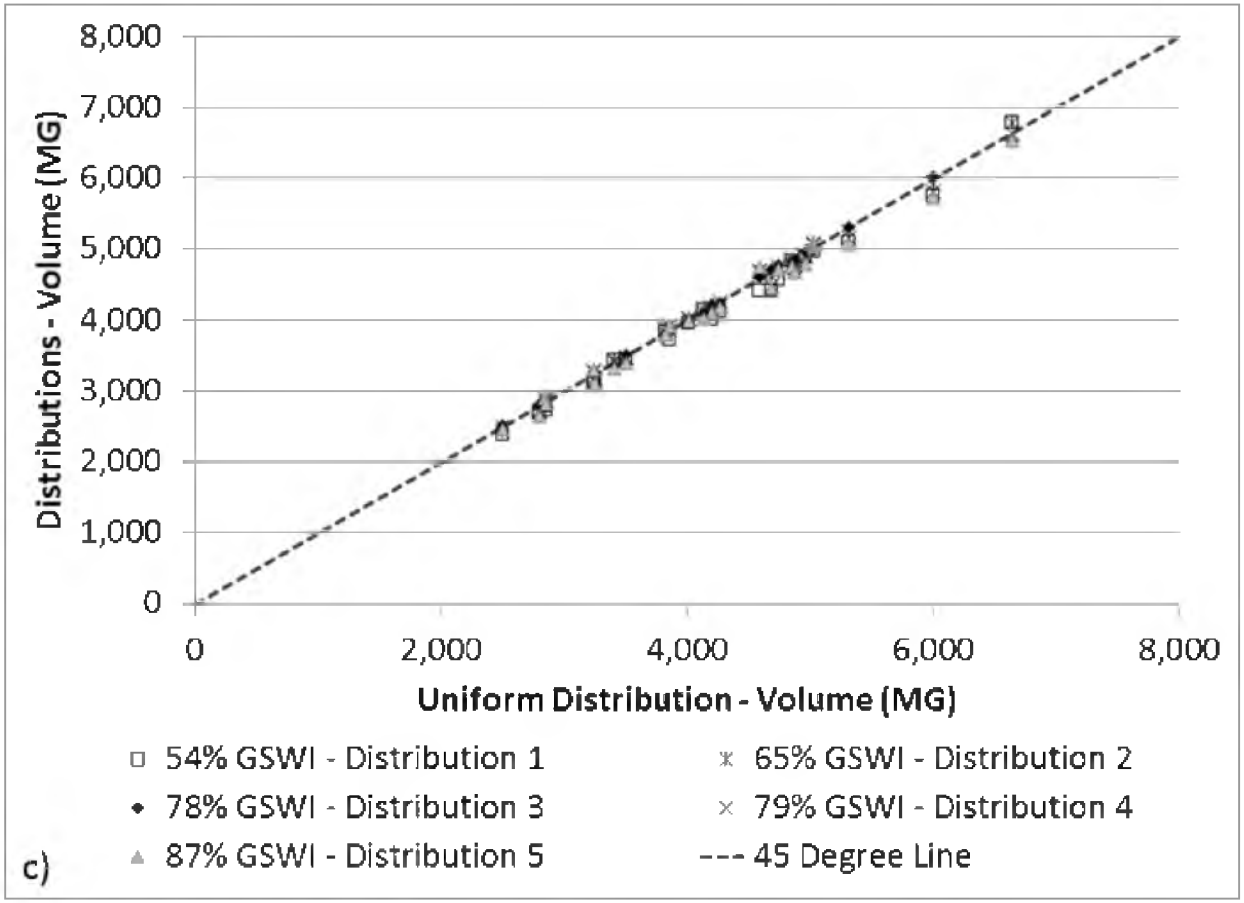

Figure 56. Continued

APPENDIX E

GSWI INFILTRATION STUDIES

Review Monte Carlo Methods for use in Assessing Infiltration Depths

Introduction

In my initial response to Dr. McPherson's exam question for this section, I proposed applying Monte Carlo methods at the subcatchment level to evaluate simulated infiltration depths produced from planned green stormwater infrastructure (GSWI) implementation. I hypothesized that the aggregated infiltration depths could be used to derive a practical expression of potential total watershed infiltration depths, with a goal to maximize this value, for a target level of spatial implementation of GSWI within the watershed area. The major advantage to this approach would allow the estimated infiltration to be determined without the time intensive tasks of simulating the models and organizing and analyzing the output dataset to arrive at the estimate, thus reducing overall project planning costs while at the same time exploiting the resources of multiple analysis methods used to evaluate the watershed area. The process could be completed for a number of GSWI implementation scenarios to compare the differences in estimated stormwater infiltration for the GSWI system.

Methods

Model Setup and Site Characterization

A model representation of the Salt Lake City, Utah area lying east of the Jordan River was used for this analysis (Figure 57). The area was represented with 54 subcatchments, each having a unique set of Green-Ampt infiltration parameters. The infiltration parameters were established using USGS soil data for the study area. Many of the subcatchments represent urban residential and commercial areas. These subcatchments have characteristically high values of impervious area (e.g., ~ 30-80%) and reduced infiltration capabilities (i.e., lower hydraulic conductivity values). Conversely, the region also contains large areas representing the lower bench of the Wasatch Front canyons. The representative subcatchments for these areas have a lower impervious area percentage (e.g., ~ 10-20%) and greater capacity for infiltration (Figure 58). Thus, the modeled area has a wide range of infiltration values and capacities. Indeed, the soil diversity within the region is represented by infiltration rates as low as 0.002 inches/hour and a few subcatchments with rates greater than 1 inch/hour (Figure 59). The area weighted hydraulic conductivity for this model is 0.8 inches/hour. This is a relatively high infiltration rate for an urban area, but falls within the range of the majority of subcatchment's hydraulic conductivity values (Figure 59). The results from this study are applicable to this study region, but further analyses could be conducted to determine if they may be extrapolated to represent regions with similar hydrologic surface characteristics.

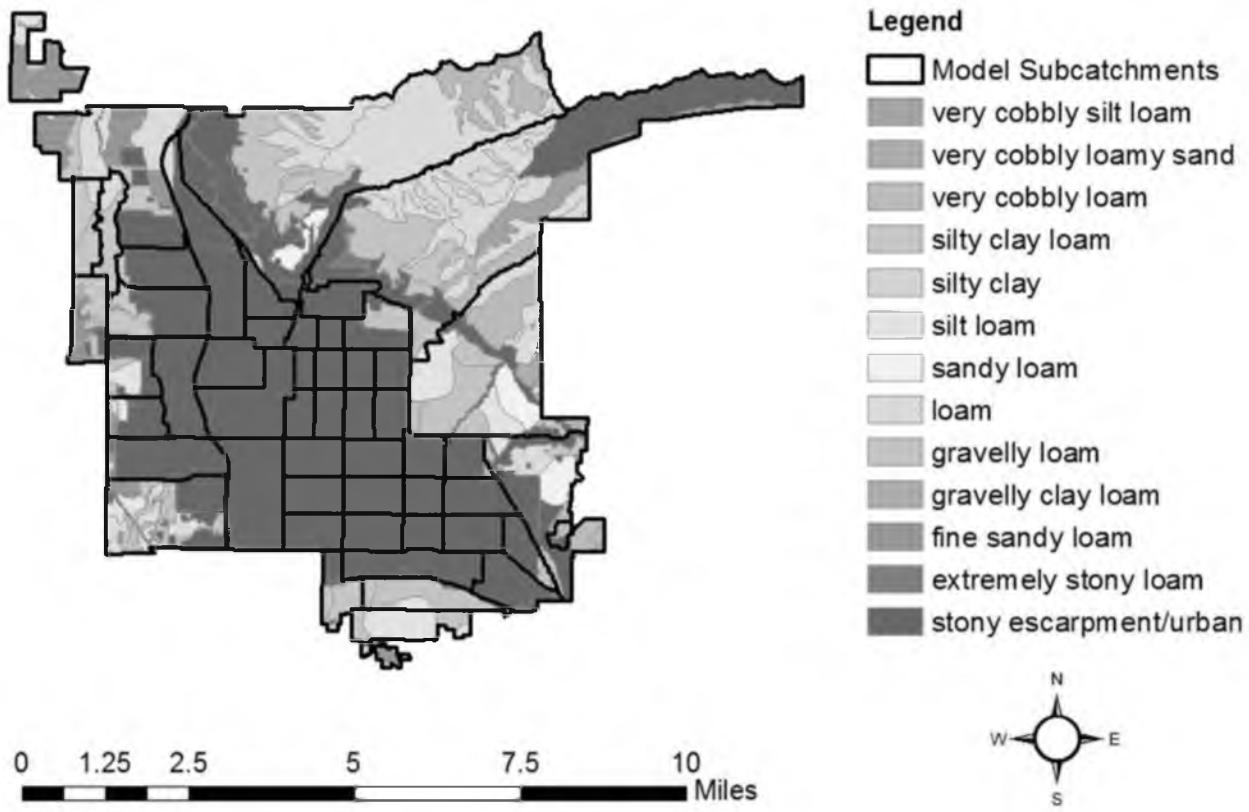

Figure 57**.** The area modeled within this study representing the eastern portion of Salt Lake City, Utah. The outlined areas are the subcatchments used to generate infiltration data within SWMM5. The colored regions indicate the various soil types present in the region. The dark red areas in the center reflect the urban area and have varying impervious percentages within the 40-80% range.

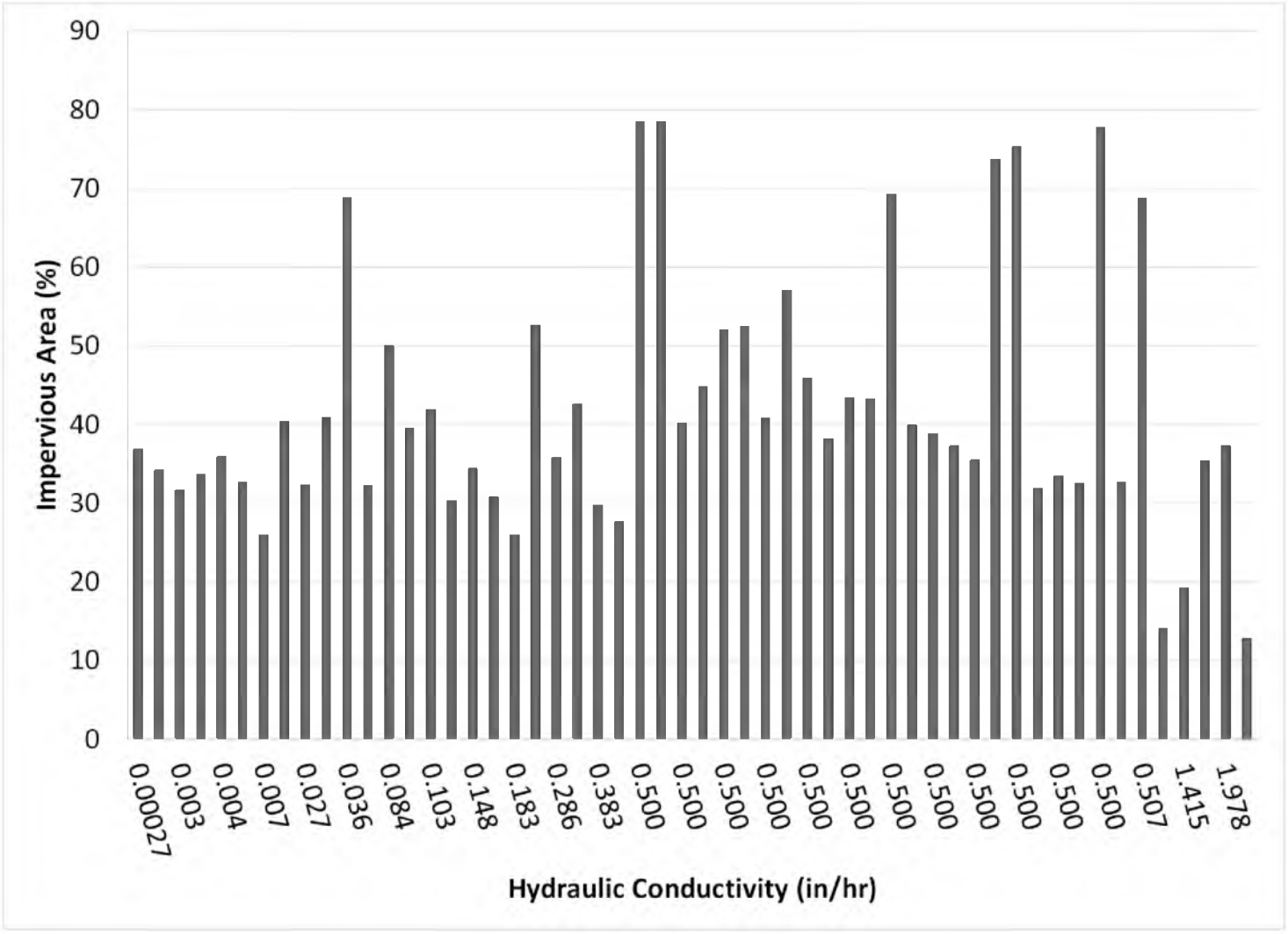

Figure 58. The hydraulic conductivities for each subcatchment and its corresponding percent impervious area. The percent impervious value reflects the magnitude of urban density, and generally shows that increased impervious percentage correlates to a reduced hydraulic conductivity.

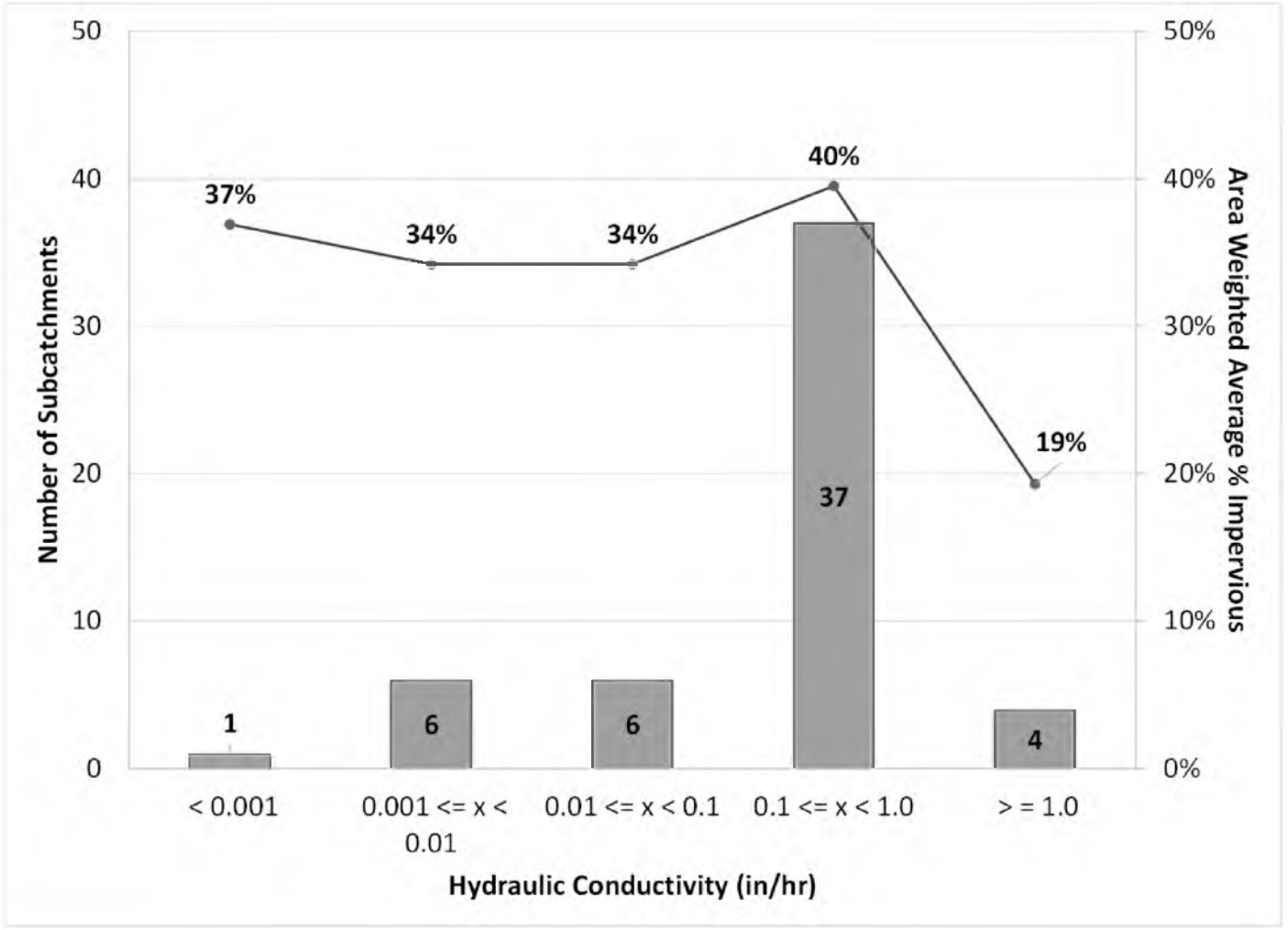

Figure 59**.** A histogram showing the distribution of subcatchments based on the range of hydraulic conductivities. The majority of the subcatchments have hydraulic conductivities between 0.1 and 1.0 inches /hour. The area weighted average hydraulic conductivity for the entire region is 0.8 inches/hour. The area weighted average percent impervious for each data range shows the higher proportion of impervious area for lower hydraulic conductivities for the study region.

Scenario Descriptions

Three simulation scenarios were developed for this analysis: 1) a baseline condition, 2) GSWI implementation of 37%, and 3) GSWI implementation of 75%. The percent of GSWI implementation represents the amount of impervious area within each subcatchment managed by a green system. A green system, as defined for this analysis, is one that uses pervious areas to intercept runoff from the managed amount of impervious areas. Thus, for these scenarios, 37% and 75% of impervious area runoff within each subcatchment was intercepted by pervious area. The estimated subcatchment infiltration depths were aggregated by SWMM5 to represent the depths for the entire study area. The infiltrated depths for each rainfall event were exported from SWMM5 for each scenario. A frequency analysis was conducted on the percent increases (relative to the baseline condition) of infiltrated depth per event for both GSWI scenarios. In this way, the distribution of expected increases to infiltration can be presented for each GSWI implementation.

Monte Carlo Method

The four major steps followed to complete the Monte Carlo simulations were: 1) Derivation of an equation to describe the infiltration process, 2) Describe the factors within the process equation, 3) Generate a large set of random data points, and 4) Calculate output using the random dataset. The details for how these steps were addressed with this analysis are provided in the sections below.

Step 1. Derivation of an equation to describe the infiltration process: The Green-Ampt equations were used to estimate infiltration depth at each subcatchment. For

efficiency, the SWMM5 model was used to perform all Green-Ampt infiltration calculations.

Step 2. Describe the factors within the process equation: The Green-Ampt equation is a complicated one that accounts for the wetness of the soil (both before and during infiltration), the rate of infiltration during saturated conditions (i.e., Hydraulic conductivity), and suction properties at the surface of the soil. Adjustments can be made to these parameters as the soil becomes saturated (which reduces the infiltration rate) or if ponding occurs (essentially introducing a hydraulic head on the surface). The swmm5 model requires four input parameters to estimate infiltration depth with the Green-Ampt equations: rainfall depth (inches), suction head (inches), saturated hydraulic conductivity (inches/hour), and the initial soil moisture deficit ratio. For each subcatchment, the suction head, saturated hydraulic conductivity, and initial deficit values varied and were dictated by the soil properties of the area being represented, as discussed previously. These three soil parameters at each subcatchment were kept constant for all simulations. The rainfall depth was established as the random variable.

Step 3. Generate a large set of random data point: A rainfall timeseries for 11-years' data (2000-2010) was used to drive the infiltration calculations in SWMM5. Each rainfall event, which naturally resulted in a corresponding infiltration event, was considered a randomly generated data point. In total, 586 rainfall events or data points were used for each simulated scenario.

Step 4. Calculate output using the random dataset: The 586 rainfall events were applied to each subcatchment. The calculated infiltration depth for each event at all subcatchments was aggregated by SWMM5 to estimate the total watershed infiltration for

all rainfall events.

Results

The statistical data for each simulation showed small differences in infiltration depth on an event basis (Table 35). The total volumes increased by 2.2% and 4.4% for the 37% GSWI and 75% GSWI simulation, respectively. The mean, median, and standard deviation of each dataset showed very little difference. To gain a deeper understanding of these results, the estimated infiltration depths for the 37% GSWI scenario were subtracted from the output for the baseline condition and the statistics for these data were summarized (Table 36). These differences were further analyzed to understand how estimated infiltration percentages change in response to incorporating GSWI. The same analysis was conducted using the 75% GSWI output relative to the baseline condition (Table 36). The average estimated increase in infiltration per event was 3% and 6% for the 37% and 75% GSWI scenarios, respectively. The standard deviation is higher for the 75% GSWI scenario, which indicates the spread of potential infiltration values is greater than that of the 37% GSWI scenario. This is also seen in the scatter plot of each scenarios output contained in Figure 60. The confidence interval, which identifies the boundary conditions within which the true mean exists at a 95% confidence, is small for both simulations. The standard errors of 0.1% and 0.2% for the 37% and 75% GSWI indicate the sample datasets are an adequate representation of the actual response. Of course, observed data are necessary to validate these results, but these observations are not available. Therefore, these results can only be estimations of the potential observed value.

While the confidence intervals established the average increase of infiltration that

Table 35. Summary of simulated infiltration statistics for all scenarios.

Statistical Variables	Baseline	37% GSWI	75% GSWI
No. of Events	586	586	586
Minimum Volume (in.)	0.0	0.0	0.0
Maximum Volume (in.)	3.59	3.65	3.80
Total Volume (in.)	136	139	142
Mean (in.)	0.49	0.51	0.52
Median (in.)	0.30	0.31	0.32
Standard Deviation (in.)	0.56	0.58	0.59
Variance ($in.^2$)	0.31	0.33	0.35
Coeff. Of Variation	0.63	0.65	0.67
Skewness	2.08	2.07	2.07

Table 36. Summary of statistics for the percent difference relative to the baseline condition for each GSWI implementation.

Statistical Variables	37% GSWI Difference	75% GSWI Difference
Minimum Increase (%)	-7%	-7%
Maximum Increase (%)	20%	23%
Mean Increase (%)	2.6%	5.8%
Median Increase (%)	2.4%	5.6%
Standard Deviation (%)	1.8%	2.6%
Standard Error	0.1%	0.2%
95% Confidence	2.5% - 2.8%	5.6% - 6%
Coeff. Of Variation	0.01	0.01
Skewness	1.1	0.9
No. of Bins	25	25
Bin size (%)	1%	1%

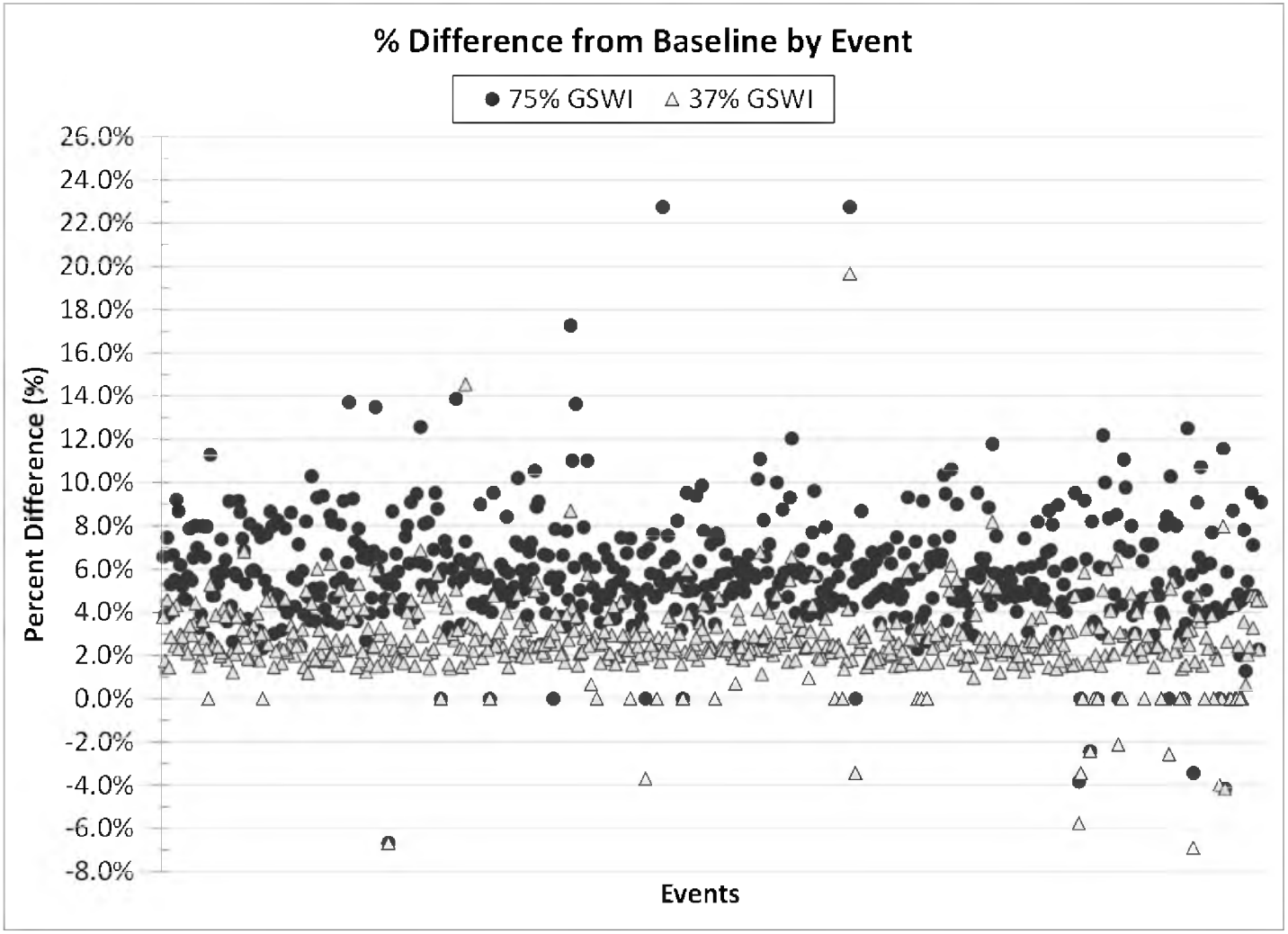

Figure 60. The scatter plot of the increase in infiltrated depth relative to the baseline condition for the 37% GSWI and 75% GSWI scenarios. The data points for the 37% scenario are more tightly clustered around the mean value of 2.6% than the data points are for the 75% scenario, indicating the spread for potential estimates of infiltration depth are greater as the percent implementation increases.

could be expected from each GSWI implementation scenario, consideration of the distribution of potential values was also required.

Review of Figure 61 shows the estimated increases from the 37% GSWI scenario form a tight configuration near the average value of 2.6%, while the 75% GSWI data points show a lower density surrounding the mean value of 5.8%. To further this point, Figure 57 explicitly shows the differences in spread of estimated percent increases in infiltration for each scenario. Over 40% of all infiltration events for the 37% GSWI scenario had an increased infiltration of 2-3% and the potential for infiltration depths beyond this value tapers off dramatically. This could be indicative of the GSWI pervious areas reaching saturated soil conditions for a number of events, which would limit the ability of the GSWI system to infiltrate more than 2-3%. However, increasing the pervious area to manage 75% of impervious area expands the capacity enough to capture more runoff from each event without reaching the saturation point of the soil. Thus, the range of probable infiltration depths is greater, or less restricted, than that of the 37% GSWI scenario. This means there is also more uncertainty in the estimated increases in infiltration depth for larger implementations of GSWI.

Conclusions

The highlights of these analyses are the following:

1. The input datasets produced a standard error of 0.1% and 0.2% at a 95% confidence for the 37% and 75% GSWI scenarios, respectively. This is a small margin of error and indicates the uncertainty associated with the calculated mean is small for both scenario sets. Thus, the average percent

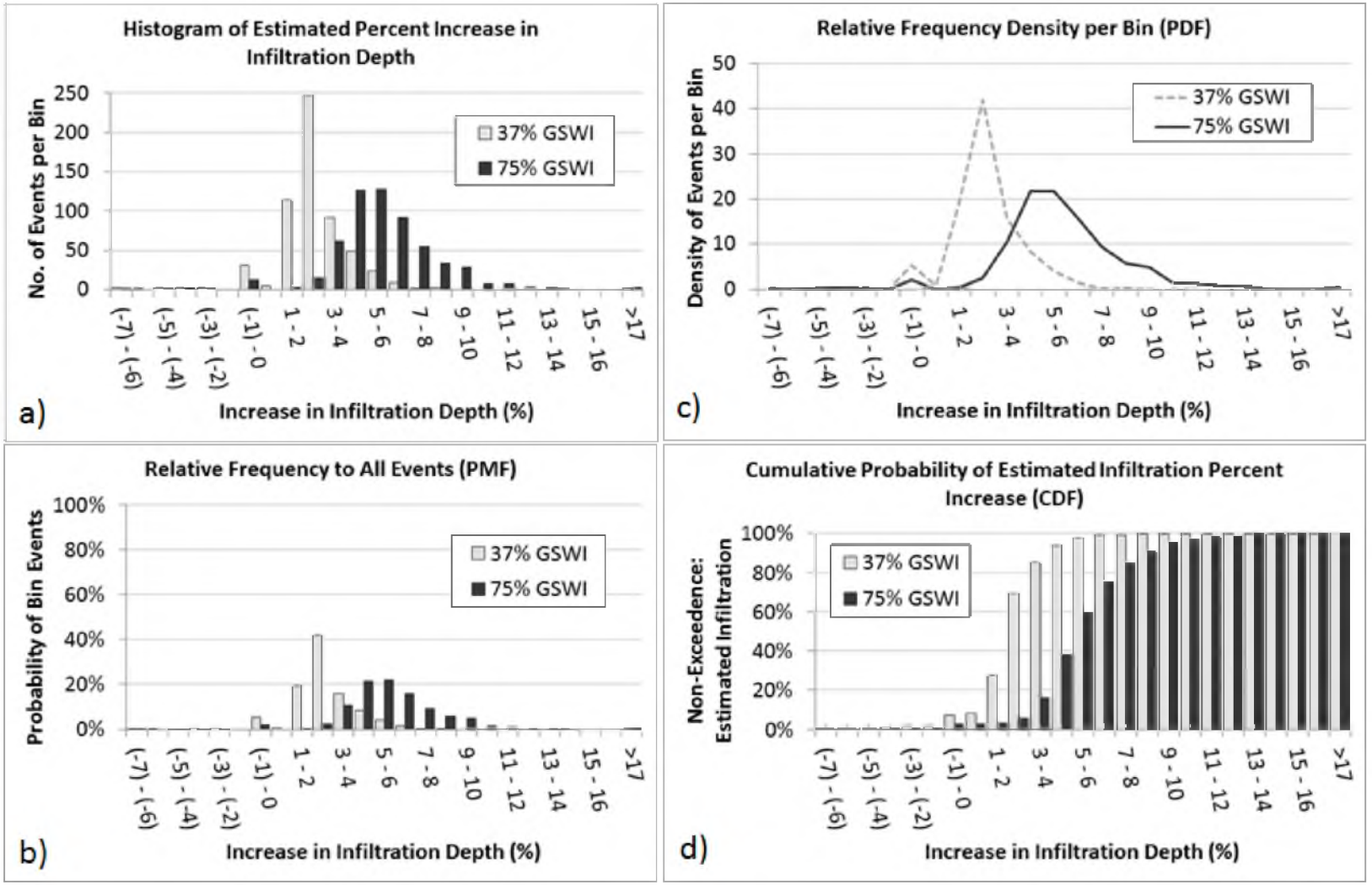

Figure 61. Frequency graphs generated using the output produced from SWMM5: a) histogram of the number of infiltration events per bin, b) the probability mass function of the histogram events calculated by dividing the number of events per bin by the total number of events, c) the probability density function generated by dividing the PMF data by the bin size, and d) the cumulative distribution frequency of the histogram data, which is the cumulative probability of events per bin.

increase in infiltrated depth relative to baseline conditions for 37% and 75% GSWI for conditions specific to this watershed model is 2.6% and 5.8%, respectively.

2. As the percent of GSWI implementation increases, so does the uncertainty associated with the range of potential percent increases in infiltration depth for each event. The pervious areas within the 37% GSWI model could be reaching saturated conditions during more rainfall events, limiting the infiltration capacity. The 75% GSWI scenario introduced a greater amount of pervious area, which expanded the infiltration capacity and reduced the incidence of saturation. Therefore, a wider range of infiltration depths were possible.
3. These results were calculated for an area weighted average hydraulic conductivity of 0.8 inches/hour and may not be representative of regions with hydraulic conductivities greater than or less than this value. Further analyses are required to establish if extrapolation is possible.

REFERENCES

Abida, H., and Sabourin, J.F. (2006). "Grass Swale-Perforated Pipe Systems for Stormwater Management." *J. Irr. Drain. Eng.*, 132, 55-63.

Arnold, C.L., and Gibbons, C.J. (1996). "Impervious Surface Coverage: The Emergence of a Key Environmental Indicator." *J. Am. Plann. Assoc.,* 62(2), 243-258.

Alfredo, K., Montalto, F., and Goldstein, A. (2010). "Observed and Modeled Performances of Prototype Green Roof Test Plots Subjected to Simulated Low- and High-Intensity Precipitations in a Laboratory Experiment." *J. Hydro. Eng.*, 15(6), 444-457.

Arabi, Mazdak, Govindaraju, Rao S., Hantush, Mohamed M., and Engel, Bernard A. (2006). "Role of Watershed Subdivision on Modeling the Effectiveness of Best Management Practices with SWAT." *J. Am. Water Resour. Assoc.,* 42(2), 513-528. doi: 10.1111/j.1752-1688.2006.tb03854.x

Bach, P.M., Rauch, W., Mikkelsen, P.S., McCarthy, D.T., and Deletic, A. (2014). "A Critical Review of Integrated Urban Water Modelling – Urban Drainage and Beyond." *Env. Modell. Software,* 54(0), 88-107.

Banting, D., Doshi, H., Li, J., Missios, P., Au, A., Currie, B., and Verrati, M. (2005). *Report on the Environmental Benefits and Costs of Green Roof Technology for the City of Toronto.* Ryerson University.

Baughman, D., Lodor, M., Bush, C., Chamblin, L., Albertin, K., Jean-Baptiste, S., and Moisio, S. (2013). "Sustainable Watershed Evaluation and Planning Process for Wet Weather Program Alternatives Development." *Paper presented at the World Environmental and Water Resources Congress 2013.* Showcasing the Future, 19-23 May 2013, Reston, Virginia.

Benedict, M.A. and McMahon, E.T. (2002). "Green Infrastructure: Smart Conservation for the 21st Century." *Renewable Resources Journal,* 20(3), 12-17.

Bhaduri, B., Harbor, J., Engel, B., and Grove, M. (2000). "Assessing Watershed-Scale, Long-Term Hydrologic Impacts of Land-Use Change Using a GIS-NPS Model." *Environ. Manage.,* 26(6), 643-658.

Booth, D.B., Leavitt, J., and Peterson, K. (1996). "The University of Washington Permeable Pavement Demonstration Project – Background and First-Year Field Results." Center for Urban Water Resources Management. University of Washington. Seattle, WA.

Bormann, H., Breuer, L., Graff,., Huisman, J.A., and Croke, B. (2009). "Assessing the Impact of Land Use Change on Hydrology by Ensemble Modelling (LUCHEM) IV: Model Sensitivity to Data Aggregation and Spatial (re-) Distribution." *Adv. Water Resour.*, 32(2009), 171-192.

Boyd, M.J., Bufill, M.C., and, Knee, R.M. (1994). "Predicting Pervious and Impervious Storm Runoff from Urban Drainage Basins." *Hydrol. Sci.*, 39(4), 321-332.

Burian, S.J., Nix, S.J., Durrans, S.R., Pitt, R.E., Fan, C., and Field, R. (1999). "The Historical Development of Wet-Weather Flow Management." U.S. Environmental Protection Agency. Washington, D.C.

Carson, T. B., Marasco, D. E., Culligan, P. J., and McGillis, W. R. (2013). "Hydrological Performance of Extensive Green Roofs in New York City: Observations and Multi-Year Modeling of Three Full-Scale Systems." *Environmental Research Letters,* 8(2).

Carter, T. and Jackson, C.R. (2007). "Vegetated Roofs for Stormwater Management at Multiple Spatial Scales." *Landscape and Urban Plan.*, 80(2007), 84-94.

City of Lancaster. (2011). "Green Infrastructure Plan." The City of Lancaster.

Conan, C., Marsily, G., Bouraoui, F., and Bidoglio, G. (2003). "A Long-Term Hydrological Modelling of the Upper Guadiana River Basin (Spain)." *Physics and Chemistry of the Earth,* 28(2003), 193-200.

CTDEP (2004). "Connecticut Stormwater Quality Manual." The Connecticut Department of Environmental Protection.

Damodaram, C., Giacomoni, C., Khedun, P., Holmes, H., Ryan, A., Saour, W., and Zechman, E.M. (2010). "Simulation of Combined Best Management Practices and Low Impact Development for Sustainable Stormwater Management." *J. Am. Water Resour. Assoc.*, 46(5), 907-918.

Dietz, M.E. and Clausen, J.C. (2008). "Stormwater Runoff and Export Changes with Development in a Traditional and Low Impact Subdivision." *J. Env. Manage.*, 87(2008), 560-566.

Elliott, A. (2009). "Effect of Aggregation of On-Site Stormwater Control Devices in an Urban Catchment Model." *J. Hydrol. Eng.*, 14(9), 975-983.

Elliott, A. H., and Trowsdale, S. A. (2007). "A Review of Models for Low Impact Urban

Stormwater Drainage." *Env. Modelling & Software,* 22(3), 394-405. doi: http://dx.doi.org/10.1016/j.envsoft.2005.12.005.

Emerson, C.H., and Traver, R.G. (2008). "Multiyear and Seasonal Variation of Infiltration from Stormwater Best Management Practices." *J. Irr. Drain. Eng.,* 134(5), 598-605. doi: 10.1061/(ASCE)0733-9437(2008)134:5(598).

Eric, M., Fan, C., Joksimovic, D., and Li, J. (2013). "Modeling Low Impact Development Potential with Hydrological Response Units." *Water Sci. and Technology,* 68(11), 2382-2390.

Ghosh, I., and Hellweger, F. L. (2011). "Effects of Spatial Resolution in Urban Hydrologic Simulations." *J. Hydrol. Eng.,* 17(1), 129-137.

Hamel, P., Daly, E., and Fletcher, T.D. (2013). "Source-Control Stormwater Management for Mitigating the Impacts of Urbanisation on Baseflow: A Review." *J. Hydrology,* 485(0), 201-211. doi: http://dx.doi.org/10.1016/j.jhydrol.2013.01.001.

HCFCD (2011). "Harris County Low Impact Development & Green Infrastructure Design Criteria for Storm Water Management." Harris County Flood Control District. Houston, Texas.

James, M.B., and Dymond, R.L. (2012). "Bioretention Hydrologic Performance in an Urban Stormwater Network." *J Hydrol. Eng.,* 17(3), 431-436. doi: 10.1061/(ASCE)HE.1943-5584.0000448.

Jayasooriya, V.M. (2014). "Tools for Modeling of Stormwater Management and Economics of Green Infrastructure Practices: A Review." *Water, Air, & Soil Pollution,* 225(8), 2-20.

Jia, H., Lu, Y., Yu, S.L., and Chen, Y. (2012). "Planning of LID-BMPs for Urban Runoff Control: The Case of Beijing Olympic Village." *Separation and Purification Technology,* 84(2012), 112-119.

Kertesz, R., Heaney, J., and Sansalone, J. (2007). "Disaggregated modeling for urban hydrologic controls." *Paper presented at the 2007 World Environmental and Water Resources Congress: Restoring Our Natural Habitat*, May 15, 2007 - May 19, 2007, Tampa, Florida, United states.

Lee, J.G. and Heaney, J.P. (2002). "Directly Connected Impervious Areas as Major Sources of Urban Stormwater Quality Problems –Evidence from South Florida." *Proceedings from the Seventh Biennial Stormwater Research & Watershed Management Conference*, Tampa, Florida, May 22-23.

Lee, J.G. and Heaney, J.P. (2003). "Estimation of Urban Imperviousness and its Impacts on Storm Water Systems." *J. Water Resour. Plann. Manage.,* 129(5), 419-426.

Lee, J.G., Selvakumar, A., Alvi, K., Riverson, J., Zhen, J.X., Shoemaker, L., and Lai, F. (2012). "A Watershed-Scale Design Optimization model for Stormwater Best Management Practices." *Env. Modell. Software,* 37(2012), 6-18.

Lee, J.G., and Struck, S.D. (2009). "Evaluation and Optimization of Distributed Stormwater Controls in Spreadsheet." *Paper presented at the World Environmental and Water Resources Congress 2009: Great Rivers*, May 17, 2009 - May 21, 2009, Kansas City, Missouri, United States.

Leopold, L. (1968). "Hydrology for Urban Land Planning – A Guidebook on the Hydrologic Effects of Urban Land Use." Geological Survey Circular 554. Department of the Interior, Washington, D.C.

Lloyd-Davies, D.E. (1906). "The Elimination of Storm-Water from Sewerage Systems." The Institution of Civil Engineers. Paper No. 3560.

Lowndes, M.A., Eds. Bubenzer, G. (2000). "The Wisconsin Storm Water Manual: Overview and Screening Criteria." G3691-1.

Lucas, W.C. (2004). "Delaware Urban Runoff Management Model: Hydrology and Hydraulics." *World Water & Environmental Resources Congress 2003*, ASCE, 1-10.

Lucas, W.C. and Sample, D.J. (2014). "Reducing Combined Sewer Overflows by Using Outlet Controls for Green Stormwater Infrastructure: Case Study in Richmond, Virginia." *J. Hydrol.,* 520(2015), 473-488.

Maher, M. and Lustig, T. (2003). "Sustainable Water Cycle Design for Urban Areas." *Water Sci. Tech.,* 47(7), 25-31.

MMSD (2011). "Determining the Potential of Green Infrastructure to Reduce Overflows in Milwaukee." Milwaukee Metropolitan Sewerage District.

Mohamoud, Y. M., Parmar, Rajbir, and Wolfe, Kurt. (2010). "Modeling best management practices (BMPs) with HSPF." *Paper presented at the Watershed Management Conference 2010: Innovations in Watershed Management under Land Use and Climate Change*, August 23, 2010 - August 27, 2010, Madison, Wisconsin, United States.

Muleta, M. (2007). "Sensitivity of a Distributed Watershed Simulation Model to Spatial Scale." *J. Hydrol. Eng.,* 12(2), 163-172.

Nickel, D., Schoenfelder, W., Medearis, D., Dolowitz, D.P., Keeley, M., Shuster, W. (2014). "German Experience in Managing Stormwater with Green Infrastructure." *J. Env. Plann. Manage.,* 57(3), 403-423.

NRDC (2006). "Rooftops to Rivers: Green Strategies for Controlling Stormwater and Combined Sewer Overflows." National Resource Defense Council.

NRDC (2011). "Rooftops to Rivers II: Green Strategies for Controlling Stormwater and Combined Sewer Overflows." National Resource Defense Council.

Osmond, D.L., Line, D.E., Gale, J.A., Gannon, R.W., Knott, C.B., Bartenhagen, K.A., Turner, M.H., Coffey, S.W., Spooner, J., Wells, J., Walker, J.C., Hargrove, J.C., Foster, M.A., Robillard, P.D., and Lehning., D.W. (1995). "WATERSHEDSS: Water, Soil and Hydro-Environmental Decision Support System," http://h2osparc.wq.ncsu.edu.

Pappas, E.A., Smith, D.R., Huang, C., Shuster, W.D., and Bonta, J.V. (2008). "Impervious Surface Impacts to Runoff and Sediment Discharge Under Laboratory Rainfall Simulation." *Catena,* 72(2008), 146-152.

Park, S. Y., Lee, K. W., Park, I. H., and Ha, S. R. (2008). "Effect of the Aggregation Level of Surface Runoff Fields and Sewer Network for a SWMM Simulation." *Desalination,* 226(1–3), 328-337. doi: http://dx.doi.org/10.1016/j.desal.2007.02.115.

PGC (1999). "Low-Impact Development Hydrologic Analysis." Prince George's County, Maryland. Department of Environmental Resources Programs and Planning Division.

Pitt, R. and Voorhees, J. (2010). "Integrated Modeling of Green Infrastructure Components in an Area Served by Combined Sewers." Low Impact Development 2010: Redefining Water in the City, ASCE, 1617-1630.

Pitt, R., Talebi, L., O'Bannon, D., Bambic, D., Wright, J., and Simon, M. (2013). "Comparison of Winslamm Modeled Results with Monitored Bioinfiltration Data During Kansas City Green Infrastructure Demonstration Project." *World Environmental and Water Resources Congress 2013: Showcasing the Future 2013*. 2936-2950.

PWD (2009). "Green City Clean Waters: The City of Philadelphia's Program for Combined Sewer Overflow Control." Philadelphia Water Department, Philadelphia, PA. Submitted to USEPA September 1, 2009.

PWD (2014). "Stormwater Management Guidance Manual. Version 2.1." Philadelphia Water Department, Philadelphia, PA.

Rossman, L. (2010). "Stormwater Management Model: User's Manual Version 5." U.S. Environmental Protection Agency. Cincinnati, OH. EPA/600/R-05/040.

Roy, A. H., Wenger, S. J., Fletcher, T. D., Walsh, C. J., Ladson, A. R., Shuster, W. D., and Brown, R. R. (2008). "Impediments and Solutions to Sustainable, Watershed-Scale Urban Stormwater Management: Lessons from Australia and the United

States." *Env. Manage.*, 42(2), 344-359. doi: 10.1007/s00267-008-9119-1.

Schueler, T. (1994). "The Importance of Imperviousness." *Watershed Protection Techniques,* 1(3), 100-111.

Schueler, T., Fraley-McNeal, L., and Cappiella, K. (2009). "Is Impervious Cover Still Important? Review of Recent Research." *J. Hydrol. Eng.*, 14, 309-315.

Shapiro, N. (2010). "LID Policy Innovations for Watershed Management in Retrofitting an Ultra-Urban Infrastructure: Addressing Water Quantity and Quality Challenges." *Paper presented at the Watershed Management Conference 2010: Innovations in Watershed Management under Land Use and Climate Change*, August 23, 2010 - August 27, 2010, Madison, Wisconsin, United States.

She, N., Chase, A., and Pang, J. (2008). "Evaluation of Low Impact Development Models for Stormwater Flow Reduction and Demand Management in Downtown Seattle." *Paper presented at the World Environmental and Water Resources Congress 2008: Ahupua'a*, May 12, 2008 - May 16, 2008, Honolulu, HI, United States.

Shuster, W. and Rhea, L. (2013). "Catchment-Scale Hydrologic Implications of Parcel-Level Stormwater Management (Ohio USA)." *J. Hydrol.*, 485(2013), 177-187.

SLCo. (2009). "Salt Lake Countywide Water Quality Stewardship Plan (WaQSP)." Salt Lake County.

Smullen, J.T., Myers, R.D., Reynolds, S.K., and Maimone, M. (2008). "A Green Approach to Combined Sewer Overflow Control: Source Control Implementation on a Watershed Scale." *11th International Conference on Urban Drainage.* Edinburgh, Scotland, UK.

Spicer (2008). "Low Impact Development (LID) in a Combined Sewer Overflow (CSO) District: Evaluating the Effectiveness of LID in Reducing CSOs." City of Saginaw. Project #117352SG2008.

Strecker, E., Leisenring, M., Rathfelder, K., and Barrett, M. (2010). "Linking BMP Performance to Receiving Water Protection, Task 3C, Part 2: Distributed BMP Modeling Approach." Draft Memorandum. October, 29.

Struck, S.D., Carter, S., Brescol, J., Christian, D., Hufnagel, C.L., and Sim, Y. (2011). "Applying Low Impact Development Practices to Meet Multiple Objectives: Case Studies." *Paper presented at the World Environmental and Water Resources Congress 2011: Bearing Knowledge for Sustainability,* May 22, 2011 - May 26, 2011, Palm Springs, California, United States.

Struck, S.D., Hufnagel, C.L., and Field, R. (2012). "Prioritization of Green Infrastructure for CSO Communities - Identifying Effective Implementation Opportunities." *Paper*

presented at the World Environmental and Water Resources Congress 2012: Crossing Boundaries, May 20, 2012 - May 24, 2012, Albuquerque, New Mexico, United States.

Tong, S.T., Sun, Y., Ranatunga, T., He, J., and Yang, Y.J. (2012). "Predicting Plausible Impacts of Sets of Climate and Land Use Change Scenarios on Water Resources." *Applied Geography,* 32(2012), 477-489.

UDFCD (2011). "Urban Storm Drainage: Criteria Manual Volume 3 - Best Management Practices." Urban Drainage and Flood Control District, Denver, CO.

U.S. EPA (2000). "Low Impact Development (LID): A Literature Review." U.S. Environmental Protection Agency. Washington, D.C. EPA-841-B-00-005.

U.S. EPA (2006). "Pilot Projects for LID Urban Retrofit Program in the Anacostia River Watershed Phase III." U.S. Environmental Protection Agency. Washington, D.C. Grant No. X-9731220.

U.S. EPA (2007). "SUSTAIN – A Framework for Placement of Best Management Practices in Urban Watersheds to Protect Water Quality." U.S. Environmental Protection Agency. Washington, D.C. EPA-600-R-09-095. p3.63-3.66.

U.S. EPA (2010). "Stormwater Management Model: User's Manual Version 5. U.S. Environmental Protection Agency." Cincinnati, OH. EPA/600/R-05/040.

U.S. EPA (2010). "Green Infrastructure Case Studies: Municipal Policies for Managing Stormwater with Green Infrastructure." U.S. Environmental Protection Agency. Washington, D.C. EPA-841-F-10-004.

U.S. EPA (2013). "National Stormwater Calculator User's Guide." U.S. Environmental Protection Agency. Washington, D.C. EPA-600-R-13-085.

U.S. EPA (2014). "Greening CSO Plans: Planning and Modeling Green Infrastructure for Combined Sewer Overflow (CSO) Control." U.S. Environmental Protection Agency. Washington, D.C. EPA-832-R-14-001.

Verbeiren, B., Van De Voorde, T., Canters, F., Binard, M., Cornet, Y., and Batelaan, O. (2013). "Assessing Urbanisation Effects on Rainfall-Runoff using a Remote Sensing Supported Modelling Strategy." *Intern. J. Applied Earth Observation and Geoinformation,* 21(2013), 92-102.

Voyde, E., Fassman, E., and Simcock, R. (2010). "Hydrology of an Extensive Living Roof Under Sub-tropical Climate Conditions in Auckland, New Zealand." *J. Hydrol.,* 394(3-4), 384-395.

Wang, J. L., Che, W., Zhang, W., Li, J. Q., and Yi, H. X. (2010). "Roadside Stormwater

Master Plan Using Low Impact Development (LID)." *Paper presented at the 2010 International Low Impact Development Conference - Redefining Water in the City*, April 11, 2010 - April 14, 2010, San Francisco, California, United States.

WERF (2012). "User's Guide to the BMP SELECT Model." SW1R06a. Water Environment Research Foundation, Alexandria, VA.

Wulliman, P.E. and Thomas, P. (2005). "Learning from Nature: Reducing Urban Stormwater Impacts." http://www.udfcd.org/downloads/pdf/tech_papers/Wulliman-LakeLine%20Article.pdf.

Wulliman, P.E. and Urbonas, B. (2005). "Peak Flow Control for Full Spectrum Designs." http://www.udfcd.org/downloads/pdf/tech_papers/Full%20Spectrum%20Detention%202005-01-01%20Concept%20Paper.pdf.

Urbonas, B. and Wulliman, P.E. (2007). "Full Spectrum Detention to Control Stormwater Runoff." http://www.udfcd.org/downloads/pdf/tech_papers/Full%20Spectrum%20Detention%202007.pdf.

Ya, L., Youpeng, X., and Yi, S. (2012). "Hydrological Effects of Urbanization in the Qinhuai River Basin, China." *2012 International Conference on Modern Hydraulic Engineering. Procedia Engineering,* 28(2012), 767-771.

Yang, G., Bowling, L.C., Cherkauer, K.A., and Pijanowski, B.C. (2011). "The Impact of Urban Development on Hydrologic Regime from Catchment to Basin Scales." *Landscape and Urban Planning,* 103(2011), 237-247.

Yeo, I.Y. and Guldmann, J.M. (2010). "Global Spatial Optimization with Hydrlogical Systems Simulation: Application to Land-Use Allocation and Peak Runoff Minimization." *Hydrology and Earth System Sciences*. European Geosciences Union, 14, p325-338.